Doctoral Thesis,

Rahimi, Amir

Semi-probabilistic approach to durability design and assessment of reinforced concrete members exposed to the action of chlorides

BAW
Federal Waterways Engineering and Research Institute

Competence for Waterways

Semi-probabilistic approach to durability design and assessment of reinforced concrete members exposed to the action of chlorides

Amir Rahimi

DAfStb

Semi-probabilistic approach to durability design and assessment of reinforced concrete members exposed to the action of chlorides

Amir Rahimi

Karlsruhe · Januar 2020

Impressum

Herausgeber (im Eigenverlag):
Bundesanstalt für Wasserbau (BAW)
Kußmaulstraße 17, 76187 Karlsruhe
Postfach 21 02 53, 76152 Karlsruhe
Telefon: +49 (0) 721 97 26-0
Telefax: +49 (0) 721 97 26-4540
E-Mail: info@baw.de, www.baw.de

ISBN 978-3-939230-65-6 (Onlinefassung)

Verfügbar unter: https://henry.baw.de/handle/20.500.11970/106976

Karlsruhe · Januar 2020

Die deutsche Originalausgabe erschien 2016 als Dissertation unter dem Titel:

Semiprobabilistisches Nachweiskonzept zur Dauerhaftigkeitsbemessung und -bewertung von Stahlbetonbauteilen unter Chlorideinwirkung

"… no prediction of future developments can be made without some form of model, no matter how crude…"

fib bulletin 53:2009

Preface

A very important aspect of the environmental actions to which reinforced concrete structures are subjected is the action of chlorides. A great number of civil engineering structures are affected by chloride-induced corrosion, such as bridges, tunnels, multi-storey car parks, etc., where de-icing agents are used in winter for reasons of traffic safety, and marine structures, such as dams, flood barriers and locks, which are surrounded by salt water every day.

After long-time applied descriptive design for chloride-induced corrosion safety performance-based concepts have been developed which are based on probabilistic approaches. To ease their use semi-probabilistic design concepts (partial safety factors) have been worked out to enable durability design of new structures and repair decisions for existing structures. A correspondent research project was carried out from 2011 to 2016 with collaboration of Federal Waterways Engineering and Research Institute (BAW) and Center for Building Materials of Technical University of Munich (cbm TUM). The aim of the project was to develop a performance-based easy-to-use tool for durability design and assessment of reinforced concrete structures with regard to chloride-induced corrosion. Easy-to-use leads to nomograms where design results can be gripped in dependence of relevant parameters.

The results were presented in a dissertation titled „Semiprobabilistisches Nachweiskonzept zur Dauerhaftigkeitsbemessung und -bewertung von Stahlbetonbauteilen unter Chlorideinwirking", also published in German language in the publication series of the German Committee for Structural Concrete (DAfStb) as Issue no. 626.

The current document is the English translation of the dissertation which – at the instigation of BAW and DAfStb – wants to provide global access to the achieved results among experts.

The editors would like to see a lively application and are open to comments and suggestions.

Claus Kunz
(Head of Department Structural Engineering, BAW)

Andreas Westendarp
(Head of Section Construction Materials, BAW)

Udo Wiens
(Chief Executive Officer, DAfStb)

TECHNISCHE UNIVERSITÄT MÜNCHEN
LEHRSTUHL FÜR WERKSTOFFE UND WERKSTOFFPRÜFUNG IM BAUWESEN

Semi-probabilistic approach to durability design and assessment of reinforced concrete members exposed to the action of chlorides

Amir Rahimi

This is the full text of the dissertation approved by the Department of Civil, Geo and Environmental Engineering of the Technical University of Munich as satisfying the requirements for a

PhD in Engineering.

Head of examination committee: Univ.-Prof. Dr.-Ing. Detlef Heinz
Dissertation examiners:
1. Univ.-Prof. Dr.-Ing. Christoph Gehlen
2. Univ.-Prof. Dr.-Ing. Wolfgang Breit, TU Kaiserslautern
3. Univ.-Prof. Dr.-Ing. Viktor Mechtcherine, TU Dresden

The dissertation was submitted to the Technical University of Munich on 16th March 2016 and approved by the Department of Civil, Geo and Environmental Engineering on 1st June 2016.

Foreword

This dissertation was written between 2011 and 2016 during the time I spent as a guest research assistant at the Department of Civil, Geo and Environmental Engineering of the Technical University of Munich, with support and funding by the Federal Waterways Engineering and Research Institute (BAW).

I wish to extend my warmest thanks to *Univ.-Prof. Dr.-Ing. Christoph Gehlen*, my doctoral supervisor, for his excellent guidance, the confidence he placed in me and his personal manner. It gives me great pleasure to recall the time we worked together and I greatly appreciate his kind support.

My warmest thanks also go to *BDir Dipl.-Ing. Andreas Westendarp* and *Dr.-Ing. Thorsten Reschke*, my supervisors at the BAW, for their support in technical matters as well as for giving me the time and freedom to pursue my work on this dissertation.

The research project was overseen by a group of dedicated experts. In addition to my supervisors, I would also like to thank the other members of the supervision group, *Dr.-Ing. Udo Wiens (DAfStb)* and *Ir. Joost Gulikers (Rijkswaterstaat, Netherlands)* for the great interest they took in my work as well as their advice and motivating support.

I also wish to thank *Univ.-Prof. Dr.-Ing. Wolfgang Breit* and *Univ.-Prof. Dr.-Ing. Viktor Mechtcherine* for reporting and *Univ.-Prof. Dr.-Ing. Detlef Heinz* for chairing the Examination Committee.

Furthermore, I would like to express my appreciation to *Mr Steinar Helland (SKANSKA, Norway)* for his constructive advice and the discussions we had when working together to draft *fib* bulletin 76 in connection with my dissertation.

I would also like to take this opportunity to thank *Dipl.-Ing. (FH) Philipp Tamm M.Sc.* and *Mr Dimitar Konstadinov M.Sc.,* whose theses were of great help to me in writing this dissertation.

My wholehearted thanks also go to *Dipl.-Math. Hanns Heiß* for checking my work so thoroughly.

Finally, I wish to express my gratitude to *my parents* for their unconditional support and the confidence they placed in me throughout the years.

Karlsruhe, June 2016

Abstract

Over the past three decades, performance-based concepts for the durability design of reinforced concrete structures with regard to corrosion of the reinforcement have been developed using a fully probabilistic approach in order to remedy the shortcomings of the current standard rules in which descriptive requirements are specified. However, applying the design approaches at a fully probabilistic level is not only time-consuming but also requires specialist know-how and special numerical software. Descriptive approaches are usually inadequate or not practicable for assessment of the remaining service life of existing structures in terms of durability, whether repair measures have been carried out or not, owing to the lack of information available on the composition of the construction materials. There are currently no performance-based design approaches available that are suitable for use in practice. This dissertation discusses the development of semi-probabilistic concepts that permit new structural elements and repair measures involving the replacement of damaged concrete to be designed for durability with regard to chloride-induced corrosion of the reinforcement. The concepts also enable the remaining service life of existing members to be assessed. Design nomograms have been established to provide designers with an easy-to-use tool that enables the durability of reinforced concrete structures to be addressed in a transparent manner.

List of symbols and abbreviations

a	initial part of a distribution (e.g. for BetaD)
α_i	sensitivity factors [–]
α	ageing exponent [–] (general; irrespective of time)
α_{app}	ageing exponent [–] according to Approach C
α_{nss}	ageing exponent [–] according to Approach A
α_{RCM}	ageing exponent [–] according to Approach B
b	final part of a distribution (e.g. for BetaD)
b_e	temperature coefficient [K], regression parameter
BetaD	Beta distribution
β	reliability index [–]
β_0	target reliability index [–]
c	concrete cover [mm]
c_{min}	minimum concrete cover to reinforcement [mm], corresponds to the design concrete cover to reinforcement c_d
c_{nom}	nominal concrete cover to reinforcement [mm], corresponds to the characteristic (i.e. mean) concrete cover to reinforcement c_k
c_{new}	thickness of (new) repair layer [mm] when damaged concrete is removed and replaced
c_{remain}	thickness of remaining concrete layer over the reinforcement (concrete cover to reinforcement) [mm] when damaged concrete is removed and replaced
$C(x, t)$	chloride concentration at depth x at time t [% by mass/b]
C_0	initial chloride content [% by mass/b]
C_{crit}	critical chloride content (at which corrosion is initiated) [% by mass/b]
C^*_{crit}	difference between the critical chloride content C_{crit} and the residual chloride content determined at the surface of the rebars C_r; $C^*_{crit} = C_{crit} - C_r$ [% by mass/b]
$C_{new}(x, t)$	time- and depth-dependent chloride concentration in the (new) repair layer [% by mass/b] when damaged concrete is removed and replaced

C_r residual chloride content at the surface of the rebars [% by mass/b] when damaged concrete is removed and replaced

$C_{remain}(x, t)$ time- and depth-dependent chloride concentration in the remaining concrete layer [% by mass/b] when damaged concrete is removed and replaced

$C_{s,0}$ chloride concentration at the surface of the concrete member at the time of observation as a function of the available chloride source which is taken to be a constant action (surface chloride concentration) [% by mass/b]

$C_{s,\Delta x}$ chloride concentration at depth Δx as a function of the available chloride source which is taken to be a constant action (equivalent surface chloride concentration) [% by mass/b]

$C_{s,g}$ concentration of residual chlorides at the surface of the concrete member [% by mass/b] when damaged concrete is removed and replaced

CoV coefficient of variation of a variable

$d_{E,min}$ minimum layer thickness of the repair layer (= $c_{new,min}$) [mm]; 5 % quantile of the measured or calculated thickness; design thickness of repair layer

$d_{E,nom}$ nominal thickness of the repair layer (= $c_{new,nom}$) [mm]; corresponds to the characteristic (i.e. mean) thickness of the repair layer

$D(t_0)$ collective term for $D_{app}(t_0)$, $D_{nss}(t_0)$ and $D_{RCM}(t_0)$ [m²/s]

$D_{app}(t)$ apparent chloride diffusion coefficient [m²/s] at time t

$D_{app}(t_0)$ apparent chloride diffusion coefficient at reference time t_0 [m²/s] converted from $D_{app}(t_{insp})$

$D_{app}(t_{insp})$ apparent chloride diffusion coefficient of the concrete member [m²/s], measured at the time of inspection t_{insp}

$D_{in}(t)$ instantaneous chloride diffusion coefficient [m²/s]

$D_{nss}(t)$ non-steady state chloride diffusion coefficient [m²/s] according to the unidirectional diffusion test based on *DIN EN 12390-11:2015*

$D_{RCM}(t_0)$ chloride migration coefficient [m²/s] according to the rapid chloride migration test (RCM) at reference time t_0

$D_{test}(t_0)$ chloride diffusion coefficient [m²/s] of a concrete at reference time $t_{0,}$ determined by laboratory tests or chloride profiles from existing structures

Δc allowance for deviations of the concrete cover to reinforcement [mm] ensuring that most of the concrete cover (95 % of a normal distribution) exceeds the minimum concrete cover to reinforcement c_{min}

Δc_n	partial factor for the thickness of the layer of repair material [mm]; corresponds to the allowance for deviations in the thickness of the layer of the repair material (Δd_E)
Δc_r	partial factor for the thickness of the remaining concrete cover to reinforcement [mm]
Δd_E	allowance for deviations of the thickness of the layer of repair material when damaged concrete is removed and replaced [mm]
Δx	convection zone; depth range in which the chloride penetration behaviour may deviate from the behaviour according to Fick's law owing to intermittent chloride attack [m]
FA	fly ash
$\Phi( )$	function of a standard normal distribution
g(X, t)	limit state function
f	fly ash content [kg/m³]
f( )	general way of expressing a function
γ_α	partial factor for the ageing exponent
$\gamma_{\alpha,n}$	partial factor for the ageing exponent of the repair material
$\gamma_{\alpha,r}$	partial factor for the ageing exponent of the remaining concrete layer
γ_D	partial factor for the chloride migration coefficient at the reference time
$\gamma_{D,n}$	partial factor for the chloride migration coefficient of the repair material at the reference time
$\gamma_{D,r}$	partial factor for the chloride migration coefficient of the remaining concrete layer at the reference time
γ_C	partial factor for the surface chloride concentration
k_e	environmental parameter to take account of the ambient temperature [–]
K	constant for the regression analysis to determine α_{app} [–]
K_D	design variable, used when damaged concrete is removed and replaced, to take account of the ratio between the chloride penetration resistance of the new and existing layers [–]
λ	uncertainty in the probabilistic model according to *LNEC E 465:2007*
LogND	log-normal distribution
% by mass/b	percentage by mass of binder

% by mass/B	percentage by mass of concrete or sample
% by mass/c	percentage by mass of cement
μ	mean value of a random variable
n	time-independent ageing exponent [–] used to determine the instantaneous chloride diffusion coefficient
ND	normal distribution
p_f	probability of failure or occurrence [–]
R	resistance
R^2	coefficient of determination of a regression analysis [–]
r. h.	relative humidity [%]
S	action (stress)
SN	spray zone
SW	splash zone
σ	standard deviation of a random variable
t_0	reference time [year] or [d]
t_{ex}	time at the beginning of exposure to an environment containing chloride [year], [d] or [s]
t_{SL}	life span (service life) of a member [year]
T_{real}	ambient temperature [K]
T_{ref}	reference temperature [K]
u	q % quantile of a normal distribution
U	value of a normally distributed quantity dividing the area of the distribution into q % and (1-q) %
UW	underwater (submerged) zone
w/b	water/binder ratio [–]
w/c	water/cement ratio [–]
w/c_{eq}	equivalent water/cement ratio [–]
WW	tidal zone (zone of fluctuating water levels)
x	depth [mm]
X	random variable

$x_{crit}(t)$	depth of critical chloride content (at which corrosion is induced) at time t [m]
x^*_{crit}	depth with chloride content $C^*_{crit} = C_{crit} - C_r$
c	cement content [kg/m³]
c_{eq}	equivalent cement content [kg/m³]
Z	state; difference between resistance and action

Indices

d	design variable
k	characteristic variable
insp	parameter determined during the inspection or testing of a member
new	variable for the repair layer used to replace damaged concrete
remain	variable for the remaining concrete layer when damaged concrete is removed and replaced

Table of contents

1 Introduction

1.1 Background and problem statement

Current standards (DIN EN 206 / DIN 1045-2 / DIN EN 1992-1/NA) deal with the durability of new concrete structures descriptively by specifying compliance with certain minimum requirements for the concrete composition and cover to reinforcement that are based on experience. Performance-based assessment according to the performance concept, as in the case of structural design, is not available. The reliability-based approach of *DIN EN 1990:2010* is not currently implemented.

Experience and findings for existing structures have shown that, when the current descriptive approach set out in standards is applied, the intended service life in terms of chloride-induced corrosion of the reinforcement cannot always be achieved with a sufficient level of probability and, in some cases, is even far lower than originally projected. Performance-based durability design based on fully probabilistic calculations (e.g. *Gehlen et al. 2008*, *fib bulletin 76:2015*) has also demonstrated that, in the case of structures exposed to the action of chlorides, compliance with the descriptive normative requirements for the resistance of materials and members does not always result in the safety level aspired to in standards.

According to *DIN EN 206:2014*, performance-based design methods may (only) be used in connection with proof of suitability for use issued by a building inspectorate. The only standardized method available for designing concrete members exposed to the action of chlorides is the laboratory test method for rapid chloride migration described in *BAW-Merkblatt "Chloride penetration resistance"* published in 2012, in conjunction with the general acceptance criteria set out in that code. The evaluation is only based on the material resistance determined at an early age. No consideration is given to the crucial long-term behaviour of the material, exposure-related factors or member design. The fully probabilistic design approaches (in particular in *fib bulletin 34:2006: fib Model Code for Service Life Design*) permit sound durability design but they are time-consuming and require specialist knowledge and the use of special numerical software. Simplified instruments for engineers and designers are not available.

When assessing the remaining service life of existing structures in terms of durability, whether repairs have been carried out or not, the descriptive approaches are usually inadequate or not practicable owing to the lack of data on the composition of the

construction materials. Performance-based design approaches suitable for use in practice are not available.

A semi-probabilistic performance concept for the durability design of reinforced concrete members with regard to carbonation-induced corrosion of the steel reinforcement was recently developed and design nomograms drawn up to provide a user-friendly instrument for designers (*Greve-Dierfeld 2015*). It was demonstrated in that publication that, in contrast to the design of components subjected to the action of chlorides, the descriptive requirements set out in standards for the design of members under XC-exposure result in high levels of reliability in a large proportion of cases and may therefore even lead to concrete members being designed uneconomically.

1.2 Objectives

This dissertation aims to provide simplified, performance-based instruments for designers permitting the

1. durability design of new reinforced concrete members,
2. assessment of the durability of existing reinforced concrete members and
3. durability design of reinforced concrete members to be repaired by removing and replacing the damaged concrete

with regard to chloride-induced corrosion of the reinforcing steel, taking the following boundary conditions into account:

- the limit state to be considered is the depassivation of the reinforcement,
- safety levels must be specified and must be consistent with standards and current research (*DAfStb Positionspapier 2008*),
- concepts based on the fully probabilistic model described in *fib bulletin 34:2006* are to be developed,
- input values used to assess the material resistance must be quantifiable by testing,
- the classification of actions according to exposure classes specified in *DIN EN 206:2014* should be taken into consideration.

The concepts to be developed will be described and any relevant uncertainties will be discussed.

1.3 Approaches

The three objectives of the dissertation outlined above will be dealt with in the same order in Chapters 2, 3 and 4 when elaborating the design concepts concerned. The design concepts will first be developed and described on a fully probabilistic level. After determining the partial factors for the variables in the fully probabilistic model, a semi-probabilistic design tool will be developed and subsequently simplified for application in practice by drawing up design nomograms. The design formats and the way in which they are interrelated are shown in Fig. 1.1.

Exposure classes XS1 and XD1 are not considered in the semi-probabilistic design approaches and design nomograms as the action of chloride is generally not the dominant action in these types of exposure and the required safety levels can be achieved by complying with the descriptive requirements (see *Gehlen et al. 2008*, *fib bulletin 76:2015* and Chapter 2.2).

To provide a better overview, the laboratory tests conducted by the author of this dissertation are presented in three separate annexes, Annex A, B and C. The nomograms developed are presented in Annexes D and E. The work is summarized in Chapter 5 which also includes an outlook.

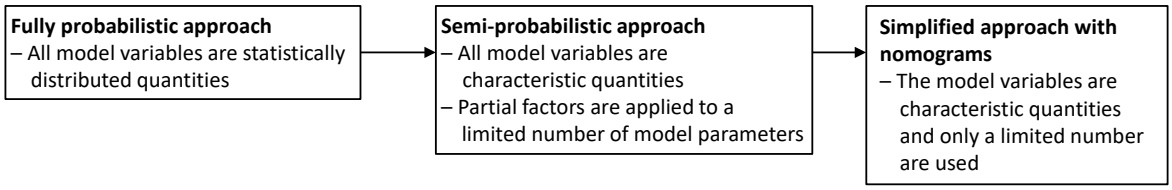

Fig. 1.1: Design formats and the relationship between them

2 Durability design of new reinforced concrete members exposed to the action of chlorides

2.1 Introduction

One very important aspect of the environmental actions to which reinforced concrete structures are subjected is the action of chlorides. It affects a great number of civil engineering structures such as bridges, tunnels, multi-storey car parks, etc., where de-icing agents are used in winter for reasons of traffic safety, and marine structures such as dams and locks. Chlorides penetrating concrete as far as the surface of the reinforcing steel and reaching a critical concentration at this point will damage the protective passive layer of concrete surrounding the rebars. These will start to corrode if certain boundary conditions are present. This phase (corrosion-initiation phase) does not in itself cause any visible damage to the structure. Yet subsequent corrosion of the rebars affects the serviceability and load-bearing capacity of the structure (damage phase). Cracking, spalling of the concrete cover, loss of the bond between the concrete and the steel, a reduction in the cross-section of the steel or even failure of the structural element may occur.

The resistance of a concrete member to chloride-induced corrosion of the rebars can be assessed and controlled by means of the following three parameters:

- the chloride penetration rate in connection with the thickness of the concrete cover,
- the threshold value of the critical chloride concentration C_{crit} and
- the rate of corrosion.

There are tried-and-tested mathematical models for determining the chloride penetration rate which are able to compute the time- and depth-dependent chloride concentration in concrete with sufficient accuracy. The critical chloride content at which corrosion is initiated depends on a variety of factors specific to concrete technology, the environment and the reinforcement (see Chapter 2.4.4.9). The critical chloride content is not normally determined for individual cases, a general threshold value being used instead to take it into account. The time at which depassivation of the surface of the rebars occurs and therefore the corrosion initiation phase usually begins can be estimated by calculating the chloride penetration rate in the concrete and assuming a critical chloride content.

Apart from the anodic dissolution of the iron in reinforcing steel, which is caused amongst other things by depassivation of the surface of the rebars, other conditions also have to be fulfilled before oxygen corrosion of the reinforcement is initiated. These are as follows: the reinforcing steel must be electrically conductive – uncoated steel always conducts

electricity; the concrete must be electrolytically conductive – this is generally true of the majority of concrete members exposed to chlorides owing to the prevailing moisture conditions; the formation of anodic and cathodic regions in the concrete member caused by the differences in potential, e.g. due to local depassivation of the reinforcing steel; and the oxygen supply to the cathodic region. Lack of oxygen may inhibit the initiation of corrosion in underwater structures even if depassivation of the surface of the reinforcing steel has occurred. However, the cathodic subprocess of corrosion may occur in low oxygen environments as the passive steel surface (cathode) is frequently extensive. In addition, a large proportion of the cathodic region of underwater structures often lies in the wet concrete above water level which is exposed to the oxygen in the atmosphere. Depassivated areas of reinforcing steel may also be protected from corrosion (cathodically) by structural boundary conditions (being connected to metal elements). Thus, in the majority of cases, corrosion of the rebars may be initiated by chloride-induced depassivation of the surface of the rebars. Structural and exposure-related factors must always be taken into account.

Recent years have seen the development of models for determining the corrosion rate of reinforcing steel after depassivation in which one or several of the mechanisms involved in corrosion are taken into account by means of the relevant influencing parameters. *Osterminski 2013* grouped these models into oxygen diffusion models (such as *Takewka et al. 2003*, *Hussain & Ishida 2011*), electrolyte resistance models (such as *Alonso et al. 1988*. *Duracrete 1998a*), equivalent circuit models (such as *Schwenk 1972*, *Osterminski 2013*) and numerical models (such as *Bažant 1978*, *Ghods et al. 2008*). However, there are no tried-and-tested models that are suitable for estimating the corrosion damage-phase between depassivation of the rebars and cracking or spalling of the concrete cover or failure of the structural element. Splitting stresses from the reinforcement occurring in the concrete cover due to the effects of mechanical loads must be taken into account when considering the consequences of corrosion for the structure (*ISO 16204:2012*).

It is for these reasons that depassivation of the reinforcing steel is often regarded as a limit state for the purpose of durability design (including in this dissertation) while the damage phase is disregarded. The durability of concrete structures in respect of chloride-induced corrosion of the reinforcing steel is also ensured by the descriptive methods set out in standards by means of provisions for controlling the chloride penetration resistance of the concrete and preventing depassivation of the reinforcement or initiation of corrosion of the reinforcing steel.

2.2 Descriptive and performance-based approaches

The durability of new concrete structures has hitherto been ensured by complying with certain minimum requirements for concrete composition and concrete cover to reinforcement in accordance with the descriptive approach specified in standards and codes (e.g. DIN EN 206 / DIN 1045-2 / DIN EN 1992-1-1/NA / ZTV-W LB 215 / ZTV-ING). Compliance with the requirements for certain parameters is required for reinforced concrete structures exposed to the action of chlorides:

- maximum water/cement ratio,
- minimum cement content,
- maximum permissible fines content,
- permitted cement type,
- minimum compressive strength,
- minimum concrete cover to reinforcement and a permitted allowance for deviations,
- maximum initial chloride content of the concrete and
- maximum crack width.

These parameters describe the resistance of the concrete and the concrete member to possible depassivation of the rebars due to chloride ingress from the environment. The minimum requirements for the parameters concerned depend on the environmental actions. The intensity of the actions is defined by classifying the environment according to the type of exposure, the classification depending on the relevant chloride solution. In this particular case, the relevant exposure classes are XD (de-icing salt) and XS (seawater) which are split into three sub-groups depending on the moisture condition of the concrete member (see Table 2.1).

Requirements for the concrete composition and minimum compressive strength are specified for each exposure class in *DIN 1045-2:2008* which, in conjunction with *DIN EN 206:2014*, deals with concrete performance in Germany. *DIN EN 1992-1-1/NA:2013* (*EC 2*), the principal German standard on the design of reinforced concrete structures, also includes requirements for the minimum concrete cover for each exposure class. These requirements are based on an intended service life of at least 50 years, assuming normal maintenance conditions. Other specifications, such as maximum crack width, are set out in publications for specific types of structure and specific situations, either in guidelines such as *ZTV-W*-, *ZTV-ING*-, *DAfStb*-Richtlinien etc. or in standards such as *DIN 19702:2010*.

Table 2.1: Exposure classes related to chloride action according to DIN 1045-2:2008

Class	Description of the environment	Examples of where exposure classes may occur (informative)
Corrosion induced by chlorides other than from seawater (when concrete containing reinforcement or other embedded metal is subject to contact with water containing chlorides, including de-icing salts, from sources other than from seawater, the exposure shall be classified as follows:		
XD1	Moderately humid	Concrete members exposed to spray from trafficked areas; private garages
XD2	Wet, rarely drey	Salt water pools; Concrete members exposed to industrial waste water containing chlorides
XD3	Cyclic wet and dry	Parts of bridges with frequent exposure to splashing; road pavements; car park slabs in direct contact with traffic[a]
Corrosion induced by chlorides from seawater (where concrete containing reinforcement or other embedded metal is subject to contact with chlorides from seawater or air carrying salt originating from seawater, the exposure shall be classified as follows)		
XS1	Exposed to airborne salt but not in direct contact with seawater	Exterior concrete members near to or on the coast
XS2	Permanently submerged	Permanently submerged parts of structures in harbours
XS3	Tidal, splash and spray zones	Quay walls in harbours

[a] *Additional protection (e.g. crack-bridging coating) will be required, see also DAfSt-Heft 526.*

These standardized minimum requirements are based not only on scientific findings and on product standards for concrete constituents but also to a great extent on national experience. The rules that apply in individual European countries and the resulting concrete and member resistances are not always compatible or clear. This can be demonstrated, for example, by comparing the descriptive rules valid in European countries and the resulting reliabilities in *fib bulletin 76:2015*. The classification of concrete according to exposure classes was introduced with the publication of *EN 206* in 2000. However, *EN 206* only specified the overall framework and supplementary national application rules within this framework were permitted. As a result, the national annexes to *EN 206* include a wide variety of different provisions in spite of the regional proximity of the countries. These differences cannot always be easily explained and the provisions do not always result in the same levels of resistance. Fig. 2.1 shows national provisions for the maximum water/cement ratio and the minimum concrete cover for exposure classes XS1 to XS3 for nine countries: six European countries in which *EN 206* is valid (Portugal, United Kingdom, Netherlands, Germany, Denmark and Norway), Spain, a European country which has not adopted *EN 206*, and two non-European countries (USA and Australia).

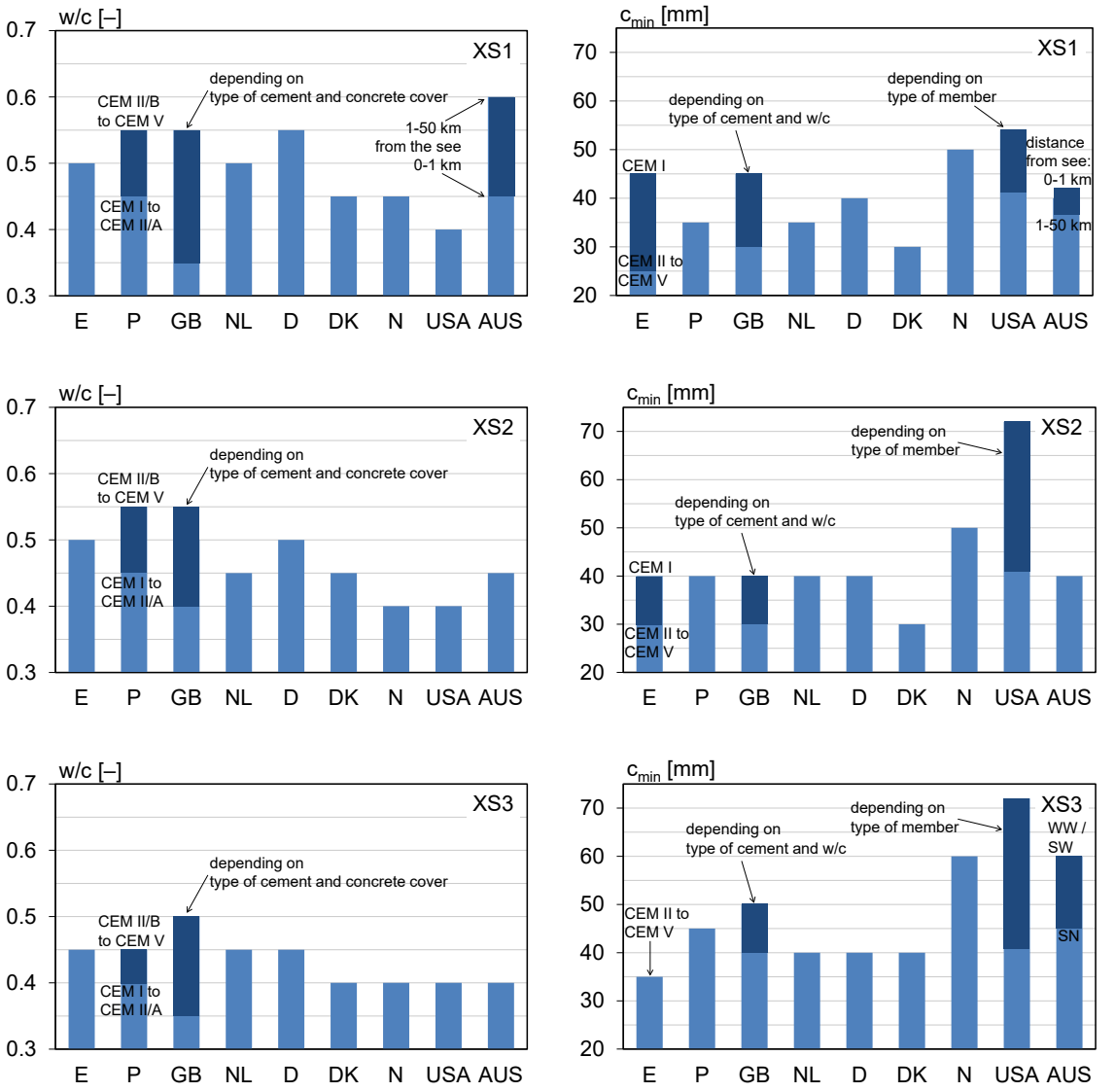

WW: tidal zone, SW: splash zone, SN: spray zone

Fig. 2.1: Diversity of the national requirements of different countries for maximum water/cement ratio (left) and minimum concrete cover (right) for exposure classes XS1 to XS3 (fib bulletin 76:2015)

It can be seen in Fig. 2.1 that some national annexes or standards permit the value of a parameter to be selected freely or parameters to be combined. The result is a certain degree of flexibility in design and the influence of individual parameters on the member resistance can also be considered, even if only to a limited extent. For example, *NP EN 206-1+NA:2007* (the Portuguese national annex to *EN 206*) permits a higher water/cement ratio for concrete with CEM II/B to CEM V cement while, in the United Kingdom (*BS 8500-1:2006*), the type of cement, water/cement ratio and minimum concrete cover are linked. It is not disputed that the type of binder has a significant effect on the durability of concrete structures. The descriptive approach to ensuring durability dates back to a time when the choice of binder was a relatively simple matter as the range of available types of cement

was very limited. The growing range of available binders means that the limits of this concept have now been reached.

Each of the countries considered above has, as can be expected, more stringent requirements for exposure classes XS2 and XS3 than for XS1 (with the exception of Spain where the requirements for XS1 are more stringent than for XS2 for the use of CEM I). Apart from NL and USA, in which no distinction is made between exposure classes XS2 and XS3, the other countries each have more stringent requirements for exposure class XS3. This is because it is assumed that the penetration of chlorides owing to capillary suction will be more rapid in concrete members exposed to XS3 conditions (see Chapter 2.4.4.7), thus leading to a more rapid depassivation of the rebars, and/or there is a greater probability of corrosion of the rebars being initiated after depassivation (see Chapter 2.1).

The range of resulting reliabilities was calculated in *fib bulletin 76:2015* (see Fig. 2.2) to compare the member resistances to chloride-induced corrosion of the rebars resulting from the provisions specified in national standards. This was done using the performance-based fully probabilistic concept presented in Chapter 2.4. Favourable and unfavourable design situations specific to each country were considered in order to determine the range of reliability for the national provisions of each country. The unfavourable design situations were derived by comparing low member resistances with regard to chloride-induced depassivation of the rebars – by selecting the permitted values of material parameters resulting in a concrete with a low resistance to chloride penetration (unfavourable cement type, maximum permitted water/cement ratio) and the lowest permissible minimum concrete cover - and the most unfavourable action scenarios (environments with high levels of available chloride). The favourable design situations were derived by comparing high member resistances and favourable action scenarios. On the action side, the temperature considered was the average of the annual mean temperature for each country while a common range of available chlorides was assumed. Detailed information on this particular benchmarking can be found in *fib bulletin 76:2015*.

The reliability ranges calculated for a life span of 50 years are shown in Fig. 2.2. . It can be seen that, in some cases, the national provisions result in significant differences in the ranges of reliability indices. For instance, the reliability indices calculated for exposure class XS3 were $-0.4 \leq \beta \leq 1.7$ for the United Kingdom and $-1.3 \leq \beta \leq 1.3$ for the Netherlands. These differences are difficult to understand in view of the regional proximity of the two countries and their similar environmental conditions. Moreover, shows that the average reliability index for exposure classes XS2 and XS3 is far below the target value of $\beta = 1.5$ specified in *DIN EN 1990:2010*, indicating a lack of certainty in the descriptive concept in the standards of individual countries. For exposure class XS1, the provisions of the national annexes to *EN 206* result in acceptable reliabilities, even for unfavourable

design situations. The reliability analyses for exposure classes XD1 to XD3 (in *fib bulletin 76:2015*) yielded results that were comparable to those for the XS exposure classes.

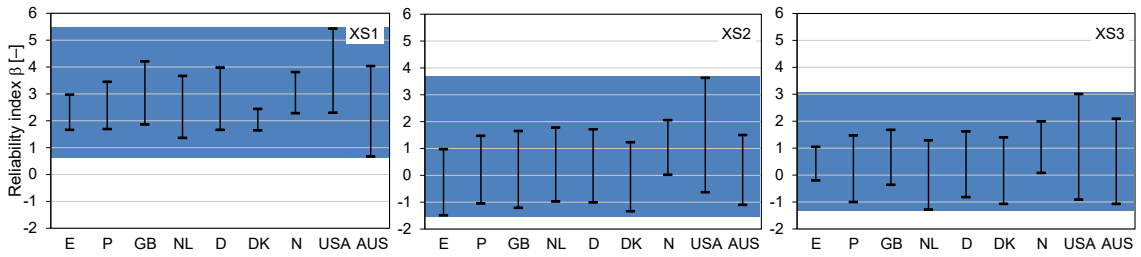

Fig. 2.2: Spectra of reliabilities provided by deemed-to-satisfy rules for XS1 to XS3 exposure classes for a design service life of 50 years determined by reliability design (fib bulletin 76:2015)

By contrast to the descriptive approach, performance-based durability design involves determining the potential concrete and member resistances and comparing them with the expected environmental actions (cf. the benchmarking in *fib bulletin 76:2015* referred to above).

From the mid-1980s, probabilistic performance-based prediction models were developed to permit performance-based durability evaluation and design (for initial work on this subject see, for example, *Siemes et al. 1985*, *Hergenröder 1992*, *CEB 238:1997*, *DuraCrete 1998*). These performance concepts assume that the following basic information is needed for realistic estimations of durability:

- definition of limit states,
- mathematical models to describe the time-related damage mechanisms and transport processes,
- statistical quantification of place- and time-related actions,
- measurement and statistical quantification of member resistances,
- assumption of appropriate probabilities of occurrence of unintended states of the structural elements (failure).
- A fully probabilistic performance concept was developed for the durability of concrete members in intact areas (without cracking) for cases in which depassivation of the rebars due to the action of chlorides (an unintended member state) occurs (*Gehlen 2000*). This concept has been adopted internationally in design practice. The design model published in *fib bulletin 34:2006: fib Model Code for Service Life Design* and later in *fib Model Code for Concrete Structures 2010* and *ISO 16204:2012* is based on the ***limit state*** that depassivation of the surface of the reinforcement must be ruled out. Depassivation of the rebar surface occurs when a critical chloride content is reached at the surface of the rebars. The time- and depth-dependent chloride concentration in concrete members is determined by a ***mathematical model***. The variables of the ***action*** are taken to be the available

chloride from the chloride source in the environment and the ambient temperature, which are regarded as stochastic parameters. The variable of the ***resistance*** is taken to be the measured resistance of concrete to chloride penetration in conjunction with the dimensions of the concrete cover. A maximum ***probability of occurrence*** *or* ***probability of failure*** for the limit state under consideration is assumed to be dependent on the effort required to minimize the risk of occurrence or failure.

- The performance-based concepts for the durability design of reinforced concrete members developed as part of the work on this dissertation are based on the fully probabilistic concept published in *fib bulletin 34:2006*. Modelling the process of chloride penetration in concrete is dealt with in the following chapter and constitutes the most important component of the concept. The fully probabilistic concept is then described. This is followed by a detailed account of the development of the semi-probabilistic approach and a simplified format with design nomograms.

2.3 Modelling chloride transport in concrete

2.3.1 History of the development of the model

Chloride transport in concrete was first modelled in *Collepardi et al. 1970*. The model known as Fick's second law of diffusion is shown in equation (2.1) in its original form as a differential equation.

$$\frac{\partial C}{\partial t} = D \cdot \frac{\partial^2 C}{\partial x^2} \qquad (2.1)$$

where D is the chloride diffusion coefficient of the concrete [m²/s] which is assumed to be constant, i.e. not time-dependent.

When the model was applied during the 1980s the calculated chloride penetration depths were shown to be very unfavourable, resulting in unrealistically short life spans being estimated for concrete members. Furthermore, the chloride diffusion coefficient of older concrete members was revealed to be considerably lower (more favourable) than that of comparable concretes at an early age (for example *Østmosen et al. 1993*). When plotted on a double-logarithmic scale, the chloride diffusion coefficient was shown to decrease linearly over time (*Bamforth 1993, Maage et al. 1993, Maage et al. 1996*). This resulted in the constant chloride diffusion coefficient being replaced by a time-dependent chloride diffusion coefficient in the early 1990s (see Eq. (2.2)). The chloride diffusion coefficients were determined by fitting chloride profiles taken at different times from structures subjected to constant exposure to chloride solutions into the mathematical solution of differential equation (2.1).

$$D_{app}(t) = D_{test}(t_0) \cdot \left(\frac{t_0}{t - t_{ex}}\right)^{\alpha} \qquad (2.2)$$

and for $t_{ex} << t$, which is the usual case:

$$D_{app}(t) = D_{test}(t_0) \cdot \left(\frac{t_0}{t}\right)^{\alpha} \qquad (2.3)$$

where $D_{test}(t_0)$ is the chloride diffusion coefficient of a concrete [m²/s] at reference time t_0 [s] determined by laboratory tests or chloride profiles from existing structures, α is the ageing exponent [–] which takes account of the reduction in the apparent chloride diffusion coefficient over time ($0 < \alpha < 1.0$) and t_{ex} is the time at which exposure to an environment containing chlorides begins. For the sake of simplicity, t_{ex} can be ignored as its influence generally only lasts a few days and is thus of no consequence as longer periods of several

years are used when modelling the chloride transport in concrete to determine the time at which depassivation of the rebars occurs.

The parameter $D_{app}(t)$ represents the apparent chloride diffusion coefficient of the concrete for the entire period of time under consideration, t_{ex} (~ 0) to t, as a constant mean value. The term "apparent" denotes that the chloride bond is considered (*Lay 2007*) in addition to the transport of free chloride ions in the pore solution owing to the concentration gradient, i.e. the diffusion process alone; it is used to differentiate the parameter from the instantaneous chloride diffusion coefficient $D_{in}(t)$ (see Chapter 2.3.2.3).

It has not yet been possible to fully explain why the chloride diffusion coefficient decreases over time and thus why the resistance of the concrete to the penetration of chlorides increases. In addition to the increase in the density of the structure of the concrete owing to continuing hydration of the binder, there are also other influences which slow down chloride transport in concrete over time, such as blockage of pores owing to ion exchange with seawater and partial drying of the concrete due to the moisture gradient (see Chapter 2.4.4.4).

This has led to the development and publication of several models based on Fick's second law of diffusion and a time-dependent chloride diffusion coefficient.

Possibly the most frequently used model based on Fick's law of diffusion is the one developed in *DuraCrete 1998* and *Gehlen 2000* and published in *fib bulletin 34:2006: fib Model Code for Service Life Design*. Differential equation (2.1) is solved in this case with the aid of the Gauss error function. An important boundary condition is the assumption that the chloride concentration at the surface of the concrete member is constant. In addition, the influence of a convection zone, which forms near the surface due to the intermittent action of chlorides and in which the redistribution of chlorides deviates greatly from Fick's law of diffusion, is taken into account by a variable by way of simplification.

Mejlbro 1996 presented a model in which the surface chloride concentration could be considered as a function of time. In this case, differential equation (2.1) is solved by the Ψ_p function which is far more complex than the Gauss error function. Additional parameters, which require verification, are needed to take account of the variation in the surface chloride concentration over time.

The various versions of the model use different parameters to describe the material properties and ambient conditions. The appropriate data must therefore be used when applying and comparing the models. However, validated models should lead to results of a similar magnitude provided they have been calibrated using the same structural and laboratory data.

The exploration of the durability design in this dissertation is based on the model in *fib bulletin 34:2006: fib Model Code for Service Life Design* which is described in the following chapters.

2.3.2 Selected model

2.3.2.1 Basic principle and mathematical formula

There are various physical and chemical processes involved in the penetration of chlorides into concrete. The aim of modelling is to illustrate the result of these processes, i.e. the chloride profiles, in a practicable manner and with sufficient accuracy.

The engineering model described in *fib bulletin 34:2006: fib Model Code for Service Life Design* solves the differential equation (2.1) for Fick's law of diffusion as follows (Eq. (2.4)). The model has been slightly simplified and technically modified:

$$C(x,t) = C_0 + \left(C_{S,0} - C_0\right) \cdot erfc \frac{x}{2 \cdot \sqrt{D_{app}(t) \cdot t}} \qquad (2.4)$$

where:

$C(x, t)$: is the chloride concentration at depth x at time t [% by mass/b]

C_0: is the initial chloride content of the concrete [% by mass/b]

$C_{s,0}$: is the chloride concentration at the surface of the member at the time of observation as a function of the available chloride source which is taken to be a constant action (surface chloride concentration) [% by mass/b]

x: is the depth with a corresponding chloride content $C(x, t)$ [m]

t: is the concrete age [s]

$D_{app}(t)$: is the apparent chloride diffusion coefficient of the concrete [m²/s], its magnitude depending on the exposure period. However, the variable is taken to be constant over the period under consideration, from t_{ex} (~ 0) to t, in all calculations

erfc: is the complementary Gauss error function (= 1-erf)

It can be concluded from equation (2.4) that the chloride penetration rate in concrete is governed by the diffusivity and chloride-binding capacity of the concrete (material resistance) and the different levels of chloride action (environmental actions).

For the sake of simplicity, the period prior to exposure of the concrete to chlorides in the environment, t_{ex}, is not included in the ageing term ($D_{app}(t) \cdot t$) in equation (2.4) ($D_{app}(t) \cdot t$) as it does not significantly affect the calculation of the chloride concentrations for the period of several years under consideration (see also Chapter 2.3.1, equation (2.2)). An accurate expression of the ageing term is $D_{app}(t) \cdot (t - t_{ex})$.

The chloride transport close to the surface may, however, greatly deviate from Fick's law of diffusion if members are subject to cyclic exposure to chlorides. These include trafficked areas (treatment with de-icing agents in winter) and parts of coastal structures exposed to fluctuating water levels and spray water. For such cases, the equivalent surface chloride concentration $C_{s,\Delta x}$ was introduced in *Gehlen 2000.* To err on the safe side, the chloride concentrations within the convection zone Δx are disregarded and equation (2.4) is amended as follows for intermittent chloride action (cf. Fig. 2.3, right):

$$C(x,t) = C_0 + \left(C_{S,\Delta x} - C_0\right) \cdot erfc \frac{x - \Delta x}{2 \cdot \sqrt{D_{app}(t) \cdot t}} \qquad (2.5)$$

where:

$C_{s,\Delta x}$: is the chloride concentration at depth Δx as a function of the available chloride source which is taken to be a constant action (equivalent surface chloride concentration) [% by mass/b]

Δx: is the depth range in which the chloride penetration behaviour may deviate from the behaviour according to Fick owing to intermittent chloride attack [m]

The (equivalent) surface chloride concentration is time-dependent, particularly at the start. However, this parameter is taken to be constant over time for the sake of simplicity to satisfy the boundary condition for applying the Gauss error function to solve the differential equation of Fick's law of diffusion.

The material resistance is taken into consideration by the apparent chloride diffusion coefficient $D_{app}(t)$. The term "apparent" is used to differentiate this parameter from the instantaneous chloride diffusion coefficient $D_{in}(t)$. It also covers the chloride-binding capacity and the transport of chloride ions in the pore solution due to the concentration gradient, i.e. the diffusion process alone (*Lay 2007*). The magnitude of $D_{app}(t)$ varies over the exposure period (concrete age), decreasing as the period under consideration increases in length, i.e. $D_{app}(t_2)$ is generally lower than $D_{app}(t_1)$, with $t_2 > t_1$. For individual calculations, the apparent chloride diffusion coefficient is introduced as a constant input variable representing a chloride diffusion coefficient averaged over the period under consideration (t_{ex} (~ 0) to t). Various ways of describing this variable of the material resistance are proposed in the following chapter.

This model is also based on several assumptions and simplifications, as are all engineering models of relevance to actual practice.

The application of Fick's law of diffusion to modelling chloride transport in concrete is a simplifying assumption as – although diffusion is the principal transport mechanism – the

chlorides in partially saturated concrete can be transported convectively by capillary suction, permeation or the micro ice lens pump. Several transport mechanisms may also occur simultaneously, particularly in road structures subject to greatly varying levels of exposure to de-icing agents. The few models that have been developed explicitly for road structures and take account of convective chloride transport in concrete in addition to diffusion are of limited value or no value at all in practical terms. The progress of chloride penetration, taking diffusion, convection and dispersion into account, is calculated analytically in the model in *Lay 2007*. However, the model is very complex and includes numerous variables, some of which cannot be quantified directly. The empirical model of *Ungricht 2008* considers the convection and diffusion mechanisms consecutively. However, the progress of chloride penetration can only be calculated analytically for very short periods of time and several of the model variables are not directly quantifiable. It is not possible to perform a probabilistic design with this model owing to the lack of data (*Kapteina 2011*).

The following principal assumptions have to be made if Fick's law of diffusion and the Gauss error function are to be used to address the problem at hand:

- the concrete has a homogeneous structure,
- diffusion is unidirectional in a semi-finite medium,
- the chloride-binding capacity of the concrete is constant,
- the surface chloride concentration is constant,
- ions other than chlorides are not taken into account.

Furthermore, the model can be used to predict the development of the chloride concentration in the concrete over long periods of time after exposure. The transport process initially deviates greatly from Fick's law of diffusion, the length of time depending on the type of exposure (under water, zone of fluctuating water levels, salty air, etc.). The model only maps the time- and depth-dependent chloride concentration in the structural element with a sufficient degree of accuracy after relatively stable conditions have been reached within the element.

2.3.2.2 Apparent chloride diffusion coefficient $D_{app}(t)$

2.3.2.2.1 General

The general formulation of the apparent chloride diffusion coefficient $D_{app}(t)$ was shown in equation (2.3). The parameter $D_{test}(t_0)$, which describes the resistance of the concrete (in general, of the product) to chloride penetration, is usually determined by fitting chloride profiles from existing structures or accelerated laboratory tests into equation (2.4) or (2.5). This is done by means of a regression analysis in which the differences (v_i) between the

calculated values and the measurements are minimized (least squares method), cf. Fig. 2.3. The result of the regression analysis is the pair of values $D_{test}(t_0)$ and either the surface chloride concentration $C_{S,0}$ or the chloride concentration at depth Δx (convection zone) $C_{S,\Delta x}$ (equivalent surface chloride concentration). The chloride content can be taken into account by the cement mass C (or the equivalent cement mass c_{eq} or the mass of binder b) or by the mass of the finely ground sample (for example, if the composition of the material is unknown).

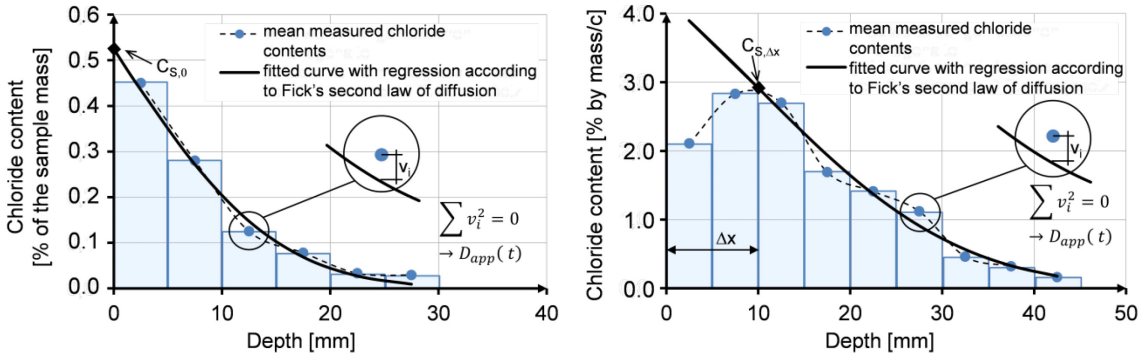

Fig. 2.3: Determination of $D_{test}(t_0)$, $C_{S,0}$ and $C_{S,\Delta x}$ by evaluating chloride profiles of laboratory specimens or structural elements exposed to chlorides

The second parameter of the apparent chloride diffusion coefficient, i.e. the ageing exponent α, describes the long-term behaviour of the product under investigation. The magnitude of the ageing exponent expresses the intensity of the decrease in $D_{app}(t)$ over time. Unlike $D_{test}(t_0)$, the ageing exponent cannot be determined by a single laboratory test. This parameter is estimated by considering structural data and/or observing the development of $D_{app}(t)$ over time in long-term laboratory tests.

Three methods of measuring or estimating the parameters $D_{test}(t_0)$ and α by different methods are presented below. The objective is to determine the apparent chloride diffusion coefficient $D_{app}(t)$ required for the durability models in this dissertation (fully probabilistic and semi-probabilistic approach and simplified approach using nomograms) for practical situations with different materials (conventional concretes, novel materials) and other necessary information (composition of the material, data available from laboratory or structural investigations, etc.) as well as a realistic estimate of the time and cost involved and the required reliability.

2.3.2.2.2 Determination of the material resistance $D_{app}(t)$ by means of diffusion tests (Approach A)

In this approach, the apparent chloride diffusion coefficient $D_{app}(t)$ is characterized by determining the parameters $D_{nss}(t_0)$ and α_{nss} in diffusion tests based on *DIN EN 12390-11:2015* and calculated using the following equation:

$$D_{app,A}(t) = k_e \cdot D_{nss}(t_0) \cdot \left(\frac{t_0}{t}\right)^{\alpha_{nss}} \qquad (2.6)$$

where:

$D_{nss}(t_0)$ is the non-steady state chloride diffusion coefficient [m²/s] according to the unidirectional diffusion test based on *DIN EN 12390-11:2015*

t_0 is the reference time; length of time during which the test specimen is exposed to a chloride solution in the diffusion test (t_0 = 28 d)

α_{nss} is the ageing exponent [–], determined by diffusion tests based on *DIN EN 12390-11:2015*

$D_{app,A}(t)$ is the apparent chloride diffusion coefficient [m²/s] according to Approach A

k_e is the environmental parameter to take account of the ambient temperature [–] (see Chapter 2.4.4.5)

The diffusion test must be carried out on test specimens cured under water for 28 days after production. The non-steady state chloride diffusion coefficient $D_{nss}(t_0)$ is determined by testing the specimens after t_0 = 28 d exposure to a chloride solution and establishing the chloride profiles. The ageing exponent α_{nss} is determined by conducting the diffusion test on the test specimens over a period of at least two years and determining the chloride diffusion coefficients for at least another three points in time (after approx. 90, 365 and 730 days' exposure to a chloride solution). An example of the development of the chloride diffusion coefficient D_{nss} of a material over time is shown on an ordinary and a double-logarithmic scale in Fig. 2.4. The ageing exponent α_{nss} is quantified by a regression analysis. The regression function (power: $y=a \cdot x^{-\alpha}$) and the coefficient of determination R^2 are shown in Fig. 2.4. The ageing exponent α_{nss} (here $\alpha_{nss} \sim 0.35$) is derived from the exponent of the regression function.

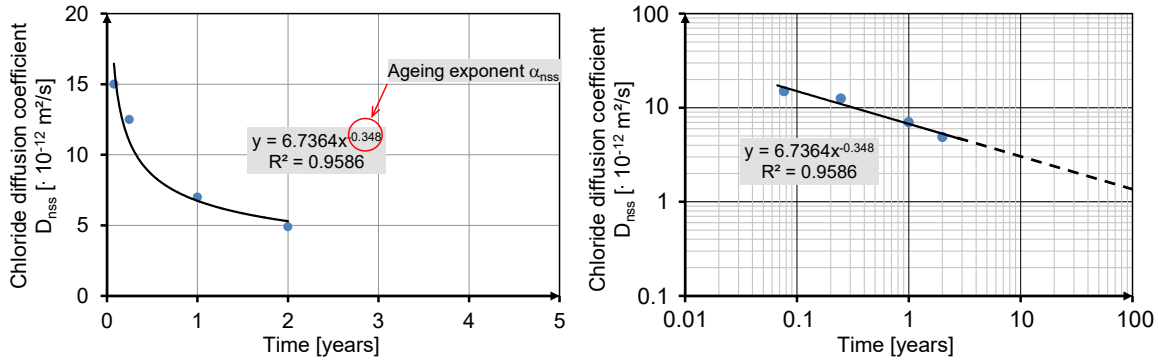

Fig. 2.4: Deriving the ageing exponent α_{nss} by regression analysis of the chloride diffusion coefficients D_{nss}. Each single D_{nss} represents the concrete resistance for different exposure periods (t_0 = 28 d, t_1 = 90 d, t_2 = 365 d, t_3 = 730 d) as a constant value over the considered time period. Development of D_{nss} over time in ordinary (left) and double-logarithmic (right) scale

Observations of how the non-steady state chloride diffusion coefficient develops over a period of at least two years are based on the latest findings of JWG TC 104 / SC1 and TC 250 / SC2 (see *Leivestad 2014*) dealing with the development of performance-based approaches for the durability design of reinforced concrete structures. The choice of an investigation period of two years is a compromise between the necessary accuracy and the time and expense involved. Finally, the results for parameters $D_{nss}(t_0)$ and α_{nss} are used to extrapolate the chloride diffusion coefficient $D_{app}(t)$ for long periods of time of up to t = 100 years for the purpose of durability design.

The ageing exponent α_{nss} derived as shown above must be limited to a value between 0.20 and 0.80 in accordance with the provisions of *fib Model Code for Concrete Structures 2010*.

This approach is particularly suitable for products of unknown composition or for which insufficient practical experience is available. Approach B, which is described in the following chapter, can be used for conventional concretes and products whose long-term resistance to the penetration of chlorides has been verified by structural data.

2.3.2.2.3 Determination of the material resistance $D_{app}(t)$ by means of the migration test and data from existing structures (Approach B)

A method of determining $D_{app}(t)$ was developed in *DuraCrete 1998* und *Gehlen 2000* in which structural data is used to determine the ageing exponent and the material resistance at reference time $D_{test}(t_0)$ is determined in an accelerated laboratory test. For this approach, the apparent chloride diffusion coefficient $D_{app}(t)$ is calculated by equation (2.7):

$$D_{app,B}(t) = k_e \cdot D_{RCM}(t_0) \cdot \left(\frac{t_0}{t}\right)^{\alpha_{RCM}} \qquad (2.7)$$

where:

$D_{RCM}(t_0)$ is the chloride migration coefficient [m²/s] obtained in the rapid chloride migration test RCM according to *BAW-Merkblatt 2012*

t_0 is the reference time; beginning of RCM test on test specimens, age of concrete (t_0 = 28 d)

α_{RCM} is the ageing exponent [–], determined according to Approach B

$D_{app,B}(t)$ is the apparent chloride diffusion coefficient [m²/s] according to Approach B

k_e is the environmental parameter to take account of the ambient temperature [–] (see Chapter 2.4.4.5)

The rapid chloride migration test RCM (Rapid Chloride Migration) was developed in *Tang 1996* and introduced into several European codes (such as *NT Build 492:1999* and *BAW-Merkblatt 2012*). The RCM test method involves applying an electrical field to speed up

the penetration of chlorides into the concrete. Once application of the voltage has been terminated and the test specimens have been split, the penetration depth of the chloride front is determined by means of indicator solutions. The chloride migration coefficient is calculated from the penetration depth, the voltage applied and other parameters. The length of the test varies between a few hours and a week and is far shorter than the accelerated laboratory diffusion test. The test method involves far less time and effort than the diffusion test.

After having been shown to be highly dependent on the type of binder, the ageing exponent of concretes with the principal types of binder, Portland cement (CEM I), Portland fly ash cement (CEM I + FA ($f \geq 0.20 \cdot c$)) and blast furnace cement (CEM III/B) was quantified as described below in *Gehlen 2000*.

Numerous chloride profiles for various concrete members made with the relevant types of binder were first determined at different times and compiled for each of the concretes mentioned above (data from literature and structural investigations by the author in *Gehlen 2000*). The structural elements were selected from the exposure environments “below water”, “zone of fluctuating water levels” and “splash zone” (XS2, XS3). The concretes had water/cement ratios between 0.40 and 0.60. The apparent chloride diffusion coefficients $D_{app}(t)$ determined from the chloride profiles by regression according to Fick’s law of diffusion (Eq. (2.4) or (2.5)) were compared with the age of the concrete in a double-logarithmic diagram (Fig. 2.4). Laboratory concretes with similar compositions, i.e. with the same type of binder and $0.40 \leq w/c \leq 0.60$, were produced and subjected to the RCM test at an age of 28 days. A regression analysis was performed on the structural data and the resulting regression line was forced through the mean value of $D_{RCM}(t_0=28d)$. The resulting regression line represents the ageing exponent according to Approach B. The ageing exponent as a function of the type of binder is quantified using this approach in Table 2.5.

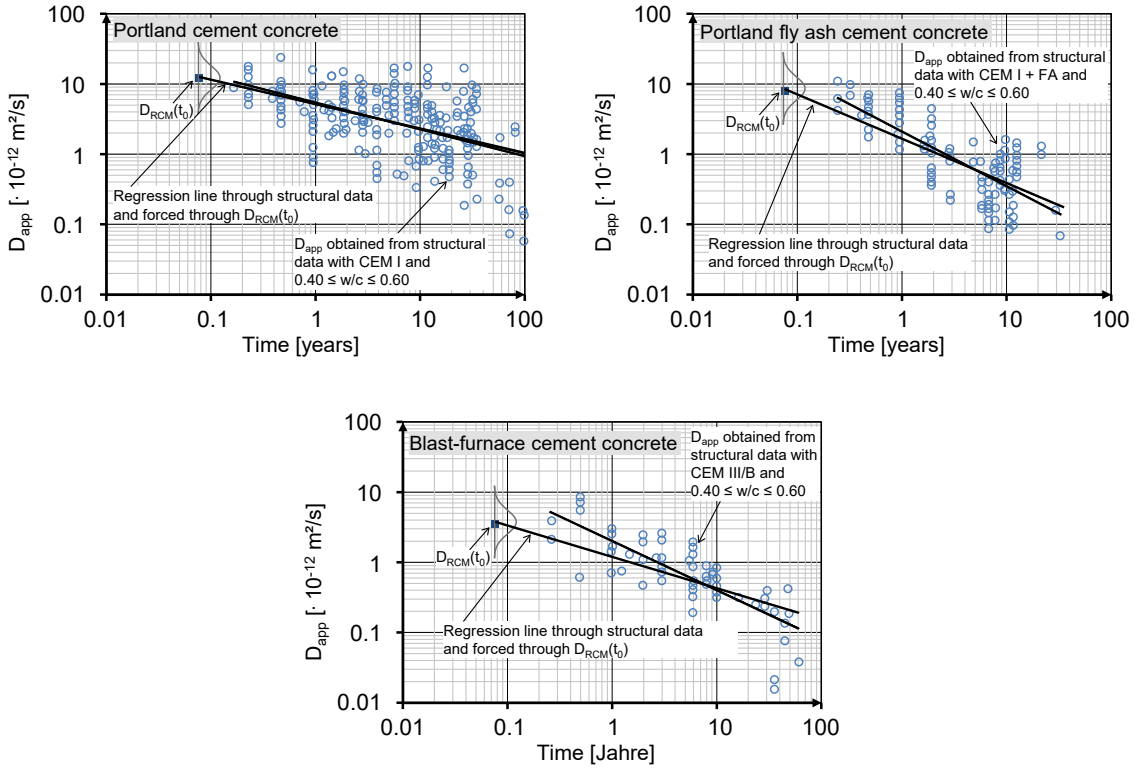

Fig. 2.5: Development of the apparent chloride diffusion coefficient over time for concretes with Portland cement (left), with Portland cement and fly ash (right) and with ground granulated blast-furnace slag cement (bottom), modified from Gehlen 2000

Forcing the regression line originally determined from structural data through $D_{RCM}(t_0)$ reduced the steepness of its slope in all three cases although the gradients differ (see Fig. 2.4). This is because, in each case, the value of $D_{RCM}(t_0)$ is lower than the chloride diffusion coefficient at time t_0 determined by regression of the structural data. This means that the ageing exponent decreases when $D_{RCM}(t_0)$ is considered, in other words it becomes more unfavourable. It can also be seen that, in all three cases, the regression lines intersect at a point between 5 and 10 years. After the intersection point, the line forced through $D_{RCM}(t_0)$ yields higher (less favourable) values for $D_{app}(t)$ than the regression line for the structural data, leading to results that are relatively "safe" (more conservative) in terms of durability design (see also *Gehlen et al. 2015*). The difference between the two regression lines is greatest for the blast furnace cement concretes. The regression lines for Portland cement concretes are almost identical.

On the one hand, this approach enables the long-term behaviour of concrete to be taken into account over several decades using data from existing structures. On the other hand, the potential resistance of concrete can be measured with relatively little effort and taken into account.

The ageing exponents statistically quantified in *Gehlen 2000* for concretes made with the three main types of binder, CEM I, CEM I + FA and CEM III/B, are shown in

Chapter 2.4.4.4, Table 2.5. Table 2.5 also includes ageing exponents derived from this data for several other types of cement and binder. The assumptions are based on the values determined for the three types of binder mentioned above, experience with each type of binder and relevant findings.

Extensive experience with this approach has been gathered thanks to its application in numerous fully probabilistic durability designs over the past 15 years. The work on durability design in this dissertation is based solely on this approach to determining the apparent chloride diffusion coefficient $D_{app}(t)$.

2.3.2.2.4 Determination of the material resistance $D_{app}(t)$ by means of the diffusion test and data from existing structures (Approach C)

This approach to determining $D_{app}(t)$ is suitable for application in specific design cases in which the long-term behaviour of the design product is determined using data from individual structures that are very similar to the design case in terms of material composition and exposure conditions. $D_{app}(t)$ is calculated as follows:

$$D_{app,C}(t) = k_e \cdot D_{nss}(t_0) \cdot \left(\frac{t_0}{t}\right)^{\alpha_{app}} \qquad (2.8)$$

where:

$D_{nss}(t_0)$ is the non-steady state chloride diffusion coefficient [m²/s] according to the unidirectional diffusion test based on *DIN EN 12390-11:2015*

t_0 is the reference time; length of time during which the test specimen is exposed to the chloride solution in the diffusion test (t_0 = 28 d)

α_{app} is the ageing exponent [–], determined according to Approach C

$D_{app,C}(t)$ is the apparent chloride diffusion coefficient [m²/s] according to Approach C

k_e is the environmental parameter to take account of the ambient temperature [–] (see Chapter 2.4.4.5)

In this approach, the potential material resistance is determined on a 28-day-old test specimen exposed to a chloride solution for 28 days (t_0 = 28 d) in the diffusion test based on *DIN EN 12390-11*:2015 (analogous to Approach A, Chapter 2.3.2.2.2). The ageing exponent α_{app} is calculated by means of a regression analysis of the chloride diffusion coefficients determined by fitting the chloride profiles obtained from structures (cf. Fig. 2.4 and Fig. 3.2). To ensure that these chloride diffusion coefficients realistically reflect the resistance of the concrete member to chloride penetration under exposure conditions, the first chloride profile included must be determined at least 10 years after initial exposure of the concrete member. The intervals between each of the following chloride profiles must be at least 5 years.

2.3.2.2.5 Summary

The apparent chloride diffusion coefficient $D_{app}(t)$ representing the material resistance over time must be determined before the chloride transport in concrete can be modelled and to permit performance-based durability design of concrete members. Three approaches to calculating this parameter for the durability design concepts presented in this dissertation have been presented and are summarized in Table 2.2. They are dependent on the design product, the available information, a realistic estimate of the time and expense involved and the required reliability.

Table 2.2: Approaches for determining the apparent chloride diffusion coefficient $D_{app}(t)$ for modelling the chloride transport in concrete and the durability design of concrete structural elements

	Approach A	Approach B	Approach C
Test method/ aids	Diffusion tests	RCM test + (extensive) structural data	Diffusion test + (limited) structural data
Applications	New products for which no experience is available, products of unknown composition	Conventional products for which experience is available and with a known composition	Structural data available for relevant design product and design exposure
Time and cost involved	Very high	Very low	Medium
Duration of test *	At least two years	Approx. 5 weeks	Approx. 9 weeks
Equation	$D_{app,A}(t) = k_e \cdot D_{nss}(t_0) \cdot (\frac{t_0}{t})^{\alpha_{nss}}$	$D_{app,B}(t) = k_e \cdot D_{RCM}(t_0) \cdot (\frac{t_0}{t})^{\alpha_{RCM}}$	$D_{app,C}(t) = k_e \cdot D_{nss}(t_0) \cdot (\frac{t_0}{t})^{\alpha_{app}}$

* *From preparing the specimens to obtaining the results, i.e. measuring the penetration depths for RCM or chemical analysis of finely-ground samples in the diffusion test*

2.3.2.3 Instantaneous chloride diffusion coefficient $D_{in}(t)$

Modelling chloride transport with the error function as a solution to Fick's law of diffusion is discussed in the literature, in which the instantaneous chloride diffusion coefficient is also considered (e.g *Tang & Gulikers 2007*, *Frederiksen et al. 2008*, *Tang et al. 2012)*. The instantaneous or point-wise $D_{in}(t)$ is valid for a particular point in time t while the apparent chloride diffusion coefficient $D_{app}(t)$ represents a constant value averaged over a period of time (t_{ex} (~ 0) to t). The parameter $D_{in}(t)$ is determined in a similar way to $D_{app}(t)$ using a reference value, i.e. a chloride diffusion coefficient $D_{test}(t_0)$ at a reference time t_0, and an ageing exponent n (Eq. (2.9)).

$$D_{in}(t) = D_{test}(t_0) \cdot (\frac{t_0}{t})^n \qquad (2.9)$$

Similar to the calculation of $D_{app}(t)$ in equation (2.3), $D_{test}(t_0)$ is determined using chloride profiles for existing structures or by laboratory tests performed at reference time t_0. By contrast to ageing exponent α (for determining $D_{app}(t)$), the ageing exponent n is a time-

dependent variable and is different from the former. This variable must be integrated over the entire duration of exposure when modelling the chloride concentration in concrete with $D_{in}(t)$. The ageing term in the model for determining the chloride concentration in concrete (Eq. (2.4)) for this particular case is shown in equation (2.10), right.

$$D_{app}(t) \cdot (t - t_{ex}) = \int_{t_{ex}}^{t} D_{in}(t) \cdot dt \qquad (2.10)$$

The relationship between the two chloride diffusion coefficients can thus be determined as follows:

$$\rightarrow D_{app}(t) \cdot (t - t_{ex}) = \int_{t_{ex}}^{t} D_{test}(t_0) \cdot \left(\frac{t_0}{t}\right)^n \cdot dt \qquad (2.11)$$

$$\rightarrow D_{app}(t) = \frac{D_{test}(t_0)}{1-n} \cdot \left(\frac{t_0}{t}\right)^n \cdot \left[t - t_{ex} \cdot \left(\frac{t}{t_{ex}}\right)^n\right] \cdot \frac{1}{t - t_{ex}} \qquad (2.12)$$

The following applies to the usual case where $t_{ex} << t$ (see Chapter 2.3.1):

$$\rightarrow D_{app}(t) = \frac{1}{1-n} \cdot D_{in}(t) \qquad (2.13)$$

The relationship between ageing exponents α and n is as follows (*Frederiksen et al. 2008*, *Tang et al. 2012*):

$$n = \alpha + \frac{ln\left[(1-\alpha) + \alpha \cdot \frac{t_{ex}}{t}\right]}{ln\left(\frac{t_{ex}}{t}\right)} \qquad (2.14)$$

which means:

$$n > \alpha \qquad (2.15)$$

and

$$D_{in}(t) < D_{app}(t) \qquad (2.16)$$

The equations shown above can be summarized as follows:

$$\begin{cases} D_{app}(t) = \dfrac{1}{1-n} \cdot D_{in}(t), \\ D_{in}(t) < D_{app}(t), \\ n > \alpha \end{cases} \tag{2.17}$$

Both the instantaneous and the apparent chloride diffusion coefficients can be used to model the chloride transport in concrete. However, the author of this dissertation is not currently aware of any method of determining ageing exponent n for the purpose of calculating the instantaneous chloride diffusion coefficient $D_{in}(t)$. By contrast, approaches to determining ageing exponent α for calculating the apparent chloride diffusion coefficient $D_{app}(t)$ have been presented in Chapter 2.3.2.2. The relationships shown above were not used correctly in some publications and academic work, resulting in incorrect results and assessments (e.g. *Tang & Gulikers 2007*).

2.4 Fully probabilistic durability design

2.4.1 General

The fully probabilistic approach to performance-based durability design considers each model variable as a statistically distributed quantity. The following chapter presents the methodology used to predict the condition states of structural elements with the design model. Chapter 2.4.3 specifies the safety level for the design approach. The individual model variables are explained and described statistically in Chapter 2.4.4 while several examples demonstrating the correspondence between the design model and practical applications are given in Chapter 2.4.5.

2.4.2 Methodology for prediction of a condition state

It is well-known from structural design that problems relating to assessment and design are basically resolved by contrasting the action *S* and the resistance *R*. The difference between actions and resistances is referred to as condition Z. A structural element is considered to have failed if the value of condition Z is less than zero. Actions and resistances are in fact uncertain quantities, not deterministic ones. They are therefore introduced into probabilistic calculations as random variables and compared in a limit state function *g(X)* (see Eq. (2.18)). The difference between action and resistance is then also a random variable.

$$g(X,t) = R(t) - S(t) = Z(t) \qquad (2.18)$$

This principle can also be applied to the verification of the service life carried out as part of durability design. By contrast to structural design, verification of the service life takes account of the random variables “action” and “resistance” as a function of time. The random variable “condition” is therefore shown as a function of the control variable “time”, see Fig. 2.6.

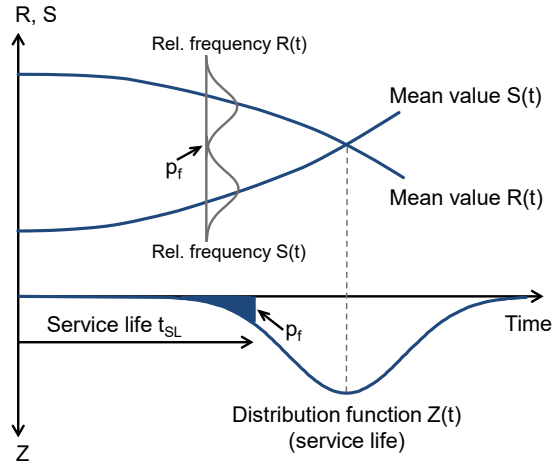

Fig. 2.6: Comparison of variable action and variable resistance and the definition of service life, based on fib bulletin 53:2009

The service life t_{SL} is defined in as the length of time during which the probability that the action will be greater than the resistance does not exceed a specified target probability (see Eq. (2.19)).

$$t_{SL} = t\left\{p_f\left(\left(R(t) - S(t)\right) < 0\right) < p_{f,Ziel}\right\} \qquad (2.19)$$

A convolution integral must be resolved when calculating the probability of failure, or probability of occurrence, p_f. The integral cannot generally be resolved analytically. Commercial software programmes (e.g. *STRUREL*) offer simulation and structural reliability analysis methods for this purpose, e.g. approximation methods such as FORM (First Order Reliability Method) and SORM (Second Order Reliability Method). It is also possible to substitute the reliability index β for the probability of occurrence p_f. The correlation between the probability of occurrence and the reliability index is as follows for normally distributed random variables (*Probabilistic Model Code 2001*):

$$p_f = \phi(-\beta) = \phi\left(-\frac{\mu_Z}{\sigma_Z}\right) \qquad (2.20)$$

bzw.

$$\beta = -\emptyset^{-1}(p_f) \qquad (2.21)$$

where $\phi()$ is the function of the standard normal distribution and μ_Z and σ_Z are the mean and standard deviations respectively of the random variable condition Z. The relationship is shown in the graph in Fig. 2.7.

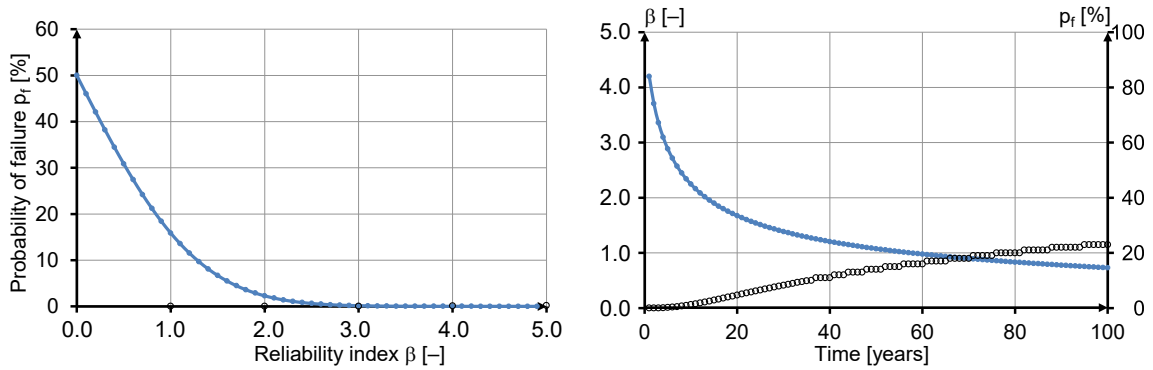

Fig. 2.7: Relationship between probability of failure p_f and reliability index β (left) and an example of p_f- and β-run over time (right)

The limit state for chloride-induced corrosion of the reinforcement is the point at which a critical chloride content is reached at the surface of the rebars (cf. Chapter 2.1). The limit state equation can be formulated as follows:

$$g(X,t) = C_{crit} - C(c,t_{SL}) \qquad (2.22)$$

where:

C_{crit}: is the critical corrosion-inducing chloride content [% by mass/b]
$C(c,t_{SL})$: is the chloride content at the surface of the rebars at time t_{SL} [% by mass/b]
c: is the concrete cover [m]
t_{SL}: is the service life [years]

The critical chloride content is an assumed threshold value that is governed by the thickness and quality of the concrete cover, amongst other things, and represents the resistance in the limit state equation. The chloride content at the surface of the rebars at time t represents the action. The limit state equation can also be described as follows:

$$g(X,t) = c - x_{crit}(t_{SL}) \qquad (2.23)$$

where:

$x_{crit}(t_{SL})$: is the depth of the critical chloride content at time t_{SL} [m]

The condition state is predicted by means of a reliability analysis with the aid of the limit state equation and by specifying a target reliability index β_0. For this purpose, each of the input parameters must be introduced into the limit state equation stochastically. Chapter 2.4.4 includes recommendations on which values can be selected for each model variable.

2.4.3 Target reliability

The target reliability is used to express the level of safety of the structure required for the condition under consideration. Distinctions in the target reliability are obtained by varying the target reliability index β_0. The relevant standards and literature (in particular *ISO 2394:1998*, *DIN EN 1990:2010*, *Probabilistic Model Code 2001*) recommend or specify values of β_0 that are differentiated primarily according to the ultimate and serviceability limit states. Owing to the comparatively severe and serious consequences of the ultimate limit state being exceeded, the target values for the ultimate limit state are higher than those for the serviceability limit state. The target values are generally stated for reference periods of one year and/or 50 years. The reference period is the period of time selected for the statistical evaluation of the variable components of the action (*DIN EN 1990:2010*). The target values for the reference period of one year are higher than those for the reference period of 50 years although both values result in the same safety level (*Holický 2011*). Thus, *DIN EN 1990:2010* specifies, for example, a design service life of 50 years for the structural element and a target reliability index of 4.7 and 3.8 for a reference period of one and fifty years respectively for the ultimate limit state (for reliability class RC 2 (medium consequences)).

Hitherto, reliability has mainly been considered and analysed in terms of the ultimate limit state and the mechanical loads to which structural elements are subjected. The same applies to the specification of target reliability indices. With regard to the serviceability limit state, a distinction is made primarily between reversible and irreversible consequences of the limit state being exceeded. The unintended conditions of structural elements dealt with under the durability aspect, including depassivation and initiation of corrosion of the rebars, are allocated to the serviceability limit state and generally have irreversible consequences.

In practice, reliability in relation to serviceability is frequently considered in the context of cost-benefit analyses (*Rackwitz 1999*, *Ang & Wyatt 1999*, *Hermann 1999*, *DuraCrete 2000*) as economic considerations dominate serviceability-related issues (*DAfStb Positionspapier 2008*).

DAfStb Positionspapier 2008 includes exposure-related information on the target reliability index for the unintended condition “initiation of the corrosion of the rebars”, i.e. for exposure classes XC1-4, XD1-3 and XS1-3. Depassivation of the reinforcement is not the only criterion; the possibility that corrosion of the reinforcement may be initiated after depassivation and the degree to which corrosion progresses are also taken into account. Thus, there is no safety requirement (no β_0) for exposure class XC1 (dry), for example, as the lack of moisture in the environment under this particular type of exposure means that there is a negligible risk of corrosion of the rebars being initiated and progressing after depassivation due to carbonation of the concrete. Consideration is also given to the

relationship between the effort involved in minimizing risk when producing a structural element and that involved in repairing it after the limit state has been exceeded.

Based on these points, *DAfStb Positionspapier 2008* states that it is preferable to use the target reliability index β_0 of 1.5 (p_f = 6.7 %) recommended in *DIN EN 1990:2010* for the serviceability limit state (with a medium level of irreversible consequences). Given that compliance with this target for exposure classes XD2, XD3, XS2 and XS3 may involve very thick concrete cover and can be very costly (*Gehlen et al. 2008*), a lower target value of β_0 = 0.5 (p_f = 30 %) is permitted for these particular exposure classes in certain cases provided that corrosion of the reinforcement can be detected at an early stage by regular monitoring and inspection and the structural element can be repaired. This is because the effort involved in repair measures at an early stage of rebar corrosion can be kept to a minimum.

Target values for the reliability index stated in the *DAfStb Positionspapier 2008* and in other codes and standards for a reference period of 50 years are given in Table 2.3. These values can be used for durability design with regard to chloride-induced corrosion of the reinforcement. The target values either relate to the serviceability limit state in general or to depassivation of the reinforcement or initiation of rebar corrosion in particular. The values of β_0 for conditions with a medium level of irreversible consequences for structural elements range from 0.5 to 1.5.

Table 2.3: Target reliability indices β_0 for a reference period of 50 years in different standards and guidelines which are used for service life design regarding chloride-induced corrosion

Document	Target reliability index β_0	Event / remark
ISO 2394:1998	0.0 1.5	Serviceability limit state; reversible: 0.0, irreversible: 1.5
DIN EN 1990:2010	1.5	Serviceability limit state, irreversible with medium consequences
fib bulletin 34:2006	1.3 (1.0 – 1.5)	Depassivation of the reinforcement
LNEC E 465:2007	2.0 1.5 1.2	Serviceability limit state, irreversible, depending on the consequences (high: 2.0, medium: 1.5, low: 1.2)
NEN 6700:2005	1.8	Initiation of corrosion of the reinforcement
NS-EN 206/NA 2014 *	1.3	Chloride-induced initiation of corrosion of the reinforcement
DAfStb Positionspapier 2008	0.5 1,5	Chloride-induced initiation of corrosion of the reinforcement; for XD2, XD3, XS2 and XS3 depending on the accessibility of the structural element for inspection and repair (easy access: 0.5, difficult access: 1.5); for XD1 and XS1 the value of 1.5 always applies.

* *Source: Fluge 2003*

The elaboration of semi-probabilistic and simplified design formats in this dissertation is based on the specifications in *DAfStb Positionspapier 2008*, in other words β_0= 1.5 and 0.5. The durability design of marine structures (structures in exposure classes XS1 to XS3) and a large proportion of road structures (structures in exposure classes XD1 to XD3) is generally based on a target reliability index $\beta_0$of 1.5 as a great deal of effort is generally associated with the inspection and repair of these types of structure.

2.4.4 Describing the model variables

2.4.4.1 Overview and remarks

The model variables and the relationships between them have been described in detail in numerous publications (e.g. *DuraCrete 1998*, *Gehlen 2000*, *fib bulletin 34:2006*). Based on *fib bulletin 76:2015,* the individual statistically quantified model variables used to develop further design formats (semi-probabilistic and nomograms) are briefly described in Chapters 2.4.4.2 to 2.4.4.10. Approach B has been used to determine the apparent chloride diffusion coefficient $D_{app}(t)$ as a wide range of relevant experience with this approach has already been gathered (see Chapter 2.3.2.2.3). An overview of the model variables and their statistical distributions is given in Table 2.4.

Table 2.4: Overview of the model variables

Variable			Unit	Distribution * and values	Quantification
$D_{app}(t)$	$D_{RCM}(t_0)$		m²/s	ND (μ / σ mit CoV = 0.20)	Chapter 2.4.4.2
	t_0		d	constant (28)	Chapter 2.4.4.3
	α_{RCM}		–	BetaD (μ / σ / 0 / 1)	Chapter 2.4.4.4
	k_e	b_e	K	ND (4800 / 700)	Chapter 2.4.4.5
		T_{ref}	K	konstant (293)	
		T_{real}	K	ND (μ / σ)	
$C_{S,0}$ / $C_{S,\Delta x}$			% by mass/b	LND (μ / σ)	Chapter 2.4.4.6
Δx			mm	BetaD (10 / 5 / 0 / 50) or constant (0)	Chapter 2.4.4.7
C_0			% by mass/b	constant (0)	Chapter 2.4.4.8
C_{crit}			% by mass/b	BetaD (0.60 / 0.15 / 0.2 / 2)	Chapter 2.4.4.9
c			mm	ND (μ / σ)	Chapter 2.4.4.10

* *A summary of the common types of distribution can be found in Faber 2007, for example.*

The model does not yet include a variable to take account of possible influences on the resistance of structural elements to chloride penetration arising from execution, curing and design. The model for durability design with regard to carbonation-induced corrosion of the reinforcement in *Gehlen 2000* and *Greve-Dierfeld 2015* includes a variable to take account of the influence of the duration of curing on the carbonation resistance of concrete. The characteristics of the surface zone of the concrete may have a significant influence on the durability of structural elements. The type of formwork and curing selected are particularly important for the development of the structure of the concrete in the surface zone. The extent to which the resistance of the concrete to chloride penetration is affected by curing and the type of formwork has hitherto been investigated insufficiently. This subject is dealt with in Annex C.3, based on the author's own investigations. In the case of structural elements in constant contact with a chloride solution (XS2, XD2), the method of curing is relatively unimportant as continuing hydration is ensured due to the steady supply of water (*Gehlen 2000*). In the design model, the surface zone of the concrete, with a mean value of 10 mm, can be safely neglected for exposure classes XS3 and XD3 in which intermittent action of moisture can lead to chlorides being drawn into the near-surface zone of the structural element due to capillary suction (see Chapters 2.3.2. and 2.4.4.7). Several studies have limited the influence of curing on the properties of hardened concrete to a zone with a depth of 10 mm at the surface of the structural element (for example *Jaegermann 1999*, *Huber 2008*). In the RCM test (*BAW-Merkblatt 2012* and *NT Build 492:1999*), the resistance of the concrete to the penetration of chloride is evaluated without taking the 10 mm surface zone into account while, in the diffusion test (*DIN EN 12390-11:2015*), the unsealed surface of the specimen is exposed to the chloride solution.

Model uncertainties, i.e. the differences between model calculations and actual measurements arising from model imperfections, can generally be treated as independent random variables in a model (*Probabilistic Model Code 2001*). They are quantified with the aid of studies and practical observations. For example, the model uncertainty was taken into account by the normally distributed variable λ in the probabilistic model for durability design with regard to chloride-induced corrosion of the reinforcement in *LNEC E 465:2007*. However, the variable λ is generally taken to have a mean value μ of 1.0 and a coefficient of variation CoV of 15 % as it cannot be verified owing to a lack of data (*Marques et al. 2012*). In this dissertation, the uncertainty in the probabilistic model is taken into account indirectly by the ageing exponent α_{RCM} verified by structural data instead of by a separate variable.

2.4.4.2 Chloride migration coefficient $D_{RCM}(t_0)$

The apparent chloride diffusion coefficient $D_{app}(t)$ is calculated with the chloride migration coefficient $D_{RCM}(t_0)$ at reference time t_0 and ageing exponent α_{RCM} to describe the material resistance to the penetration of chloride (Approach B for determining $D_{app}(t)$, see Chapter 2.3.2.2.3).

The chloride migration coefficient is determined by the RCM accelerated laboratory test (see Chapter 2.3.2.2.3) and expresses the resistance of the material to the migration of chloride ions in terms of the voltage applied. The RCM test has been shown to be a suitable test method for evaluating the resistance of concrete to the penetration of chlorides owing to its short duration, comparatively straightforward handling, low susceptibility to faults and adequate precision; it is therefore frequently used instead of the diffusion test. Both the chloride migration coefficient $D_{RCM}(t_0)$ and the chloride diffusion coefficient $D_{nss}(t_0)$ are mainly influenced by the diffusivity of the test specimen which is dependent on the pore structure, i.e. the overall porosity, pore size distribution and tortuosity. Binding of chloride ions by the binder has a significant effect on the chloride diffusion coefficient although its influence is mitigated to a large extent by the short duration of the RCM test (*Castellote 1997*, *Castellote et al. 1999, Andrade et al. 2000, Spiesz 2013*).

Numerous publications refer to a good correlation between D_{RCM} (in concrete at an early age of between 28 and 90 days) and D_{nss} (duration of exposure between 28 and 90 days) (*Frederikson et al. 1996*, *Andrade & Whiting 1996*, *Gehlen & Ludwig 1999*, *Gehlen 2000*, *Tang et al. 2010*). This applies to Portland cement concretes in particular. However, the author's own investigations have shown that parameters $D_{RCM}(t_0)$ and $D_{nss}(t_0)$ result in different evaluations of the resistance of concrete to the penetration of chloride (see Annex A).

The chloride migration coefficients $D_{RCM}(t_0=28d)$ determined for several concretes are shown in Fig. 2.8. It can be seen that $D_{RCM}(t_0=28d)$ is clearly dependent on the water/binder ratio and in particular, on the type of binder. The lowest (most favourable) values can be observed for blast-furnace cement concretes (CEM III/B, CEM III/A, CEM II/B-S) owing to their dense structure and good capacity to bind chlorides. By contrast, CEM I and CEM II/A-LL concretes have the highest (most unfavourable) values due to their high level of porosity and poor capacity to bind chlorides. Concretes containing fly ash (CEM II/A-V) harden at a slower rate (pozzolanic reaction) and have values similar to CEM I concretes. An increase in the water/binder ratio results in an increase in the chloride migration coefficient owing to the increase in the porosity of the concrete, although this effect is minimal in blast furnace cement concretes. A more comprehensive comparison of the chloride migration coefficients of various concretes with different water/cement ratios and different types of binder can be found in *Jacobs &*

Leemann 2007, for example. This particular publication also established that the type of binder has a significant influence on the chloride migration coefficient, followed by the water/cement ratio.

Other influences on the chloride migration coefficient related to concrete technology are regarded as insignificant. A possible influence of the cement content on the chloride migration coefficient of the concrete was investigated comprehensively in *Lay 2006* and shown to be negligible (provided a minimum cement content permits adequate compaction of the concrete). It was not possible to establish any systematic or significant influence of the type, shape or size of the aggregate either in *Lay 2006*. The issue of whether the addition of air-entraining admixtures to concrete to improve freeze- and freeze-thaw resistance influences the chloride migration coefficient has hitherto not been investigated extensively. Individual tests in *Lay 2006* have shown any influence to be insignificant.

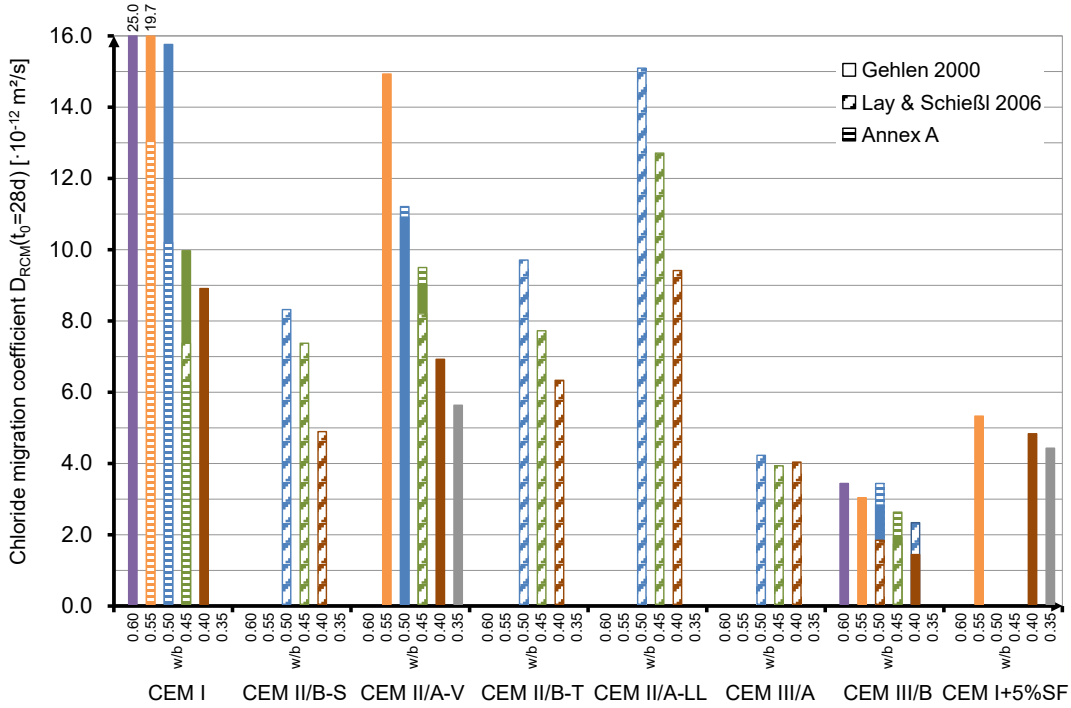

Fig. 2.8: Chloride migration coefficients of different concretes at the age of 28 days (tested according to BAW-Merkblatt 2012), dependency upon binder type and water/binder-ratio

A standardized method for the RCM laboratory test is not yet available. The differences between the test methods described in various codes, such as *NT Build 492:1999* and *BAW-Merkblatt 2012*, however small, lead to chloride migration coefficients of different magnitudes. The chloride migration coefficients determined according to *BAW-Merkblatt 2012* are generally lower (more favourable) than those determined according to *NT Build 492:1999* (e.g. *Gulikers 2011* and Annex C.1). In particular, this is because the high test voltages used in the method according to *NT Build 492:1999* cause an increase in the

temperature of the test specimens, speeding up the migration of ions (Joule effect) (*Andrade et al. 2000*, *Ghosh et al. 2011*). Furthermore, chloride binding during the test, which is shorter due to the higher test voltage used, is less likely to occur and is less intensive (*Andrade et al. 2000*). In contrast to *BAW-Merkblatt 2012*, *NT Build 492:1999* allows for a voltage of 2.0 V for polarization of the electrodes when calculating D_{RCM} which contributes minimally to the higher value of D_{RCM}. The differences between the RCM tests according to *BAW-Merkblatt 2012* and *NT Build 492:1999* are summarized in Annex C.1.

The test durations considered, which are selected depending on the initial amperage measured, apply to concretes with common binder contents, ensuring a penetration depth of at least 10 mm (and up to around 30 mm) in the test specimen. *NT Build 492:1999* permits an increase in the duration of the test in line with the binder content for materials with higher binder contents (e.g. PCC and SPCC) (see Annex A.3.3).

Several authors have questioned the precision of the chloride migration coefficient (e.g. *Spiesz & Brouwers 2012*, *Spiesz et al. 2012*) as it is determined assuming a linear chloride-binding isotherm and a linear relationship between the free and bound chloride ions although this is not the case, particularly because of the short test duration.

The scatter of the chloride migration coefficients in the test is expressed by a coefficient of variation CoV of 11 % for repeatability and 20 % for reproducibility in *BAW-Merkblatt 2012* (adopted from *Gehlen 2000*), the reproducibility being taken as the 90 % quantile of the repeatability. In *NT Build 492:1999*, the coefficient of variation CoV is 9 % for the repeatability whereas, for the reproducibility, it is taken to be 13 % for concretes with Portland cement or the admixture silica fume and 24 % for blast-furnace cement concretes.

The model variable $D_{RCM(t_0)}$ can be adequately described statistically according to *Gehlen 2000* by a normal distribution with a coefficient of variation of 20 %:

$D_{RCM(t_0)}$: ND (μ / σ with CoV = 0.20) [m²/s]

2.4.4.3 Reference time t_0

In the model, the reference time t_0 refers to the age of the test specimens at the beginning of the RCM test and is taken to be a constant variable in the design model:

t_0 = 28 [d] constant

2.4.4.4 Ageing exponent α_{RCM}

Together with the chloride migration coefficient at the reference time, this variable describes the resistance of the material to chloride penetration. The decrease in the

apparent chloride diffusion coefficient $D_{app}(t)$ is taken into account with the ageing exponent. It has hitherto not been possible to fully explain the decrease in $D_{app}(t)$ over time. The following effects may contribute to the decrease in the apparent chloride diffusion coefficient over the duration of exposure and to the general time dependency of this parameter (*DARTS 2004*):

- compaction of the structure of the concrete owing to the continuing hydration of the binder,
- blockage of the pores in the concrete by chloride ions,
- dependence of the chloride-binding capacity of the concrete on concentration and temperature,
- variations in the water saturation of the concrete over time and with depth (e.g. due to internal self-drying of the structural element).

Furthermore, blockage of the pores and compaction of the concrete structure owing to ion exchange (magnesium and calcium) between the surface of the structural element and the seawater were also established in several investigations (*Mohammed et al. 2002*, *Mohammed et al. 2002a*, *Maage & Helland 2009*). It has also been demonstrated that the decrease in the chloride diffusion coefficient over time in concrete test specimens stored in tap water is considerably lower than for comparable test specimens exposed to seawater (*Maage et al. 1999*).

Wiens 2005 states that the reason for the far greater decrease in the chloride diffusion coefficient (along with the chloride migration coefficient) over time is the "geometrical" and "ionogenic" blockage of the pores in concretes containing fly ash compared with Portland cement concretes. The pozzolanic reaction leads to the development of a specific pore structure with a pore cross-section that is both smaller and more variable. Thus, on the one hand, there are fewer (capillary) transport paths available for chloride ions while, on the other hand, the interaction between the chloride ions and the pore surfaces or the electric double layers slows down the process (*Wiens 2005*).

Although environmental conditions influence the development of the chloride diffusion coefficient over time, binders have characteristic ageing exponents. The methodology used in *Gehlen 2000* to determine the ageing exponents of concretes made with the three main types of binder, CEM I, CEM I + FA and CEM III/B, was described in Chapter 2.3.2.2.3 when presenting Approach (B) for determining the apparent chloride diffusion coefficient. The long-term behaviour of these concretes in terms of chloride penetration was considered using extensive structural data and by performing the RCM accelerated laboratory test to determine the resistance of laboratory concretes to chloride penetration. The ageing exponents determined for concretes with the three types of binder mentioned above are shown in Table 2.5. Ageing exponents for other types of cement and binder that,

according to *DIN 1045-2:2008*, may be used in situations with exposure to chlorides are based on values determined for the three types of binder mentioned above and other relevant available findings, see Table 2.5. α_{RCM} may be taken as 0.30 for conventional concretes with an unknown composition. An even lower α_{RCM} value of 0.20 is assumed for polymer-modified materials (PCC and SPCC, see Annex A).

In theory, the ageing exponent can be taken to be between 0 (no increase in the material resistance, i.e. $D_{app}(t)$ does not decrease over time) and 1 (full compaction of the structure of the concrete, no further chloride penetration being possible). *fib Model Code for Concrete Structures 2010* specifies values in the range of 0.20 to 0.80 as practical (mean) values of the ageing exponent, calculated from structural data and/or diffusion tests (i.e. α_{app} and α_{nss}, see Chapter 2.3.2.2).

Portland cement concretes (CEM I) and concretes containing powdered limestone (CEM II/A-L & LL) have the lowest ageing exponents owing to their relatively high porosity, very low degree of continuing hydration and very low chloride-binding capacity. Concretes with silica fume (CEM II/A-D) and a low proportion of blast furnace slag (CEM II/A-S) have relatively low ageing exponents owing to their low chloride-binding capacity. Higher ageing exponents are associated with concretes with a high proportion of blast furnace slag (CEM III/B & C). The most favourable ageing exponents can be assumed for concretes containing fly ash (CEM II/A & B-V) due to continuing hydration on account of the pozzolanic reaction and to the high chloride-binding capacity. There is very little relevant experience available for concretes containing pozzolans (CEM II/A & B-P & -Q) or burnt shale (CEM II/A & B-T); relatively favourable ageing exponents can be assumed for such concretes owing to their pronounced pozzolanic and hydraulic properties.

For binders comprising combinations of cement and an additive, the ageing exponent of the most closely related cement type can be selected from Table 2.5 (e.g. CEM I + 6 % silica fume → CEM II/A-D).

The ageing exponent was described statistically in *Gehlen 2000* by means of a beta-distribution. Both the mean value and standard deviation of the ageing exponent greatly influence service life designs based on the model. Results of sensitivity analyses show that the ageing exponent is the dominant variable in the model (see *Gehlen et al. 2011* and Fig. 2.11).

The chloride profiles used to determine the ageing exponent in *Gehlen 2000* were taken from structural elements under XS2- and XS3-type exposures. It is assumed that the ageing exponents determined are also valid for exposure classes XD2 and XD3. By contrast, a distinction is drawn between the ageing exponent for exposure classes XS1 and XD1 and

those for other exposure classes. In this case, the mean ageing exponent is taken as 0.65, irrespective of the type of binder (see Table 2.6), which is higher than the values determined and assumed for exposure classes XD2, XD3, XS2 and XS3 in Table 2.5. This is because the long-term behaviour of concrete is different under these types of exposure in which the concrete is not exposed directly to water containing chlorides but only to salty air or spray fog and is dry over long periods of time. The near-surface zone of the concrete will therefore rarely be water-saturated so that diffusion of chloride ions occurs only occasionally. The lower chloride penetration rate results in a pronounced reduction in the apparent chloride diffusion coefficient over time which is taken into account by a high ageing exponent.

Table 2.5: Ageing exponent α_{RCM} dependent on the cement type for exposure classes XD2, XD3, XS2 and XS3

Cement type according to DIN EN 197-1:2014		Ageing exponent α_{RCM} [–] BetaD (μ / σ) with a = 0.0 & b = 1.0
CEM I		0.30 / 0.12 [3]
CEM II	CEM II/A-S	0.35 / 0.16 [4]
	CEM II/B-S	0.37 / 0.17 [4]
	CEM II/A-D	0.40 / 0.16 [4]
	CEM II/A-P	0.40 / 0.16 [4]
	CEM II/B-P	0.40 / 0.16 [4]
	CEM II/A-Q	0.40 / 0.16 [4]
	CEM II/B-Q	0.40 / 0.16 [4]
	CEM II/A-V [1]	0.60 / 0.15 [3]
	CEM II/B-V	0.60 / 0.15 [4]
	CEM II/A-W	–
	CEM II/B-W	–
	CEM II/A-T	0.40 / 0.16 [4]
	CEM II/B-T	0.40 / 0.16 [4]
	CEM II/A-L	0.30 / 0.12 [4]
	CEM II/B-L	–
	CEM II/A-LL	0.30 / 0.12 [4]
	CEM II/B-LL	–
	CEM II/A-M	–
	CEM II/B-M	–
CEM III	CEM III/A	0.40 / 0.18 [4]
	CEM III/B	0.45 / 0.20 [3]
	CEM III/C	0.45 / 0.20 [4]
CEM IV	CEM IV/A	–
	CEM IV/B	–
CEM V	CEM V/A	–
	CEM V/B	–
CEM III/A + approx. 10% fly ash [2]		0.50 / 0.20 [4]

[1] *Fly ash content at least 18 % of the overall mass*

[2] *effective binder type; cannot be modelled for compositions with cement types according to DIN EN 197-1*

[3] *derived value based on investigations (Gehlen 2000)*

[4] *assumed value based on cement composition*

Table 2.6: Ageing exponent α_{RCM} dependent on the cement type for exposure classes XD1 and XS1 (according to Gehlen 2000)

Cement type according to DIN EN 197-1:2014	Ageing exponent α_{RCM} [–]
All cement types permitted for XD1 and XS1	BetaD (μ = 0.65 / σ = 0.12 / a = 0.0 / b = 1.0)

2.4.4.5 Variables to take account of the ambient temperature, k_e, b_e, T_{ref}, T_{real}

Fick's law of diffusion follows thermodynamic laws (*Einstein 1905*). Numerous authors (such as *Page et al. 1981*, *Nguyen et al. 2006*, *Carré 2008*, *Yuan et al. 2008*, *Dousti et al. 2013*) have confirmed that the chloride transport in concrete is dependent on temperature. An increase in the ambient temperature generally causes an increase in the rate of ion movement, leading to an increase in the chloride penetration rate in concrete. Higher temperatures may also lead to a reduction in the chloride-binding capacity of the concrete or a partial liberation of the bound chloride ions (*Benjamin & Sykes 1990*, *Hussain et al. 1995*), thus accelerating chloride penetration.

The environmental parameter k_e was introduced (see Chapter 2.3.2.2) to take account of the influence of the ambient temperature on the chloride penetration rate in concrete members when calculating the apparent chloride diffusion coefficient $D_{app}(t)$. The effect of temperature on the chloride transport in concrete can be allowed for by using the Arrhenius equation by way of simplification as shown below, in line with the temperature-dependent descriptions of the rate of corrosion and the electrolyte resistance of concrete:

$$k_e = exp\left(b_e \cdot \left(\frac{1}{T_{ref}} - \frac{1}{T_{real}}\right)\right) \qquad (2.24)$$

where:

b_e is the temperature coefficient [–]; regression parameter proportional to the activation energy of the material

T_{ref} is the reference temperature [K]

T_{real} is the surface temperature of the structural element or ambient temperature [K]

exp is the exponential function (e^x)

The variable T_{real} can be taken as the mean annual temperature of the ambient air recorded at the nearest weather station. It can be described precisely by a normal distribution:

T_{real}: ND (μ [K] / σ [°C])

A mean value of 10 °C (283 K) can be assumed for T_{real} in Germany, taking global warming into account. The standard deviation can be taken as 8 °C for XD-exposure classes (road structures) while a lower value of 5 °C can be assumed for XS-exposure classes (coastal structures) owing to the lower degree of scatter.

T_{ref} generally refers to the temperature in laboratory tests performed according to the RCM or diffusion test and is taken to be a constant 20 °C (293 K) for design purposes:

T_{ref} = 293 [K] (20 °C) constant

The functional relationship between the parameters k_e und T_{real} at a reference temperature T_{ref} of 20 °K in Portland cement paste samples was examined in *Page et al. 1981*, with a mean temperature coefficient b_e of 4800 K being determined (regression analysis). This value was then applied to concretes and other types of binder. However, the temperature only affects the chloride transport in the binder matrix so that concrete, by contrast to cement paste, generally has a lower activation energy and thus a lower temperature coefficient b_e, implying that the k_e-value for concrete is lower (*Dousti et al. 2013*). In addition, a lower activation energy for blast furnace cement concretes compared with Portland cement concretes was determined in *Dousti et al. 2013*, indicating that the chloride penetration rate in blast furnace cement concretes is less sensitive to temperature. *Maage et al. 1999* found that the temperature did not have any significantly adverse effect on the chloride penetration in blast-furnace cement concretes and concretes with silica fume (CEM I + SF and CEM III/B).

In this dissertation, the temperature coefficient b_e is quantified as follows, irrespective of the product (*Gehlen 2000*):

b_e: ND (μ = 4800 [K] / σ = 700 [K])

2.4.4.6 Surface chloride concentrations $C_{S,0}$ and $C_{S,\Delta x}$

In the model, the action is expressed by the model variables surface chloride concentration $C_{S,0}$ and equivalent surface chloride concentration $C_{S,\Delta x}$ (chloride concentration at depth Δx, see Chapter 2.3.2.1) (in addition to the ambient temperature). $C_{S,0}$ and $C_{S,\Delta x}$ are functions of both the material and the environment.

The material dependency of $C_{S,0}$ and $C_{S,\Delta x}$ is expressed by the chemical and physical chloride-binding capacity of the concrete, which is governed by the type of binder used, and the pore volume to be saturated with chloride ions, which is governed by the mix composition. The sum of the maximum quantity of bound and free chloride ions in the concrete, i.e. the maximum possible overall chloride content, can be taken as the magnitude of the action, i.e. $C_{S,0}$ or $C_{S,\Delta x}$. This is the basis for the development of an

analytical model for calculating the surface chloride concentration in *Tang 1996*. The model is based on two assumptions: 1) that there is an equilibrium between the concentration of chloride ions in the surrounding solution and the free chloride ions in the pore water in the near-surface zone of the concrete member and 2) the relationship between the free and bound chloride ions in the concrete follows a Freundlich adsorption isotherm (*Freundlich 1907*). Application of the model requires the chloride adsorption isotherm of the binder under consideration to be determined, a process which is time-consuming. The other parameters considered in the model are the binder content, capillary pore volume and degree of hydration as well as the chloride concentration of the surrounding solution and the ambient temperature. Calculating the surface chloride concentration with this model generally results in higher values for concretes made with fly ash or blast furnace cement than for Portland cement concretes as the former types of concrete have a higher chloride-binding capacity. However, the opposite result was obtained for surface chloride concentrations $C_{S,0}$ and $C_{S,\Delta x}$ derived from chloride profiles based on laboratory and structural investigations (cf. Annex C.2 and Annex B.2). This inconsistency can be explained on the one hand by the selected boundary conditions and assumptions used to determine the chloride adsorption isotherms which have little to do with actual practice (storing crushed or ground hardened cement paste in a specific quantity of solution with a defined chloride concentration and defining the free chloride content as the equilibrium concentration determined in the solution). On the other hand, the surface chloride concentration determined on laboratory specimens or concrete structures is a chloride content smeared over one or several millimetres, depending on the depth intervals selected for sampling purposes. Several structural investigations and field tests (e.g. *Bamforth 1999)* yielded higher surface chloride concentrations for concretes made with fly ash and blast-furnace cement than for Portland cement concretes. However, the chloride content in this case was considered in relation to the mass of concrete (% by mass/B). If the chloride contents are considered in relation to the mass of binder instead, the differences in the surface chloride concentration are very low to negligible owing to the higher binder contents of the composite concretes.

With regard to the environmental influences affecting the surface chloride concentration $C_{S,0}$ and $C_{S,\Delta x}$, exposure types XS and XD must be considered separately. The most important environmental parameter, which has a significant effect on the surface chloride concentration in both types of exposure, is the chloride concentration of the surrounding solution. The action of chlorides for XS-type exposure in Germany varies in magnitude depending on the salinity of the chloride source: North Sea water having a salinity of approx. 35 g/l, Baltic Sea water approx. 3-19 g/l and brackish water approx. 1-10 g/l.

Other parameters that may affect the surface chloride concentration in structural elements exposed to class XS conditions are, for example, wind speed and direction (*Fluge 1997*),

distance of the structural element from sea level (*Fluge 2003, Helland et al. 2010*), geometry and orientation of the structural element (*Wall 2007, Helland et al. 2010*) and temperature (*LNEC 465:2007*).

By contrast to seawater with its relatively constant chloride concentration, the chloride concentrations to which structural elements are exposed under class XD conditions exhibit a large degree of scatter. Seasonal variations, the differences in the quantity of de-icing agents used and the method of their application as well as greatly varying moisture gradients in the structural elements make it very difficult to quantify the action of chlorides in such cases.

The time dependency of the surface chloride concentrations $C_{S,0}$ and $C_{S,\Delta x}$ is caused by the influencing factors referred to above. In addition, the surface chloride concentration builds up over time after the start of exposure. For practical reasons, $C_{S,0}$ and $C_{S,\Delta x}$ are introduced into the model as time-independent variables. The time dependency of $C_{s,0}$ in Fick's law of diffusion is taken into consideration in several empirical (*Nilsson 2002*), analytical (*Mejlbro 1996*, *Frederiksen et al. 1997*) and numerical (*Boddy et al. 1999*) models, albeit with great limitations (*CHLORTEST 2005*).

LNEC 465:2007 describes an empirical approach to calculating the surface chloride concentration for marine structures in Portugal, taking into account the influencing factors water/cement ratio, exposure class (XS1, XS2 and XS3), vertical distance above sea level, horizontal distance from the coast and ambient temperature using predetermined factors.

To sum up, it is very difficult in practice to perform a material-specific and time-dependent calculation of the surface chloride concentration while taking other environmental and structural influences into account. However, meaningful values of $C_{S,0}$ and $C_{S,\Delta x}$ may be derived on the basis of data for existing structures exposed to similar conditions.

The surface chloride concentrations $C_{S,0}$ and $C_{S,\Delta x}$ can be described with sufficient accuracy by a log-normal distribution (*Gehlen 2000*). For structures exposed to class XD conditions, a relatively high coefficient of variation CoV of 75 % is recommended in *DARTS 2004* owing to the large variation in the frequency with which de-icing agents are used as well as the quantity used and type of application. A lower coefficient of variation, CoV = 25 %, is given for underwater structures (XS2). Scattering and spatial variations increase with the distance from sea level and the coast so that a coefficient of variation CoV of 45 % is assumed for exposure classes XS1 and XS3. Exposure-specific values of the surface chloride concentrations $C_{S,0}$ and $C_{S,\Delta x}$ based on experience are given in Table 2.7.

Table 2.7: Surface chloride content $C_{S,0}$ and $C_{S,\Delta x}$

Exposure class	$C_{S,0}$ and $C_{S,\Delta x}$ [% by mass/b] LND	
XD1	$0.5 \leq \mu \leq 1.5$	CoV = 0.75
XD2	$2.0 \leq \mu \leq 5.0$	
XD3	$2.0 \leq \mu \leq 5.0$	
XS1	$1.0 \leq \mu \leq 2.0$	CoV = 0.45
XS2	$2.0 \leq \mu \leq 5.0$	CoV = 0.25
XS3	$2.0 \leq \mu \leq 5.0$	CoV = 0.45

2.4.4.7 Depth of the convection zone Δx

During intermittent exposure to moisture, the water in the near-surface zone evaporates in the dry phase. If a structural element is exposed to chlorides at this point, capillary suction of the solution will cause the chlorides to be rapidly transported to a depth Δx where a steady-state chloride concentration is reached.

The depth Δx at which the capillary action causes rapid penetration of the chlorides, depending on the moisture content of the structural element, was quantified as follows in *Gehlen 2000* by analysing 127 chloride profiles that had been observed to deviate from Fick's law of diffusion: BetaD (μ = 8.9 mm / σ = 5.6 mm / a = 0 mm / b = 50 mm). Investigations in *Bakker & Roessink 1991* showed that weather-dependent variations in moisture are limited to a depth of approx. 15 mm below the surface of the structural element (*Gehlen 2000*). Diffusion-controlled chloride transport is assumed to occur from a depth of approx. 10 mm below the surface of the structural element in *Bamforth 1999*. Table 2.8 shows the values for the depth of the convection zone Δx used in this dissertation.

Table 2.8: Depth of convection zone Δx

Exposure class	Δx [mm]
XD1 / XS1	0
XD2 / XS2	
XD3 / XS3	BetaD (μ = 10 / σ = 5 / a = 0 / b = 50)

The boundary conditions (action) for exposure classes XD3 and XS3 in the modified chloride penetration model introduced in *Gehlen 2000*, in which the variable Δx is taken into account (Eq. (2.5)), are more severe than for other types of exposure. The surface chloride concentration thus shifts by Δx towards the interior of the structural element, resulting in a reduction in the calculated time to depassivation of the rebar surface. The increase in the severity of the actions for members under XS3- and XD3-type exposures due to the convection zone is in keeping with the desired levels of reliability for durability design with regard to chloride-induced corrosion of the reinforcement. This is because the boundary conditions in structural elements subject to intermittent moisture exposure are more favourable to the initiation of corrosion of depassivated reinforcement than in underwater structures (see Chapter 2.1). Thus the initiation of corrosion is taken into account in this case by the selected limit state "depassivation of the reinforcement".

It has not yet been definitely established whether the rate at which depassivation of the reinforcement occurs is higher under intermittent exposure than in situations where there is constant contact with the chloride solution.

2.4.4.8 Initial chloride content C_0

The initial chloride content depends on the chloride contents of the concrete constituents such as cement, additives, aggregates and water. According to *DIN EN 206:2014*, admixtures containing chlorides may not be used for reinforced and prestressed concrete. *DIN EN 206:2014* introduced two classes, Cl 0.40 and Cl 0.20, for reinforced concrete which specify the maximum permissible chloride content in (as yet unexposed) concrete as 0.40 % by mass/c and 0.20 % by mass/c respectively. The National Annexes to the standard allow higher chloride contents for blast-furnace cement concretes although a higher initial chloride content of 0.65 % by mass/c has hitherto only been allowed in *NF EN 206/CN:2014* (France) (*Helland 2015*). *NS-EN 206/NA:2014* (Norway) places stricter limitations on the initial chloride content of reinforced concrete exposed to the action of chlorides, specifying a value of $C_0 \leq 0.1$ % by mass/c. The initial chloride content of current conventional concrete mixes is generally considerably lower than 0.1 % by mass/b. However, higher initial chloride contents (in the internal, non-contaminated part of the structural elements) have been determined in older reinforced concrete structures (e.g. *Martin 1975*).

Chloride diffusion in concrete is driven by the different concentrations of chloride ions moving freely in the pore water. Depassivation and the initiation of corrosion of the reinforcement are also caused by free chloride ions. There are two questions that need to be addressed where the initial chloride content is higher:

- To what extent are the initial chlorides bound in the binder matrix and
- do the initial chlorides constitute a risk for depassivation and corrosion of the reinforcing steel; if so, to what extent and how is the critical chloride content influenced by the initial chloride content?

Numerous authors studied specimens made of a mix to which a defined amount of chlorides had been added in order to determine the chloride adsorption isotherms, critical chloride content and other parameters. The free chloride contents determined in the pore water in several studies are shown in Table 2.9. It can be seen that the chloride ions are not completely bound by the binder matrix, even when only a small amount of chloride was added.

In the context of the studies conducted to determine the critical chloride content, *Breit 2001* concluded that adding chlorides directly to test specimens may result in a reduction in the critical chloride content as the corrosion-inhibiting effect of the contact zone between the steel and concrete and the formation of a passive oxide layer are suppressed either partially or completely. Contrasting with this conclusion, several studies (e.g. *Rasheeduzzafar et al. 1992*) found that a greater proportion of the chlorides is bound by the binder matrix when they are added to the mix than when they penetrate into the hardened test specimen from outside.

For the purposes of this dissertation, it is assumed that, for contents lower than 0.1 % by mass/b, the initial chlorides contribute neither to the ingress of external chlorides into the concrete nor to depassivating the reinforcement and initiating corrosion of the rebars. The initial chloride content of the products was assumed to be negligible, i.e. $C_0 < 0.1$. The variable C_0 was taken to be a constant with a value of zero:

$C_0 := 0$ constant [% by mass/b]

Table 2.9: Free chloride content in pore water of specimens with chloride additions (NaCl) of less than 0.1% Cl^{-1} by mass of cement

Literature	Amount added Cl^{-1} * [% by mass/c]	Free chloride content in the pore water	Unit
Arya et al. 1990 Hardened Portland cement specimens	0.5	0.184	% by mass/c
Haque & Kayyali 1995 Four concrete mixes with different binders and w/c ratios	0.2	up to 0.021	
	0.4	up to 0.074	
	0.6	up to 0.072	
	0.8	up to 0.225	
Hussain et al. 1995 Hardened cement specimens, varying C_3A and sulfate contents and alkalinity	0.3	up to 2.5	g/l
	0.6	up to 10.6	
Tritthart 2002 Hardened cement specimens made with three different binders	0.4	up to approx. 5	g/l
	0.6	up to approx. 8	
	0.8	up to approx. 13	

* *from NaCl*

2.4.4.9 Critical chloride content C_{crit}

In accordance with the selected limit state (see Chapter 2.4.2), the critical chloride content is defined in the model as the overall chloride content which causes depassivation of the surface of the rebars and initiation of corrosion of the reinforcement (provided the other boundary conditions are satisfied). This criterion cannot be applied for practical reasons even though the Cl^-/OH^- ratio in the pore water and thus the pH value at the surface of the rebars form the basis for evaluating the initiation of corrosion of the rebars. Similarly, the free chloride content of the concrete cannot be used as a criterion for C_{crit} as it is difficult to determine with the methods currently used in practice. In addition, bound chloride ions may be mobilized under certain circumstances (e.g. carbonation of the concrete, available sulfate (*Neville 1995*, *Justnes 1996*) and a rise in temperature (*Hussain et al. 1995*)) and lead to depassivation of the surface of the rebars.

Numerous publications cited in this dissertation report on the numerous factors influencing C_{crit}, some of which have been intensely debated. According to those publications, C_{crit} may be influenced by the type of binder, mix composition and concrete quality (for example, *Schießl & Raupach 1990*), the steel/concrete contact zone (for example, *Glass & Reddy 2002*, *Harnisch & Raupach 2011*), the chemical composition and structure of the concrete and the surface of the steel (for example, *Angst & Elsener 2015*), the rest potential

of the steel (*Breit et al. 2011*) and environmental conditions (available moisture) (for example, *Schießl & Raupach 1990a*). Detailed evaluations of the literature in *Breit 2001* and *Angst et al. 2009* show that the critical chloride contents that have been determined vary, with ranges between 0.18 – 2.5 by mass/b and 0.02 – 3.08 % by mass/b. The wide range of values for C_{crit} determined in various studies can be attributed to the different definitions of the critical chloride content and the differences in the test and verification methods, assessment criteria, etc. (*Breit 2001*).

The influence of the type of binder on C_{crit} is evaluated in very different ways in the literature (*Alonso et al. 2012*). For example, the increase in C_{crit} due to the addition of fly ash observed in *Schießl & Breit 1996* contrasts with the findings of *Thomas 1996* and *Oh et al. 2003* in which the opposite was found to be the case. The binder influences the pH-value and the concrete/steel contact zone. Replacing Portland cement by additives inhibits the development of Portlandite in the concrete /steel contact zone, resulting in a possible reduction in C_{crit} (*Yonezawa et al. 1988*). It was concluded in *Breit 2001* that parameters related to concrete technology (type of binder, w/c ratio, cement content etc.) do not significantly affect C_{crit} when concrete specimens are subsequently exposed to a solution contaminated with chlorides and only influence the time to depassivation of the reinforcement. These findings are in line with those of *Hansson & Sørensen 1990*. However, the parameters will affect the critical chloride content of specimens to which chlorides have been added.

The critical chloride content was quantified as follows in *Gehlen 2000* by analysing the set of data (64 values) prepared in *Breit 1997* and considering boundary conditions of relevance to construction practice:

C_{crit}: BetaD ($\mu = 0.60$ / $\sigma = 0.15$ / $a = 0.20$ / $b = 2.00$) [% by mass/b]

The lower limiting value of 0.20 % by mass/b determined from the dataset and verified by *Breit 2001* and other authors was adopted in this case and the mean value of 0.48 % by mass/b determined from the dataset was increased to 0.60 % by mass/b to take account of practical aspects, in particular the thickness of the concrete cover.

Evaluation of the data from 14 corrosion sensors installed in a breakwater (Portland cement concrete) in northern Norway in *Markeset 2009* resulted in a critical chloride content with a log-normal distribution, a mean value of 0.77 % by mass/b and a standard deviation of 0.25 % by mass/b which correlates well with the values in *Gehlen 2000*.

DAfStb RiLi SIB 2001 specifies a threshold value of 0.5 % by mass/c for the critical chloride content and a designer must be consulted to assess which counter-measures are required if it is exceeded at the surface of the rebars. The value is referred to in *DAfStb Positionspapier 2015* as the “lower threshold” of the critical chloride content. The

quantification in *Gehlen 2000* referred to above was used for the purposes of this dissertation.

2.4.4.10 Concrete cover *c*

In addition to providing an adequate bond between concrete and reinforcement, the purpose of the concrete cover is to ensure the durability of the concrete member. The dimensions of the concrete cover *c* vary depending on the type of execution. The concrete cover is a geometrical variable which, in the case of large cover depths, is generally statistically quantified by a normal distribution. Negative value ranges are unavoidable in a normal distribution so that the statistical description of concrete covers with low mean values may lead to unrealistic assessments and designs. Small cover depths can be quantified by log-normal or beta distributions, for instance (*Gehlen 2000*).

In the majority of standards and directives, the concrete cover is characterized as follows by means of the three parameters nominal concrete cover c_{nom}, minimum concrete cover c_{min} and allowance for deviations of the concrete cover Δc:

$$c_{nom} = c_{min} + \Delta c \qquad (2.25)$$

With regard to durability, *EN 1992-1-1:2004* specifies the minimum concrete cover as a function of the exposure class and the structural class; S-classes S1 to S6). The structural class reflects the intended service life of the structural element. The German National Annex to the standard (*DIN EN 1992-1-1/NA:2013*) includes values for the exposure-dependent minimum concrete cover for structural class S3 with an intended service life of 50 years.

The nominal concrete cover c_{nom} is the mean value of this variable. The permitted tolerance for the concrete cover as executed is expressed by the allowance for deviation Δc, specified as 15 mm in *DIN EN 1992-1-1/NA:2013*. The minimum concrete cover is often taken to be the 5 % quantile of a normal distribution. The standard deviation of the concrete cover can thus be calculated using the following equation:

$$U_{0.05} = \mu + \sigma \cdot u_{0.05} \qquad (2.26)$$

$$\rightarrow \ \sigma = \frac{(U_{0.05} - \mu)}{u_{0,05}} \ \rightarrow \ \sigma = \frac{\Delta c_{dev}}{1.64} \qquad (2.27)$$

where:

$U_{0.05}$: is the value of the normally distributed quantity dividing the distribution range into 5 % and 95 % (in this case the minimum concrete cover c_{min}) [mm]

μ: is the mean value of the normally distributed quantity (in this case the nominal concrete cover c_{nom}) [mm]

σ: is the standard deviation of the normally distributed quantity [mm]

$u_{0.05}$: is the 5 % quantile of the normal distribution (= -1.64) [–]

The allowance for deviation Δc of 15 mm according to *DIN EN 1992-1-1/NA:2013* thus yields a standard deviation of around 9 mm; the value of Δc = 10 mm specified in *ZTV-W LB 215:2012* (the code dealing with the design of structural elements under XS-type exposure) results in a value of 6 mm for σ. The following is assumed for the geometrical variable concrete cover in the design model:

c: ND (μ / σ) [mm]

2.4.5 Validation of the model

2.4.5.1 Methodology

While the results of deterministic approaches can easily be checked against observations, there is no consistent and obvious methodology that enables the results of probabilistic models to be verified, for example, how to assess a model calculation yielding a probability of 13 % that depassivation of the rebar surface in structural elements will occur after 50 years' exposure.

The interpretation of "probability" is of crucial importance when dealing with probability-based approaches – from their development to their application and validation. Probability may be defined in many different ways (see *Schneider 2007*, for instance). It may represent the limit of the relative frequency with which an event occurs, for example. This is referred to as "frequentist probability" and requires numerous random experiments to be considered. This particular interpretation of probability is not relevant to structural design in which the variables of the probabilistic models are characterized statistically using only a limited number of verifications.

According to *Probabilistic Model Code 2001*, the interpretation of probability relevant for structural design is to be found in the Bayesian concept of probability. In this case, probability is ideally the best estimate of the frequency of events and serves as an aid to decision-making by expressing the degree of expectation or confidence that an event will occur, bearing the uncertainties in mind. In the aforementioned example, the result is an aid to deciding whether an action should be taken (e.g. repair measure) or, at the design

stage, an aid to selecting materials and geometries and deciding whether repair measures need to be planed.

According to the Bayesian interpretation, the probability resulting from the model calculation is not always realistic. When based on a large number of cases it can be taken to mean the average probability that an event will occur.

Unlike errors in a model or in the model validation process, the differences between the results obtained for a model and those obtained in practice depend on the information available at the time at which the prediction was computed. Bayes' theorem enables the a-priori probabilities calculated on the basis of the information available at an earlier date (design data) to be updated by taking account of new data and findings (a-posteriori probability).

Structural investigations enable the actions and resistances in the model to be determined more or less realistically and thus the uncertainties in the model to be reduced. The structural data is subject to scatter and uncertainty and is taken into account by statistical variables. Predictions are updated as follows using the calculation rules for conditional probabilities based on Bayes' theorem: (*Straub 2010*):

$$P\left(F/I\right) = \frac{P(F \cap I)}{P(I)} = \frac{1}{P(I)} \cdot P\left(I/F\right) \cdot P(F) \qquad (2.28)$$

where:

P(F/I): is the a-posteriori probability that a limit state will be exceeded, *F*; a-priori probability updated by information *I*

P(F): is the a-priori probability that a limit state will be exceeded, *F*; calculated on the basis of design data

P(I): is the probability that the information *I* from a structural inspection is true

P(I/F): is the likelihood of information *I*; probability that the information *I* is true when the limit state is exceeded, *F*

The information obtained from structural inspections is considered as a boundary condition $h_i(X)$ which is regarded as an equality constraint or an inequality constraint, depending on the investigation method:

$$\begin{cases} h_i(X) = 0 & Equality\ constraint \\ h_i(X) \leq 0 & Inequality\ constraint \end{cases} \qquad (2.29)$$

equation (2.28) is solved by calculating integrals over the boundaries of the defined limit state equation *g(X)* and boundary conditions $h_i(X)$:

$$P(F/I) = \frac{\int_{X\in\{g(X)<0 \cap h(X)\leq 0\}} f(X)dx}{\int_{X\in\{h(X)\leq 0\}} f(X)dx} \qquad (2.30)$$

The approximation methods used to analyse structural reliability, such as FORM and SORM, do not always provide a solution as equality constraints imply surface integrals, some of which cannot be calculated by these particular methods (*Straub 2011*). More precise, albeit very time-consuming calculation methods, such as importance sampling or subset simulation, are suitable in such cases (*Straub 2011*). The simpler methods Crude FORM or Crude Monte Carlo may also be used although the results obtained with these methods include uncertainties. As part of this dissertation (Chapter 2.4.5.2), the reliability analyses for updating the a-priori probabilities were performed using the *STRUREL* software package which used the Crude FORM method when the FORM and SORM methods failed. The individual linearization of the limit state equation occasionally leads to the results being roughly approximated (*Schall et al. 1988*).

Information on the actual concrete cover and chloride penetration can be used to update the a-priori probability if chloride-induced depassivation of the reinforcement has taken place. The concrete cover (representing the resistance) can be described with little effort, being measured on the structural element – mainly non-destructively using electromagnetic methods (*Maierhofer 2010*) – and described statistically. The interaction between action and resistance can be deduced by taking samples at different depths in the structure (drill powder samples or drill cores) and by drawing up chloride profiles. The chloride contents obtained at each inspection time are formulated as depth-dependent equality constraints in which the chloride content is taken into account as a statistical variable (usually with a log-normal distribution) owing to inaccuracies in the measurements and the measurement depth is assumed to be constant:

$$h_i(X) = C\left(x_{insp}, t_{insp}\right) - C_{S,0} \cdot erfc \frac{x_{insp}}{2 \cdot \sqrt{D_{app}\left(t_{insp}\right) \cdot t_{insp}}} \qquad (2.31)$$

2.4.5.2 Validating and updating the model prediction with structural data

Three examples are shown below in which known chloride profiles for various structural elements exposed to class XS conditions are used to

- check whether the chloride contents calculated using the model agree with the actual values measured on the structural element and
- update the reliability curves prediction on the basis of the design data.

Further examples can be found in *fib bulletin 76:2015* and *Rahimi et al. 2013*.

The prediction drawn up using design data in Example 2.1 indicates an unfavourable development of the reliability index over time. The chloride profiles determined for a 32-year-old structure at depths up to around 50 mm are lower than the mean value obtained in the model calculation. By contrast, some of the chloride contents measured at a depth of around 75 mm exceed the 95 % quantile of the model calculation. Updating the prediction leads to an even more unfavourable β-t curve for structural elements comprising Portland cement concrete (without additives) which does not do well under this type of exposure.

Example 2.2 shows chloride profiles for the structural element at two different times. The update for each time causes the reliability index to jump to a higher value. Entering the information from the chloride profiles in the shape of equality constraints greatly reduces the uncertainties in the model at the time of inspection and results in an increase in the value of β. After the update, the descending β-t curve is always steeper than in the first prediction (a-priori). The updates using the chloride profiles for 55-year-old structural elements and 70-year-old structural elements improve the β-t curve for the design service life of 120 years. Based on the results of the inspections, the structure was considered to be in good condition and there was no evidence of any chloride-induced corrosion of the reinforcement (*Reschke et al. 2014*).

The chloride profiles for a 28-year-old structure shown in Example 2.3 include high chloride values at the level of the reinforcement. The updated prediction indicates a more unfavourable development of the reliability index over time. Inspection of the structural element revealed severe corrosion of the reinforcement and the structural element was subsequently repaired (*Westendarp 1991*). As noted in Table ex. 2-3-2, the chloride content was determined by carrying out hot water extraction of the finely ground samples and then deducing the free chloride content. The results are therefore lower than the overall chloride content obtained by digesting finely ground samples with nitric acid.

Example 2.1: (from *fib bulletin 76:2015*)

Table ex. 2.1-1: Information on the structural element

Type and location of structural element	Bridge pier above the Baltic Sea in Denmark, XS3
Concrete composition	CEM I, w/c: 0.35 – 0.50
Age of structural element at time of inspection	32 years

Table ex. 2.1-2: Measured chloride contents at the inspection time of 32 years

Mean depth of measurements [mm]	No. of measurements [–]	Chloride content [% by mass/b]	
		μ	σ
7.5	17	1.39	0.66
22.5	17	0.83	0.39
45	17	0.59	0.24
75	17	0.36	0.20

Table ex. 2.1-3: Input values of the model variables

Variable	Unit	Type of distribution	μ	σ	a	b
$D_{RCM}(t_0)$	$\cdot 10^{-12}$ m²/s	ND	8.9	1.78	–	–
α_{RCM}	–	BetaD	0.30	0.12	0	1.0
t_0	year	constant	0.0767	–	–	–
t	year	constant	50	–	–	–
T_{ref}	K	constant	293	–	–	–
T_{real}	K	ND	281	5	–	–
b_e	K	ND	4800	700	–	–
$C_{S,\Delta x}$	% by mass/b	LogND	3.0	1.4	–	–
Δx	mm	BetaD	10	5	0	50
C_{crit}	% by mass/b	BetaD	0.60	0.15	0.2	2.0
C_0	% by mass/b	constant	0	–	–	–
c [1)]	mm	ND	45	3	–	–

[1)] *assumed concrete cover according to DS/EN 1992-1-1 DK NA:2011; c_{min} = 40 mm, Δc = 5 mm*

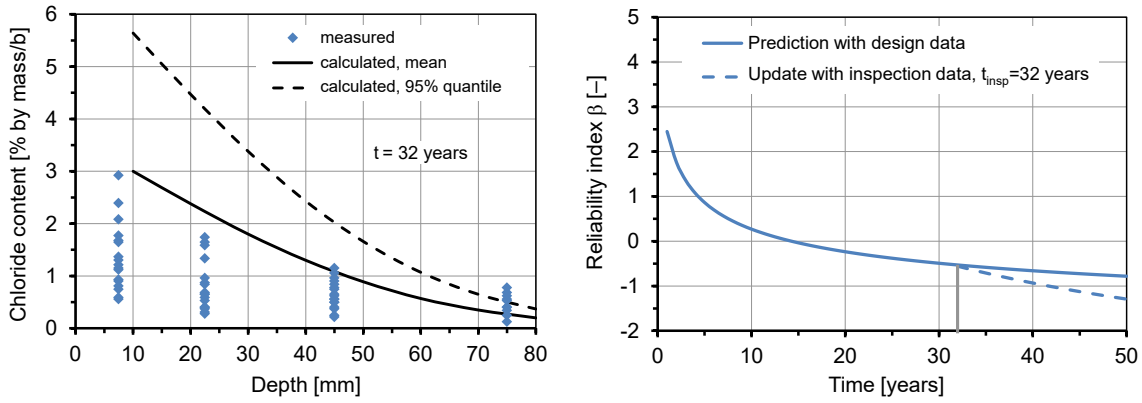

Fig. ex. 2.1-1: left: measured and calculated chloride content after 32 years' exposure; right: development of reliability index over time before and after updating

Example 2.2:

Table ex. 2.2-1: Information on the structural element

Type and location of structural element	Faces of a quay on the North Sea in Germany, XS3
Concrete composition	CEM III/A, w/c: 0.55 – 0.60
Age of structural element at time of inspection	55 and 70 years

Table ex. 2.2-2: Measured chloride contents at the inspection time of 55 years

Mean depth of measurements [mm]	No. of measurements [–]	Chloride content [% by mass/b]	
		μ	σ
10	3	2.02	0.46
30	3	1.25	0.33
50	3	0.18	0.12

Table ex. 2.2-3: Measured chloride contents at the inspection time of 70 years

Mean depth of measurements [mm]	No. of measurements [–]	Chloride content [% by mass/b]	
		μ	σ
10	2	2.30	0.28
30	2	1.31	0.41
50	2	0.46	0.38

Table ex. 2.2-4: Input values of the model variables

Variable	Unit	Type of distribution	μ	σ	a	b
$D_{RCM}(t_0)$	$\cdot 10^{-12}$ m²/s	ND	5.0	1.0	–	–
α_{RCM}	–	BetaD	0.40	0.18	0	1.0
t_0	year	constant	0.0767	–	–	–
t	year	constant	120	–	–	–
T_{ref}	K	constant	293	–	–	–
T_{real}	K	ND	283	5	–	–
b_e	K	ND	4800	700	–	–
$C_{S,\Delta x}$	% by mass/b	LogND	3.0	1.35	–	–
Δx	mm	BetaD	10	5	0	50
C_{crit}	% by mass/b	BetaD	0.60	0.15	0.2	2.0
C_0	% by mass/b	constant	0	–	–	–
c [1)]	mm	ND	60	6	–	–

[1)] *assumed concrete cover according to ZTV-W LB 215 :2012; c_{min} = 50 mm, Δc = 10 mm*

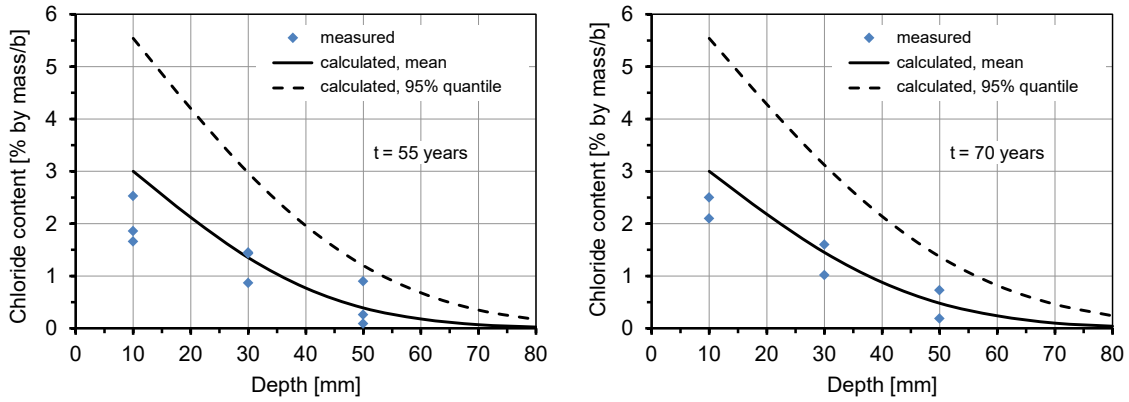

Fig. ex. 2.2-1: Measured and calculated chloride contents after 32 (left) and 70 (right) years' exposure

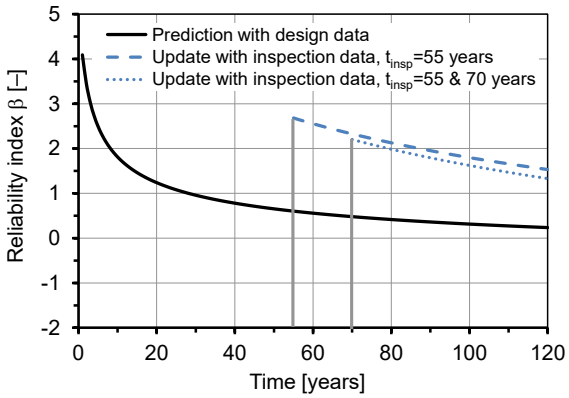

Fig. ex. 2.2-2: Development of reliability index before and after updating

Example 2.3:

Table ex. 2.3-1: Information on the structural element

Type and location of structural element	Soffit of a bridge slab on the Baltic Sea in Germany, XS3
Concrete composition	CEM III/A, w/c: 0.55 – 0.60
Age of structural element at time of inspection	28 years

Table ex. 2.3-2: Measured chloride contents at the inspection time of 28 years

Mean depth of measurements [mm]	No. of measurements [–]	Chloride content * [% by mass/b]	
		μ	σ
10	12	2.61	0.97
30	12	0.87	0.39
50	12	0.39	0.15
70	12	0.31	0.16

* *determined by hot water extraction*

Table ex. 2.3-3: Input values of the model variables

Variable	Unit	Type of distribution	μ	σ	a	b
$D_{RCM}(t_0)$	$\cdot 10^{-12}$ m²/s	ND	5.0	1.0	–	–
α_{RCM}	–	BetaD	0.40	0.18	0	1.0
t_0	year	constant	0.0767	–	–	–
t	year	constant	100	–	–	–
T_{ref}	K	constant	293	–	–	–
T_{real}	K	ND	283	5	–	–
b_e	K	ND	4800	700	–	–
$C_{S,\Delta x}$	% by mass/b	LogND	3.0	1.35	–	–
Δx	mm	BetaD	10	5	0	50
C_{crit}	% by mass/b	BetaD	0.60	0.15	0.2	2.0
C_0	% by mass/b	constant	0	–	–	–
c [1)]	mm	ND	60	6	–	–

[1)] *assumed concrete cover according to ZTV-W LB 215 :2012; c_{min} = 50 mm, Δc = 10 mm*

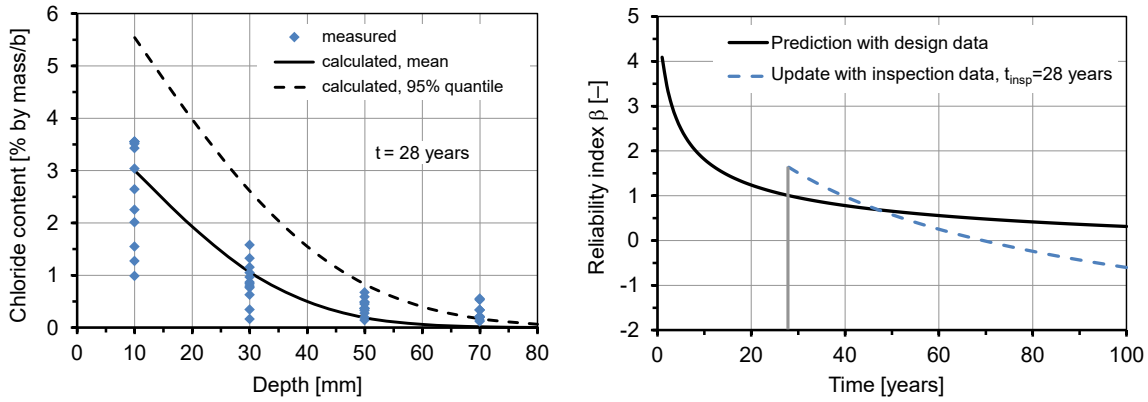

Fig. ex. 2.3-1: Left: measured and calculated chloride content after 28 years' exposure; right: development of reliability index over time before and after updating

Whenever structural data is used to validate and verify design models a question that needs to be addressed is to what extent such data is representative of the structure concerned and relevant for design purposes. Attention is drawn to the following points that need to be considered in connection with the reliability and significance of the chloride contents measured on structures:

Sampling: The sampling locations and procedure are of great importance. The chloride samples used to validate the model must be appropriate for the type of exposure, be taken at representative locations and must not include any singularities (such as cracks). Sampling is either performed by drilling cores which are then sawn into segments or by taking drill powder samples. In the latter case, care must be taken to prevent chlorides from the upper portion being transported into lower depths. Incorrect sampling and specification of sampling locations will yield chloride contents resulting in incorrect evaluations of the structural element and the model.

Sample preparation and analysis: Preparation and chemical analysis of the samples are dealt with in *DIN EN 14629:2007* although other codes, such as *DAfStb Heft 401:1989*, are also used. The codes differ with regard to the extraction method (hot / cold), fineness, homogenization and chemical test method (potentiometric / photometric), all of which affect the results obtained for the chloride content. A round robin test (*Hunkeler et al. 2000*) revealed significant differences in the results of the chloride analyses which were caused by the different methods of sample preparation and chemical analysis. Furthermore, water extraction is often used to obtain an approximation of the free chloride content (see example 2.3) although the design model considers the overall chloride content which has to be determined by acid digestion of ground samples.

Initial chloride content: The initial chloride content of the concrete is taken into account in the design model as a variable with a constant value. While the initial chloride content of current conventional concrete mixes is negligible, that of older reinforced concrete structures can be very high. The initial chloride content to be considered for design purposes must be determined on samples taken from the interior of unexposed structural concrete.

Interaction with other actions: Apart from chloride-induced corrosion of the reinforcement, reinforced concrete structures are also exposed to degradation mechanisms such as carbonation, alkali-silica reaction, scaling, internal damage and so on caused by environmental and mechanical actions. These damage mechanisms may interact with each other and also influence each other. This aspect must be taken into account when assessing the measured chloride contents.

Carbonation and chloride ingress may influence each other and the order in which the actions occur is significant. Carbonation-induced corrosion of the reinforcement is generally of minor significance for structural elements exposed to chlorides from the outset as the continuous exposure to moisture means that the depth of carbonation can be expected to be limited. However, the chlorides in the carbonation front are released from their chemical bond and are then available for the steel corrosion process once more. Where exposure to chlorides only starts at a later point in time, structural elements in

which carbonation has already occurred will react sensitively to any subsequent chloride action. Previous carbonation not only alters the pore structure of the concrete but also permanently affects its chloride-binding capacity. Chloride ions will penetrate more quickly into concrete that has undergone carbonation owing to its reduced chloride-binding capacity. In addition, changes in the pore structure will influence the transport process, depending on the type of binder used (*Wierig et al. 1995*, *Jung et al.2007*). During attack by frost/de-icing salt, chlorides penetrate into concrete more rapidly due to frost suction (micro ice lens pump) (*Jiang et al. 2011*, *Wittmann et al. 2006*). The effect of low temperatures followed by short thawing phases has been shown to be less significant. In addition, the "loosening" of the internal structure of concrete due to the action of frost makes it easier for chloride ions to penetrate into the concrete by capillary action. Mechanical loads also affect the internal structure of the concrete and the transport of water and therefore also influence chloride transport in concrete. (*Yan et al 2013*)

2.5 Semi-probabilistic durability design with partial factors

2.5.1 Basic principles

ISO 2394:1998, in general, and *ISO 16204:2012*, which deals with service life in particular, describe the basic principles of the design formats for structures. Semi-probabilistic formats for the durability design of reinforced concrete structures were described explicitly for the limit states carbonation-induced and chloride-induced corrosion of reinforcement in *Gehlen et al. 2011*.

The transport and damage models used in the semi-probabilistic format are the same as those employed in the fully probabilistic design format. The limit state equations (2.22) and (2.23) of the fully probabilistic format are modified as follows for durability design with regard to chloride-induced corrosion of the reinforcement:

$$g(X,t) = C_{crit,d} - C_d(c_d, t_{SL}) \qquad (2.32)$$

$$g(X,t) = c_d - x_{crit,d}(t_{SL}) \qquad (2.33)$$

where

$C_{crit,d}$: is the design value of the critical chloride content [% by mass/b]

$C_d(c_d, t_{SL})$: is the design chloride content at the depth of the minimum concrete cover at time t_{SL} [% by mass/b]

c_d: is the design concrete cover; corresponds to the minimum concrete cover [m]
$x_{crit}(t_{SL})$: is the design depth of the critical chloride content at time t_{SL} [m]
t_{SL}: is the service life [year]

In semi-probabilistic design formats, design values of the model variables are used instead of statistically distributed characteristic values. The design values are obtained by applying multiplicative or additive partial factors to characteristic values, e.g. mean values, of the variables. The partial factors take account of possible unfavourable deviations of the actual values of the actions, resistances and geometrical quantities from the characteristic values and the uncertainties in the model.

The partial factors are selected in such a way that compliance with the target reliability is always achieved if the limit state is exceeded within the design service life. For the purposes of the present concept, the partial factors are either based on fully probabilistic designs or on long-term experience with existing structures.

The partial factors may be taken into account as global factors in the action and/or resistance function or applied to individual or even all variables. The safety concept with global safety factors was used for structural design in *DIN 1045:1972*. It was superseded by the concept with partial factors introduced in the Eurocodes and *DIN 1045:2001*. The advantages of applying partial factors to several model variables as opposed to global safety factors are as follows (*Gehlen et al. 2011*):

- The variables affecting reliability in different ways in the design equation can be weighted using partial factors with different values, either by multiplication or addition, and
- the large number of partial factors enables the model variables to be modified specifically to suit the target reliability and thus achieve more economic designs.

However, the practicability of the design method is reduced if partial factors are considered for all model variables. The design variables, i.e. the model variables weighted with partial factors, therefore have to be limited to the most important variables taking account of the actions, resistances and geometry.

2.5.2 Differentiation of the exposure classes

In this dissertation, the partial factors are determined by fully probabilistic calculations performed for several relevant design situations. The design situations are simulated by varying the material resistance, i.e. the variables $D_{RCM(t_0)}$ and α, and the action, i.e. the variables $C_{S,\Delta x}$, Δx and T_{real}. The classification of actions according to the exposure classes specified in *DIN EN 206:2014* will be taken into account in the semi-probabilistic design format. Table 2.10 shows to what extent the model variables differ for individual exposure classes. Exposure classes XS1 and XD1 are not considered in the semi-probabilistic design format as structural elements in these classes can be designed with sufficient reliability by applying the descriptive rules (see Chapter 2.2 and *fib bulletin 76:2015*). It can be seen from Table 2.10 that the only differences between exposure classes XS and XD are the magnitude of the coefficient of variation for the surface chloride concentration and the standard deviation of the ambient temperature in the design model.

Table 2.10: Input values of the model variables dependent on exposure class (for Germany)

Exposure class	$C_{S,\Delta x}$ [% by mass/b] LgND		Δx [mm]	T_{real} [°C] ND	
				μ	σ
XS2	$2.0 \leq \mu \leq 5.0$	CoV = 0.25	0	10	5
XS3		CoV = 0.45	BetaD (10/5/0/50)		
XD2		CoV = 0.75	0		8
XD3			BetaD (10/5/0/50)		

The effect on durability design of the different values of the variables given above for the XS- and XD-exposure classes is illustrated in Fig. 2.9 in which three design cases are shown as examples. It can be seen that the β-t curves yield very similar results for exposure classes XS2 and XD2 as well as for exposure classes XS3 and XD3, particularly for a target reliability index of around 1.5 ($1.0 \leq \beta \leq 2.0$). The exposure-related differences are also moderate for a target reliability index β of 0.5. Exposure classes XD2 and XS2 and exposure classes XD3 and XS3 are therefore treated as equivalent for the purpose of drawing up a semi-probabilistic design format in this dissertation. This is also consistent with the descriptive approach of *DIN 1045-2:2008* in which the same minimum requirements are specified for exposure classes XS and XD (i.e. XS1 ≡ XD1, XS2 ≡ XD2, XS3 ≡ XD3).

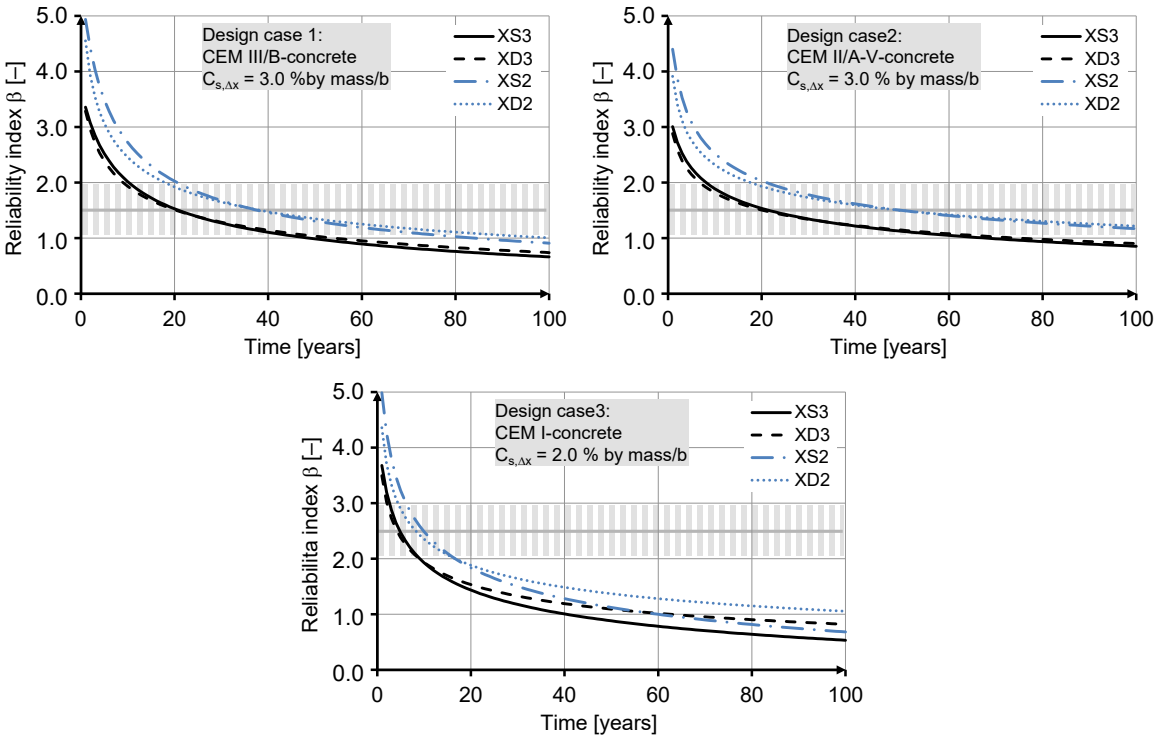

Fig. 2.9: Comparison of the exposure classes XS and XD; comparison of the service life reached for $\beta \sim 1.5$ in three different cases

2.5.3 Specification of the design variables and partial factors

As explained in the previous chapter, the partial factors are derived by evaluating fully probabilistic calculations for several design cases. These were based on four different material resistances covering a relatively wide range of materials, from favourable to unfavourable. Three surface chloride concentrations, 2.0, 3.0 and 4.0 % by mass/b, simulating actions ranging from mild to severe, were selected for the chloride attack. An extremely high surface chloride concentration of 5.0 % by mass/b was also considered for certain design cases. The target service life selected was mainly either 50 or 100 years although a value of 10 or 70 years was selected in certain design cases. The target service life of 10 years was considered as it is also intended for the same semi-probabilistic approach to be used to determine the remaining service life of existing structures before and after repairs involving the removal and replacement of damaged concrete (see Chapters 3 and 4). Exposure classes XS2 and XS3 were considered, taking account of the different magnitudes of the convection zone Δx and the coefficients of variation of the surface chloride concentration $C_{S,\Delta x}$. Exposure classes XD2 and XD3 are treated as equivalent to exposure classes XS2 and XS3 (see Chapter 2.5.2) and are not considered separately here. Table 2.11 shows the input values of the variables used in the fully probabilistic calculation of the design cases.

Table 2.11: Input values of the model variables for the calculation of the design cases in order to determine the partial factors

Variable	Unit	Type of distribution	Case [1)]	μ	σ	a	b
$D_{RCM}(t_0)$	$\cdot 10^{-12}$ m²/s	ND	Mat. 1	10.0	CoV=0.20	–	–
			Mat. 2	1.9			
			Mat. 3	9.0			
			Mat. 4	3.5			
α_{RCM}	–	BetaD	Mat. 1	0.30	0.12	0	1.0
			Mat. 2	0.45	0.20		
			Mat. 3	0.60	0.15		
			Mat. 4	0.50	0.20		
t_0	year	constant	all	0.0767	–	–	–
t	year	constant		50, 100 (10, 70) [2)]	–	–	–
T_{ref}	K	constant	all	293	–	–	–
T_{real}	K	ND	all	283	5	–	–
b_e	K	ND	all	4800	700	–	–
$C_{S,\Delta x}$	% by mass/b	LogND	XS2	2.0, 3.0, 4.0 (5.0) [3)]	CoV=0.25	–	–
			XS3		CoV=0.45		
Δx	mm	constant	XS2	0	–	–	–
		BetaD	XS3	10	5	0	50
C_{crit}	% by mass/b	BetaD	all	0.60	0.15	0.2	2.0
C_0	% by mass/b	constant	all	0	–	–	–
c	mm	ND		X	6 (Δc=10)	–	–

[1)] *Mat. 1: Material no. 1 simulates a chloride penetration resistance similar to CEM I concrete*
Mat. 2: Material no. 2 simulates a chloride penetration resistance similar to CEM III/B concrete
Mat. 3: Material no. 3 simulates a chloride penetration resistance similar to CEM II/A-V concrete
Mat. 4: Material no. 4 simulates a chloride penetration resistance similar to CEM III/A+FA concrete

[2)] *t = 10 and 70 years in certain design cases only*

[3)] *$C_{S,\Delta x}$ = 5.0 % by mass/b in certain design cases only*

X: the magnitude of the variable varies according to the design case

For reasons of practicability, the number of design variables, i.e. model variables whose characteristic values are modified by applying partial factors, was limited to four essential variables. Relevant variables of the material resistance (the chloride migration coefficient at the reference time $D_{RCM}(t_0)$ and the ageing exponent α_{RCM}), the action (surface chloride concentration $C_{S,\Delta x}$) and the geometry of the structural element (concrete cover *c*) were selected. In *Gehlen et al. 2011* and *Tamm 2014*, the three variables ageing exponent, surface chloride concentration and concrete cover were shown, in sensitivity analyses, to have a significant influence on the design results and were thus selected as design

variables. The authors' aim was to minimize the number of design variables while covering each of the three partial functions of the limit state equation, i.e. resistance, action and geometry. By including the fourth design variable, $D_{RCM(t_0)}$ it was possible, within the framework of this dissertation, to achieve a better adaptation of the designs to suit the target reliability. The mean values of the variables are taken as the characteristic values.

The magnitudes of the other model variables, to which no partial factors are applied (t_0, T_{ref}, T_{real}, b_e, Δx, C_{crit}, C_0), are generally the same for all design cases, or vary only slightly, and have little effect on the design result. t_0 and T_{ref} are set constant variables. T_{real} is generally taken to be around 10 °C for Germany. The variables b_e and Δx are not quantified for each case as this would be very time-consuming and they are each taken into account using the values given in Table 2.11. The variable C_{crit} has a considerable effect on the result of the design; its value is linked to the safety concept underlying the semi-probabilistic design format and variations are not permitted.

A process of trial and error was used to specify the values of the partial factors. It involved performing calculations with various values until a narrow reliability spectrum at the required level of reliability (i.e. $\beta \sim 1.5$ or $\beta \sim 0.5$) was achieved when the limit state was reached, taking all design cases into account. In doing so, the mean, i.e. nominal, concrete cover, which acted as a control variable, was modified so that the target reliability index for the relevant design case was achieved while the quantities of the remaining model variables stated in Table 2.11 were used. A certain deviation from the target reliability index, including towards lower values, was accepted when specifying the partial factors in order to limit the upper boundary of the reliability spectrum for economic reasons and to simplify construction practice. The partial factors determined in this way are as follows (see also Table 2.12):

γ_α: partial factor for the ageing exponent ($\alpha_{RCM,d} = \alpha_{RCM,k} / \gamma_\alpha$)

$\gamma_\alpha = 1.2$ for $\beta_0 = 1.5$

$\gamma_\alpha = 1.05$ for $\beta_0 = 0.5$

γ_D: partial factor for the chloride migration coefficient at the reference time ($D_{RCM,d}(t_0) = D_{RCM,k}(t_0) \cdot \gamma_D$)

$\gamma_D = 1.6$ for $\beta_0 = 1.5$

$\gamma_D = 1.0$ for $\beta_0 = 0.5$

γ_C: partial factor for the surface chloride concentration ($C_{S,\Delta x,d} = C_{S,\Delta x,k} \cdot \gamma_C$)

$\gamma_C = 1.9$ for $\beta_0 = 1.5$

$\gamma_C = 1.05$ for $\beta_0 = 0.5$

Δc: partial factor for the concrete cover; identical to the allowance for deviation of the concrete cover ($c_d = c_k - \Delta c \equiv c_{min} = c_{nom} - \Delta c$)

specified as $\Delta c = 10$ mm

The partial factors selected for structural design were also determined in such as way as to minimize the differences between the reliabilities achieved for individual design cases and the target reliability (*Sørensen et al. 1994*).

Table 2.12: Partial factors determined for the semi-probabilistic design format for exposure classes XS2, XS3, XD2 and XD3

Target reliability index β_0	Partial factors			
	γ_α	γ_D	γ_C	Δc
1.5 (p_f = 6.7 %)	1.2	1.6	1.9	10 mm
0.5 (p_f = 30.9 %)	1.05	1.0	1.05	10 mm

The same partial factors were obtained for exposure classes XS2 and XS3 when the calculations were evaluated.

The design cases considered when determining the partial factors are listed in Table 2.13 to Table 2.16. These include the nominal concrete cover required to achieve the target reliability index (β_0 =1.5 or 0.5), the nominal concrete cover calculated by applying the semi-probabilistic concept with the specified partial factors (Table 2.12) and the reliability index obtained for each design case.

Fig. 2.10 illustrates the safety level obtained by applying partial factors, with design case no. 16 from Table 2.13 being taken as an example.

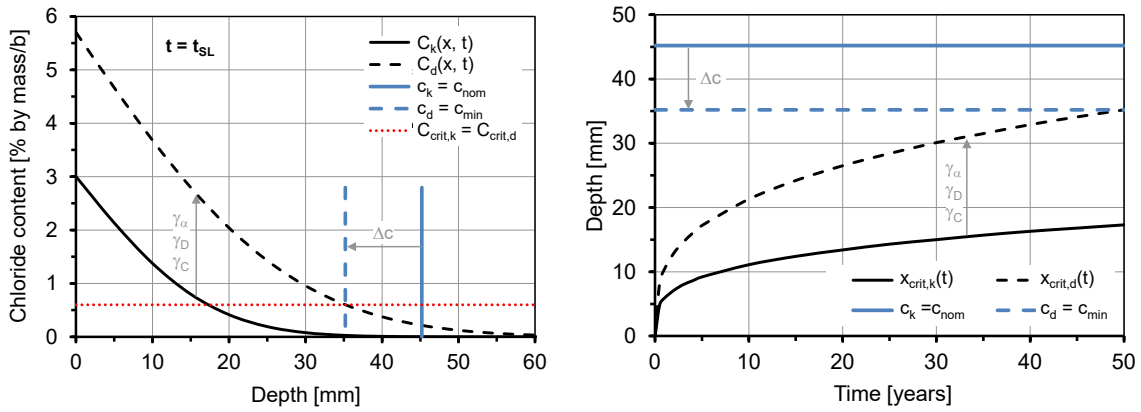

Fig. 2.10: Semi-probabilistic design format. impact of the partial factors on the calculated chloride contents (left) and on the calculated depth of the critical corrosion-inducing chloride content (right) in the example of design case no. 7 in Table 2.13; $C_k(x, t)$: characteristic run of the chloride content; $C_d(x, t)$: design run of the chloride content

The additive partial factor and the allowance for deviation for the concrete cover are taken to be equal. The factor was specified as 10 mm when determining the other three partial factors. The allowance for deviation takes account of unavoidable deviations due to bending and placing the reinforcement, different types of spacer and their installation,

erecting formwork and placing and compacting the concrete (*DBV-Merkblatt 2011*). *DIN 1045-2:2008* specifies an allowance for deviation of 15 mm for the concrete cover (Δc = 10 mm for XC1). This ensures compliance with the 5% quantile of the minimum concrete cover (see Chapter 2.4.4.10). The semi-probabilistic design format with the determined partial factors can also be used to calculate the layer thickness for repairs involving the removal and replacement of damaged concrete (see Chapter 4). The allowance for deviation in such cases is generally much lower than 15 mm owing to the comparatively small dimensions, the shallow installation depths and the absence of reinforcement. The magnitude of the allowance for deviation affects that of the other partial factors. Selecting a lower allowance for deviation generally results in more unfavourable (higher) values being determined for the other partial factors to ensure that the level of reliability is maintained (for the same minimum concrete cover). It can thus be concluded that a higher degree of reliability can be achieved by applying the semi-probabilistic design format with the specified partial factors and an allowance for deviation of the concrete cover greater than 10 mm, and vice versa. The differences in the resulting reliability indices are relatively small for allowances for deviation between 5 and 15 mm. By way of an example, reliability indices of 1.44 for Δc = 15 mm and 1.15 for Δc = 5 mm (instead of 1.31) for design case no. 20 in Table 2.13 as well as 1.61 for Δc = 15 mm and 1.37 for Δc = 5 mm (instead of 1.68) for design case no. 33 in Table 2.14 are obtained by applying the semi-probabilistic concept and an allowance for deviation of 15 mm and 5 mm (instead of 10 mm). Most national annexes to *EN 1992-1-1:2004* (with the exception of *BS 8500-1:2006* (Great Britain)) specify an allowance for deviation for the concrete cover of less than 15 mm. The author of this dissertation is not familiar with the underlying safety concepts in this case (e.g. c_{min} as a 5% quantile). *ZTV-W LB 215:2012* specifies an allowance for deviation of 10 mm.

It can be seen from the design cases (Table 2.13 to Table 2.16) that, as expected, the reliability index obtained by applying the semi-probabilistic design format decreases for each material as the surface chloride concentration and the target service life increase. The reliability indices obtained vary between 1.13 ($\equiv p_f$ = 12.9 %) and 2.06 ($\equiv p_f \sim$ 2 %) for β_0 = 1.5 ($\equiv p_f$ = 6.7 %) and between 0.32 ($\equiv p_f$ = 37.4 %) and 0.87 ($\equiv p_f \sim$ 19.2 %) for β_0 = 0.5 ($\equiv p_f$ = 30.9 %). The differences between the required and calculated nominal values of the concrete cover are shown in Table 2.13 to Table 2.16 for design cases in which the value obtained for β differs significantly from β_0, i.e. lies outside the ranges of $1.3 \leq \beta \leq 1.8$ for β_0 = 1.5 and $0.3 \leq \beta \leq 0.7$ for β_0 = 0.5 ($\equiv$ 3.5 % $\leq p_f \leq$ 9.7 % or 24.2 % $\leq p_f \leq$ 34.4 %). The reliability indices obtained differ according to the material.

For a target reliability β_0 of 1.5, the reliability indices achieved for materials no. 1 and no. 3 with the selected partial factors are higher than for materials no. 2 and 4. For material no. 1 (CEM I concrete), the concrete cover required and that calculated with the partial

factors are always very high so that, as expected, this particular material should not generally be used for exposure classes XS2 / XD2 / XS3 / XD3 for economic and practical reasons. β_0 exceeds 1.5 in many design cases with material no. 3 (CEM II/A-V-concrete), while it is lower than 1.5 in the majority of design cases with materials no. 2 (CEM III/B-concrete) and no.4 (CEM III/A+FA). This would result in uneconomical design for material no. 3 and design with a poor level of reliability in the case of materials no. 3 and no.4. However, the following can be seen if the input values of the ageing exponent (Table 2.11) are considered. The ageing exponent with a relatively low coefficient of variation of 25 % is used for material no. 3 whereas the CoV is 44 % and 40% for materials no. 2 and no.4 respectively. This means that, for materials no. 2 and no. 4, comparatively large uncertainties are taken into account in the fully probabilistic approach, resulting in a more conservative design (e.g. higher values of the concrete cover) for these materials. The uncertainties associated with the ageing exponent are of minor significance in the semi-probabilistic design format owing to the partial factors selected. The model variable with the greatest influence on the design results is the ageing exponent which also takes the uncertainties in the model into account (see Chapter 2.4.4.1), The sensitivity analysis for design case no. 34 in Table 2.14 illustrates the dominating impact of this particular variable (see Fig. 2.11).

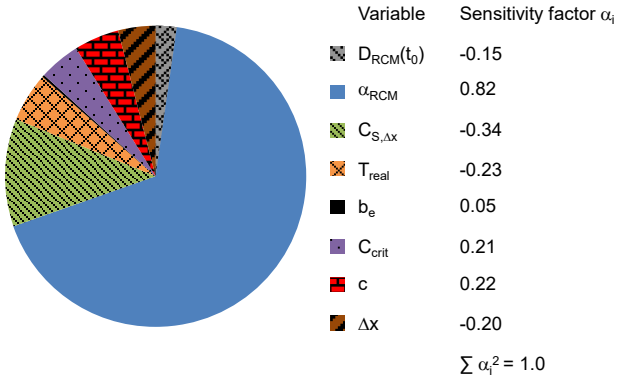

Fig. 2.11: Sensitivity analysis in the example of design case no. 34 in table 2.14; dominating impact of the variable ageing exponent α_{RCM}

The design chloride content at the level of the reinforcement is calculated as follows in the semi-probabilistic design format:

$$C(c_{min},t) = C_{0,k} + \left(C_{S,\Delta x,k} \cdot \gamma_C - C_{0,k}\right) \cdot erfc \frac{c_{min} - \Delta x_k}{2 \cdot \sqrt{k_{e,k} \cdot D_{RCM,k}(t_0) \cdot \gamma_D \cdot \left(\frac{t_0}{t_{SL}}\right)^{\frac{\alpha_{RCM,k}}{\gamma_\alpha}} \cdot t_{SL}}} \quad (2.34)$$

The mean values of the variables are taken as the characteristic values.

If the apparent chloride diffusion coefficient $D_{app}(t)$ is determined by one of the other approaches, i.e. Approach A or C (see Chapter 2.3.2.2), the mean values of the variables $D_{nss}(t_0)$ and α_{nss} or $D_{nss}(t_0)$ and α_{app} can be used as characteristic values in the design. The partial factors used for Approaches A and C are the same as those specified for Approach B.

Table 2.13: Design cases considered to determine the partial factors for β_0 =1.5

Case no.	Material see Table 2.11	XS2/ XS3	$C_{S,\Delta x}$ [% by mass/b]	t [years]	c_{nom} [mm] required for β_0 =1.5		c_{nom} [mm] calculated using factors	β [–] obtained using factors
1	Mat. 1	XS2	2.0	50	101.3	+14.4	115.7	1.85
2			3.0		121.7		131.2	1.70
3			4.0		135.5		141.5	1.62
4		XS3	2.0		113.0		125.7	1.78
5			3.0		132.5		141.2	1.67
6			4.0		1145.5		151.5	1.61
7		XS2	2.0	100	134.8		147.0	1.71
8			3.0		162.6		167.1	1.57
9			4.0		181.1		180.5	1.49
10		XS3	2.0		146.4		157.0	1.66
11			3.0		173.0		177.2	1.56
12			4.0		191.0		191.0	1.50
13			2.0	70	128.0		139.9	1.72
14			2.0	10	65.3	+12.5	77.8	2.06
15	Mat. 2	XS2	2.0	50	39.9		40.7	1.54
16			3.0		48.1		45.2	1.38
17			4.0		53.6		48.2	1.31
18		XS3	2.0		50.5		50.7	1.51
19			3.0		58.5		55.2	1.38
20			4.0		63.6		58.2	1.31
21			5.0		67.6	-7.1	60.5	1.26
22		XS2	2.0	100	52.2		48.2	1.37
23			3.0		63.4	-9.6	53.8	1.23
24			4.0		70.8	-13.3	57.5	1.16
25		XS3	2.0		62.3		58.2	1.37
26			3.0		73.0	-9.2	63.8	1.25
27			4.0		80.3	-12.8	67.5	1.18
28			5.0		85.7	-15.5	70.2	1.13
29			4.0	70	71.1	-8.6	62.5	1.24
30			2.0	10	35.0		38.6	1.80

Table 2.14: Design cases considered to determine the partial factors for β_0=1.5 (Table 2.13 continued)

Case no.	Material see Table 2.11	XS2/ XS3	$C_{S,\Delta x}$ [% by mass/b]	t [years]	c_{nom} [mm] required for β_0 =1.5		c_{nom} [mm] calculated using factors	β [–] obtained using factors
31	Mat. 3	XS2	2.0	50	44.4	+10.2 →	54.6	1.88
32			3.0		53.5		61.2	1.75
33			4.0		59.6		65.5	1.68
34		XS3	2.0		55.2	+9.4 →	64.6	1.83
35			3.0		64.0		71.2	1.73
36			4.0		69.7		75.5	1.67
37		XS2	2.0	100	54.3		63.1	1.75
38			3.0		65.8		70.9	1.63
39			4.0		73.4		76.0	1.56
40		XS3	2.0		64.6		73.0	1.73
41			3.0		75.7		80.9	1.63
42			4.0		83.0		86.0	1.57
43			5.0		88.6		89.8	1.53
44			4.0	70	75.8		80.3	1.62
45			2.0	10	41.0	+8.9 →	49.9	2.08
46	Mat. 4	XS2	2.0	50	46.7		46.4	1.49
47			3.0		56.6		51.8	1.35
48			4.0		63.1	-7.8 →	55.3	1.28
49		XS3	2.0		57.0		56.4	1.48
50			3.0		66.5		61.8	1.45
51			4.0		73.0	-7.7 →	65.3	1.29
52			5.0		77.6	-9.6 →	68.0	1.25
53		XS2	2.0	100	60.6		54.6	1.35
54			3.0		73.8	-12.6 →	61.2	1.22
55			4.0		82.5	-17.0 →	65.5	1.15
56		XS3	2.0		70.4		64.6	1.36
57			3.0		83.1	-11.9 →	71.2	1.24
58			4.0		91.7	-16.2 →	75.5	1.17
59		XS3	2.0	70	63.0		60.2	1.42
60			3.0		74.0		66.1	1.30
61			4.0		81.3	-11.3 →	70.0	1.23
62			2.0	10	38.6		42.8	1.79

Table 2.15: Design cases considered to determine the partial factors for β_0 =0.5

Case no.	Material see Table 2.11	XS2/ XS3	$C_{S,\Delta x}$ [% by mass/b]	t [years]	c_{nom} [mm] required for β_0 =0.5	c_{nom} [mm] calculated using factors	β [–] obtained using factors
1	Mat. 1	XS2	2.0	50	65.6	66.3	0.52
2			3.0		81.0	74.0	0.44
3			4.0		91.0	87.2	0.40
4		XS3	2.0		73.7	76.3	0.58
5			3.0		89.0	89.0	0.50
6			4.0		99.0	97.4	0.46
7		XS2	2.0	100	85.1	82.1	0.43
8			3.0		105.3	-6.9 → 98.4	0.36
9			4.0		118.4	-9.5 → 108.9	0.32
10		XS3	2.0		92.1	92.1	0.5
11			3.0		112.3	108.4	0.42
12			4.0		125.5	-6.6 → 118.9	0.38
13	Mat. 2	XS2	2.0	50	21.2	+4.2 → 25.4	0.76
14			3.0		25.9	28.9	0.66
15			4.0		28.9	31.2	0.61
16		XS3	2.0		30.9	+4.5 → 35.4	0.77
17			3.0		35.6	38.9	0.67
18			4.0		38.7	41.2	0.62
19		XS2	2.0	100	26.2	28.9	0.63
20			3.0		32.2	33.1	0.54
21			4.0		35.9	35.9	0.50
22		XS3	2.0		35.4	38.9	0.66
23			3.0		41.5	43.1	0.57
24			4.0		45.4	45.9	0.52
25	Mat. 3	XS2	2.0	50	25.0	+6.1 → 31.1	0.87
26			3.0		30.5	+5.4 → 35.9	0.78
27			4.0		34.1	+4.9 → 39.0	0.74
28		XS3	2.0		34.9	+6.2 → 41.1	0.86
29			3.0		40.3	+5.7 → 46.0	0.79
30			4.0		43.9	+5.1 → 49.0	0.74

Table 2.16: Design cases considered to determine the partial factors for β_0 =0.5 Table 2.15 continued)

Case no.	Material see Table 2.11	XS2/ XS3	$C_{S,\Delta x}$ [% by mass/b]	t [years]	c_{nom} [mm] required for β_0 =0.5		c_{nom} [mm] calculated using factors	β [–] obtained using factors
31	Mat. 4	XS2	2.0	100	29.0	+5.6 →	34.6	0.78
32			3.0		35.6		40.1	0.69
33			4.0		39.8		43.7	0.65
34		XS3	2.0		38.5	+6.1 →	44.6	0.79
35			3.0		45.1	+5.0 →	50.1	0.71
36			4.0		49.3		53.7	0.67
37		XS2	2.0	50	23.9	+4.1 →	28.0	0.72
38			3.0		29.3		32.0	0.62
39			4.0		32.8		34.6	0.58
40		XS3	2.0		33.5	+4.5 →	38.0	0.74
41			3.0		38.9		42.0	0.64
42			4.0		42.4		44.7	0.60
43		XS2	2.0	100	29.0		31.6	0.61
44			3.0		35.8		36.4	0.52
45			4.0		40.1		39.6	0.48
46		XS3	2.0		38.2		41.6	0.64
47			3.0		45.0		46.4	0.55
48			4.0		49.4		49.6	0.51

2.6 Simplified design format for durability design using nomograms

By contrast to the fully probabilistic design format, which requires specialist knowledge and specialized numerical software, the semi-probabilistic design format provides designers with an easy-to-use tool for durability design. Design nomograms may be developed on the basis of the semi-probabilistic format to avoid having to deal with equations and to simplify the design process even further.

The functional correlation between the weighted model variables from the semi-probabilistic format is represented graphically in the format using nomograms which takes only a very limited number of model variables into account (cf. Fig. 1.1).

Nomograms are generally graphical aids enabling complex equations with several unknowns to be solved. Well-known examples in structural design are, for example, nomograms for reduction factors for flexural buckling and torsional flexural buckling in the design of steel structures or tables for determining the creep factor in reinforced concrete structures.

The design nomograms that have been developed are shown in Fig. D.1 to Fig. D.19 in Annex D. They were prepared by splitting the mathematical equation for calculating the design chloride content at the level of the reinforcement (Eq. (2.34))) into several partial functions (Eq. (2.35) to (2.38)) so that each partial function contains one of the variables taken into account in the nomogram and the initial equation is obtained again when these partial functions are multiplied. To obtain the limit state equation, the critical chloride content C_{crit} was taken as the chloride content at the level of the reinforcement and the target service life t_{SL} as the time.

$$c_{min} - \Delta x_k = f\left(C_{S,\Delta x}\right) \cdot f\left(D_{RCM}(t_0)\right) \cdot f(\alpha_{RCM}, t_{SL}) \tag{2.35}$$

$$f\left(C_{S,\Delta x}\right) = 2 \cdot erfc\left(\frac{C_{crit,k}}{C_{S,\Delta x,k} \cdot \gamma_C}\right) \tag{2.36}$$

$$f\left(D_{RCM}(t_0)\right) = \sqrt{D_{RCM}(t_0) \cdot \gamma_D} \tag{2.37}$$

$$f(\alpha_{RCM}, t_{SL}) = \sqrt{k_{e,k} \cdot \left(\frac{t_0}{t_{SL}}\right)^{\frac{\alpha_{RCM,k}}{\gamma_\alpha}} \cdot t_{SL}} \tag{2.38}$$

Ideally, all four design variables – the chloride migration coefficient at the reference time $D_{RCM}(t_0)$, the ageing exponent α_{RCM}, the surface chloride concentration $C_{S,\Delta x}$ and the concrete cover c as well as the target service life t_{SL} – should be taken into account separately in the nomogram, cf. Fig. 2.12. However, the model variables ageing exponent α_{RCM} and target service life t_{SL} cannot be inserted into two partial functions that are independent of each other. For this reason, each nomogram was established for a particular (constant) target service life so that the lower quadrant in Fig. 2.12 was no longer needed. In order to minimize the number of nomograms, only the target service lives of 10, 20, 30, 40, 50, 70 and 100 years were considered. Where necessary, the nomograms have been split into two separate diagrams to enhance their resolution, with the values of $D_{RCM}(t_0)$ ranging from 0 to 2 m²/s and 2 to 20 m²/s respectively.

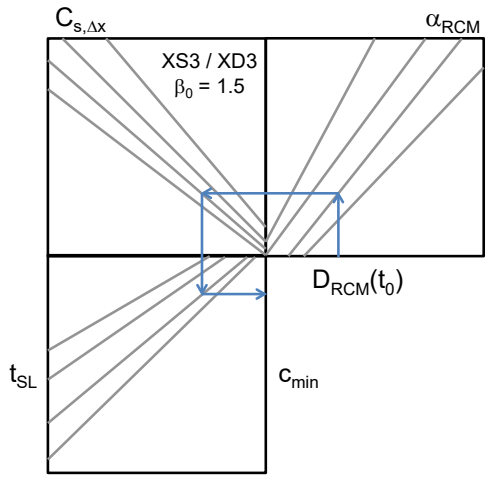

Fig. 2.12: Ideal format of the design nomogram considering each of the design variables and the target service life

In this case, the input variable is the chloride migration coefficient at the reference time $D_{RCM}(t_0)$. The other variables are taken into account by sets of lines in each quadrant. Each line in a set represents a specific value relating to the characteristic value of an (unfactored) variable. The partial factors γ_α, γ_D and γ_C are taken into account by the slope of the lines. The minimum concrete cover, i.e. the design concrete cover, required for a particular target service life to achieve the target reliability (β_0 = 0.5 or 1.5) can then be read from the diagram. It goes without saying that the nomogram is also reversible so that the chloride migration coefficient required at reference time $D_{RCM}(t_0)$ can be determined for a specific minimum concrete cover.

As in the semi-probabilistic design format, the design format using the nomograms can also be used to determine the apparent chloride diffusion coefficient in accordance with Approaches A and C (see Chapter 2.3.2.2). The corresponding characteristic values of the variables $D_{nss}(t_0)$ and α_{nss} or $D_{nss}(t_0)$ and α_{app} are taken into account in the nomograms.

The same nomograms are also used to determine the remaining service life of existing structures (Chapter 3) and the layer thicknesses for repair measures involving the removal

and replacement of damaged concrete (Chapter 4). The nomograms therefore include additional variables ($d_{E,min}$ and $D_{app}(t_0)$) which are defined in Chapters 3 and 4.

The nomograms have been established for exposure classes XS3 / XD3. They can also be used for structural elements in exposure classes XS2 / XD2 if the minimum concrete cover is reduced by 10 mm (assumed mean depth of the convection zone) when used as the output parameter (result of the design) or increased by 10 mm when used as the input parameter (e.g. to determine the required value of $D_{RCM}(t_0)$).

For reasons relating to design and execution, the minimum and maximum values of the concrete cover were taken as 20 mm and 80 mm respectively.

The conditions for using the design nomograms are described in Annex D.

By way of an example, the nomograms are used to design a concrete made with a CEM III/B cement for placement in the submerged zone (XS2) of a quay wall on the North Sea coast (assumed value of $C_{S,\Delta x}$ = 4.0 % by mass/b) with a minimum concrete cover of 50 mm, a target service life of 70 years and a target reliability β_0 of 1.5. Selecting an ageing exponent α_{RCM} of 0.45 (Table 2.5) and applying the nomogram in Fig. D.4 in Annex D, the concrete must be shown to have a value of $D_{RCM}(t_0=28d)$ with a mean value of not more than approx. $2.65 \cdot 10^{-12}$ m²/s (see Fig. 2.13). It must be noted that the minimum concrete cover (the input value) must be taken as 60 mm (XS2) for the nomogram in Fig. D.4.

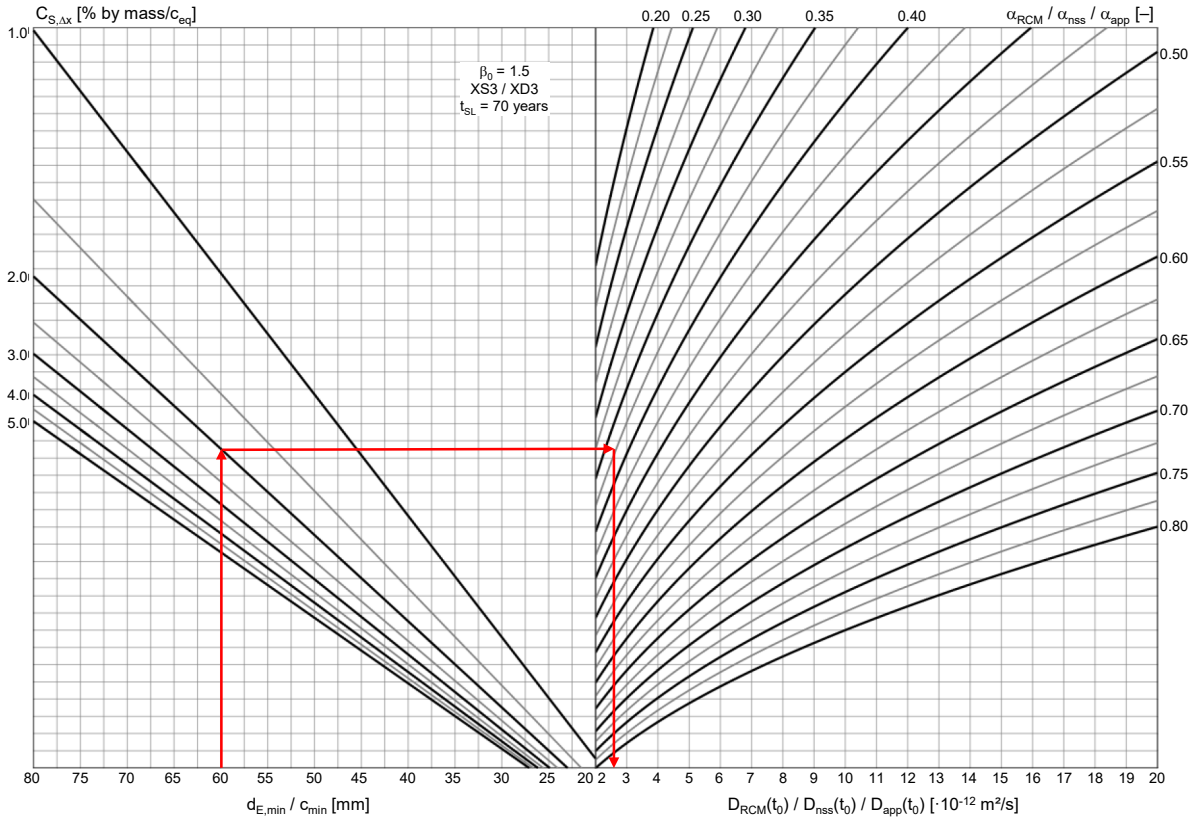

Fig. 2.13: Design nomogram for XS3 / XD3, target service life t_{SL}=70 years, target reliability index β_0=1.5, $2 \leq D(t_0) \leq 20$ (Fig. D.4 Annex D)

3 Assessment of the durability of reinforced concrete members exposed to the action of chlorides

3.1 Introduction

A large proportion of the activities in the construction sector concern existing structures. As structures age, the time and effort required for inspection, maintenance and repair increases. Concepts for determining the remaining service life are needed to enable existing structures to be assessed.

A simplified design approach is presented in Chapter 3.2. It enables the durability of reinforced concrete members exposed to the action of chlorides to be assessed by estimating their remaining service life. The design approach is based on the same limit state and the same design model for the durability of new structures as described in Chapter 2. The nomograms established in Annex D are used. The parameters required for this purpose are derived from data obtained during structural inspections. The safety level specified for the design of new structures in *DAfStb Positionspapier 2008* with a target reliability index $\beta_0 = 1.5$ or 0.5 is also applied in this case.

At a fully probabilistic level, the remaining service life is determined by considering the development of the reliability index over time, cf. Fig. 3.1, left. A comparison of the reliability index achieved at the time under consideration, which represents the actual condition, with the target reliability, which specifies the minimum target condition for the defined limit state, yields the available wear margin as defined in *DIN 31051:2012*.

At a semi-probabilistic level, the remaining service life is determined by considering the development of the design depth of the critical chloride content (at which corrosion is initiated), cf. Fig. 3.1, right. The available wear margin is obtained by calculating the difference between the depth of the critical chloride content at the time under consideration and the minimum concrete cover.

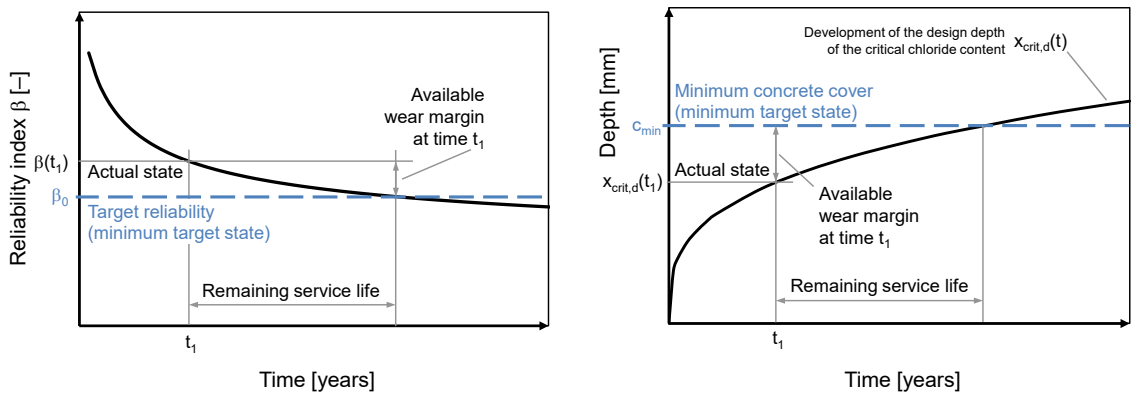

Fig. 3.1: Determination of the remaining service life in the fully probabilistic (left) and semi-probabilistic (right) design format

3.2 Simplified design approach using nomograms to determine the remaining service life

A method of approximating the remaining service life of existing structures with the aid of the design nomograms in Annex D is presented below. Two examples of its application are presented in the following chapter.

The input parameters for the nomograms for determining the remaining service life are $D_{app}(t_0)$, α_{app}, $C_{S,\Delta x}$ and c_{min}; they can be obtained by measuring the concrete cover and the depth-dependent chloride content of the structural element. The minimum concrete cover c_{min} (input parameter) is taken to be the 5% quantile of the different values of the concrete cover obtained for the structural element. The other input parameters are derived from the chloride profile representing the mean value of the chloride contents measured at various depths and established by means of a regression analysis.

The apparent chloride diffusion coefficient at the time of the inspection, $D_{app}(t_{insp})$, and the surface chloride concentration or the chloride concentration at depth Δx (convection zone), $C_{S,\Delta x,insp}$, are calculated by means of a regression analysis according to equation (2.5) berechnet (see Chapter 2.3.2.2.1). Any measurements obtained in the near-surface zone that deviate from the diffusion behaviour alone (Δx) are not considered in the regression analysis if they have a favourable effect on the development of the chloride profile. Measurements within the convection zone must be taken into consideration if disregarding them would result in lower chloride contents within the convection zone (see Example 3.1). In other words, the convection zone is taken as zero in this case for the purpose of determining parameters $D_{app}(t_{insp})$ and $C_{S,\Delta x,insp}$. However, for parameter $C_{S,\Delta x,insp}$, the chloride content at a depth Δx of 10 mm must be calculated from the chloride profile and

used for designs performed with the aid of the nomograms. For structural elements in exposure classes XS3 / XD3, a convection zone Δx of 10 mm shall be assumed. A convection zone is not required for structural elements in exposure classes XS2 / XD2 ($\Delta x = 0$).

To obtain a realistic idea of how the chloride content will develop, the spacing between the measuring depths should be as small as possible. At least three measurements are required for the regression analysis and the chloride content must be measured at a minimum of three different depths within the concrete cover. The first mean measuring depth should be less than 10 mm in the near-surface zone for XS2 / XD2, i.e. samples must be taken in a 20 mm surface zone. For structural elements on exposure classes XS3 / XD3, the depth of the first measurements after the convection zone should be between 10 and 40 mm.

The input parameters for the nomograms, the non-steady state chloride diffusion coefficient $D_{nss}(t_0)$ and the chloride migration coefficient $D_{RCM}(t_0)$, relate to a reference time of 28 days. When using the nomograms to determine the remaining service life, the apparent chloride diffusion coefficient at the time of inspection, $D_{app}(t_{insp})$, must be converted to the corresponding value at the reference time of 28 d ($D_{app}(t_0)$). A distinction is made between whether chloride profiles are available only for one or more than one inspection time when determining the input parameter $D_{app}(t_0)$ and the ageing exponent α_{app}.

The apparent chloride diffusion coefficient at the reference time $D_{app}(t_0=28d)$ is calculated is follows if a mean chloride profile from a single inspection time only is available:

$$D_{app}(t_0) = \frac{1}{k_e} \cdot D_{app}(t_{insp}) \cdot \left(\frac{t_0}{t_{insp}}\right)^{-\alpha_{app}} \qquad (3.1)$$

where k_e = 0.56 [–] (see below), t_0 = 28 [d] or 0.0767 [year] and α_{app} is a function of the type of binder from Table 2.5 (i.e. $\alpha_{app} = \alpha_{RCM}$). The value of α_{app} may be taken as 0.20 if the type of binder is not known.

The parameters at time t_0 ($D_{RCM}(t_0)$, $D_{nss}(t_0)$, $D_{app}(t_0)$) in the nomograms are based on an assumed temperature of 20 °C. The structure-specific parameter $D_{app}(t_{insp})$ relates to a mean annual temperature of 10° C. The temperature coefficient k_e is therefore taken to be 0.56 when determining the parameter $D_{app}(t_0)$, corresponding to T_{ref} = 20 °C and T_{real} = 10 °C (cf. Chapter 2.4.4.5).

The ageing exponent α_{app} can be determined in accordance with Fig. 3.2 if chloride profiles from inspections for different times are available, as for Approach C for determining $D_{app}(t)$ in Chapter 2.3.2.2.4. The prerequisite for this is that the first inspection

considered took place at least 10 years after the start of exposure and there must be an interval of at least 5 years between each of the following inspections. This is to ensure that the chloride profiles realistically reflect the resistance of the concrete member to the ingress of chlorides from the environment to which it is exposed. Alternatively, the ageing exponent can be determined by field tests on structures with the same concrete composition, quality of workmanship and exposure conditions. The maximum ageing exponent α_{app} must not exceed 0.80.

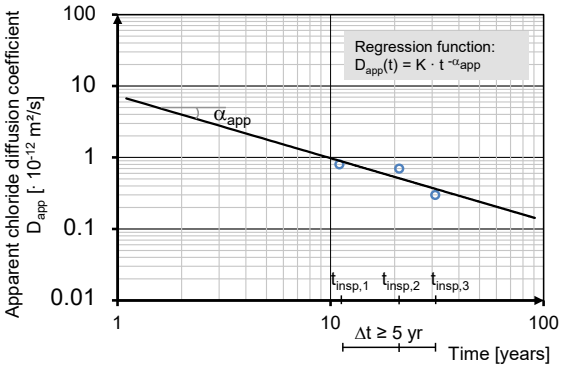

Fig. 3.2: Determination of the ageing exponent α_{app} by means of chloride profiles obtained at different points in time; K: constant derived from the regression analysis

$D_{app}(t_0=28d)$ is calculated from the derived regression function as follows:

$$D_{app}(t_0) = \frac{1}{k_e} \cdot K \cdot t_0^{-\alpha_{app}} \qquad (3.2)$$

where K is a constant obtained from the regression analysis.

The remaining service life can be estimated with the calculated ageing exponents α_{app} and $D_{app}(t_0)$ as well as $C_{S,\Delta x,insp}$ from the last inspection using the nomograms in Annex D Fig. D.1 to Fig. D.19.

A flow chart for determining the remaining service life of a structural element, depending on the availability of inspection data, is shown in Fig. 3.3.

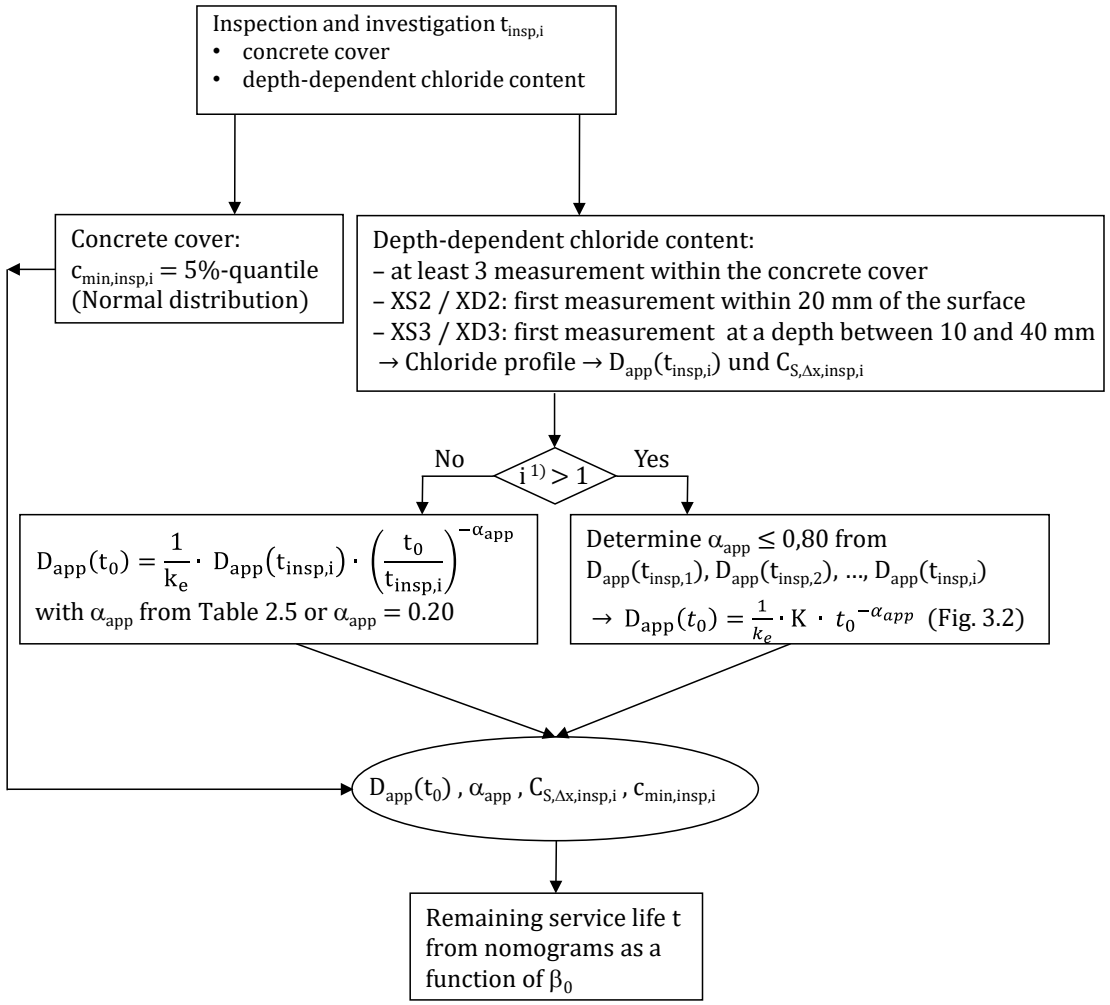

[1] $t_{insp,i=1} \geq 10$ *years; where* $i > 1$, *the interval between measurements should be at least 5 years*

Fig. 3.3: Flow chart for determining the remaining service life

3.3 Examples of how to apply the nomograms to determine the remaining service life

The two examples given below illustrate how the nomograms can be used to determine the remaining service life. Example 3.1 corresponds to Example 2.1 used to validate the design model in Chapter 2.4.5.2. The measured chloride contents in the other examples in Chapter 2.4.5.2 do not satisfy the boundary conditions for establishing the chloride profile and for application of the nomograms.

Example 3.1: Example 2.1 from Chapter 2.4.5.2

Table ex. 3.1-1: Information on the structural element

Type and location of structural element	Bridge pier over the Baltic Sea in Denmark, XS3
Concrete composition	CEM I, w/c: 0.35 – 0.50
Concrete cover	c_{nom} = 45 mm, Δc = 5 mm (c_{min} = 40 mm)
Age of structural element at time of inspection	32 years
Target reliability	β_0 = 0.5

Table ex. 3.1-2: Measured chloride contents at the inspection time of 32 years

Mean depth of measurements [mm]	No. of measurements [–]	Chloride content [% by mass/b]	
		μ	σ
7.5	17	1.39	0.66
22.5	17	0.83	0.39
45	17	0.59	0.24
75	17	0.36	0.20

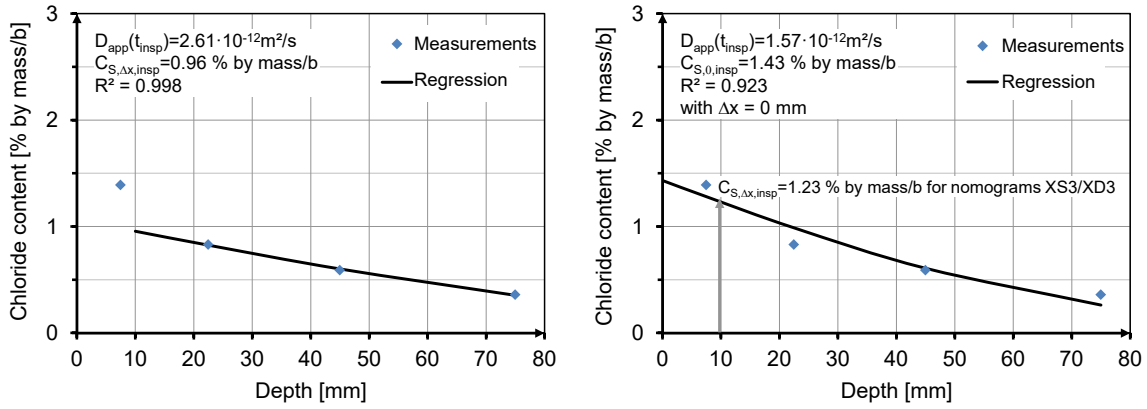

Fig. ex. 3.1-1: Deriving $D_{app}(t_{insp})$ and $C_{S,\Delta x,insp}$ from the regression analysis (e.g. by means of "solver" function in Microsoft Excel); left: the first measured chloride content within the convection zone (Δx = 10 mm) is not considered; right: all of the measured chloride contents are considered

Figure Example 3.1-1, right → $D_{app}(t_{insp})$ = 1.57 · 10^{-12} m²/s and $C_{S,\Delta x,insp}$ = 1.23 % by mass/b

The ageing exponent α_{app} = 0.30 (Table 2.5, CEM I)

$$D_{app}(t_0) = \frac{1}{k_e} \cdot D_{app}(t_{insp}) \cdot \left(\frac{t_0}{t_{insp}}\right)^{-\alpha_{app}} = 17.1 \cdot 10^{-12} \ \frac{m^2}{s}$$

Figure D.19 (t_{SL} = 10 years) → c_{min} = 38 mm

Figure D18 (t_{SL} = 20 years) → c_{min} = 46 mm

The service life for the required reliability β_0 of 0.5 is thus calculated to be around 12 years which correlates well with the result of the fully probabilistic calculation (Chapter 2.4.5.2, Example 2.1) with around 18 years, cf. Figure Example 3.1.2.

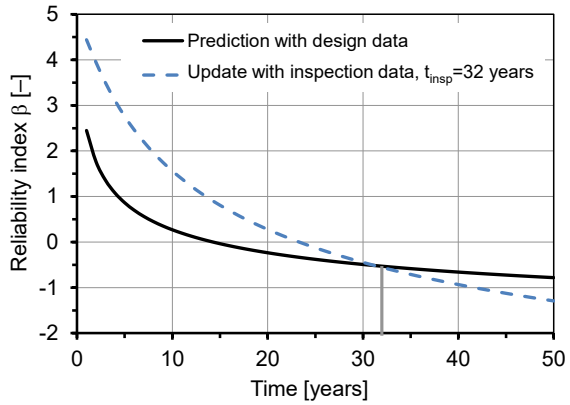

Fig. ex. 3.1-2: Fully probabilistic calculation of the remaining service life; example 2.1 from Chapter 2.4.5.2, β-t-run before and after updating

Example 3.2:

Table ex. 3.2-1: Information on the structural element

Type and location of structural element	Marine structure on the North Sea coast, XS3
Concrete composition	CEM III/A
Age of structural element at time of inspection	10 and 20 years
Concrete cover	c_{nom} = 60 mm, Δc = 10 mm (c_{min} = 50 mm)
Target reliability	β_0 = 1.5

Table ex. 3.2-2: Measured chloride contents at the inspection time of 10 years

	Chloride content [% by mass/b] Mean depth of measurements [mm]				
	5	15	25	35	45
1	2.85	2.23	0.77	0.23	0.06
2	2.01	1.86	0.76	0.13	0.08
3	2.75	2.33	0.73	0.17	0.06
4	1.83	1.67	0.55	0.19	0.06
5	2.00	1.79	0.56	0.15	0.06
Mean	**2.29**	**1.98**	**0.67**	**0.17**	**0.06**
Standard deviation	0.474	0.288	0.110	0.038	0.009

Table ex. 3.2-3: Measured chloride contents at the inspection time of 20 years

	Chloride content [% by mass/b] Mean depth of measurements [mm]					
	5	15	25	35	45	55
Mean	**2.65**	**2.15**	**0.72**	**0.21**	**0.035**	**0.01**
Standard deviation *	0.530	0.430	0.144	0.042	0.007	0.0002

* *taken to be 20 % of the mean value (for the fully probabilistic calculation)*

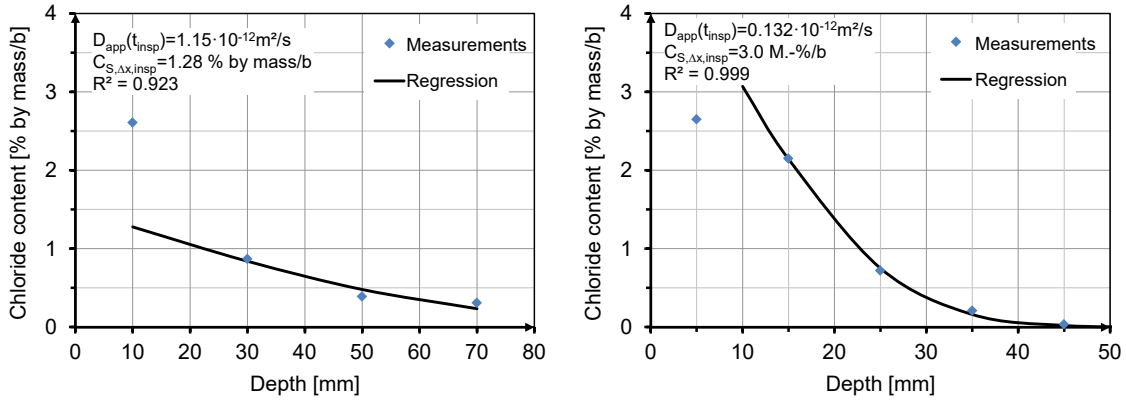

Fig. ex. 3.2-1: Deriving $D_{app}(t_{insp})$ and $C_{S,\Delta x,insp}$ at t_{insp}=10 (left) and t_{insp}=20 years (right) from the regression analysis (e.g. by means of "solver" function in Microsoft Excel)

Figure example 3.3-1, left → $D_{app}(t_{insp,1})$ = 0.201 · 10^{-12} m²/s and $C_{S,\Delta x,insp,1}$ = 3.0 % by mass/b

Ageing exponent α_{app} = 0.40 (Table 2.5, CEM III/A)

$$D_{app}(t_0) = \frac{1}{k_e} \cdot D_{app}(t_{insp}) \cdot \left(\frac{t_0}{t_{insp}}\right)^{-\alpha_{app}} = 2.5 \cdot 10^{-12} \frac{m^2}{s}$$

Figure D.10 (t_{SL} = 30 years) → c_{min} ~ 49 mm

Figure D.8 (t_{SL} = 40 years) → c_{min} ~ 53 mm

→ t_{SL} ~ 32 years → the remaining service life is around 22 years.

Figure example 3.2-1, right → $D_{app}(t_{insp,2})$ = 0.132 · 10^{-12} m²/s and $C_{S,\Delta x,insp,2}$ = 3.0 % by mass/b

$$D_{app}(t_{insp,2}) = D_{app}(t_{insp,1}) \cdot \left(\frac{t_{insp,1}}{t_{insp,2}}\right)^{\alpha_{app}}$$

→ α_{app} = 0.607

$$D_{app}(t_0) = \frac{1}{k_e} \cdot D_{app}(t_{insp,2}) \cdot \left(\frac{t_0}{t_{insp,2}}\right)^{-\alpha_{app}} = 7.02 \cdot 10^{-12} \frac{m^2}{s}$$

Figure D.8 (t_{SL} = 40 years) → c_{min} ~ 52 mm

Figure D.10 (t_{SL} = 30 years) → c_{min} ~ 49 mm

→ t_{SL} ~ 35 years → the remaining service life is around 15 years.

The development of the reliability index over time obtained in fully probabilistic calculations results in an overall service life of 47 years if the chloride profiles at $t_{insp,1}$ = 10 years are taken into account and 67 years if the chloride profiles at $t_{insp,1}$ = 10 years and $t_{insp,2}$ = 20 years are taken into account.

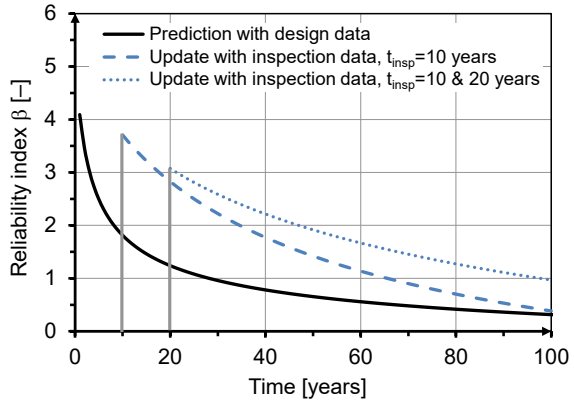

Fig. ex. 3.2-2: Fully probabilistic calculation of the remaining service life (input values of the model variables from Table ex. 2.3-3 in Chapter 2.4.5.2)

4 Durability design of reinforced concrete members exposed to the action of chlorides and to be repaired by replacing damaged concrete

4.1 Introduction

Repairing concrete members by replacing damaged concrete, i.e. partially removing the concrete and replacing it with a repair material, is a tried-and-tested, common method of repairing reinforced concrete structural elements contaminated with chlorides. Depending on the penetration depth and concentration of chlorides in the member, the concrete cover is removed either partially or fully, including deeper areas behind the reinforcement if necessary, and replaced by repair material. The aim of such repair measures is to repassivate the reinforcing steel and increase the resistance of the structural element to further chloride ingress. Repairs can be either extensive or only carried out at selected points. Durability design within the context of this dissertation is based on extensive repairs to concrete members and any risk of damage to adjacent areas without repairs can be ruled out.

Concepts for the performance-based design of repair measures and for assessing the ability of such measures to prolong the service life of concrete members do not yet exist. Based on the approach for the durability design of new structures, a simplified approach to the design and assessment of repair measures involving the replacement of damaged concrete has been developed in this dissertation.

The repair materials frequently used to replace damaged concrete are polymer-modified cement-bound systems whose compositions are not disclosed by the manufacturers. Their properties are determined by laboratory tests. These are used to determine the density, modulus of elasticity and chloride penetration resistance of such systems. Hitherto, only limited experience and knowledge of the performance of the materials concerned is available, in particular with regard to their durability and long-term behaviour when exposed to the action of chlorides.

The following “milestones” are an essential part of developing a performance-based durability design of repair measures involving the replacement of damaged concrete with a repair material:

- Modelling the chloride transport in concrete members comprising more than one layer, i.e. the remaining concrete and the repair material applied on top of it.
- Assessing the performance of repair materials and their long-term behaviour.

The studies published so far (*Rahimi et al. 2013a*. *2014*. *2014a*. *2015*. *2015a*. *2015b*. *Gehlen et al. 2015*) on modelling chloride transport in two-layer systems, fully probabilistic prediction of the condition after repairs have been carried out, determining the minimum removal depth and the influence of the redistribution of chlorides on the determination of the service life are summarized in Chapter 4. This is followed by the development of design approaches at a semi-probabilistic level and with nomograms. Laboratory testing and field tests to assess the resistance of repair materials to chloride ingress and the chloride transport in repaired concrete members are described in Annex A and Annex B respectively.

4.2 Fully probabilistic design approach

4.2.1 Principle

The main features of the concept for the durability design of new structures (Chapter 2) are also applied in a slightly modified form when developing a similar approach for the repair of structural elements by replacing damaged concrete with repair material. The limit state relevant for designing new structures, the variables of the action and resistance together with their statistical characterization and the target reliability remain the same. Three separate cases are described in the following chapters, differing with regard to how the chloride transport in concrete members is modelled and the limit state equation is formulated:

- Case 1: The concrete cover is completely removed and replaced by a repair material. The remaining layer of concrete behind the reinforcement is not contaminated with chlorides.
- Case 2: The concrete cover is only partially removed and replaced by a repair material. The remaining layer of concrete in the concrete cover and behind the reinforcement is not contaminated with chlorides.
- Case 3: The concrete cover is only partially removed and replaced by a repair material. The remaining layer of concrete is contaminated with (residual) chlorides. There is a similar case in which the contaminated concrete cover remains in place and is covered with a layer of repair material.

4.2.2 Repair involving complete replacement of the concrete cover (Case 1)

The durability of the repair measure can be verified using the approach for new structures (Chapter 2) when the concrete is removed to the depth of the reinforcement or beyond it and replaced with a repair material (Fig. 4.1), so that the concrete cover comprises a single material. The relevant properties of the repair material used are needed in order to determine the material resistance. The compositions of the repair materials are frequently unknown to the users. Approach A (Chapter 2.3.2.2.2)) is suitable for determining the apparent chloride diffusion coefficient $D_{app}(t)$ (cf. Annex A) in this case.

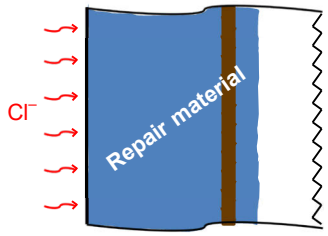

Fig. 4.1: Complete removal of cover and replacement with repair material, no residual chlorides (case 1)

4.2.3 Repair involving partial replacement of the concrete cover, without residual chlorides (Case 2)

4.2.3.1 Modelling chloride transport

Partial removal of the concrete cover may be appropriate for economic reasons, reasons relating to execution or design or as a preventive measure and so on (Fig. 4.2, left). In this case, the concrete cover comprises two layers, each with different material properties. The lifetime, i.e. the time to depassivation of the reinforcement, depends on the chloride penetration behaviour of both layers. For the case that the remaining concrete layer is not contaminated with chlorides, the time- and depth-dependent chloride content of both layers can be calculated using equations (4.1) to (4.4). This mathematical formulation is based on the diffusion equation for "semi-finite composite media" developed by *Carslaw & Jaeger 1959* and *Crank 1975* and adapted to suit the model for new structures, i.e. a one-layer system (Eq. (2.5)).

$$C_{new}(x,t) = C_{S,\Delta x} \cdot \sum_{n=0}^{\infty} \gamma^n \cdot \left\{ erfc \frac{(2n+1)\cdot(c_{new}-\Delta x)+x}{2\sqrt{D_{app,new}(t)\cdot t}} - \gamma \cdot erfc \frac{(2n+1)\cdot(c_{new}-\Delta x)-x}{2\sqrt{D_{app,new}(t)\cdot t}} \right\} \quad (4.1)$$

$$C_{remain}(x,t) = \frac{2k_D \cdot C_{S,\Delta x}}{k_D+1} \cdot \sum_{n=0}^{\infty} \gamma^n \cdot erfc \frac{(2n+1)\cdot(c_{new}-\Delta x)+k_D \cdot x}{2\sqrt{D_{app,new}(t)\cdot t}} \quad (4.2)$$

mit:

$$k_D = \sqrt{\frac{D_{app,new}(t)}{D_{app,remain}(t)}} \quad (4.3)$$

und

$$\gamma = \frac{1-k_D}{1+k_D} \quad (4.4)$$

where $D_{app,new}(t)$ and $D_{app,remain}(t)$ are the apparent chloride diffusion coefficients of the repair material and the remaining concrete respectively; c_{new} is the thickness of the new repair layer. The chloride concentration in repair layer $C_{new}(x,t)$ is described using equation (4.1) (with $x \leq 0$), the chloride concentration in the remaining layer $C_{remain}(x,t)$ using equation (4.2) (with $x \geq 0$). The equations are a modification of the calculation model with the error function of Fick's law of diffusion. The boundary conditions are a constant external surface chloride concentration in the repair layer ($C_{s,\Delta x}$ = constant) and an equilibrium concentration at the layer boundary ($C_{new}(x=0,t) = C_{remain}(x=0,t)$). Comparative analytical and numerical calculations have shown that the chloride concentration can be calculated with a sufficient degree of accuracy if a control variable $n = 0$ is used in equations (4.1) and (4.2).

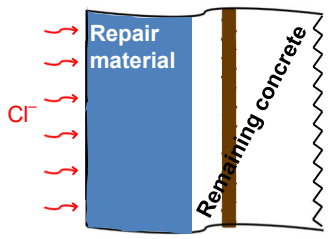

Fig. 4.2: Partial removal of cover and replacement with repair material, no residual chlorides (case 2)

Any possible interfacial resistance at the interface between the repair layer and the remaining concrete layer is disregarded here. Interfacial resistance may occur in a layer owing to incoherency of the pore structure of the two materials and the presence of a large proportion of impermeable aggregates (*Zhang et al. 1998*). In this case, the boundary condition of the concentration equilibrium at the interface is no longer fulfilled in the above approach and the chloride transport is modelled using other mathematical equations that are similar (see *Crank 1975*).

4.2.3.2 Prediction of the condition state and design

The limit state equation can be formulated as follows, by analogy to the durability design of new structures (Eq. (2.22) or (2.23)):

$$g(X,t) = C_{crit} - C_{remain}(c_{remain}, t_{SL}) \tag{4.5}$$

i.e. (using Eq. (4.2) with $n = 0$):

$$C_{crit} = \frac{2k_D \cdot C_{S,\Delta x}}{k_D + 1} \cdot \; erfc\,\frac{c_{new} - \Delta x + k_D \cdot c_{remain}}{2\sqrt{D_{app,new}(t_{SL}) \cdot t_{SL}}} \tag{4.6}$$

or

$$g(X,t) = c_{remain} - x_{crit}(t_{SL}) \tag{4.7}$$

i.e. (using Eq. (4.2) with $n = 0$):

$$c_{remain} = \frac{\left[2erf^{-1}\left(1 - \frac{C_{crit}}{C_{S,\Delta x}} \cdot \frac{k_D + 1}{2k_D}\right) \cdot \sqrt{D_{app,new}(t_{SL}) \cdot t_{SL}} - c_{new} + \Delta x\right]}{k_D} \tag{4.8}$$

c_{remain} is the thickness of the remaining concrete layer over the surface of the reinforcement.

Results of examples of reliability analyses for such two-layer systems are shown in Fig. 4.3, left. However, the same material properties are attributed to both layers (see Fig. 4.3, right) to enable the results to be compared with those obtained for a reliability analysis for a one-layer system (as for new structures). It can be seen from Fig. 4.3, left, that the development of the reliability index over time is always more favourable for two-layer systems than for one-layer systems with distinct differences for the materials comprising CEM III/B and CEM II/A-V. That means that the two different mathematical formulations used to calculate the development of the chloride penetration (Eq. (2.5) and (4.2)) lead to different results for the reliability analyses although both result in the same chloride penetration profile (deterministic) (if both layers have the same material properties). This is because the relative uncertainty of a sum of two or more random variables is lower than that of individual random variables (*Straub 2015*). For reliability analyses of two-layer systems, the material properties $D_{RCM}(t_0)$ and α_{RCM} are each taken into account twice with the same coefficient of variation (uncertainties) as for the analysis of the one-layer system.

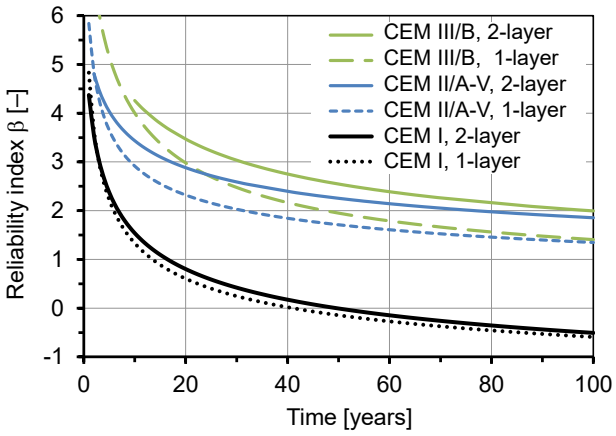

Variable	Distribution & Values		
	CEM III/B	CEM II/A-V	CEM I
$D_{RCM}(t_0)$ [10^{-12} m²/s]	ND (μ / σ)		
	1.9 / 0.38	9.0 / 1.8	10.0 / 2.0
α_{RCM} [–]	BetaD (μ / σ / 0 / 1)		
	0.45 / 0.20	0.60 / 0.15	0.30 / 0.12
c [mm] (1-layer Sys.)	ND (60 / 6)		
c_{new} [mm]	ND (30 / 6)		
c_{remain} [mm]	ND (30 / 6)		
t_0 [d]	constant 28		
T_{ref} [K]	constant 273		
T_{real} [K]	ND (283 / 5)		
b_e [K]	ND (4800 / 700)		
$C_{S,\Delta x}$ [% by mass/b]	LND (3.0 / 0.75)		
Δx [mm]	constant 0		
C_{crit} [% by mass/b]	BetaD (0.60 / 0.1 5/ 0.2 /2)		

Fig. 4.3: Left: comparison of the reliability analyses of 1- and 2-layer systems; right: values used for the variables for the reliability analyses

By contrast, the uncertainties of the above variables increase if the concrete cover is divided (*Gollwitzer 2015*). While the coefficient of variation of the concrete cover in one-layer systems is $\mathrm{CoV} = 6/60 = 0.10$, a higher coefficient of variation of $\mathrm{CoV}\,(c_{new} + c_{remain}) = \sqrt{6^2 + 6^2}/60 = 0.14$ is obtained for two-layer systems. The influence of the concrete cover on the results of the reliability analysis is, however, far less significant, particularly when compared with the ageing exponent (cf. Fig. 2.11), so that, on the whole, the reliability is greater for two-layer systems. The considerable differences in the development of the reliability index of the two types of system for materials comprising CEM III/B and CEM II/A-V (Fig. 4.3) are due to their ageing exponents being far greater than those of materials with CEM I.

This probability-based advantage of two-layer systems does not apply in construction practice, at least not entirely. On the other hand, the favourable influence of the age of the remaining concrete layer at the time of repair on the chloride penetration resistance is not taken into consideration in the reliability analyses for the sake of simplicity and to err on the safe side.

4.2.4 Repair with partial replacement or covering of the concrete cover, with residual chlorides (Case 3)

4.2.4.1 Modelling the chloride transport

In cases in which the remaining concrete layer is contaminated the residual chlorides will be redistributed over both layers after the new repair layer has been applied (Fig. 4.4). The error function as a solution to Fick's second law of diffusion cannot be used to describe the redistribution of the residual chlorides mathematically as the required boundary condition of a constant concentration at the phase boundary, $\partial C_s / \partial t = 0$, does not apply. The chloride transport in the structural element cannot be formulated mathematically in a way that is generally valid for this case.

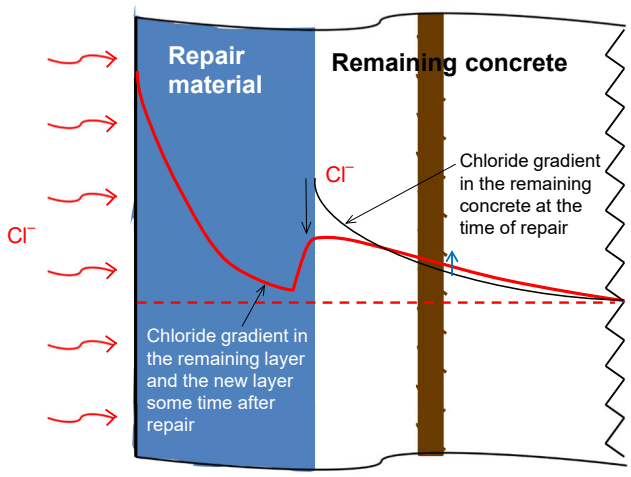

Fig. 4.4: Partial removal of cover and replacement with repair material, residual chlorides are available (case 3)

The convolution integral in Eq. (4.9) was developed for the theoretical case where both layers have the same apparent chloride diffusion coefficient $D_{app}(t)$ (the same material properties) (*Kostadinov 2014*). The integral enables the time- and depth-dependent chloride concentration due to redistribution of the residual chlorides to be calculated, on condition that the residual chloride profile follows Fick's second law of diffusion.

$$C(x,t) = \frac{1}{\sqrt{4\pi D_{app}(t) \cdot t}} \int_{x}^{\infty} e^{-\frac{(x-y)^2}{4D_{app}(t) \cdot t}} \cdot C_{S,g} \cdot erfc\left(\frac{y}{\sqrt{4D_{app}(t) \cdot t}}\right) dy \qquad (4.9)$$

However, the integral does not provide a closed-form solution, i.e. it cannot be expressed by a finite number of known functions. A closed-form solution can be approximated by the Riemann integral, for example (see Chapters 4.2.4.2 and 4.2.4.4). The interval x to ∞ indicates the boundaries of the remaining concrete layer; $C_{S,g}$ is the residual chloride content of the boundary layer.

The diffusion-controlled chloride ingress and diffusion-controlled redistribution of chlorides in two-layer systems in the presence of residual chlorides will be considered numerically with the aid of the finite element method in the following chapters.

A significant mobilization of the residual chlorides can be expected to occur immediately after application of the repair material. This is caused by the moisture present in the new layer. As a result, the residual chlorides can either penetrate further into the remaining concrete layer due to capillary suction or move in the other direction and thus be transported into the new layer (diffusion-controlled). The quantity of chloride ions moving into the new layer can vary depending on the moisture content of the remaining concrete layer. This important issue was considered in laboratory experiments conducted by the author (see Annex B.1).

If the remaining concrete layer contains residual chlorides it needs to be considered how high a level of contamination is permitted and how this affects the remaining service life of the structural element after the repair measure has been carried out. These issues are dealt with in Chapters 4.2.4.2 and 4.2.4.4.

4.2.4.2 Minimum depth of removal of the concrete cover

As explained in the previous chapter, it is not possible to model the chloride transport in repaired concrete members using mathematical functions if residual chlorides are present in the remaining concrete layer. However, it is possible to track the migration of chlorides by means of the finite element method (FEM) or finite difference method and with the aid of the appropriate software.

The chloride transport in a two-layer system is investigated below using the finite element method and with the aid of the *COMSOL Multiphysics*® software. The aim of the numerical investigations is to determine the boundary conditions for the depth to which the concrete cover has to be removed and for the residual chloride gradient below which the risk of depassivation of the rebars owing to redistribution of residual chlorides is negligible. To this end, the chloride transport was regarded solely as a diffusion process

and described by Fick's law of diffusion. The mechanisms were modelled in the programme using differential equations and resolved by applying the FEM.

Based on the results of studies of numerous (numerical) cases, the following two boundary conditions were specified. Compliance with these is required in order to minimize the probability of depassivation of the rebars (which occurs when the critical chloride content C_{crit} is reached at the surface of the rebars) by redistribution of the residual chlorides in the remaining concrete layer:

1. The depth at which the critical chloride content occurs should be at least 10 mm from the surface of the reinforcement.
2. The maximum residual chloride content in the remaining concrete layer must not exceed 2.0 % of the mass of the binder (% by mass/b).

This means that the concrete layer contaminated with chlorides must be removed to a depth at which the boundary conditions stated above are fulfilled. However, the prerequisite for this is that the actual residual chloride profile corresponds to Fick's law of diffusion.

The results of selected theoretical cases shown in Fig. 4.5 to Fig. 4.13 illustrate the redistribution and penetration of chlorides by diffusion in a repaired concrete member, along with the plausibility of the specifications set out above.

Fig. 4.5 shows how chlorides were redistributed in a concrete member when the 55 mm-thick concrete cover was partially (25 mm) removed and the surface of the member was subsequently sealed. The residual chloride profile (residual Cl, cf. Fig. 4.5) satisfies both of the boundary conditions stated above and is within the maximum permissible limiting values. The concrete is a very porous material with a very low resistance to chloride ingress (e.g. made with Portland cement with a w/c ratio of 0.60). The diffusion-controlled redistribution of the residual chlorides 1, 5, 10, 20 and 50 years after the concrete had been repaired is shown in the figure. A distinct decrease in the chloride content in the near-surface zone can be seen, being very pronounced at the beginning ($t = 1$ year) and becoming less marked over time. At the level of the surface of the reinforcing steel, the chloride content first increases ($t = 1$ and 5 years) but decreases again over time and always remains below the critical chloride content C_{crit} of 0.50 % by mass/b. Thus it can be assumed that there is no risk of the residual chlorides causing depassivation of the reinforcing steel in this case. The critical chloride content C_{crit} was taken as 0.50 % by mass/binder, based on *DAfStb RiLi SIB 2001*.

Erring on the safe side, the calculations considered the apparent chloride diffusion coefficient $D_{app}(t)$ of the remaining concrete layer from the time at which the repair was

carried out, while the age of the concrete member prior to repair was not taken into account.

In a second case (cf. Fig. Fig. 4.6) the maximum chloride content was increased to 3.0 % by mass/b by way of departure from the first boundary condition (the concrete and concrete cover being the same as in the first case). It can be seen in Fig. 4.6 that the critical chloride content at the surface of the reinforcing steel was reached at t = 1 and 5 years so that the risk of the residual chlorides causing depassivation of the reinforcing steel cannot be ruled out.

Fig. 4.7 illustrates the theoretical case in which – deviating from the second boundary condition – the critical chloride content C_{crit} in the residual chloride profile occurs at a distance of only 7.5 mm from the surface of the reinforcing steel. The chloride content at a distance of 10 mm from surface of the reinforcing steel is 0.60 % by mass/b. Similar to the previous case in Fig. 4.6, the chloride profiles at t = 1 and 5 years also exhibit chloride contents equal to or slightly higher than C_{crit} at the surface of the reinforcing steel.

By way of comparison with the first case (Fig. 4.5) a concrete with a greater resistance to chloride ingress (e.g. with CEM III/A, w/c ratio = 0.50) is considered in Fig. 4.8. The specified boundary conditions are also shown to be adequate in this case so that depassivation of the reinforcement by redistribution of the residual chlorides can be ruled out. The chloride redistribution is considerably slower. By contrast with the previous cases, in which the chloride content at the surface of the reinforcing steel initially increased rapidly (t = 1 and 5 years) and then decreased (t = 10, 20 and 50 years), the chloride content at the surface of the reinforcing steel increases continuously from t = 1 years to t = 50 years but remains below the critical content C_{crit} at all times.

In the cases considered so far, the nominal concrete cover was taken as 55 mm as specified in *DIN EN 1992-1-1/NA:2013* for exposure classes XD and XS. In addition, the national code *ZTV-W LB 215:2012* also applies to structures on waterways and in coastal areas in Germany and specifies a higher nominal concrete cover of 60 mm for exposure classes XD and XS. The first case in Fig. 4.5 was therefore considered with a concrete cover of 60 mm (cf. Fig. 4.9), not only for this reason but also for the purpose of investigating whether the specified boundary conditions are also valid for other dimensions of the concrete cover. A residual chloride profile corresponding to the error function solution of Fick's second law of diffusion and with the limiting values of both boundary conditions resulted in a depth of 27 mm for removal of the concrete cover. As shown in Fig. 4.9, the chloride content at the surface of the reinforcing steel always remains below C_{crit}.

Fig. 4.10 illustrates the case in which, by contrast to the previous case (Fig. 4.9), the removed concrete cover is replaced with a repair material (instead of the remaining

concrete being sealed). The thickness of the concrete cover is the same, i.e. 60 mm. The repair material used was made of the same porous material with a very low chloride diffusion resistance as the remaining part of the structural element (Portland cement with a w/c ratio of 0.60). The repaired surface of the concrete member was then sealed to prevent ingress of external chlorides. In this case, the residual chlorides will diffuse into the new layer as well as being redistributed in the remaining concrete layer. The extraction of the residual chlorides by the new layer results in a lower degree of redistribution in the remaining layer and thus in a lower chloride content at the surface of the reinforcing steel at each of the considered times than is the case in Fig. 4.9 in which the concrete member was only sealed after removal of the concrete cover.

Furthermore, a case was investigated in which the repair material has a very high resistance to chloride ingress (e.g. CEM III/B concrete with a w/c ratio of 0.45) (cf. Fig. 4.11). In contrast to the previous case, in which a porous repair material was used, residual chlorides diffuse into the new layer to a far lesser extent. A diffusion-open repair material is thus more favourable as regards extraction (back diffusion) of the residual chlorides.

In practice, the surface of the structural element is not usually sealed after application of the repair material so that ingress of external chlorides into the concrete can be expected. Fig. 4.12 and Fig. 4.13 show the last two cases described above (Fig. 4.10 and Fig. 4.11) but with ingress of external chlorides into the structural element in addition to the residual chlorides. The figures clearly show that, as expected, the resistance of the structural element to chloride ingress increases significantly if a diffusion-tight repair material is used rather than a diffusion-open material. A comparison of Fig. 4.11 and Fig. 4.13 shows that, at t = 20 years, the external chlorides have not yet reached the remaining concrete layer. In each case, a slight difference between the chloride profiles in the vicinity of the remaining concrete layer can only be detected at t = 50 years, indicating that external chlorides have penetrated into the repair layer.

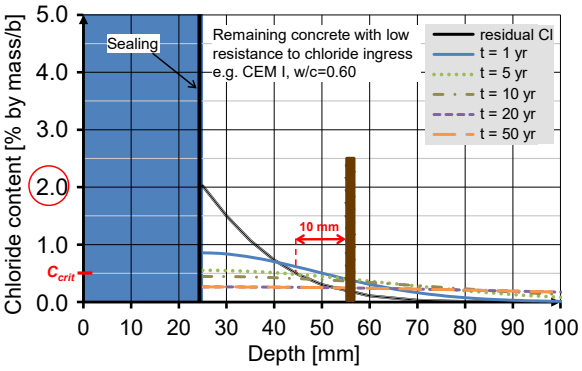

Fig. 4.5: Redistribution of residual chlorides in a concrete with low chloride diffusion resistance after partial removal (25 mm) of cover and sealing. The residual chloride profile exhibits a maximum of 2.0 wt.-%/c and falls below C_{crit}=0.50 wt.-%/c at 10 mm from the rebar surface

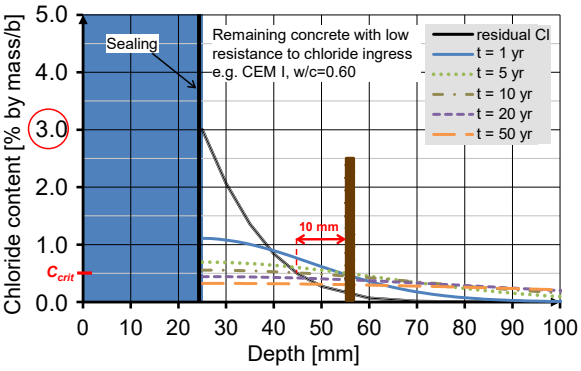

Fig. 4.6: Redistribution of residual chlorides; same case as in Fig. 4.5 but the residual chloride profile exhibits a higher maximum of 3.0 wt.-%/c; impact of maximum chloride content in remaining concrete on the chloride content at rebar surface

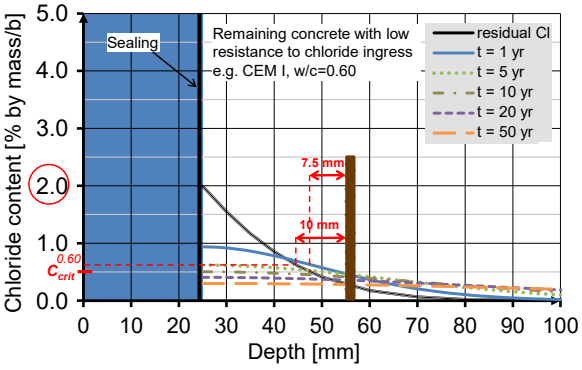

Fig. 4.7: Redistribution of residual chlorides; same case as in Fig. 4.5but the depth with C_{crit} is only 7.5 mm (less than 10 mm) from the rebar surface; impact of the distance of the depth with C_{crit} to rebar surface

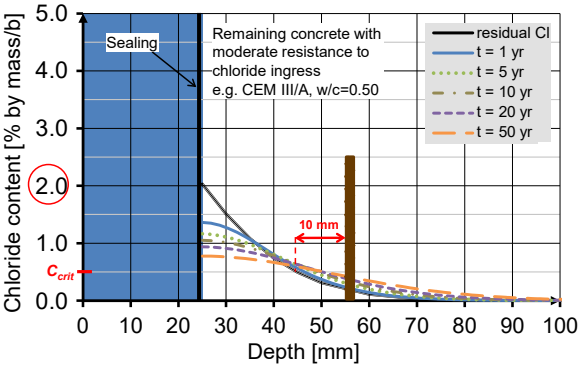

Fig. 4.8: Redistribution of residual chlorides; same case as in Fig. 4.5but remaining concrete has a higher resistance against chloride diffusion; impact of the diffusivity of remaining concrete

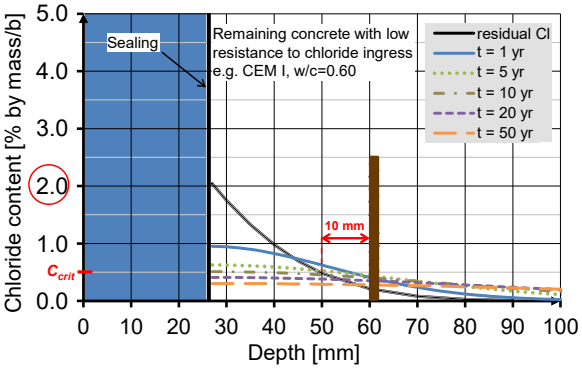

Fig. 4.9: Redistribution of residual chlorides; same case as in Fig. Fig. 4.5 but with a different concrete cover (60 mm instead of 55 mm) and thickness of repair layer (27 mm instead of 25 mm); impact of variation in cover dimension

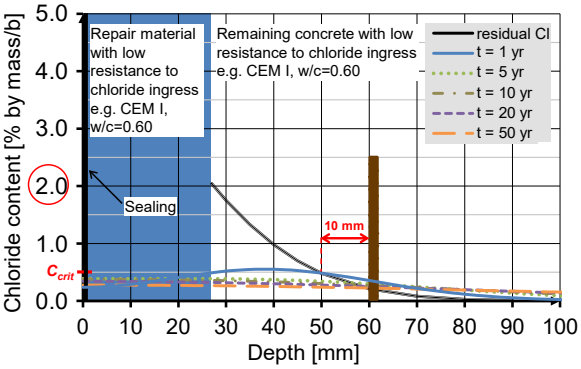

Fig. 4.10: Redistribution of residual chlorides; same case as in Fig. 4.9 but the removed cover is replaced by a repair material followed by sealing the surface; impact of chloride extraction ("back-diffusion") by the repair layer

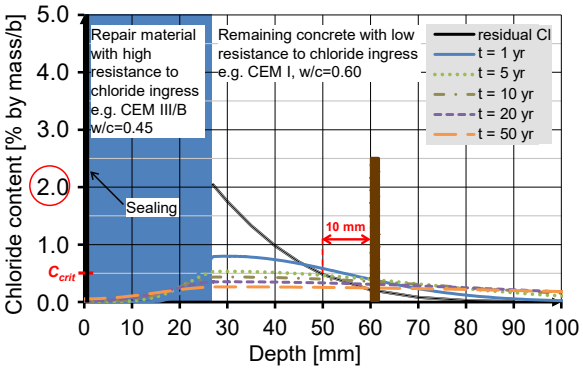

Fig. 4.11: Redistribution of residual chlorides; same case as in Fig. 4.9 but the repair material exhibits a much higher resistance to chloride diffusion; impact of diffusivity of repair material

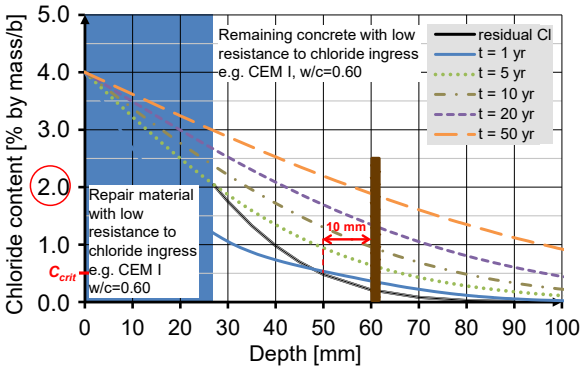

Fig. 4.12: Ingress and redistribution of chlorides; same case as in Fig. 4.9 but external chlorides ingress through the repair layer (surface is not sealed)

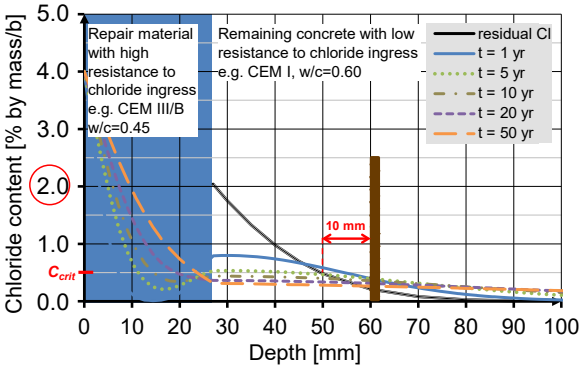

Fig. 4.13: Ingress and redistribution of chlorides; same case as in Fig. 4.12 but the repair material exhibits a much higher resistance to chloride diffusion; impact of diffusivity of repair material

The validity of the defined boundary conditions in terms of preventing residual chlorides causing corrosion of the reinforcing steel was examined and verified in the cases illustrated above. Unfavourable cases of relevance in practice were considered and, to err on the safe side, the possibility of the residual chlorides being extracted by capillary suction and washed out of the freshly applied repair layer was disregarded (cf. Annex B.1), as was the favourable influence of the age of the structural element when the repair was carried out on the chloride penetration resistance of the remaining concrete. Thus the defined boundary conditions can be considered as general, conservative criteria for the execution of repairs to concrete members.

The results presented above are based on deterministic calculations using mean values, i.e. with a probability of occurrence p_f of 50 %. Considering the conservative assumptions stated above (disregarding the age of the structural element and the extraction of chlorides by capillary suction) and the assumed critical chloride content with a low limiting value of

0.5 % by mass/b, the defined boundary conditions for the depth to which the concrete cover has to be removed in order to achieve the target reliabilities β_0 = 0.5 and 1.5 can be regarded as valid without the need to quantify them specifically.

The probability of depassivation of the reinforcement occurring due to the redistribution of the residual chlorides can be quantified using equation (4.9) in cases in which the surface of the structural element is sealed after removal of the damaged concrete or where it is assumed that the remaining concrete layer and the repair layers have the same material properties. However, as the integral does not provide an exact, closed-form solution, the solution is approximated with the aid of the Riemann integral. The limit state equation for the reliability analysis is established using the approximated equation for the time- and depth-dependent residual chloride profile. The results of such reliability analyses for the cases in Fig. 4.5, Fig. 4.8 and Fig. 4.10 are shown in Fig. 4.14. For the case in Fig. 4.10, the results in Fig. 4.14 indicate that the probability of the critical chloride content C_{crit} of 0.6 % by mass/b being reached at the surface of the reinforcement following redistribution of the residual chlorides can virtually be ruled out (very high reliability indices increasing over time). This is due to the "back diffusion" of the residual chlorides present in the new repair layer. By contrast, a relatively low reliability index (β = 0.9) was determined for the case in Fig. 4.5 immediately after the repair measure had been carried out although it increases over time. This is consistent with the results of the FE calculations in Fig. 4.5 in which the chloride content at the surface of the reinforcement is shown to increase although it decreases again over time. The reliability index for the case in Fig. 4.8 decreases over time and more or less stagnates after around 20 years. Its value is always high so that a very low probability (p_f < 4 %) of depassivation of the reinforcement was determined in this case. The different reliability profiles for the cases shown in Fig. 4.5 and Fig. 4.8 are due to the great differences in the chloride penetration resistance of the two materials.

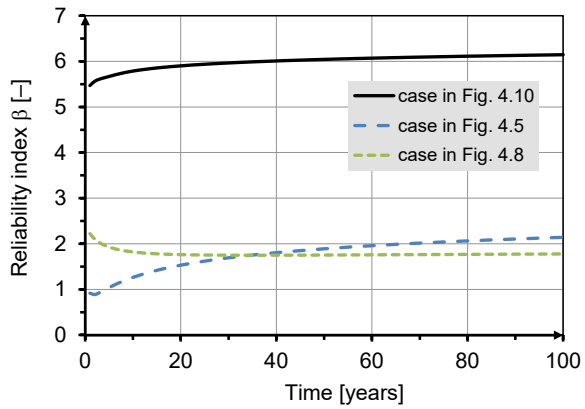

Fig. 4.14: Probability of corrosion initiation due to redistribution of residual chlorides

equation (4.10) shows the way the time- and depth-dependent redistribution of the residual chlorides has been formulated with the aid of the Riemann integral for the case in Fig. 4.10 (using the *Maxima* software). For the Riemann approximation, the required area of a function (in this case the integral in Eq. (4.9)) is determined according to the following principle. The overall area is divided into several partitions comprising inscribed or superscribed rectangles, the areas of which are subsequently added together. The inscribed rectangles assume the lowest value of the function (minimum) in each partition while the superscribed rectangles assume the highest value (maximum). The overall area lies between the sums of all of the inscribed rectangles (upper sum) and all of the superscribed rectangles (lower sum). The difference between the higher and lower sums decreases as the number of partitions increases, in other words the finer the partitions become. Consequently, both values will be approximately equal to the number indicating the overall area of the function.

In this case, the residual chloride profile was divided into very small partitions in 2 mm depth intervals so that equation (4.10) comprises a total of 76 conditions (not presented in full here). $D_{app}(t)$ was abbreviated to D for the purposes of the equation.

$$
\begin{aligned}
C(x,t) = -\Bigg(& erf\left(\frac{x+103}{2\sqrt{D\cdot t}}\right) + erf\left(\frac{x+101}{2\sqrt{D\cdot t}}\right) + erf\left(\frac{x+99}{2\sqrt{D\cdot t}}\right) \\
& + erf\left(\frac{x+95}{2\sqrt{D\cdot t}}\right) + 2erf\left(\frac{x+93}{2\sqrt{D\cdot t}}\right) + 2erf\left(\frac{x+91}{2\sqrt{D\cdot t}}\right) \\
& + 2erf\left(\frac{x+89}{2\sqrt{D\cdot t}}\right) + 3erf\left(\frac{x+87}{2\sqrt{D\cdot t}}\right) + 5erf\left(\frac{x+83}{2\sqrt{D\cdot t}}\right) \\
& + 5erf\left(\frac{x+81}{2\sqrt{D\cdot t}}\right) + 7erf\left(\frac{x+79}{2\sqrt{D\cdot t}}\right) + \cdots + 189erf\left(\frac{x+29}{2\sqrt{D\cdot t}}\right) \\
& - 1940erf\left(\frac{x+27}{2\sqrt{D\cdot t}}\right) + 1940erf\left(\frac{x-27}{2\sqrt{D\cdot t}}\right) \\
& - 189erf\left(\frac{x-29}{2\sqrt{D\cdot t}}\right) - \cdots - 7erf\left(\frac{x-79}{2\sqrt{D\cdot t}}\right) - 5erf\left(\frac{x-81}{2\sqrt{D\cdot t}}\right) \\
& - 5erf\left(\frac{x-83}{2\sqrt{D\cdot t}}\right) - 3erf\left(\frac{x-87}{2\sqrt{D\cdot t}}\right) - 2erf\left(\frac{x-89}{2\sqrt{D\cdot t}}\right) \\
& - 2erf\left(\frac{x-91}{2\sqrt{D\cdot t}}\right) - 2erf\left(\frac{x-93}{2\sqrt{D\cdot t}}\right) - erf\left(\frac{x-95}{2\sqrt{D\cdot t}}\right) \\
& - erf\left(\frac{x-99}{2\sqrt{D\cdot t}}\right) - erf\left(\frac{x-101}{2\sqrt{D\cdot t}}\right) - erf\left(\frac{x-103}{2\sqrt{D\cdot t}}\right)\Bigg)/2000
\end{aligned}
\qquad (4.10)
$$

4.2.4.3 Design approach

One of the most important conditions for predicting the service life is the availability of mathematical models to describe the relevant transport and/or damage mechanisms (see Chapter 2.2). As explained in the previous chapters, a generally valid mathematical formulation of the chloride transport in repaired structural elements with residual chlorides is not available. Nonetheless, a simplified approach for the durability design of such repair measures is presented below. The approach was first described in *Gehlen & Fischer 2007*.

The approach in *Carslaw & Jaeger 1959* (Eq. (4.1) to (4.4)) is used as the mathematical model. The residual chloride content at the surface of the rebars, C_r, is determined/ defined. The limit state is defined as the chloride content being reached at the surface of the rebars due to the ingress of external chlorides, its value being the difference between the critical chloride content C_{crit} and the residual chloride content, i.e. $C_{crit} - C_r = C^*_{crit}$. The gradient of the residual chloride profile and its redistribution are not taken into account. The procedure described here is illustrated in Fig. 4.15.

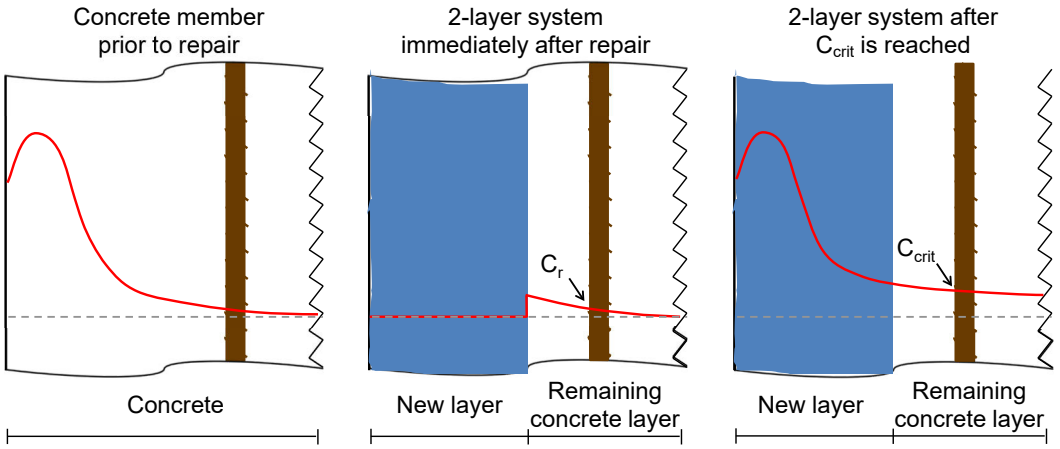

Fig. 4.15: Schematic representation of the chloride profiles in a concrete structural element before and after repair

The limit state equation for the reliability analysis is as follows, by analogy to the 2-layer system without residual chlorides (Eq. (4.5) or (4.7)):

$$g(X,t) = C^*_{crit} - C_{remain}(c_{remain}, t_{SL}) \qquad (4.11)$$

or

$$g(X,t) = c_{remain} - x^*_{crit}(t_{SL}) \qquad (4.12)$$

In Eq. (4.12), x^*_{crit} is the depth with the critical chloride content $C^*_{crit} = C_{crit} - C_r$.

Fig. 4.16, left, shows the results of reliability analyses for a 2-layer system comprising a 25 mm thick repair layer made of a CEM III/A concrete (w/c = 0.55) and a 35 mm thick remaining layer of CEM I concrete (w/c = 0.45) by way of an example. The residual chloride content at the surface of the rebars C_r is shown in Fig. 4.16, right, and satisfies both of the boundary conditions stated in Chapter 4.2.4.2. The residual chloride content at the surface of the rebars is 0.29 % by mass/b. By way of comparison, the case in which there are no residual chlorides in the remaining concrete layer (C_r = 0) is also considered. A target reliability index β_0 = 1.5 is achieved after 14 years (C_r = 0.29) or 23 years (C_r = 0).

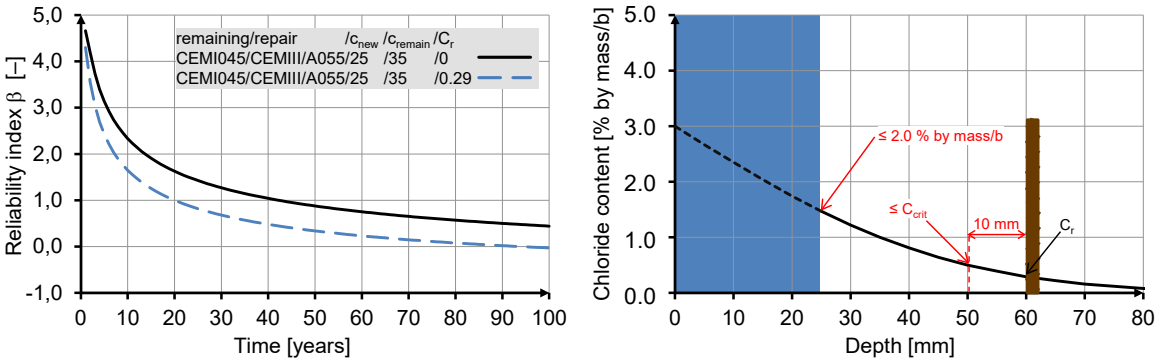

Fig. 4.16: Left: development of the reliability index over time after repairing a structural element containing residual chlorides – example; right: residual chloride profile

To verify the design approach, the impact of disregarding the redistribution of the residual chloride gradient on durability design according to the approach is first demonstrated in the following chapter. Comparative numerical studies with FEM follow in Chapter 4.2.4.5. Fig. 4.17 gives an overview of the process of verifying the design approach.

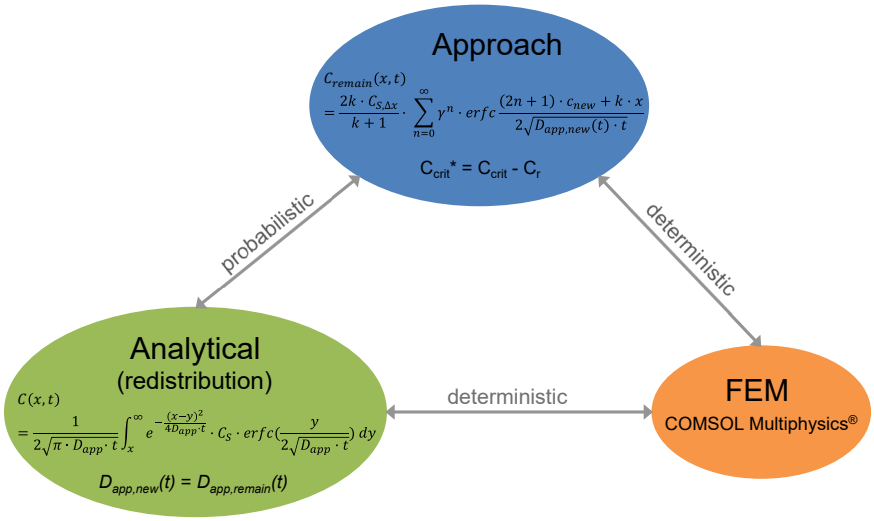

Fig. 4.17: Concept for verification of the design approach

4.2.4.4 Considering the redistribution of chlorides in the reliability analysis

At the end of Chapter 4.2.4.2, the boundary conditions defined for the residual chloride profile to prevent depassivation of the reinforcing steel due (solely) to the redistribution of the residual chlorides was demonstrated by sample probabilistic calculations. The convolution integral was included in Eq. (4.9) as an aid to calculation and applies when the repair layer and the remaining concrete layer have the same material properties, i.e. $D_{app.new}(t) = D_{app,remain}(t)$.

In the following, the redistribution of the residual chlorides with additional chloride ingress from an external source is considered in the same way as above and compared with the simplified design approach presented above with the aid of reliability analyses. Three cases are considered by way of examples (Fig. 4.18). The remaining concrete layer and the new repair layer are assumed to have the same material properties. The residual chloride profiles and the materials used are shown in Fig. 4.18, right. The design cases were all performed for a uniform action (coastal area, under water, $C_{S,0}$ = 3.0 % by mass/b, T_{real} = 10 °C). The residual chloride profiles were divided into 10 mm depth intervals for the purpose of approximating the convolution integrals (Eq. (4.9)) using the Riemann integral. The formulation determined for the design case with the residual chloride profile in Fig. 4.18, right, with C_r = 0.21 % by mass/b (dotted curve) is shown in equation (4.13) ($D = D_{app}(t)$). Larger intervals than those in Chapter 4.2.4.2 (10 mm instead of 2 mm) can be selected in this case as the redistribution of the residual chlorides had a comparably minor impact on the reliability analyses due to the dominant influence of the external chloride ingress. equation (4.13) thus includes far fewer conditions than equation (4.10) (19 instead of 76).

$$
\begin{aligned}
C(x,t) = -\Bigg(& erf\left(\frac{x+107}{2\sqrt{D\cdot t}}\right) + 5erf\left(\frac{x+97}{2\sqrt{D\cdot t}}\right) + 15erf\left(\frac{x+87}{2\sqrt{D\cdot t}}\right) \\
& + 24erf\left(\frac{x+77}{2\sqrt{D\cdot t}}\right) + 125erf\left(\frac{x+67}{2\sqrt{D\cdot t}}\right) + 240erf\left(\frac{x+57}{2\sqrt{D\cdot t}}\right) \\
& + 450erf\left(\frac{x+47}{2\sqrt{D\cdot t}}\right) + 710erf\left(\frac{x+37}{2\sqrt{D\cdot t}}\right) \\
& - 1570erf\left(\frac{x+27}{2\sqrt{D\cdot t}}\right) - 1570erf\left(\frac{x-27}{2\sqrt{D\cdot t}}\right) \\
& - 710erf\left(\frac{x-37}{2\sqrt{D\cdot t}}\right) + 450erf\left(\frac{x-47}{2\sqrt{D\cdot t}}\right) + 240erf\left(\frac{x-57}{2\sqrt{D\cdot t}}\right) \\
& + 125erf\left(\frac{x-67}{2\sqrt{D\cdot t}}\right) + 24erf\left(\frac{x-77}{2\sqrt{D\cdot t}}\right) + 15erf\left(\frac{x-87}{2\sqrt{D\cdot t}}\right) \\
& + 5erf\left(\frac{x-97}{2\sqrt{D\cdot t}}\right) + erf\left(\frac{x-107}{2\sqrt{D\cdot t}}\right) - 2000C_{S,0} \\
& \cdot erf\left(\frac{x}{2\sqrt{D\cdot t}}\right)\Bigg)/2000
\end{aligned}
\tag{4.13}
$$

From the β-t runs in Fig. 4.18, left, it can be seen that the curves only differ significantly from each other in the initial phase, i.e. in the first few years following the repair measure. Later on, the curves are almost coincident, indicating that the approach applied here delivers reliable results. The reason for the initially significantly lower reliability index obtained for the detailed method (considering the redistribution of chlorides) lies in the initial significant drop in the residual chloride gradient due to which the chloride concentration near the surface of the rebars increases even before there is a significant ingress of external chlorides. Erring on the safe side, the favourable influence of the age of the structural element at the time of the repair measure on the resistance of the remaining concrete to chloride penetration was not taken into consideration in the calculations. On the basis of this assumption, the uncertainty described above in the period immediately after the repair measure (high reliability indices) is regarded as insignificant.

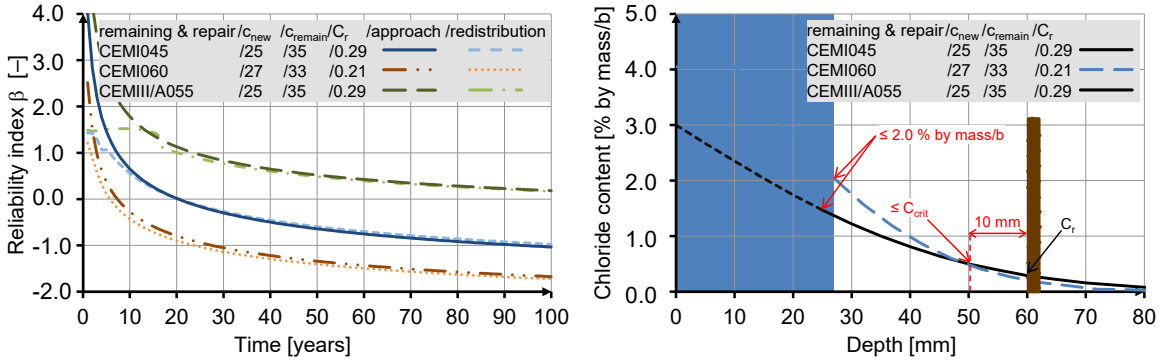

Fig. 4.18: Left: prediction of service life after repair – impact of the redistribution of the residual chlorides; right: residual chloride profiles

4.2.4.5 Comparative FE studies

Results of numerical studies conducted with the finite element method and the *COMSOL Multiphysics*® software are used below to verify the design approach presented above. As in the FE studies described in Chapter 4.2.4.2 on the required minimum depth of removal of the concrete cover, only the diffusion-controlled chloride transport was considered in this case. The calculations are deterministic, i.e. $\beta = 0$ or $p_f = 50$ %.

First of all, the plausibility of the analytical approach to taking account of the redistribution of the residual chlorides is studied with the aid of the Riemann integral. In Fig. 4.19, the results of the FE calculations are contrasted with the chloride profiles calculated with the aid of the Riemann integral shown in Fig. 4.18. The time selected for each profile was the service life calculated in Fig. 4.18 for a reliability index $\beta = 0$ (deterministic approach). The results demonstrate a perfect correlation between the analytical and numerical calculations. For the case with a CEMIII/A concrete with $w/c = 0.55$, the chloride profile obtained after 100 years is shown although the reliability index at this time is still greater than zero (see Fig. 4.18). It can also be seen in Fig. 4.19 that C_{crit} has not yet been reached at the surface of the rebars after 100 years.

The design case calculated with the simplified approach in Chapter 4.2.4.3, Fig. 4.16, left, was studied numerically in Fig. 4.20. The chloride profiles 5, 10, 50 and 105 years after a repair measure were calculated by FEM and presented. The critical chloride content, taken as $C_{crit} = 0.60$ % by mass/b in the reliability analyses, is reached at the surface of the rebars after 105 years. The time that elapses until the critical chloride content is reached, taken to be the service life of the structural element following the repair measure, is calculated as 94 years if the simplified approach is used (Fig. 4.16, left, $\beta = 0$). This result demonstrates a very good correlation between the results obtained with the simplified approach and those obtained by numerical calculations. The chloride transport is thus described with a sufficient degree of accuracy by the simplified probabilistic approach, permitting a reliable prediction of the condition.

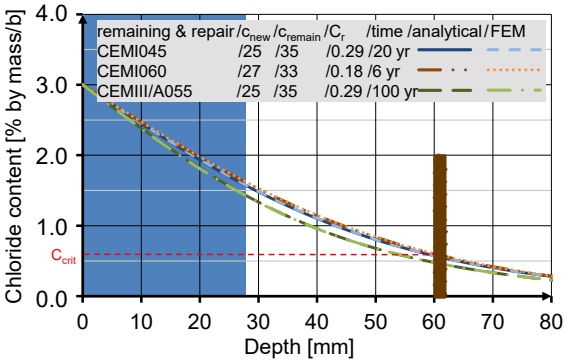

Fig. 4.19: Chloride profiles in repaired elements – Comparing the analytical approach (Rieman integral) with FEM

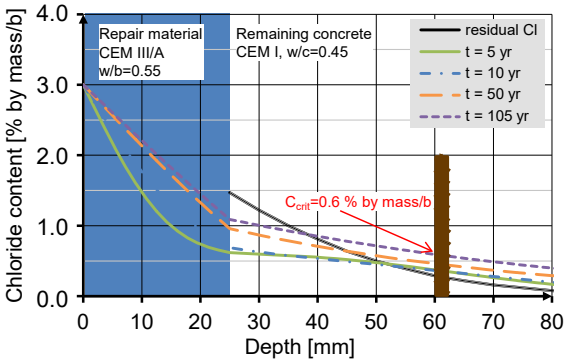

Fig. 4.20: Chloride profiles over time in a repaired element, calculated by FEM (COMSOL Multiphysics®)

4.2.4.6 Limitations of the approach

In the approach described above for estimating the remaining service life of structural elements after repair measures involving the removal and replacement of damaged concrete, only the chloride concentration at the surface of the rebars is taken into account for the residual chloride profile. The residual chloride gradient and its redistribution are not taken into account. This means that the approach is not applicable to cases in which the residual chloride profile does not reach the surface of the reinforcing steel (cf. Fig. 4.21).

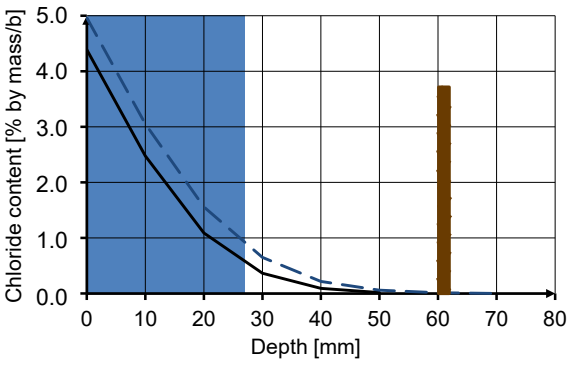

Fig. 4.21: Examples of design cases; the residual chloride profiles do not exhibit any chloride concentration at the rebar surface

For such cases, the residual service life after a repair measure may be estimated as follows. Assuming a low residual chloride concentration at the rebar surface, e.g. $C_r = 0.10$ % by mass/b, the remaining service life is calculated using the approach described above. The time that elapses until the residual chloride profile at the surface of the rebars reaches a concentration of 0.10 % by mass/b must be estimated conservatively and added to the remaining service life determined beforehand.

4.3 Semi-probabilistic design approach

In addition to the semi-probabilistic concept for the durability design of new structures, a similar concept for the design of repair measures involving the removal and replacement of damaged concrete was developed. It is based on the same principles and procedures (see Chapter 2.5).

For cases in which the concrete cover is fully replaced with a repair material and there are no residual chlorides in the remaining concrete layer behind the reinforcing steel (Case 1, Chapter 4.2.2), the semi-probabilistic design of the repair measures is performed with the same concept as for new structures (Chapter 2.5).

For other cases with partial replacement of the concrete cover, the limit state equations (4.11) und (4.12)) from the fully probabilistic design format are modified by taking account of the design values of the variables in equations (4.14) and (4.15):

$$g(X,t) = C^{*}_{crit,d} - C_{remain,d}(c_{remain,d}, t_{SL}) \qquad (4.14)$$

$$g(X,t) = c_{remain,d} - x^{*}_{crit,d}(t_{SL}) \qquad (4.15)$$

Similar to the design concept for new structures, the design variables selected for the repair layer and the remaining concrete layer were the two variables for the material resistance $D_{RCM}(t_0)$ and α_{RCM}, the layer thicknesses c_{new} and c_{remain} and the variable of the action $C_{S,\Delta x}$. Characteristic values, i.e. mean values, are used for the other variables. Thus the following partial factors are required:

$\gamma_{\alpha,r}$: partial factor for the ageing exponent of the remaining concrete ($\alpha_{RCM,remain,d} = \alpha_{RCM,remain,k} / \gamma_{\alpha,r}$)

$\gamma_{D,r}$: partial factor for the chloride migration coefficient of the remaining concrete at the reference time ($D_{RCM,remain,d}(t_0) = D_{RCM,remain,k}(t_0) \cdot \gamma_{D,r}$)

Δc_r: partial factor for the thickness of the remaining concrete layer over the reinforcing steel ($c_{remain,d} = c_{remain,k} - \Delta c_r \equiv c_{remain,min} = c_{remain,nom} - \Delta c_r$)

$\gamma_{\alpha,n}$: partial factor for the ageing exponent of the repair material ($\alpha_{RCM,new,d} = \alpha_{RCM,new,k} / \gamma_{\alpha,n}$)

$\gamma_{D,n}$: partial factor for the chloride migration coefficient of the repair material at the reference time ($D_{RCM,new,d}(t_0) = D_{RCM,new,k}(t_0) \cdot \gamma_{D,n}$)

Δc_n: partial factor for the thickness of the layer of repair material ($c_{new,d} = c_{new,k} - \Delta c_n \equiv c_{new,min} = c_{new,nom} - \Delta c_n$); corresponds to the allowance for deviation of the thickness of the layer of repair material (Δd_E)

γ_C: partial factor for the surface chloride concentration ($C_{S,\Delta x,d} = C_{S,\Delta x,k} \cdot \gamma_C$)

The limit state equations (4.14) and (4.15) can therefore be formulated as follows:

$$C_{crit,k} - C_{r,k} = \frac{2k_{D,d} \cdot \gamma_C \cdot C_{S,\Delta x,k}}{k_{D,d} + 1} \cdot erfc \frac{c_{min,new} - \Delta x_k + k_{D,d} \cdot c_{min,remain}}{2\sqrt{k_{e,k} \cdot D_{RCM,new,k}(t_0) \cdot \gamma_{D,n} \cdot \left(\frac{t_0}{t_{SL}}\right)^{\frac{\alpha_{RCM,new,k}}{\gamma_{\alpha,n}}} \cdot t_{SL}}} \tag{4.16}$$

and

$$c_{min,remain} = \frac{1}{k_{D,d}} \cdot \left(2erf^{-1}\left(1 - \frac{C_{crit,k} - C_{r,k}}{\gamma_C \cdot C_{S,\Delta x,k}} \cdot \frac{k_{D,d} + 1}{2k_{D,d}}\right) \cdot \sqrt{k_{e,k} \cdot D_{RCM,new,k}(t_0) \cdot \gamma_{D,n} \cdot \left(\frac{t_0}{t_{SL}}\right)^{\frac{\alpha_{RCM,new,k}}{\gamma_{\alpha,n}}} \cdot t_{SL}} - c_{min,new} + \Delta x_k \right) \tag{4.17}$$

with:

$$k_{D,d} = \sqrt{\frac{D_{app,new,d}(t)}{D_{app,remain,d}(t)}} = \sqrt{\frac{D_{RCM,new,k}(t_0) \cdot \gamma_{D,n} \cdot \left(\frac{t_0}{t_{SL}}\right)^{\frac{\alpha_{RCM,new,k}}{\gamma_{\alpha,n}}}}{D_{RCM,remain,k}(t_0) \cdot \gamma_{D,r} \cdot \left(\frac{t_0}{t_{SL}}\right)^{\frac{\alpha_{RCM,remain,k}}{\gamma_{\alpha,r}}}}} \tag{4.18}$$

If the apparent chloride diffusion coefficient $D_{app}(t)$ is determined by Approach A or C (see Chapter 2.3.2.2) the mean values of the variables $D_{nss}(t_0)$ and α_{nss} or $D_{nss}(t_0)$ and α_{app} can be used as characteristic values for design purposes. The partial factors used in Approach B are also used for these two approaches.

The partial factors were determined by evaluating the fully probabilistic calculations for several design cases in the same way as for the design concept for new structures. The partial factors were selected in such a way that the range of reliabilities obtained for the design cases is small and close to the target reliability index β_0. They are summarized in Table 4.1. The partial factors selected for the material properties of the two layers and for the action were less than 1.0 (0.9) to achieve a target reliability index β_0 of 0.5, i.e. the

partial factors make the characteristic values of the variables more favourable. This is because reliabilities far greater than β_0 = 0.5 are achieved if the same allowance for deviation of 10 mm is assumed for both layer thicknesses. The global safety factor determined in *Greve-Dierfeld 2015* for the semi-probabilistic design concept for durability design with regard to carbonation-induced corrosion of the reinforcing steel is also less than 1.0 (γ_f = 0.7) for β_0 = 0.5 (for XC3).

Table 4.1: Partial factors specified for the semi-probabilistic approach for exposure classes XS2, XS3, XD2 and XD3

Target reliability index β_0	Partial factors						
	$\gamma_{\alpha,r}$	$\gamma_{D,r}$	Δc_r	$\gamma_{\alpha,n}$	$\gamma_{D,n}$	Δc_n	γ_C
1.5 (p_f = 6.7 %)	1.1	1.1	10 mm	1.2	1.2	10 mm	1.9
0.5 (p_f = 30.9 %)	0.9	0.9	10 mm	0.9	0.9	10 mm	0.9

Examples of several design cases considered to determine the partial factors for exposure class XS2 for a target service life t_{SL} of 50 years and a target reliability index β_0 of 1.5 are shown in Table 4.2 to Table 4.5. For the design cases in the first two tables there are no residual chlorides present on the surface of the rebars C_r while Table 4.4 and Table 4.5 include design cases with C_r = 0.1, 0.2 and 0.3 % by mass/b.

For the design cases with C_r = 0, the reliability indices obtained with the partial factors are all greater than 1.3, with the maximum being 2.17. If residual chlorides are present on the surface of the reinforcing steel the reliability indices obtained decrease in very unfavourable cases to values as low as 1.10 (C_r = 0.3 and $C_{S,\Delta x}$ = 5.0 % by mass/b).

Examples of design cases considered to determine the partial factors for β_0 = 0.5 are shown in Table 4.6. Most of the reliability indices obtained are greater than 0.5. However, they decrease to values as low as 0.23 for the very unfavourable cases nos. 13 to 16 (extremely diffusion-open remaining concrete and extremely high loads).

In Chapter 4.2.3.2, Fig. 4.3, it was shown that, in some cases, the reliability analysis performed for the two-layer model results in higher reliability indices than for the one-layer model. This may be correct in terms of probability theory but does not fully correspond to construction practice. This means that it is not always possible to obtain the actual safety level with the reliability index calculated with the 2-layer model based on experience and an understanding of the probabilistic interpretation of the limit state under consideration. For this reason, the layer thicknesses for five different design cases were calculated using not only the semi-probabilistic concept with the two-layer model but also the concept with the one-layer model and the results compared with each other. It was assumed that the remaining concrete and the repair layer had the same material properties to enable the calculations to be performed for the one-layer model. The results are shown

in Table 4.7 (for β_0 = 1,5) and Table 4.8 (for β_0 = 0,5). Apart from one case with unrealistically large layer thicknesses (case no. 3), greater layer thicknesses are obtained with the two-layer system, i.e. a higher safety level is achieved with the two-layer system.

The same was considered in Table 4.9 (for β_0 = 1,5) and Table 4.10 (for β_0 = 0,5) for two design cases where the remaining concrete and the repair layer have different material properties. The layer thickness was calculated using the one-layer system, once for the case where the repair layer and the remaining concrete are both made of the same material and once for the case where the remaining concrete has the same material properties as the repair layer. For β_0 = 1.5, the layer thickness obtained with the two-layer system is, as expected, between the layer thicknesses obtained with the one-layer model. For β_0 = 0.5, the layer thickness obtained with the two-layer model for case no. 2 is greater than the two values calculated with the one-layer model, indicating a higher safety level for the two-layer model.

Results similar to those for XS2 are obtained for design cases in exposure class XS3 if the defined partial factors are used.

Table 4.2: Design cases considered to determine the partial factors for XS2, t_{SL}=50 years, β_0 =1.5 and C_r=0

Case no.	Remaining concrete			Repair material		$C_{S,\Delta x}$	$c_{new,nom}$ required for β_0=1.5	$c_{new,nom}$ calculated using factors	β obtained using factors
	$D_{RCM}(t_0)$	α_{RCM}	c_{nom}	$D_{RCM}(t_0)$	α_{RCM}				
	[$\cdot 10^{-12}$m²/s]	[–]	[mm]	[$\cdot 10^{-12}$m²/s]	[–]	[% by mass/b]	[mm]	[mm]	[–]
1	10.0	0.3	35	5.0	0.5	3.0	32.6	35.4	1.59
2			25				41.5	40.1	1.46
3			35	1.9	0.45		20.1	25.3	1.75
4			25				26.3	28.6	1.61
5			35	9.0	0.6		23.9	36.3	1.99
6			25				30.7	41.0	1.88
7			35	4.0	0.4		37.3	41.6	1.64
8			25				46.6	47.0	1.51
9			35	5.0	0.5	5.0	45.8	42.4	1.41
10			25				55.0	47.1	1.30
11			35	1.9	0.45		29.6	30.5	1.57
12			25				36.0	33.8	1.41
13			35	9.0	0.6		34.3	43.4	1.81
14			25				43.1	48.2	1.72
15			35	5.0	0.5	2.0	21.4	29.2	1.78
16				1.9	0.45		12.1	20.6	1.97
17				9.0	0.6		15.1	30.0	2.17
18				4.0	0.4		25.3	34.5	1.84

Table 4.3: Design cases considered to determine the partial factors for XS2, t_{SL}=50 years, β_0=1.5 and C_r=0 (Table 4.2 continued)

Case no.	Remaining concrete			Repair material		$C_{S,\Delta x}$	$c_{new,nom}$ required for β_0=1.5	$c_{new,nom}$ calculated using factors	β obtained using factors	
	$D_{RCM}(t_0)$	α_{RCM}	c_{nom}	$D_{RCM}(t_0)$	α_{RCM}					
	[$\cdot 10^{-12}$m²/s]	[–]	[mm]	[$\cdot 10^{-12}$m²/s]	[–]	[% by mass/b]	[mm]	[mm]	[–]	
19	20.0	0.3	35	1.9	0.45	3.0	21.6	24.6	1.64	
20			25				26.3	26.9	1.53	
21			35	10	0.3		83.0	91.2	1.69	
22			25				94.3	99.2	1.61	
23			35	1.9	0.45	5.0	31.8	30.2	1.44	
24			25				36.6	32.6	1.34	
25			35	10	0.3		106.0	107.0	1.52	
26			25				117.5	115.0	1.45	
27			35	1.9	0.45	2.0	12.8	19.5	1.86	
28			35	10	0.3		62.8	77.4	1.86	
29	4.0	0.4	35	5.0	0.5	3.0	17.9	28.6	1.87	
30			25				29.3	38.4	1.77	
31			35	5.0	0.5	5.0	28.1	35.0	1.70	
32			25				40.6	44.8	1.61	
33			35			2.0	9.5	23.0	2.05	
34	10.0	0.3	25	5.0	0.5	5.0	22.8	30.4	1.95	for t_{SL}=10 years
35				1.9	0.45		15.3	22.4	2.13	
36	20.0	0.3		1.9	0.45		16.6	22.4	2.01	

Table 4.4: Design cases considered to determine the partial factors for XS2, t_{SL}=50 years, β_0=1.5, c_{remain}=25 mm, C_r=0.1, 0.2 and 0.3

Case no.	Remaining concrete			Repair material		$C_{S,\Delta x}$	$c_{new,nom}$ required for β_0=1.5	$c_{new,nom}$ calculated using factors	β obtained using factors
	$D_{RCM}(t_0)$	α_{RCM}	C_r	$D_{RCM}(t_0)$	α_{RCM}				
	[$\cdot 10^{-12}$m²/s]	[–]	[% by mass/b]	[$\cdot 10^{-12}$m²/s]	[–]	[% by mass/b]	[mm]	[mm]	[–]
1	10.0	0.3	0.1	5.0	0.5	3.0	46.5	42.7	1.40
2			0.2				52.3	45.7	1.33
3			0.3				59.3	49.4	1.26
4			0.1	1.9	0.45		29.9	30.5	1.53
5			0.2				34.5	32.8	1.43
6			0.3				39.1	35.5	1.36
7			0.1	9.0	0.6		34.5	43.7	1.82
8			0.2				39.6	46.8	1.73
9			0.3				44.7	50.5	1.68
10			0.1	4.0	0.4		51.8	49.9	1.45
11			0.2				57.9	53.4	1.38
12			0.3				65.4	57.6	1.30
13			0.1	5.0	0.5	5.0	59.5	46.4	1.18
14			0.2				64.7	49.2	1.14
15			0.3				71.2	52.7	1.09
16			0.1	1.9	0.45		39.2	33.3	1.28
17			0.2				43.0	35.4	1.23
18			0.3				47.7	38.0	1.17

Table 4.5: Design cases considered to determine the partial factors for XS2, t_{SL}=50 years, β_0 =1.5, c_{remain}=25 mm, C_r=0.1, 0.2 and 0.3 (Table 4.4 continued)

Case no.	Remaining concrete			Repair material		$C_{S,\Delta x}$	$c_{new,nom}$ required for β_0=1.5	$c_{new,nom}$ calculated using factors	β obtained using factors
	$D_{RCM}(t_0)$	α_{RCM}	C_r	$D_{RCM}(t_0)$	α_{RCM}				
	[$\cdot 10^{-12}$m²/s]	[–]	[% by mass/b]	[$\cdot 10^{-12}$m²/s]	[–]	[% by mass/b]	[mm]	[mm]	[–]
19	10.0	0.3	0.1	9.0	0.6	5.0	44.8	47.5	1.58
20			0.2				49.0	50.4	1.54
21			0.3				54.1	53.9	1.49
22	20.0	0.3	0.1	1.9	0.45	3.0	30.1	29.0	1.45
23			0.2				34.5	31.5	1.38
24			0.3				40.0	34.4	1.29
25			0.1	10	0.3		102.7	105.0	1.55
26			0.2				112.7	111.8	1.48
27			0.3				125.0	120.3	1.41
28			0.1	1.9	0.45	5.0	36.6	32.0	1.20
29			0.2				44.1	34.2	1.15
30			0.3				49.0	37.0	1.10
31			0.1	10	0.3		125.4	113.4	1.27
32			0.2				134.5	119.9	1.23
33			0.3				145.8	127.9	1.19
34	4.0	0.4	0.1	5.0	0.5	5.0	44.2	44.2	1.50
35			0.2				49.0	46.8	1.45
36			0.3				54.6	50.0	1.40

Table 4.6: Design cases considered to determine the partial factors for XS2, t_{SL}=50 years, β_0=0.5, c_{remain}=25 mm, C_r=0, 0.1, 0.2 and 0.3

Case no.	Remaining concrete			Repair material		$C_{S,\Delta x}$	$c_{new,nom}$ required for β_0=0.5	$c_{new,nom}$ calculated using factors	β obtained using factors
	$D_{RCM}(t_0)$	α_{RCM}	C_r	$D_{RCM}(t_0)$	α_{RCM}				
	[$\cdot 10^{-12}$m²/s]	[–]	[% by mass /b]	[$\cdot 10^{-12}$m²/s]	[–]	[% by mass/b]	[mm]	[mm]	[–]
1	10.0	0.3	0	9.0	0.6	3.0	11.9	15.5	0.74
2			0.1				14.5	17.3	0.68
3			0.2				17.4	19.4	0.62
4			0.3				21.0	21.9	0.55
5			0	1.9	0.45		8.6	12.8	0.79
6			0.1				10.9	14.3	0.73
7			0.2				13.5	16.1	0.66
8			0.3				16.6	18.1	0.59
9			0	5.0	0.5		14.5	16.4	0.60
10			0.1				17.4	18.3	0.54
11			0.2				20.8	20.5	0.49
12			0.3				24.9	23.1	0.43
13	20.0	0.3	0	4.0	0.4	5.0	29.9	25.8	0.34
14			0.1				33.1	27.9	0.31
15			0.2				36.9	30.3	0.27
16			0.3				41.5	33.3	0.23
17	5.0	0.4		3.0	0.4		20.4	25.2	0.70
18							23.7	27.4	0.65

Table 4.7: Verification of the semi-probabilistic concept for the 2-layer system by means of the concept for the 1-layer system; remaining concrete and repair material have the same material properties; XS2, β_0=1.5, t_{SL}=50 years, C_r=0

Case no.	Remaining concrete and repair material		$c_{remain,nom}$	$C_{S,\Delta x}$	$c_{new,nom}$ [1] 2-layer system	β [2] 2-layer system	$c_{new,nom}$ [3] 1-layer system	β [4] 1-layer system	β [5] 1-layer sys. with $c_{new,nom}$ of 2-layer sys.
	$D_{RCM}(t_0)$	α_{RCM}							
	[$\cdot 10^{-12}$ m²/s]	[–]	[mm]	[% by mass/b]	[mm]	[–]	[mm]	[–]	[–]
1	5.0	0.5	25	3.0	36.6	1.85	34.9	1.31	1.35
2	9.0	0.6			37.4	2.26	36.1	1.75	1.79
3	10.0	0.3	35		88.7	1.79	96.2	1.70	1.54
4	1.9	0.45			12.1	1.98	10.2	1.38	1.46
5			25	5.0	28.2	1.88	25.4	1.25	1.35

[1] *thickness of the repair layer calculated for the 2-layer system with the semi-probabilistic concept*
[2] *reliability index obtained (with the reliability analysis for the two-layer system) with the thickness of the repair layer calculated for the two-layer system with the semi-probabilistic concept*
[3] *thickness of the repair layer calculated for the one-layer system (new structure) with the semi-probabilistic concept*
[4] *reliability index obtained (with the reliability analysis for the one-layer system) with the thickness of the repair layer calculated for a one-layer system with the semi-probabilistic concept*
[5] *reliability index obtained (with the reliability analysis for the one-layer system) with the thickness of the repair layer calculated for a two-layer system with the semi-probabilistic concept*

*Table 4.8: Verification of the semi-probabilistic concept for the 2-layer system by means of the concept for the 1-layer system; remaining concrete and repair material have the same material properties; XS2, β_0=**0.5**, t_{SL}=50 years, C_r=0*

Case no.	Remaining concrete and repair material $D_{RCM}(t_0)$	Remaining concrete and repair material α_{RCM}	$c_{remain,nom}$	$C_{S,\Delta x}$	$c_{new,nom}$ [1] 2-layer system	β [2] 2-layer system	$c_{new,nom}$ [3] 1-layer system	β [4] 1-layer system	β [5] 1-layer sys. with $c_{new,nom}$ of 2-layer sys.
	[$\cdot 10^{-12}$m²/s]	[–]	[mm]	[% by mass/b]	[mm]	[–]	[mm]	[–]	[–]
1	5.0	0.5	25	3.0	13.0	1.04	11.4	0.57	0.63
2	9.0	0.6			11.9	1.13	11.0	0.79	0.83
3	10.0	0.3	35		37.3	0.44	44	0.44	0.25
4	1.9	0.45	25		8.3	1.26	4.0	0.67	0.87
5				5.0	11.4	1.13	7.9	0.58	0.73

[1] *thickness of the repair layer calculated for the 2-layer system with the semi-probabilistic concept*
[2] *reliability index obtained (with the reliability analysis for the two-layer system) with the thickness of the repair layer calculated for the two-layer system with the semi-probabilistic concept*
[3] *thickness of the repair layer calculated for the one-layer system (new structure) with the semi-probabilistic concept*
[4] *reliability index obtained (with the reliability analysis for the one-layer system) with the thickness of the repair layer calculated for a one-layer system with the semi-probabilistic concept*
[5] *reliability index obtained (with the reliability analysis for the one-layer system) with the thickness of the repair layer calculated for a two-layer system with the semi-probabilistic concept*

Table 4.9: Verification of the semi-probabilistic concept for the 2-layer system by means of the concept for 1-layer system; remaining concrete and repair material have different material properties; XS2, β_0=1.5, t_{SL}=50 years, C_r=0

Case no.	Remaining concrete		Repair material		$c_{remain,nom}$	$C_{S,\Delta x}$	$c_{new,nom}$ [1] 2-layer system	$c_{new,nom}$ [2] 1-layer sys with remaining concrete only	$c_{new,nom}$ [3] 1-layer sys with repair material only
	$D_{RCM}(t_0)$	α_{RCM}	$D_{RCM}(t_0)$	α_{RCM}					
	[$\cdot 10^{-12}$m²/s]	[–]	[$\cdot 10^{-12}$m²/s]	[–]	[mm]	[% by mass/b]	[mm]	[mm]	[mm]
1	4.0	0.4	3.0	0.4	25	3.0	39.0	43.5	35.7
2	3.0	0.4		0.45			33.3	35.7	29.3

[1] *thickness of the repair layer calculated for the two-layer system with the semi-probabilistic concept*
[2] *thickness of the repair layer calculated for the one-layer system (new structure) with the semi-probabilistic concept for cases in which both layers are made of the remaining concrete*
[3] *thickness of the repair layer calculated for the one-layer system (new structure) with the semi-probabilistic concept for cases in which both layers are made of the repair material*

Table 4.10: Verification of the semi-probabilistic concept for the 2-layer system by means of the concept for 1-layer system; remaining concrete and repair material have different material properties; XS2, β_0=0.5, t_{SL}=50 years, C_r=0

Case no.	Remaining concrete		Repair material		$c_{remain,nom}$	$C_{S,\Delta x}$	$c_{new,nom}$ [1] 2-layer system	$c_{new,nom}$ [2] 1-layer sys. with remaining concrete only	$c_{new,nom}$ [3] 1-layer sys. with repair material only
	$D_{RCM}(t_0)$	α_{RCM}	$D_{RCM}(t_0)$	α_{RCM}					
	[$\cdot 10^{-12}$m²/s]	[–]	[$\cdot 10^{-12}$m²/s]	[–]	[mm]	[% by mass/b]	[mm]	[mm]	[mm]
1	4.0	0.4	3.0	0.4	25	3.0	16.3	17.1	12.8
2	3.0	0.4		0.45			13.4	12.8	8.8

[1] *thickness of the repair layer calculated for the two-layer system with the semi-probabilistic concept*
[2] *thickness of the repair layer calculated for the one-layer system (new structure) with the semi-probabilistic concept for cases in which both layers are made of the remaining concrete*
[3] *thickness of the repair layer calculated for the one-layer system (new structure) with the semi-probabilistic concept for cases in which both layers are made of the repair material*

4.4 Simplified design approach with nomograms

To simplify the design process, the semi-probabilistic concept for repairing concrete members by replacing damaged concrete was transferred to nomograms in the same way as for the durability design of new structures. The design nomograms thus created are presented in Annex E. Each nomogram comprises a rectangular graph in which the parameter d_C is determined from the sets of curves for $k_{D,d}$, the input parameter being d_R. The parameters $k_{D,d}$, d_R and d_c are determined/defined as follows.

The parameter $k_{D,d}$ expresses the relationship between the properties of the remaining concrete and those of the repair material. The index "*d*" indicates that this particular parameter is a design value, i.e. partial factors have to be applied to each of the variables. The time-dependent parameter k_D was presented in equation (4.18) in a previous chapter. To facilitate the use of the nomograms, $k_{D,d}$ is simplified by assuming it is not time-dependent, as shown in equation (4.19). The period of time is taken to be 50 years, in other words, the relationship between the material properties of both layers is always calculated for a lifespan of 50 years and the result taken into account in the calculations. It was demonstrated by the cases considered in Table 4.11 that simplifying $k_{D,d}$ in this way has only a negligible impact on durability design.

$$k_{D,d} = \sqrt{\frac{D_{app,new}(t)}{D_{app,remain}(t)}} \cong 0{,}04^{\left(\frac{\alpha_{new}}{\gamma_{\alpha,n}} - \frac{\alpha_{remain}}{\gamma_{\alpha,r}}\right)} \cdot \sqrt{\frac{D_{RCM,new}(t_0) \cdot \gamma_{D,n}}{D_{RCM,remain}(t_0) \cdot \gamma_{D,r}}} \qquad (4.19)$$

The parameter d_R is also a design variable and takes account of the resistance of the repair material to chloride penetration as follows during the planned service life and the service life itself:

$$d_R = \sqrt{D_{app,new,d}(t_{SL}) \cdot t_{SL}} = \sqrt{k_e \cdot D_{RCM,new}(t_0) \cdot \gamma_{D,n} \cdot \left(\frac{t_0}{t_{SL}}\right)^{\frac{\alpha_{new}}{\gamma_{\alpha,n}}} \cdot t_{SL}} \qquad (4.20)$$

The parameter d_c is the result read from the nomogram and is defined as follows:

$$d_c = 2erf^{-1}\left(1 - \frac{C_{crit,k} - C_{r,k}}{\gamma_C \cdot C_{S,\Delta x,k}} \cdot \frac{k_{D,d} + 1}{2k_{D,d}}\right) \cdot d_R \qquad (4.21)$$

The minimum layer thickness is finally calculated using equation (4.22):

$$c_{new,min} = d_c - k_{D,d} \cdot c_{remain,min} + \Delta x \qquad (4.22)$$

In contrast to the nomograms for new structures, it is not possible to invert these nomograms, i.e. to take d_c as the input parameter and d_R as the result.

Design for cases in which the entire concrete cover is replaced with a repair material (Case 1, Chapter 4.2.2) is performed using the nomograms developed for new structures in Annex D. In this case, the minimum layer thickness of the repair material is shown in accordance with *DAfStb RiLi SIB 2001*, with $d_{E,min}$ (instead of $c_{new,min}$).

A minimum layer thickness of 20 mm was selected for reasons relating to execution and construction practice.

Two examples of calculating the minimum layer thickness for repair measures involving replacement of damaged concrete are shown below.

Example 4.1: Design of the layer thickness for complete replacement of the concrete cover of a structural element under XD2 exposure (without residual chlorides)

Information:

Design service life after repair: t_{SL} = 50 years

Safety level: β_0 = 1.5

Repair material: concrete with CEM I + 22% FA with $D_{RCM}(t_0=28\ d)$ = 5.5 · 10^{-12} m²/s

Chloride action: $C_{S,0}$ = 4.0 % by mass/b

Main type of binder: CEM I + 22% FA

Solution:

α_{RCM} = 0.60 (Table 2.5, CEM II/A-V)

Fig. D.5 → $d_{E,min}$ ~ 53 mm for XD3 / XS3

For XD2: $d_{E,min}$ ~ 53 mm - 10 mm ~ 43 mm

Allowance for deviation of the layer thickness Δd_E = 10 mm → $d_{E,nom}$ ~ 53 mm

Example 4.2: Design of the layer thickness for partial replacement of the concrete cover of a structural element under XS3 exposure with residual chlorides.

Information:

Age of structural element: t = 40 years

Target service life after repair: t_{SL} = 50 years, safety level: β_0 = 1.5

Depth of concrete cover c_{nom} = 60 mm, Δc = 10 mm

Concrete composition: CEM III/A, no further details or parameters are available

Repair material: $D_{nss}(t_0=28d)$ = 3.0 · 10^{-12} m²/s, α_{nss} = 0.50

Chloride profile determined immediately before repair (from Example 3.1, Chapter 3.3):

Table ex. 4.2-1: Measured chloride contents at the inspection time of 40 years

	Chloride content [% by mass/b] Mean depth of measurements [mm]						
	5	15	25	35	45	55	65
Mean value	2.1	2.6	1.82	0.82	0.41	0.25	0.02

Solution:

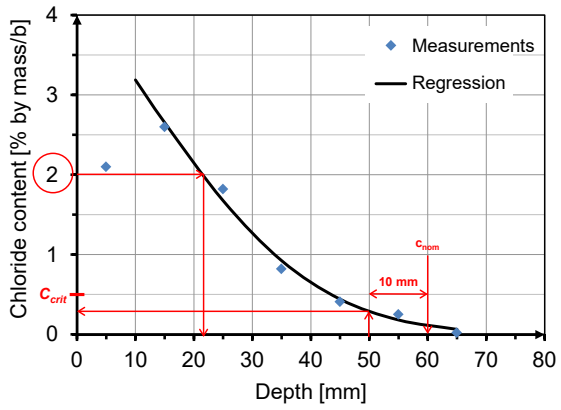

Fig. ex. 4.2-1: Deriving $D_{app}(t_{insp})$ and $C_{S,\Delta x,insp}$ at t_{insp} = 40 years from the regression analysis

from Fig. ex. 4.2-1: $D_{app}(t_{insp})$ = 0.221 · 10^{-12} m²/s and $C_{S,\Delta x,insp}$ = 3.2 % by mass/b

→ $C(x=c_{nom}, t_{insp})$ = 0.20 % by mass/b = C_r

Depth to which concrete is removed: x = 22 mm ($C(x=22mm,\ t_{insp})$ = 2.0 % by mass/b and $C(x=50mm,\ t_{insp}) \leq 0.5$ % by mass/b) → $c_{remain,nom}$ = 60 – 22 = 38 mm and $c_{remain,min}$ = 38 – 10 = 28 mm

Ageing exponent α_{app} = 0.40 (Table 2.5, CEM III/A)

$$D_{app}(t_0) = \frac{1}{k_e} \cdot D_{app}(t_{insp}) \cdot \left(\frac{t_0}{t_{insp}}\right)^{-\alpha_{app}} = 2.5 \cdot 10^{-12}\ m^2/s$$

$$k_{D,d} = 0.04^{\left(\frac{\alpha_{new}}{\gamma_{\alpha,n}} - \frac{\alpha_{remain}}{\gamma_{\alpha,r}}\right)} \cdot \sqrt{\frac{D_{RCM,new}(t_0) \cdot \gamma_{D,n}}{D_{RCM,remain}(t_0) \cdot \gamma_{D,r}}} = 0.04^{\left(\frac{0.5}{1.2} - \frac{0.4}{1.1}\right)} \cdot \sqrt{\frac{3.0 \cdot 1.2}{2.5 \cdot 1.1}} = 0.96$$

$$d_R = \sqrt{k_e \cdot D_{RCM,new}(t_0) \cdot \gamma_{D,n} \cdot \left(\frac{t_0}{t_{SL}}\right)^{\frac{\alpha_{new}}{\gamma_{\alpha,n}}} \cdot t_{SL}}$$

$$= \sqrt{0.56 \cdot (3.0 \cdot 10^{-12} \cdot 365 \cdot 24 \cdot 3600) \cdot 1.2 \cdot \left(\frac{0.0767}{50}\right)^{\frac{0.5}{1.2}} \cdot 50 \cdot 1000}$$

$$= 14.6\ mm$$

$C_{S,\Delta x,insp}$ = 3.0 % by mass/b and C_r = 0.2 % by mass/b → Fig. E.7 → d_c ~ 37.2 mm

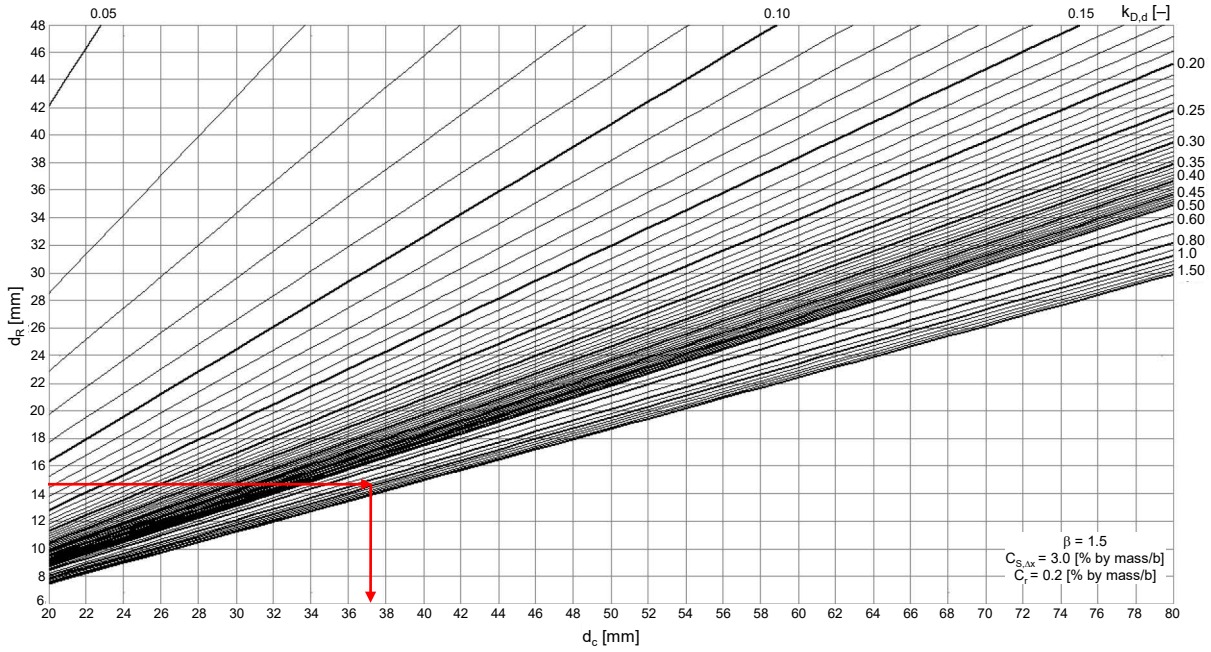

Fig. ex. 4.2-2: Design nomogram for β_0=1.5, $C_{S,\Delta x}$=3.0 wt.-%/b, C_r=0.2 wt.-%/b (see Fig. E.7, Annex E)

$$c_{new,min} = d_c - k_{D,d} \cdot c_{remain,min} + \Delta x = 37.2 - 0.96 \cdot 28 + 10 = 20.3\ mm \geq 20mm$$

→ $d_{E,min}$ = 20.3 mm

Δd_E = 10 mm → $d_{E,nom}$ = 30.3 mm

Example 4.3: Example of application from Chapter 2.6

Information:

The concrete cover is fully replaced with a repair material with:

$D_{RCM}(t_0=28d)$ = 2.65 · 10^{-12} m²/s and α_{RCM} = 0.45

$C_{S,\Delta x}$ = 4.0 % by mass/b, target service life t_{SL} = 70 years, β_0 = 1.5

Solution:

$$k_{D,d} = 0.04^{\left(\frac{0.45}{1.2}-\frac{0.45}{1.1}\right)} \cdot \sqrt{\frac{2.65 \cdot 1.2}{2.65 \cdot 1.1}} = 1.17$$

$$d_R = \sqrt{0.56 \cdot (2.65 \cdot 10^{-12} \cdot 365 \cdot 24 \cdot 3600) \cdot 1.2 \cdot \left(\frac{0.0767}{70}\right)^{\frac{0.45}{1.2}} \cdot 70 \cdot 1000} = 17.5\ mm$$

Fig. E.9 → d_c ~ 44.5 mm → $c_{new,min} = 44.5 - 1.17 \cdot 0 + 0 = 44.5\ mm$

The minimum layer thickness calculated using the nomograms in Annex E is slightly less than that calculated using the nomograms for new structures in Annex D (c_{min} = 50 mm, see example in Chapter 2.6). The nomograms in Annex D must be used for the durability design of repair measures in which the concrete cover is removed completely and replaced.

Table 4.11: Verification of the applicability of the parameter k_D in the approximated equation (4.19) (without partial factors)

Case no.	Remaining concrete			Repair material			$C_{S,\Delta x}$	t_{SL}	k_D exact	k_D approx.	C(x=$c_{new,nom}$. t) with k_D exact	C(x=$c_{new,nom}$. t) with k_D approx.	Difference between the last two columns
	$D_{RCM}(t_0)$	α_{RCM}	$c_{remain,nom}$	$D_{RCM}(t_0)$	α_{RCM}	$c_{new,nom}$							
	[$\cdot 10^{-12}$m²/s]	[–]	[mm]	[$\cdot 10^{-12}$m²/s]	[–]	[mm]	[% by mass/b]	[year]	[–]	[–]	[% by mass/b]	[% by mass/b]	[%]
1	10.0	0.3	35	5.0	0.4	25	3.0	10	0.5543	0.5125	0.0110	0.0140	+27.3
2								20	0.5354		0.0527	0.0571	+8.3
3								30	0.5246		0.1021	0.1054	+3.2
4								50	0.5114		0.1937		0
5								70	0.5029		0.2698	0.2673	-0.9
6								100	0.4940		0.3606	0.3564	-1.2
7	10.0	0.3	35	8.0	0.35	25	3.0	10	0.7919	0.7615	0.0533	0.0592	+11.1
8								20	0.7783		0.1731	0.1793	+3.6
9								30	0.7704		0.2842	0.2882	+1.4
10								50	0.7607		0.4595		0
11								70	0.7543		0.5895	0.5871	-0.4
12								100	0.7476		0.7334	0.7296	-0.5
13	20.0	0.20	35	2.0	0.55	15	4.0	10	0.1348	0.1025	0.0044	0.0057	+29.5
14								20	0.1194		0.0158	0.0167	+5.7
15								30	0.1113		0.0274	0.0277	+1.1
16								50	0.1017		0.0470		0
17								70	0.0959		0.0623	0.0632	+1.4
18								100	0.0901		0.0798	0.0831	+4.1

5 Summary and outlook

Design concepts have been developed in this dissertation with the aim of facilitating the transparent and performance-based design and assessment of reinforced concrete structures in the following cases, focusing on the chloride-induced corrosion of reinforcing steel which is relevant for durability:

- erection of new structures
- estimation of the remaining service life of existing structures and
- repair by removing and replacing damaged concrete

This enables the reliability-based concept set out in *DIN EN 1990:2010* to be implemented and the safety requirements specified in the standard to be satisfied.

The design concepts have each been developed and described on a fully probabilistic level, converted to a semi-probabilistic format by determining the relevant partial factors and simplified by establishing nomograms for practical applications.

Durability design and assessment using nomograms is performed for two different safety requirements (β_0 = 1.5 and 0.5), taking account of the expected/existing action (exposure class and available chloride source), the material resistance determined in the laboratory or for a structure, the required/desired/existing concrete cover and the design service life.

The potential resistance of the structural element to chloride ingress can be determined by means of the methods developed in this dissertation. These take account of the various types of material (conventional concretes, new materials), the available information (composition of the material, data from laboratory tests or structural investigations etc.), the time and effort required for application of the methods and the required reliability.

Particular attention is drawn to the following points regarding the outlook for further optimization and simplification of the design process:

The rapid chloride migration test (RCM) has been shown to be a suitable test method for assessing the resistance of the materials concerned to chloride ingress thanks to its short duration, general ease of use and reliability and its satisfactory level of precision. The boundary conditions of this test method still need to be standardized and specified in normative provisions.

Systematic investigations are required to enable the impact of execution/workmanship, in particular curing and the type of formwork, on the resistance of structural elements to chloride ingress to be taken into account in the design process.

Similar to durability design with regard to the carbonation-induced corrosion of reinforcing steel (*Leivestad 2013, Greve-Dierfeld 2015*), distinctions between the various levels of material resistance can be made by introducing classes of resistance to chloride ingress. This enables concretes with similar performances to be grouped together in “concrete families” (combinations of binder and w/b ratio). A first approach was described in *Leivestad 2013*.

References

Standards

BS 8500-1:2006 Concrete – complementary British Standard to BS EN 206-1 – Part 1: Method of specifying and guidance for the specifier. London, Great Britain.

DIN 1045-2:2008 Tragwerke aus Beton, Stahlbeton und Spannbeton – Teil 2: Beton – Festlegung, Eigenschaften, Herstellung und Konformität – Anwendungsregeln zu DIN EN 206-1.

DIN 1164-1:1994 Zement – Teil 1: Zusammensetzung, Anforderungen (zurückgezogen, ersätzt durch *DIN 1164-10:2013*)

DIN 4030-1:2008 Beurteilung betonangreifender Wässer, Böden und Gase – Teil 1: Grundlagen und Grenzwerte.

DIN 19702:2010 Massivbauwerke im Wasserbau – Tragfähigkeit, Gebrauchstauglichkeit und Dauerhaftigkeit.

DIN 31051:2012 Grundlagen der Instandhaltung.

DIN EN 14626:2007 Produkte und Systeme für den Schutz und die Instandsetzung von Betontragwerken – Prüfverfahren – Bestimmung des Chloridgehaltes in Festbeton; Deutsche Fassung EN 14629:2007.

DIN EN 1990:2010 Eurocode 0: Grundlagen der Tragwerksplanung; Deutsche Fassung EN 1990:2002 + A1:2005 + A1:2005/AC:2010.

DIN EN 1992-1-1/NA:2013 Nationaler Anhang – National festgelegte Parameter – Eurocode 2: Bemessung und Konstruktion von Stahlbeton- und Spannbeton-tragwerken – Teil 1-1: Allgemeine Bemessungsregeln und Regeln für den Hochbau.

DIN EN 206:2014 Beton – Festlegung, Eigenschaften, Herstellung und Konformität; Deutsche Fassung EN 206:2013.

DIN EN 197-1:2014 (Entwurf) Zement – Teil 1: Zusammensetzung, Anforderungen und Konformitätskriterien von Normalzement; Deutsche Fassung EN 197-1:2014.

DIN EN 12390-3:2009 Prüfung von Festbeton – Teil 3: Druckfestigkeit von Probekörpern.

DIN EN 12390-7:2009 Prüfung von Festbeton – Teil 7: Dichte von Festbeton.

DIN EN 12390-11:2015 Prüfung von Festbeton – Teil 11: Bestimmung des Chlorid-widerstandes von Beton – Einseitig gerichtete Diffusion.

DS/EN 1992-1-1 DK NA:2011 National annexe to EN 1992-1-1. Denmark.

EN 1992-1-1:2004 Eurocode 2: Design of concrete structures – Part 1-1: General rules and rules for buildings.

ISO 16204:2012 Durability – Service life design of concrete structures.

ISO 2394:1998 General principles on reliability of structures.

NEN 6700:2005 Technical principles for building structures. The Netherlands.

NF EN 206/CN:2014 National supplement to NF EN 206. France.

NP EN 206-1:2007 Betão – Parte 1: Especificação, desempenho, produção e conformidade. IPQ, Lisboa, Portugal.

NS-EN 206/NA 2014 National annexe to EN 206:2014. Norway.

Guidelines

BAW-Merkblatt 2012: Chlorideindringwiderstand von Beton (MCL). Bundesanstalt für Wasserbau.

CEB 238:1997 New Approach to Durability Design: An Example for Carbonation Induced Corrosion. Comité Euro-International du Béton (CEB). Bulletin d'Information, N° 238, Lausanne 1997.

DAfStb Heft 401:1989 Arbeitskreis Prüfverfahren Chlorideindringtiefe des Deutschen Ausschusses für Stahlbeton. Anleitung zur Bestimmung des Chloridgehaltes von Beton. In Schriftenreihe des Deutschen Ausschusses für Stahlbeton. Beuth Verlag, Berlin.

DAfStb RiLi SIB 2001: Richtlinie für Schutz und Instandsetzung von Betonbauteilen – Teil 1: Allgemeine Regelungen und Planungsgrundsätze. Deutscher Ausschuss für Stahlbeton.

DAfStb Positionspapier 2008: Positionspapier des Deutschen Ausschusses für Stahlbeton zur Umsetzung des Konzepts von leistungsbezogenen Entwurfsverfahren unter Berücksichtigung von DIN EN 206-1, Anhang J. In Beton- und Stahlbetonbau 103, 2008, Heft 12, Seiten 837 bis 839.

DAfStb Positionspapier 2015: Positionspapier des Deutschen Ausschusses für Stahlbeton zum aktuellen Stand der Technik – Kritischer korrosionsauslösender Chloridgehalt. In Beton- und Stahlbetonbau 110, 2015, Heft 11, Seiten 784 bis 786.

DBV-Merkblatt 2011: Betondeckung und Bewehrung – Sicherung der Betondeckung beim Entwerfen, Herstellen und Einbauen der Bewehrung sowie des Betons nach Eurocode 2. Merkblätter Deutscher Beton- und Bautechnik-Verein e.V. Berlin.

fib bulletin 34:2006 Model Code for Service Life Design. Prepared by *fib* Task Group 5.6.

fib bulletin 53:2009 Structural Concrete – Textbook on behaviour, design and performance. Volume 3: Design of durable concrete structures.

fib bulletin 76:2015 Benchmarking of Deemed-to-Satisfy Provisions in Standards – Durability of Reinforced Concrete Structures Exposed to Chlorides. Prepared by *fib* Task Group 8.6: Gehlen, C., Greve-Dierfeld, S. v., Gulikers, J., Helland, S., Rahimi, A. et al.

fib Model Code for Concrete Structures 2010.

LNEC E 465:2007 Concrete – methodology for estimating the concrete performance properties allowing to comply with the design working life of reinforced or pre-stressed concrete structures under environmental exposures XC and XS. MOPTC – Laboratório Nacional de Engenharia Civil, Portugal.

NT Build 492:1999 Concrete, Mortar and Cement-Based Repair Materials – Chloride Migration Coefficient from Non-Steady-State Migration Experiments.

Probabilistic Model Code 2001 – Part 1: Basis of design. Prepared by Joint Committee on Structural Safety (JCSS). ISBN 978-3-909386-79-6.

ZTV-W LB 215:2012 Zusätzliche Technische Vertragsbedingungen – Wasserbau (ZTV-W) für Wasserbauwerke aus Beton und Stahlbeton (Leistungsbereich 215), Ausgabe 2012. Bundesministerium für Verkehr, Bau und Stadtentwicklung (BMVBS).

ZTV-ING:2014 Zusätzliche Technische Vertragsbedingungen und Richtlinien für Ingenieurbauten. Bundesministerium für Verkehr, Bau und Stadtentwicklung (BMVBS).

Literature

Alonso, C., Andrade, C., Gonzalez, J.A. 1988: Relation between resistivity and corrosion rate of reinforcement in carbonated mortar made with several cement types. Cement and Concrete Research, 39, 3, 1988, 687-698.

Alonso, M.C., Sanchez, M., Angst, U.M., Garcia-Calvo, J.L. 2012: The effect of binder type on chloride threshold values for reinforced concrete. Proceedings of the International Conference of Concrete Repair, Rehabilitation and Retrofitting III – Alexander et al. (Eds). © 2012 Taylor & Francis Group, London, ISBN 978-0-415-89952-9.

Andrade, C., Whiting, D. 1996: A comparison of chloride ion diffusion coefficients derived from concentration gradients and non-steady state accelerated ionic migration. Materials and Structures, Vol. 29, October 1996, pp 476-484.

Andrade, C., Castellote, M., Alonso, C., González, C. 2000: None-steady-state chloride diffusion coefficients obtained from migration and natural diffusion tests. Part 1: Comparison between several methods of calculation. Materials and Structures, Vol. 33, January-February 2000, pp 21-28.

Ang, G. K. I., Wyatt, D. P. 1999: Performance Concept in the Procurement of Durability and Serviceability of Buildings. Ottowa: NRC Research Press, 1999. Durability of Building Materials and Components, Proceedings of the Eight International Conference, Vancouver, May 30-June 3, 1999, (Lacasse, M. A.; Vanier, D. J. (Ed.)), Vol. 3, pp. 1821-1832.

Angst, U., Elsener, B., Larsen, C.K., Vennesland, Ø. 2009: Critical chloride content in reinforced concrete – A review. Cement and Concrete Research, 39: 1122-1138.

Angst, U.M., Elsener, B. 2015: Forecasting chloride-induced reinforcement corrosion in concrete – effect of realistic reinforcement steel surface conditions. Proceedings of the International Conference of Concrete Repair, Rehabilitation and Retrofitting IV – Dehn et al. (Eds). 5-7 October 2015, Leipzig, Germany.

Arya, C., Buenfeld, N.R., Newman, J.B. 1990: Factors Influencing Chloride-binding in Concrete. Cement and Concrete Research, Vol. 20 (1990) pp. 291-300.

Bamforth, P.B. 1993: Concrete classification for r.c. structures exposed to marine and other salt laden environments. Structural Faults and Repair 93, Vol II, Edinburgh, June/July 1993, Engineering Technics Press, pp. 31-40.

Bamforth, P.B. 1997: Corrosion of Reinforcement in Concrete Caused by Wetting and Drying Cycles in Chloride Containing Environments. Middlesex: Taywood Engineering Ltd. BSI Supported Project PBB/BM 1746.

Bamforth, P.B. 1999: The Derivation of Input Data for Modelling Chloride Ingress from Eight-Year UK Coastal Exposure Trials. Magazine of Concrete Research 51 (1999), No. 2, pp. 87-96.

Benjamin, S.E., Sykes, J.M. 1990: Chloride-induced pitting corrosion of Swedish iron in ordinary Portland cement mortars and alkaline solutions – the effect of temperature. Corrosion of Reinforcement in Concrete, International Symposium, Wishaw, Warwickshire, UK, May 21-24, 1990, (Page, C. L.; Treadaway, K.W.J.; Bamforth, P.B. (Ed.)), S. 59-64.

Boddy, A., Bentz, E., Thomas, M.D.A., Hooton, R.D. 1999: An overview and sensitivity study of a multi-mechanistic chloride transport model. Cement and Concrete Research, Vol. 29, pp. 827-837.

Bouwmeester, W.J., Polder, R.B., Lollini, F. 2010: The effect of Curring on the Microstructure and Chloride Penetration Resistance of Concrete. Proceedings of 2nd International Symposium on Service Life Design for Infrastructure. 4-6 October 2010, Delft, The Netherlands.

Breit, W. 1997: Untersuchungen zum kritischen korrosionsauslösenden Chloridgehalt für Stahl in Beton. Schriftenreihe Aachener Beiträge zur Bauforschung, Institut für Bauforschung der RWTH Aachen, Nr. 8, Dissertation.

Breit, W. 2001: Kritischer korrosionsauslösender Chloridgehalt – Sachstand und neuere Untersuchungen. Verein Deutscher Zementwerke e.V., Verlag Bau+Technik, Düsseldorf, Germany.

Breit, W., Dauberschmidt, C., Gehlen, C., Sodeikat, C., Taffe, A., Wiens, U. 2011: Zum Ansatz eines kritischen Chloridgehaltes bei Stahlbetonbauwerken. Beton- und Stahlbetonbau , 106 (2011), Heft 5. Ernst & Sohn, Berlin.

Bunke, N. 1991: Prüfung von Beton – Empfehlungen und Hinweise als Ergänzung zu DIN 1048. Schriftenreihe des Deutschen Ausschusses für Stahlbeton, Heft 422. Beuth, Berlin.

Caré, S. 2008: Effect of temperature on porosity and on chloride diffusion in cement pastes. Construction and Building Materials 22 (2008) 1560-1573.

Carslaw, H. S., Jaeger, J. C. 1959: Conduction of Heat in Solids. Clarendon Press, Oxford, UK.

Castellote, M. 1997: Application of electrical fields for the characterisation of concrete in relation to chloride ions transport. Doctoral thesis, University of Zaragoza, in Spanisch.

Castellote, M, Andrade, C, Alonso, C. 1999: Chloride-binding isotherms in concrete submitted to non-steady-state migration experiments. Cement and Concrete Research 29 (1999) pp. 1799-1806.

CHLORTEST 2005: EU Funded Research Project under 5FP GROWTH Programme. Resistance of Concrete to Chloride Ingress – From laboratory tests to in-field performance – WP4 Report – Modelling of Chloride Ingress.

Collepardi, M., Marcialis, A., Turriziani, R. 1970: The kinetics of chloride ions penetration in concrete (in Italian). Il Cemento, No. 4 (1970) 157-164.

COMSOL Multiphysics® – Multiphysics Modeling, Finite Element Analysis, and Engineering Simulation Software, www.comsol.com.

Crank, J. 1975: The Mathematics of Diffusion. Clarendon, Oxford, UK, 2nd edition.

DARTS 2004: Durable and reliable tunnel structures – Deterioration modelling. Prepared by Ingenieurbüro Professor Schießl, Gehlen, C., Kapteina, G. Project with financial support of the European Commission under the Fifth Framework Program, GROWTH 2000 Project GRD1-25633, Contract G1RD-CT-2000-00467.

Dousti, A., Rashetnia, R., Ahmadi, B., Shekarchi, M. 2013: Influence of exposure temperature on chloride diffusion in concretes incorporating silica fume or natural zeolite. Construction and Building Materials 49 (2013) 393-399.

DuraCrete 1998: Probabilistic Performance based durability design of concrete structures, EU-Project (Brite EuRam III). No BE95-1347.

DuraCrete 1998a: Subtask 4.3.1: Statistical Quantification of the propagation period. The European Union – Brite EuRam III, Contract BRPR-CT95-0132, Project BE95-1347, Document BE95-1347/TG4/E, 1998.

DuraCrete 2000: Probabilistic performance based durability design of concrete structures: General guidelines for durability design and redesign. – Report No. BE95-1347/R14.

Einstein, A. 1905: Über die von der molekularkinetischen Theorie der Wärme geforderte Bewegung von in ruhenden Flüssigkeiten suspendierten Teilchen. Annalen der Physik, 17, S. 549–560.

Faber, M. H. 2007: Risk and Safety in Civil Engineering. Lecture Notes. ETH Swiss Federal Institute of Technology Zurich.

Fluge, F. 1997: Environmental Loads on Costal Bridges. Oslo, Norwegian Road Research Laboratory. Repair of Concrete Structures : From Theory to Practice in a Marine Environment (Blankvoll, A. (Ed.)), Svolvaer, Norway, 28-30 May, 1997, pp. 89-98.

Fluge, F. 2003: Marine chlorides – A probabilistic approach to derive provisions for EN 206-.1 DuraNet, Third workshop, Tromsø, Norway, June 2001. Reported in "Betongkonstruksjoners Livsløp" report no 19, Norwegian Road Administration, P.O.Box 8142, 0033 Oslo.

Frederikson, J.M., Sørensen, H.E., Andersen, A., Klinhoffer, O. 1996: The Effect of Water/Cement Ration on Chloride Transport into Concrete – Immersion, Migration and Resistivity Tests. Copenhagen, Danish Road Directorate, Report No 54 1996.

Frederiksen, J.M., Nilsson, L.-O., Sandberg, P., Poulsen, E., Tang, L., Andersen, A. 1997: A system for estimation of chloride ingress into concrete. Theoretical background. HETEK. Danish Road Directorate Report No 83 1997.

Frederiksen, J.M., Mejlbro, L., Nilsson, L.-O. 2008: Fick's 2nd law – Complete solution for chloride ingress into concrete, Report TVBM-3146, Lund Institute of Technology, Sweden.

Freundlich, H. 1907: Über die Adsorption in Lösungen. Z. Phys. Chem. 57, 1907, S. 385-470.

Gehlen, C.; Ludwig, H.M. 1999: Compliance Testing for Probabilistic Design Purposes. Brussels: European Union – Brite EuRam, 1999. Contract BRPR-CT95-0132, Project BE95-1347, Document BE95-1347/R8.

Gehlen, C. 2000: Probabilistische Lebensdauerbemessung von Stahlbetonbauwerken – Zuverlässigkeitsbetrachtungen zur wirksamen Vermeidung von Bewehrungskorrosion. Schriftenreihe des Deutschen Ausschusses für Stahlbeton, Heft 510. Beuth, Berlin, Dissertation.

Gehlen, C., Fischer, C. 2007: Überarbeitung des BAW-Merkblatts Chlorideindringwiderstand von Beton. Abschlussbericht-Nr. A07/1-1. Institut für Werkstoffe im Bauwesen der Universität Stuttgart.

Gehlen, C., Schießl, P. und *Schießl-Pecka, A. 2008*: Hintergrundinformationen zum Positionspapier des DAfStb zur Umsetzung des Konzeptes von leistungsbezogenen Entwurfsverfahren unter Berücksichtigung von DIN EN 206-1, Anhang J, für dauerhaftigkeitsrelevante Problemstellungen. Beton- und Stahlbetonbau 103 (2008), Heft 12, S. 840–851.

Gehlen, C., Mayer, T. F., Greve-Dierfeld, S. von 2011: Lebensdauerbemessung. Beton-Kalender 2011, Kapitel XIV. Ernst & Sohn, Berlin.

Gehlen, C., Brameshuber, W., Horbach, J., Ludwig, H.M., Meschke, G. 2013: Dauerhafte Infrastruktur aus Beton – Einfluss kombinierter Last- und Umwelteinwirkungen auf das Mikrogefüge und die Transportprozesse im Beton. Antrag an die DFG zur Einrichtung eines Schwerpunktprogramms.

Gehlen, C., Rahimi, A., Reschke, T., Westendarp, A. 2015: Bewertung der Leistungsfähigkeit von Instandsetzungsmaterialien und der Lebensdauer von instandgesetzten Stahlbetonbauteilen unter Chlorideinwirkung. Beton-Kalender 2015, Kapitel VI. Ernst & Sohn, Berlin.

Ghosh, P. Hammond, A. Tikalsky, P. J. 2011: Prediction of equivalent steady-state chloride diffusion coefficients. ACI Materials Journal, January-February 2011, Vol. 108, No. 1, pp 88-94.

Glass, G. K., Reddy, B. 2002: The Influence of the Steel Concrete Interface on the Risk of Chloride Induced Corrosion Initiation. Corrosion of Steel in Reinforced Concrete Structures, COST 521, Final Workshop, University of Applied Sciences, Luxembourg, 18-19 Febrary 2002, Weydert, R. (Ed.), S. 227-232.

Gollwitzer, S. 2015: Informationen beim persönlichen Gespräch am 17.02.2015.

Greve-Dierfeld S. von 2015: Bemessungsregeln zur Sicherstellung der Dauerhaftigkeit XC-exponierter Stahlbetonbauteile. Dissertation, Technische Universität München.

Gulikers, J. 2011: Analysis and evaluation of a European Round Robin Test on Rapid Chloride Migration. Report of Rijkswaterstaat Ministerie van Verkeer en Waterstaat, Utrecht.

Hansson, C. M., Sørensen, B. 1990: The threshold concentration of chloride in concrete for the initiation of reinforcement corrosion. Philadelphia: American Society for Testing Materials, ASTM 1065, 1990. In Corrosion Rates of Steel in Concrete, (Berke, N.S.; Chaker, V.;Whiting, D. (Ed.)), S. 3-16.

Harnisch, J., Raupach, M. 2011: Aktuelle Untersuchungsergebnisse zum kritischen Chloridgehalt von Stahl in Beton. Restoration of Buildings and Monuments, Bauinstandsetzen und Baudenkmalpflege, Vol. 17, No. 3/4, 157-168.

Haque, M.N. and Kayyali, O.A. 1995: Free and Water Soluble Chloride in Concrete. Cement and Concrete Research, Vol. 25 (1995) No. 3, pp. 532-542.

Helland, S., Aarstein, R., Maage M. 2010: In-field performance of North Sea offshore platforms with regard to chloride resistance. Structural Concrete 2010, 11, No. 1. 1464-4177 © 2010 Thomas Telford and *fib*.

Helland, S. 2015: Informationen durch Schriftverkehr.

Hergenröder, M. 1992: Zur statistischen Instandhaltungsplanung für bestehende Betonbauwerke bei Karbonatisierung des Betons und möglicher Korrosion der Bewehrung. Berichte aus dem Konstruktiven Ingenieurbau, Technische Universität München, Dissertation.

Herman, M. H.1999: Building Performance Starts at Hand-Over: The Importance of Life Span Information. Ottowa: NRC Research Press, 1999. – Durability of Building Materials and Components, Proceedings of the Eight International Conference, Vancouver, May 30-June 3, 1999, (Lacasse, M. A.; Vanier, D. J. (Ed.)), Vol. 3, pp. 1867-1873.

Holický, M. 2011: Optimization of the Target Reliability Level in Engineering. 1st International Symposium on Uncertainty Modelling in Engineering (ISUME 2011), 2 - 3 May 2011, Prague, Czech Republic.

Huber, J. 2008: Zur Nachbehandlung von Beton – Auswirkungen des Wasserverlustes durch Evaporation in jungem Alter am Beispiel von Straßenbeton. Dissertation, Technische Universität München.

Hunkeler, F., Ungricht, H., Deillon, F. 2000: Untersuchungen zur Chloridbestimmung im Beton und Durchführung eines 2-stufigen Ringversuchs. Technische Forschung und Beratung für Zement und Beton (TFB), Wildegg, Schweiz. Forschungsauftrag 88/97 auf Antrag der Arbeitsgruppe Brückenforschung. Eidgenössisches Departement für Umwelt, Verkehr, Energie und Kommunikation Bundesamt für Straßen.

Hussain, S.H., Rasheeduzzafar, Al-Musallam, A., Al-Gahtani, A.S. 1995: Factors Affecting Threshold Chloride for Reinforcement Corrosion in Concrete. Cement and Concrete Research, Vol. 25 (1995), No. 7, pp. 1543-1555.

Hussain, R.H., Ishida, T. 2011: Computer-aided oxygen transport model of mass and energy simulation for corrosion of reinforced steel. Automation in Construction, 20, 5, 2011, 559-570.

Jaegermann, C. 1990: Effect of Water-Cement Ratio and Curing on Chloride Penetration into Concrete Exposed to Mediterranean Sea. Journal of the ACI 87 (1990), No. 4, pp. 333-339.

Jacobs, F., Leemann A. 2007: Betoneigenschaften nach SN EN 206-1. ASTRA Report VSS Nr. 615.

Jiang, F., Wan, X., Wittmann, F.H., Zhao, T. 2011: Influence of combined actions on durability of reinforced concrete structures. Restoration of Buildings and Monuments, Vol. 17, No. 5, 289-298.

Jung, S.H., Choi, Y.J., Lee, B.C. 2007: Influence of Carbonation on the Chloride Diffusion in Concrete. Proceedings of the International Conference on Sustainable Building Asia, Seoul, Korea.

Justnes, H. 1996: A review of chloride binding in cementitious systems. SINTEF Civil and Environmental Engineering, Cement and Concrete, Trondheim, Norway.

Kapteina, G. 2011: Modell zur Beschreibung des Eindringens von Chlorid in Beton von Verkehrsbauwerken. Dissertation, Technische Universität München.

Kostadinov, D. 2014: Prognose der Restnutzungsdauer von instand gesetzten Betonbauteilen unter Chlorideinwirkung. Masterarbeit, Technische Universität München.

Lay, S., Schießl, P. 2006. Dauerhaftigkeitsbemessung von Stahlbetonkonstruktionen. Forschungsbericht AiF/DBV-Nr. 12525/225, Technische Universität München.

Lay, S. 2007: Abschätzung der Wahrscheinlichkeit tausalzinduzierter Bewehrungskorrosion. Dissertation, Technische Universität München. Schriftenreihe des Deutschen Ausschusses für Stahlbeton, Heft 568. Beuth, Berlin.

Leivestad, S. 2013: Durability – exposure resistance classes, a new system to specify durability in EN 206 and EN 1992. Memo, durability classes, JWG 250/104 – N19C.

Leivestad, S. 2014: Durability – Exposure resistance classes, a new system to specify durability in EN 206 and EN 1992. Memo, JWG 250/104 – N25.

Maage, M., Helland, S., Carlsen, E.J. 1993: Experience with chloride penetration in concrete exposed to marine environment in Norway, Proceedings FIP symposium 1993, Kyoto, Japan.

Maage, M., Helland, S., Poulsen, E., Vennesland, O., Carlsen, E.J. 1996: Service life prediction of existing concrete structures exposed to a marine environment. ACI Materials Journal, Vol. 93, November-Decemmber 1996, pp. 602-608.

Maage, M., Helland, S., Carlsen, E.J. 1999: Chloride penetration into concrete with lightweight aggregates. EU-Project (Brite EuRam III), report BE96-3942/R3.

Maage, M., Helland, S. 2009: Shore Approach. 26 years performance of high quality concrete in a marine environment. COIN Project report 14, SINTEF Trondheim, Norway.

Maierhofer, C., Reinhardt, H.-W., Dobmann, W. 2010: Non-Destructive Evaluation of Reinforced Concrete Structures: Volume 2: Non-Destructive Testing Methods. Woodhead Publishing Series in Civil and Structural Engineering.

Markeset, G. 2009: Critical chloride content and its influence on service life predictions. Materials and Corrosion 2009, 60, No. 8.

Marues, P.F., Costa, A., Lanata, F. 2012: Service life of RC structures: chloride induced corrosion: prescriptive versus performance-based methodologies. Materials and Structures (2012) 45:277-296.

Martin, H. 1975: Zeitlicher Verlauf der Chloridionenwanderung in Beton, der einem PVC-Brand ausgesetzt war. Betonwerk + Fertigteiltechnik, Heft 1 / 1975.

Maxima – A Computer Algebra System. Energy Science and Technology Software Center. http://maxima.sourceforge.net.

Mejlbro, L. 1996: The complete solution to Fick's second law of diffusion with time-dependent diffusion coefficient and surface concentration. Proceedings of CEMENTA's workshop on Durability of Concrete in Saline Environments. Danderyd, Sweden.

Mohammed, T.U., Yamaji, T., Hamada, H. 2002: Chloride Diffusion, Microstructure, and Mineralogy of Concrete after 15 Years of Exposure in Tidal Environment. ACI Materials Journal, May - June 2002, pp. 256-263.

Mohammed, T.U., Yamaji, T., Hamada, H. 2002a: Microstructures and Interfaces in Concrete after 15 Years of Exposure in the Tidal Environment. ACI Materials Journal, Vol. 99, No. 4, July - August 2002, pp. 352-360.

Neville, A. 1995: Chloride attack of reinforced concrete – an overview. Materials and Structures, vol. 28 (1995) pp 63-70.

Nilsson, L.-O. 2002: Concepts in Chloride Modelling – Key note paper at 3rd International RILEM workshop on Testing and Modelling Chloride Ingress into Concrete, Madrid, 9.-10. September 2002.

Nguyen, T.S., Lorente, S., Carcasses, M. 2006: Influence of the temperature on the chloride transport through cementitious materials. J. Phys. IV France 136 (2006) 63–70, © EDP Sciences, Les Ulis.

Oh, B.H., S.Y. Jang, S.Y., Shin, Y.S. 2003: Experimental investigation of the threshold chloride concentration for corrosion initiation in reinforced concrete structures. Magazine of Concrete Research 55: 117-124.

Osterminski, K. 2013: Zur voll-probabilistischen Modellierung der Korrosion von Stahl in Beton – Ein Beitrag zur Dauerhaftigkeitsbemessung von Stahlbetonbauteilen. Dissertation, Technische Universität München.

Østmosen, T., Liestøl, G., Grefstad, K.A., Sand, B.T., Farstad, T. 1993: Chloride durability of coastal bridges in concrete), Report from Norwegian Public Roads Administration, Oslo (in Norwegisch).

Page, C.L., Short, N.R., El Tarras, A. 1981: Diffusion of Chloride Ions in Hardened Cement Pastes. Cement and Concrete Research 11 (1981), No. 3, pp. 395-406.

Rackwitz, R. 1999: Zuverlässigkeitsbetrachtungen bei Verlust der Dauerhaftigkeit von Bauteilen und Bauwerken. – Kurzberichte aus der Bauforschung 40 (1999), Nr. 4, S. 297–301 Stuttgart: IRB, 1998. – Forschungsbericht Nr. T 284.

Rahimi, A., Gehlen, C., Reschke, T., Westendarp, A. 2013: Long-Term Performance of Concrete Structures in a Marine Environment – Measured and Calculated. Proceedings of 7th International Conference on Concrete Under Severe Conditions – Environment and Loading (CONSEC13), Nanjing, China.

Rahimi, A., Gehlen, C., Reschke, T., Westendarp, A. 2013a: Approaches for Modelling the Residual Service Life of Marine Concrete Structures after Repair. Proceedings of 7th International Conference on Concrete Under Severe Conditions – Environment and Loading (CONSEC13), Nanjing, China.

Rahimi, A., Gehlen, C., Reschke, T., Westendarp, A. 2014: Approaches for Modelling the Residual Service Life of Marine Concrete Structures. International Journal of Corrosion 1/2014, http://www.hindawi.com/journals/ijc/2014/432472/abs/.

Rahimi, A., Gehlen, C., Reschke, T., Westendarp, A. 2014a: Efficiency of materials used for repair measures of concrete structures exposed to chlorides. Proceedings of the 5th International Conference on Concrete Repair – Concrete Solutions, 01.-03. September 2014, Belfast, UK.

Rahimi, A., Gehlen, C., Reschke, T., Westendarp, A. 2015: Chloride transport in concrete structural elements after repair. Proceedings of the International *fib* symposium 2015, Concrete – Innovation and Design, 18.-20. May, Copenhagen, Denmark.

Rahimi, A., Gehlen, C., Reschke, T., Westendarp, A. 2015a: Restnutzungsdauer von instandgesetzten Stahlbetonbauteilen unter Berücksichtigung der Chlorid-umverteilung. Ibausil 2015, 16.-18. September 2015, Weimar, Deutschland.

Rahimi, A., Gehlen, C., Reschke, T., Westendarp, A. 2015b: Impact of Chloride Redistribution on the Service Life of Repaired Concrete Structural Elements. Proceedings of the International Conference on Concrete Repair, Rehabilitation and Retrofitting IV, 5.-7. October 2015, Leipzig, Germany.

Raupach, M. 1992: Zur chloridinduzierten Makroelementkorrosion von Stahl in Beton. Schriftenreihe des Deutschen Ausschusses für Stahlbeton (1992), Nr. 433. Beuth, Berlin, Dissertation.

Rasheeduzzafar, Hussain, H.S., Al-Saadoun, S.S. 1992: Effect of Tricalcium Aluminate Content of Cement on Chloride Binding and Corrosion of Reinforcing Steel in Concrete. ACI Materials Journal, January-February 1992, pp. 3-12.

Reschke, T., Rahimi A., Becker, H. 2014: Schleuse Wilhelmshaven – Instandsetzungs-bedarf der Kajen und mögliche Instandsetzungsvarianten. Gutachten zur Auftrags-Nr. A39510306414. Bundesanstalt für Wasserbau, Karlsruhe.

Rößler, G., Westendarp, A., Dauberschmidt, C., Meng, B., Pierkes, R., Schwamborn, B., Wiens, U. 2009: Instandsetzung von Meerwasserbauten, ibac-Forschungsbericht F647.

Schall, G., Gollwitzer, S., Rackwitz, R. 1988: Integration of Multinormal Densities on Surfaces. Proceedings of 2nd IFIP WG 7.5 Work. Conference on Reliability and Optimization on Structural Systems, London, 1988, ed. P. Thoft-Christensen, Springer, 1989.

Schießl, P., Raupach, M. 1990: Influence of concrete composition and microclimate on the critical chloride content in concrete. London: Elsevier, 1990. Corrosion of Reinforcement in Concrete, International Symposium, Wishaw, Warwickshire, UK, May 21-24, 1990, (Page, C. L.; Treadaway, K.W.J.; Bamforth, P.B. (Ed.)), S. 49-58.

Schießl, P., Raupach, M. 1990a: Einfluss der Betonzusammensetzung und der Umgebungsbedingungen auf die chloridinduzierte Korrosion von Stahl in Beton – Ergebnisse von Untersuchungen mit Betonkorrosionszellen. Beton-Informationen 30 (1990), Nr. 4, S. 43-54.

Schießl, P., Breit, W. 1996: Local repair measures at concrete structures damaged by reinforcement corrosion- aspects of durability. Proceedings of 4th Int. Symp. Corrosion of Reinforcement in Concrete Construction, The Royal Society of Chemistry, Cambridge: 525-534.

Schneider, J. 2007: Sicherheit und Zuverlässigkeit im Bauwesen – Grundwissen für Ingenieure.

Schwenk, W. 1972: Korrosionsgefährdung und Schutzmaßnahmen bei Elementbildung zwischen erdverlegten Rohren und Behältern aus unterschiedlichen Metallen. Gwf-gas/Erdgas, 113, 11, 1972, 546-550.

Siemes, T., Vrouwenvelder, T., Beukel, A. van den 1985: Durability of buildings: a reliability analysis. HERON, Vol. 30, No. 3, pp. 2-48.

Sørensen, J.D., Kroon I.B., Faber, M.H. 1994: Optimal reliability-based code calibration. Structural Safety 1994, volume 15, 197-208.

Spiesz, P., Ballari, M.M., Brouwers, H.J.H. 2012: RCM: a new model accounting for the non-linear chloride binding isotherm and the non-equilibrium conditions between the free- and bound-chloride concentrations. Construction and Building Materials 27 (2012) 293-304.

Spiesz, P., Brouwers, H.J.H. 2013: Influence of the applied voltage on the Rapid Chloride Migration (RCM) test. Cement and Concrete Research 42 (2012) 1072-1082.

Spiesz, P. 2013: Durability of concrete with emphasis on chloride migration. Doctoral thesis, Eindhoven University of Technology, the Netherlands. bouwstenen 183, ISBN 978-90-386-3431-9.

Spörel, F., Müller, H. 2012: Untersuchung des Einflusses von Schalung und Nachbehandlung auf die Dauerhaftigkeit geschalter Betonflächen massiger Betonbauteile. Bericht A39510310141, Bundesanstalt für Wasserbau, Abteilung Bautechnik, Referat Baustoffe, Karlsruhe.

Straub, D. 2010: Zuverlässigkeit und Lastannahmen. Vorlesungsunterlagen, Fachgebiet Risikoanalyse und Zuverlässigkeit, Technische Universität München. Oktober 2010.

Straub, D. 2011: Reliability updating with equality information. Probabilistic Engineering Mechanics 26 (2011) 254-258, ELSEVIER.

Straub, D. 2015: Informationen beim persönlichen Gespräch am 03.11.2015.

STRUREL – A structural reliability analysis program system by RCP GmbH (Reliability Consulting Programs), www.strurel.de.

Takewaka, K., Yamaguchi, T., Maeda, S. 2003: Simulation model for deterioration of concrete structures due to chloride attack. Journal of Advanced Concrete Technology, 1, 2, 2003, 139-146.

Tamm, P. 2014: Erstellung eines semiprobabilistischen Konzepts zur Dauerhaftigkeitsbemessung von Meerwasserbauwerken gegenüber chloridinduzierter Betonstahlkorrosion. Masterarbeit, Technische Universität München.

Tang, L. 1996: Chloride transport in concrete – measurement and prediction. Doctoral thesis, Chalmers University of Technology, Gothenburg, Sweden.

Tang, L., Gulikers, J. 2007: On the mathematics of time-dependent apparent chloride diffusion coefficient in concrete. Cement and Concrete Research 37 (2007) 589-595.

Tang, L., Utgenannt, P., Lindvall, A., Boubitsas, D. 2010: Validation of models and test methods for assessment of durability of concrete structures in road environment. Uppdragsrapport No. P802606, Lund, Sweden.

Tang, L., Nilsson, L.-O., Basheer, P.A. M. 2012: Resistance of concrete to chloride ingress – Testing and Modelling. CRC Press, ISBN: 978-0-415-48614-9.

Thomas, M. 1996: Chloride threshold in marine concrete. In Cement and Concrete Research, 26: 513–519.

Tritthart, J. 2002: Porenlösungsuntersuchungen als Schlüssel zum Verständnis von Bindungs- und Transportmechanismen in Zementstein und Beton. Materials and Corrosion 53, 385-392 (2002).

Ungricht, H. 2004: Wasserhaushalt und Chlorideintrag in Beton – Einfluss der Exposition und der Betonzusammensetzung. Dissertation, Eidgenössische Technische Hochschule ETH Zürich, Selbstverlag, Zürich, 2004.

Wall, H. 2007: Chloride profiling in marine concrete – Methods and tools for sampling. Doctoral thesis, Lund Institute of Technology, Sweden.

Weizong, G., Boes, A. 2010: Einfluss von wasserabführenden Schalungsbahnen auf die Dauerhaftigkeit von Betonbauwerken. Beton 60 (2010), Nr. 1+2, S. 32-36.

Westendarp, A. 1991: Schießstand Eckernförde Süd – Instandsetzungskonzept für die Betonaußenflächen der Zugangsbrücke. Gutachten zur Auftrags-Nr. 414253 und 413107. Bundesanstalt für Wasserbau, Karlsruhe.

Wiens, U. 2005: Zur Wirkung von Steinkohlenflugasche auf die chloridinduzierte Korrosion von Stahl in Beton. Schriftenreihe des Deutschen Ausschusses für Stahlbeton, Heft 551. Beuth, Berlin, Dissertation.

Wierig, H.-J., Langkamp, H. 1995: Über die Chloridpenetration in nicht karbonatisierte und karbonatisierte Betone. Zement Kalk Gips International, 48 Jhg., Nr. 3, 184-191.

Wittmann, F.H., Zhang, P., Zhao; T. 2006: Influence of combined environmental loads on durability of reinforced concrete structures. Restoration of Buildings and Monuments 12 (4), 349-362.

Yan, Y., Wang, L., Wittmann, F.H. 2013: Publications on Durability of Reinforced Concrete Structures under Combined Mechanical Loads and Environmental Actions: An Annotated Bibliography. RILEM TC-246 TDC. Test Methods to Determine Durability of Concrete under Combined Environmental Actions and Mechanical Load. Aedificatio Publishers.

Yonezawa, T., Ashworth, V., Procter, R.P.M. 1988: Pore solution composition and chloride effects on the corrosion of steel in concrete. Corrosion 44, 489-499.

Yu, Z., Ye, G., Hunger, M., Noort, v. R. 2013: Discussion of the evolution of the chloride coefficient of Portland cement concrete tested by rapid chloride migration (RCM) test at long-term curing periods up to 5 years. Proceedings of international conference Concrete under Sever Conditions – Environment and Loading (CONSEC13), September 2013, Nanjing, China.

Yuan, Q., Shi, C., Schutter, G. De, Audenaert, K. 2008: Effect of temperature on transport of chloride ions in concrete. In Alexander M.G., Beushausen H.D., Dehn F., Moyo P., editors. Proceedings of the 2nd international conference on concrete repair, rehabilitation and retrofitting. Cape Town; 2008, p. 345-51.

Zhang, J.-Z., McLoughlin, I. M., Buenfeld, N. R. 1998: Modelling of Chloride Diffusion into Surface-treated Concrete. Cement and Concrete Composites 20 (1998) 253-261.

A Annex A: Investigations to determine the performance of repair materials

A.1 Introduction

Polymer-modified cement-bound systems, PCC (Polymer-modified Cement Concrete) and SPCC (Sprayed Polymer-modified Cement Concrete) are frequently used to replace damaged concrete when repairing reinforced concrete members contaminated with chlorides. In addition to their high flexural and tensile strength and the good bond they form with concrete, they generally have a dense structure (partly due to the low *w/b* ratio), thus ensuring a high level of protection against the ingress of aggressive substances such as chlorides and CO_2. The high cement and binder content of these materials compared with conventional concrete results in the exposed reinforcing steel being repassivated rapidly and intensively.

Manufacturers do not generally reveal the compositions of PCC and SPCC. The long-term behaviour of these relatively new materials has not yet been adequately researched.

Results of laboratory investigations into the resistance of six different repair materials to chloride ingress are presented and discussed in Annex A. The following three objectives are pursued:

- to determine the parameters required for durability design in accordance with the concept presented in Chapter 2,
- to check whether the performance of the repair materials is correctly assessed with the design concept,
- to compare the resistance of the repair materials to chloride ingress with that of conventional concretes.

To achieve these objectives, laboratory tests were conducted on seven different conventional concretes at the same time. The composition of the materials and its impact on the results of the laboratory tests are not taken into account here.

Some of the observations in Annex A have already been published in *Rahimi et al. 2014a* and *Gehlen et al. 2015* where they were presented as the intermediate results of ongoing investigations.

A.2 Materials, specimens, tests

Six commercially available repair materials were selected for the investigations. They were all hydraulically hardening polymer-modified cement-bound mixes: four dry-mix sprayed concretes (SPCC) and two premixed dry mortars (PCC). The SPCC mixes contain aggregates with a maximum particle size between 4 mm and 8 mm and the PCC have a maximum particle size of 2 mm. Further information on the constituents and the composition of the materials is not available. The compositions of the materials are not taken into account when assessing and interpreting the test results. However, the composition of the dry mixes was estimated by means of an overall chemical analysis, X-ray diffraction analysis and the manufacturer's information, as summarized in Table A.1 (*Kostadinov 2014*). The estimate is only a rough one and the results have not been confirmed by the manufacturers.

Table A.1: Estimated composition of the investigated repair materials [1)]

Constituent	Unit	Repair materials						
		SPCC 1	SPCC 2	SPCC 3	SPCC 4	PCC I	PCC II	
Portland cement clinker	% by mass [2)]	50	47	22	45	64	60	100%
Burnt shale		18	–	18	–	10	15	
Fly ash		–	25	40	35	14	–	
Silica fume		24	23	15	14	8	15	
Polymer fibres		8	5	5	6	4	10	
Aggregate		55	65	45	70	50	65	100%
Binder content	% by mass [2)]	45	35	55	30	50	35	
	kg/m³ [3)]	?	?	?	?	675	610	

[1)] *The results obtained for the constituents and compositions of the materials have not been confirmed by the manufacturers.*

[2)] *of the dry mix*

[3)] *of the test specimen; cannot be determined for SPCC as the water content is unknown*

Seven conventional concretes were produced and subjected to the same tests with the aim of achieving a better assessment and evaluation of the results of the tests on the repair materials. The composition of the concretes is shown in Table A.2. Three types of binder - Portland cement, Portland cement with added fly ash and blast-furnace cement - were selected as the long-term behaviour of these types of binder under chloride exposure (ageing exponent) is relatively well-researched and is known (cf. Chapter 2.3.2.2.3 and 2.4.4.4).

Table A.2: Composition of the investigated concretes

Designation	Binder	w/b ratio [–]	Binder content [kg/m³]	Aggregate
CEM I w/b=0.45	CEM I 42.5 R	0.45	320	Rhine gravel AB 16
CEM I w/b=0.50		0.50		
CEM I w/b=0.55		0.55		
CEM I + FA w/b=0.45	CEM I 42.5 R + 22 % by mass/c FA	0.45	263 z 58 f	
CEM I + FA w/b=0.50		0.50		
CEM III/B w/b=0.45	CEM III/B	0.45	320	
CEM III/B w/b=0.50		0.50		

Slabs measuring 300 x 300 x 80 mm³ were made with the repair materials, water being added in accordance with the manufacturer's instructions. The dimensions of the specimens were selected on the basis of *BAW-Merkblatt 2012* for the determination of the chloride migration coefficient of repair materials. The slabs were protected against drying out by leaving them in the formwork for one day after production. After demoulding, the specimens were either cured in water for 6 days at 20 °C and subsequently at 20 °C / 65 % RH (for tests on hardened specimens, e.g. compressive strength) or cured in water at 20 °C until testing (for the RCM and diffusion tests). For SPCC, large slabs (1000 x 1000 x 80 mm³) were first produced by the dry-mix method. Smaller slabs measuring 300 x 300 x 80 mm³ were then cut out of the large slabs (at an age of 7 days).

The concrete specimens were produced and cured in accordance with the relevant test specification.

Table A.3 shows which laboratory tests were conducted, along with the test specimens made of the repair materials (300 x 300 x 80 mm³, cut from the large slabs) and the concretes.

Table A.3: Overview of the investigations

Test	Test specimens		Age at time of testing [d] (scheduled test duration)
	Repair material	Concrete	
Density	3 drill cores ϕ/L: 50/50 mm	3 10 mm cubes	28
Compressive strength			28
Water absorption	2 slices ϕ/L: 100/30 mm from drill cores		28
Hg-porosimetry	1 drill core ϕ/L: 50/50 mm	1 drill core ϕ/L: 100/50 mm	28, 365, 550, 730
Initial chloride content			28
RCM & Electrolyte resistance	3 drill cores ϕ/L: 100/50 mm from large slabs	3 drill cores ϕ/L: 100/50 mm from 100 mm cubes	28, 56, 90, 180, 365, 550, 730
Diffusion	one slab 200 x 200 x 80 mm³		28, 90, 180, 365, 550, 730 [1)]

[1)] *Time of taking drill powder; the age oft he speciment is the specified time plus 28 days curing*

The properties of the hardened test specimens determined by laboratory tests are shown in Table A.4. The properties tested were compressive strength, water absorption at atmospheric pressure W_{at}, water absorption at a pressure of 150 bar W_{150bar} and the median radius of the pore size distribution. The test specimens for the repair materials were cut from the large slabs.

The density and compressive strength were measured on drill cores with a diameter and length of 50 mm (or on 100 mm cubes in the case of the concrete specimens) at a specimen age of 28 d in accordance with *DIN EN 12390-7* and *DIN EN 12390-3* respectively. In the water absorption test, which was based on *Bunke 1991,* the water absorption at atmospheric pressure, W_{at}, and at a pressure of 150 bar, W_{150bar}, was determined using 30 mm thick slices with a diameter of 100 mm. The slices were stored in water until a constant mass was reached after which a pressure of 150 bar was applied under water for 24 hours. The pore size distribution and thus the median radius were determined by mercury intrusion porosimetry, the test being performed on fragments of the specimens.

Table A.4: Properties of the specimens determined by laboratory tests

Specimen	Density [kg/m³]	Compressive strength [N/mm²]	W_{at} [% by mass]	W_{150bar} [% by mass]	W_{150bar} * [% by volume]	Median radius [nm]
SPCC 1	2280	65.2	6.5	7.0	15.0	55
SPCC 2	2220	70.5	7.1	8.0	16.5	126
SPCC 3	2210	62.8	7.4	8.8	18.6	52
SPCC 4	2170	46.4	5.9	9.9	20.7	117
PCC I	2080	68.9	9.7	13.1	25.2	50
PCC II	2220	55.0	5.9	6.9	14.5	52
CEM I w/b=0.45	2380	48.1	4.8	6.0	13.7	60
CEM I w/b=0.50	2340	47.4	5.6	6.8	15.1	63
CEM I w/b=0.55	2330	42.9	5.8	6.8	15.3	79
CEM I + FA w/b=0.45	2330	52.5	5.0	6.4	14.4	62
CEM I + FA w/b=0.50	2310	46.9	5.9	7.5	16.5	74
CEM III/B w/b=0.45	2340	41.4	5.1	5.9	13.2	31
CEM III/B w/b=0.50	2340	41.5	5.4	6.1	13.8	32

* *taken as the overall porosity of the specimen*

The specimens made of the repair materials all have lower densities than the concrete specimens but have higher compressive strengths, with the exception of SPCC 4 which has a compressive strength comparable to that of the concrete specimens. As regards water absorption, the majority of the repair material specimens had a higher porosity than the concrete specimens which can largely be explained by the higher binder contents of the repair materials. The lowest median radii were determined for the CEM III/B concretes and the highest median radii for the specimens made of SPCC 2 and SPCC 4. The median radius is the pore radius at which precisely 50 % of the total intrusion volume of mercury has been injected. The median values generally decrease as the fineness of the pore structure increases.

The laboratory tests conducted to estimate durability include the Rapid Chloride Migration test (RCM) and the diffusion test (laboratory storage test). The RCM tests were performed on the specimens at the ages of approx. 28 d, 56 d, 90 d, 180 d, 365 d, 550 d and 730 d in accordance with *BAW-Merkblatt 2012*. In addition, the electrolyte resistance of the specimens was measured by the two electrode method (TEM) immediately before they were placed in the measuring cells.

The diffusion tests were based on *DIN EN 12390-11:2015*. A slab of each repair material that had been stored in water for 28 days was used. The slabs were cut down to 200 x 200 mm² to enable them to be placed in the containers. (The concrete slabs for the diffusion tests were made with the same dimensions.) The surfaces of the slabs – with the exception of the side to be exposed – were sealed with epoxy resin, after which the slabs were stored at 20 °C / 65 % RH for one day to allow the resin to cure. During this time, the side to be exposed was covered with a damp non-woven material to prevent water loss. The sealed slabs were then stored under water for 24 h and subsequently immersed in a 3% NaCl solution to minimize chloride absorption due to absorption / capillary suction. The slabs were stored in plastic containers with lids and placed on spacers with a height of around 5 mm, the containers being filled with the NaCl solution up to around 10 mm above the base of the slabs. The solution was occasionally topped up during the storage period to maintain the solution at a constant level. Apart from storage (immersion) of the specimens in the test solution, *DIN EN 12390-11:2015* describes two other immersion methods. Chloride exposure can either be by ponding or by fully immersing the test specimen in the test solution. Experience has shown that constant exposure of the specimens, i.e. a constant salt concentration and constant contact between the exposed face and the solution, is more easily achieved with the latter type of storage (complete immersion).

Sketches of the test set-ups for the diffusion test and RCM test are shown in Fig. A.1.

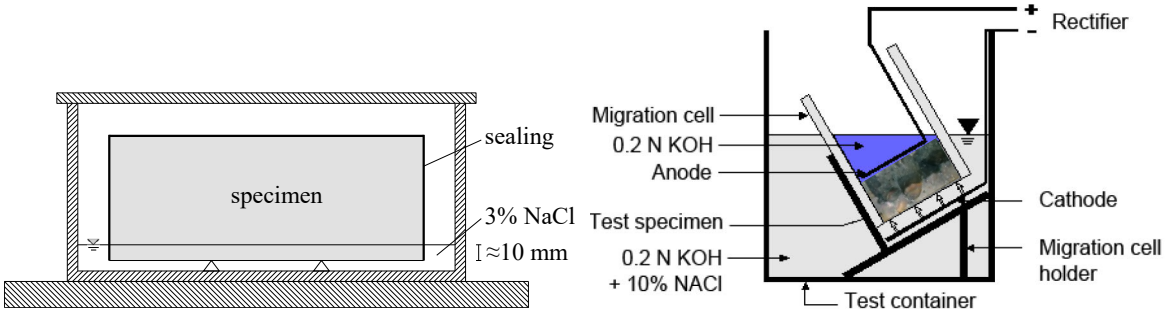

Fig. A.1: Sketches of the test set-up for diffusion test (left) and RCM test (right, from BAW-Merkblatt 2012)

For each material, samples of drill powder were obtained at three points on each slab at depth intervals of 5 mm at the specified (planned) times of around 28 d, 90 d, 180 d, 365 d, 550 d and 730 d after immersion had commenced. The drill powder samples were extracted using a bench drill with a diamond grinding point. The sampling points and the order in which the drill powder samples were taken are shown in Fig. Fig. A.2. The boreholes were subsequently filled with epoxy resin. The overall chloride content of the samples was determined acid digestion and by photometric analysis in accordance with *DAfStb Heft 401:1989*.

The method of sampling (extraction of drill powder samples) differs from the method specified in *DIN EN 12390-11:2015*. In the latter, samples are taken by grinding the sample at the end of the test, i.e. after 90 days' exposure to chlorides. As the chloride profiles needed to be established at several different times for the purposes of this dissertation, sampling was performed by taking drill powder samples to enable the same specimen to be used for the test. Grinding the specimen allows an average sample of the material to be taken over the surface of the specimen while the borehole cuts enable the material to be sampled at different points (at three points in this case). A margin of at least 10 mm around the edges of the specimen should be excluded from grinding. This is because penetration of the solution at the edges cannot be ruled out even though the surfaces of the specimen have been sealed. When obtaining samples by extracting drill powder there is a risk of material being transported from the upper to the lower sampling depths.

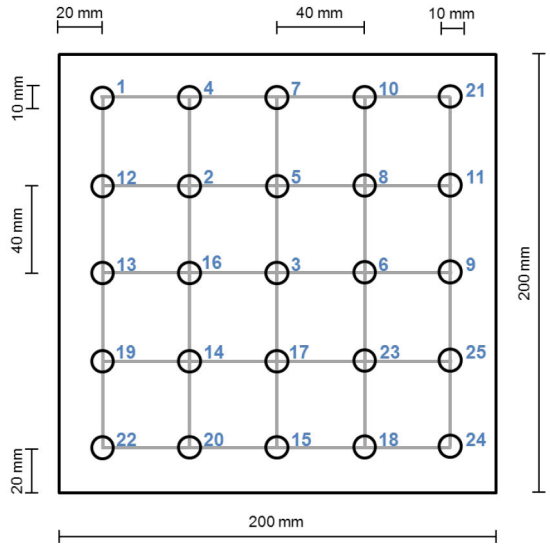

Fig. A.2: Location and order of the borehole cuts in the slabs used in the diffusion tests

The results of the RCM test and diffusion test and results obtained when measuring the electrolyte resistance are presented, evaluated and discussed in the next chapter.

A.3 Parameters and relationships

A.3.1 Chloride profiles

The chloride profiles determined in the diffusion tests (to a depth of 30 mm) on specimens (200 x 200 mm² slabs) of the repair materials or the concrete specimens are shown in Fig. A.3 and Fig. A.4. The chloride content is given as a percentage of the mass of the specimen and not of the cement or binder content as is usually the case. The values were

stated in this way as the binder contents of the repair materials are unknown. For the concrete specimens, the factors used to convert the chloride content into the percentage by mass of the binder are given in Fig. A.4.

The times selected for taking the specimens and establishing the chloride profiles were 28 d, 90 d, 180 d, 365 d, 550 d and 730 d after commencement of the diffusion test and were based on the method of determining the ageing exponent α_{nss} presented in Chapter 2.3.2.2.2. However, it was not possible to establish chloride profiles for all specimens at each of the scheduled times for a variety of reasons relating to organizational aspects, the laboratory and the measuring methods. Chloride profiles with results that were obviously incorrect were discarded.

The chloride profiles mostly indicate a continuous increase in the chloride content of the test specimens. Any incorrect results may be due to contaminated material being transported from the upper layers into the lower ones in some of the profiles. For all of the test specimens, it was possible to model the depth-dependent development of the chloride content very well with the Gauss error function based on Fick's second law of diffusion (coefficient of determination R^2 between 0.90 and 1.0). The chloride contents of test specimen SPCC 4 were considerably higher than those of the other specimens, both in the near-surface zone and at the deeper levels. The two PCC specimens and the concrete specimens CEM III/B w/b=0.45 and CEM I w/b=0.45 have the lowest chloride contents. It can be seen from the concrete specimens that the water/binder ratio *w/b* has an impact. For a Portland cement concrete, specimen CEM I w/b=0.45 has relatively low chloride contents. Compared with conventional Portland cement concretes, the values of $D_{RCM}(t_0)$ and the specific electrolyte resistance ρ (see Fig. A.6) indicate that this type of concrete has an above-average resistance to chloride ingress and a dense structure.

The chloride contents determined at the surface of the specimens (to a depth of 5 mm) developed differently over time. While the surface chloride concentration of most of the specimens increases over time, it is almost constant for SPCC 1 and increases only slightly for the two PCC samples. However, it must be noted that the surface chloride concentration tends to be rather inaccurate, possibly as a result of salt crystals adhering to the surface of the specimens.

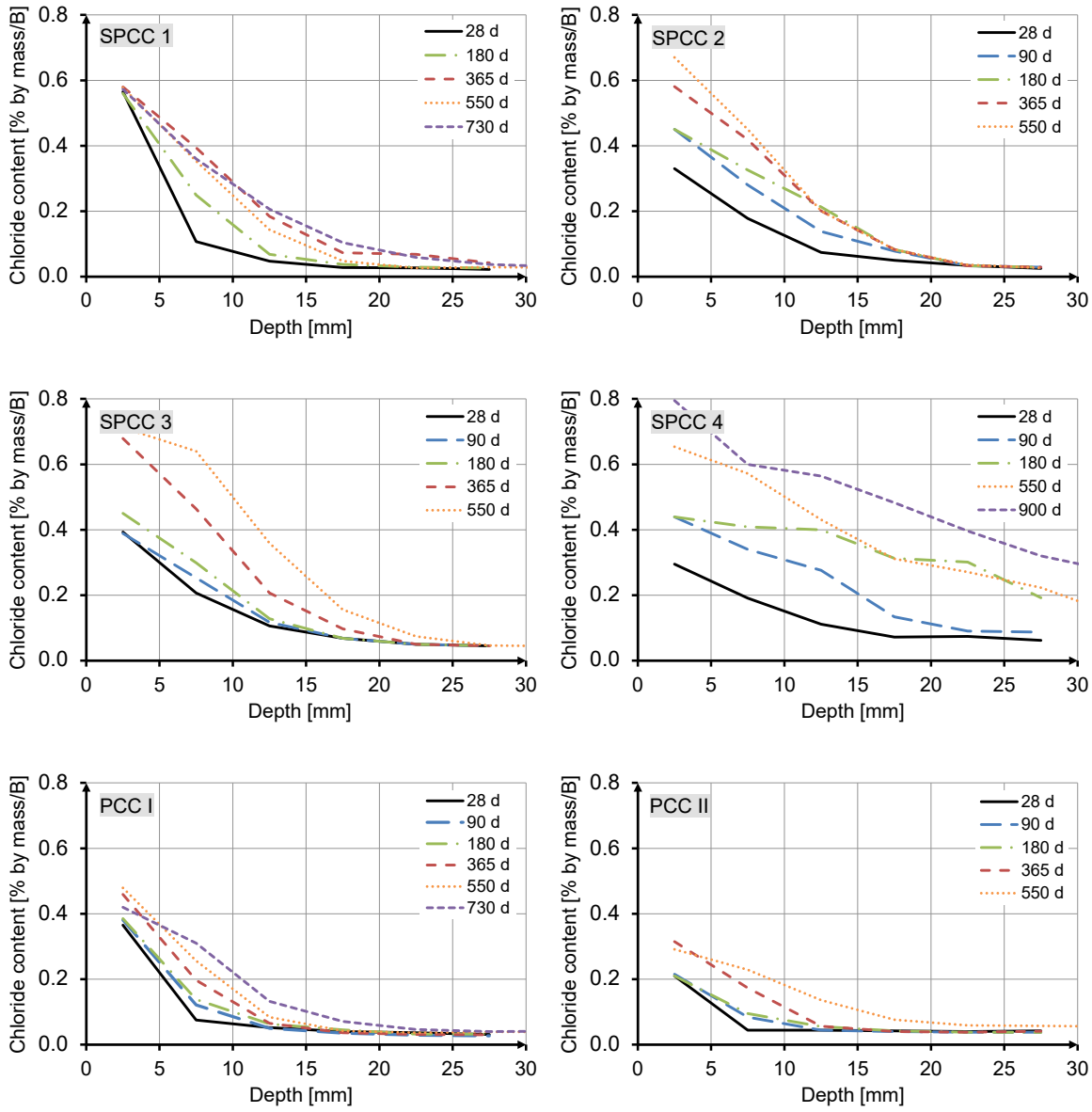

Fig. A.3: Chloride profiles of the specimens made of the repair materials derived from diffusion tests

On the whole, there was no evidence of any systematic differences between the specimens made of repair materials and the concrete specimens as regards the time- and depth-dependent chloride penetration.

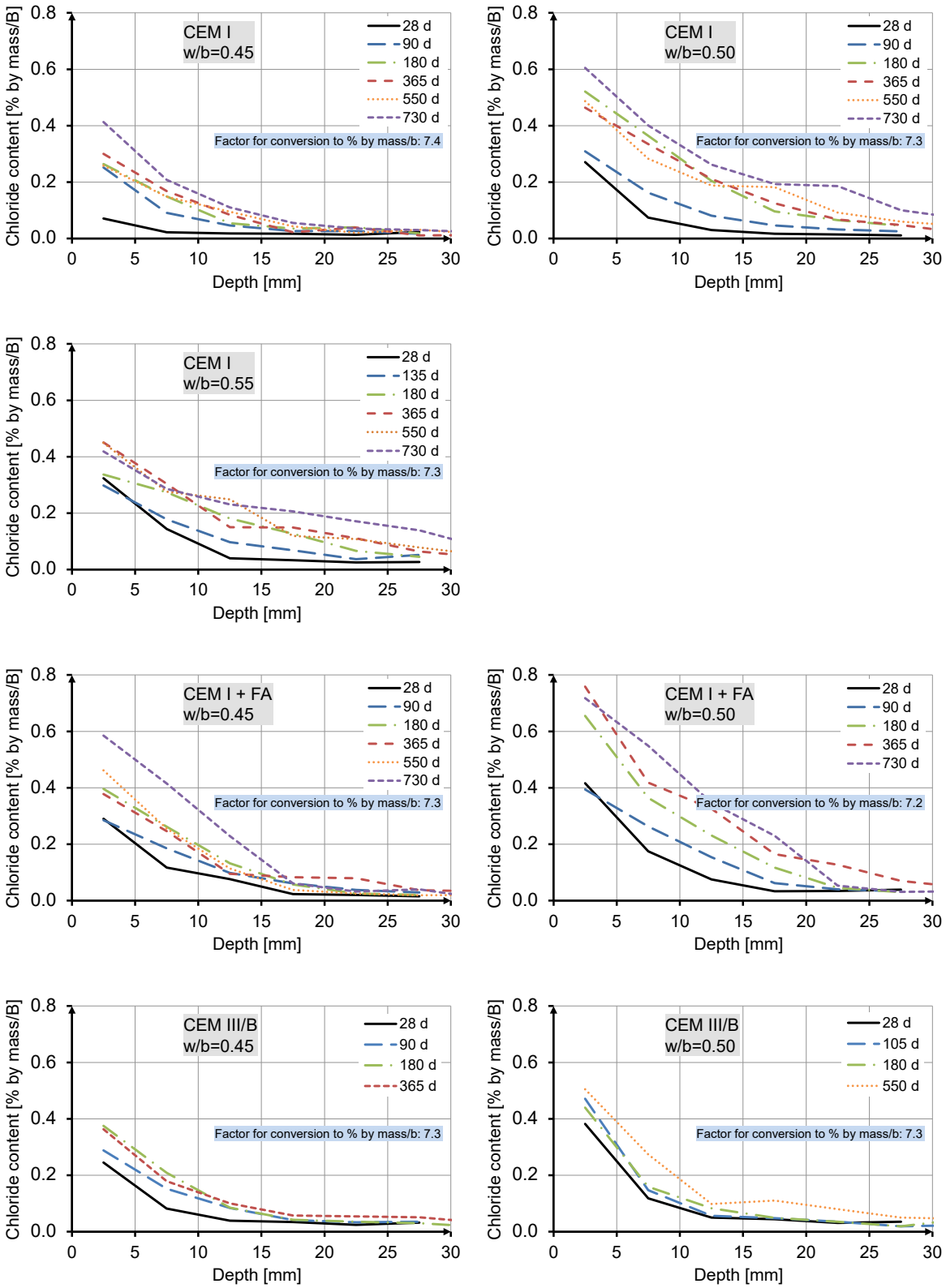

Fig. A.4: Chloride profiles of the concrete specimens derived from diffusion tests

Initial chloride contents C_0 between 0.01 and 0.03 % by mass/B were determined for the specimens made of repair materials. The concrete specimens had lower initial chloride contents, ranging between 0.002 and 0.01 % by mass/B (0.02 to 0.08 % by mass/b).

A.3.2 Development of the non-steady state chloride diffusion coefficient over time, $D_{nss}(t)$

The non-steady state chloride diffusion coefficients $D_{nss}(t)$ were calculated from the chloride profiles by carrying out regression analyses with Gauss' error function to solve Fick's law of diffusion (see Chapter 2.3.2.2). Generally speaking, the non-steady state chloride diffusion coefficient D_{nss} can be expected to decrease over time. This is due to post-hydration of the binder which leads to an increase in the density of the specimens. This tendency can be observed in all of the specimens (see Fig. A.5 and Fig. A.6), although it varies in intensity. The development of D_{nss} over time is quantified by means of a trend line in the double-log diagrams in Fig. A.5 and Fig. A.6. The regression function (power: $y=a \cdot x^{-\alpha}$) and the coefficient of determination R^2 are specified. The ageing exponent α_{nss} (see Chapter 2.3.2.2.2) is expressed by the exponent of the trend function α. The values of $D_{nss}(t_0)$ and α_{nss} for each of the test specimens are given in Table A.6.

It should be noted that the gradual development of the surface chloride concentration (ideally increasing until a constant value is reached) has a beneficial effect on ageing exponents α_{nss} determined in this way. The very high ageing exponents of several of the specimens, including SPCC 2 and SPCC 3 (0.90 and 0.81 respectively) can partly be attributed to this effect.

The other parameters shown in Fig. A.5 and Fig. A.6, D_{RCM}, ρ and $D_{app}(t=50\ a)$, are discussed in the following chapters.

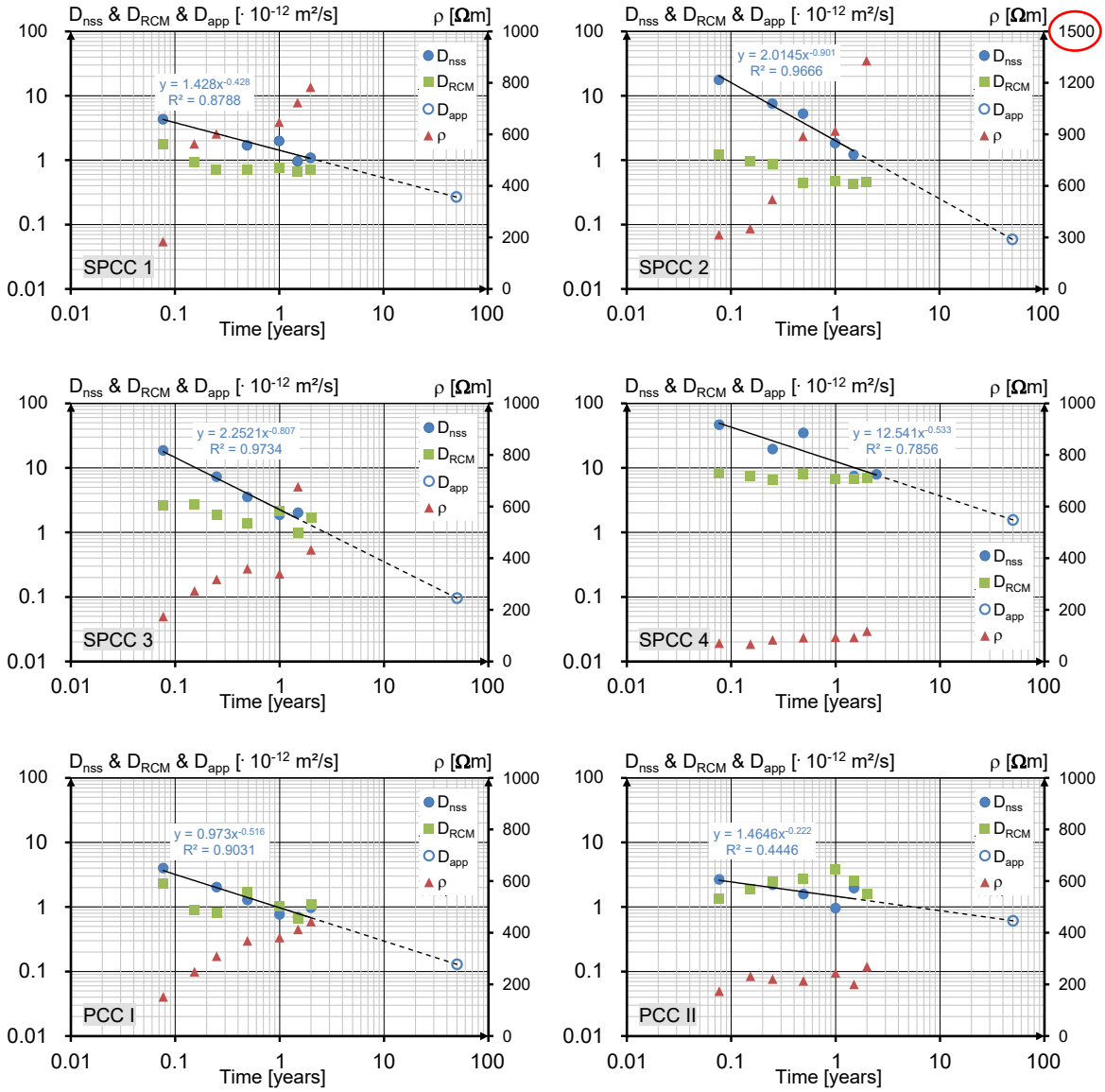

Fig. A.5: Development of the parameters chloride diffusion coefficient D_{nss}, chloride migration coefficient D_{RCM} and specific electrolyte resistance ρ; determining the ageing exponent and the apparent diffusion coefficient $D_{app}(t=50\ a)$ – investigated repair materials

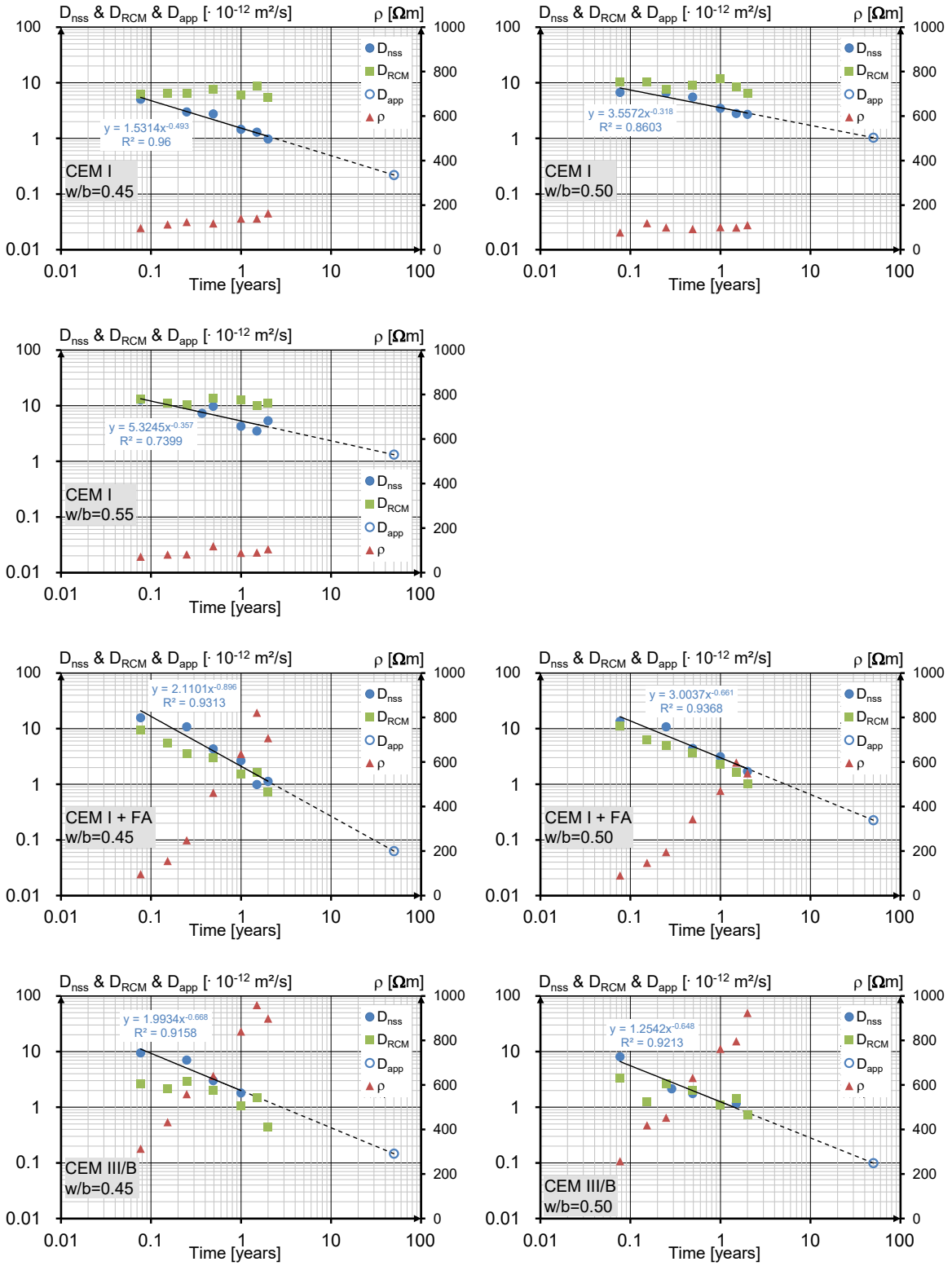

Fig. A.6: Development of the parameters chloride diffusion coefficient D_{nss}, chloride migration coefficient D_{RCM} and specific electrolyte resistance ρ; determining the ageing exponent and the apparent diffusion coefficient $D_{app}(t=50\ a)$ – investigated concretes

A.3.3 Chloride migration coefficient D_{RCM}

The RCM test is generally performed on test specimens at an early age (28 d or 56 d for slow-hardening materials according to *BAW-Merkblatt 2012*). The test is used to obtain a relatively quick and simple assessment of the resistance of concretes to chloride ingress. The parameter D_{RCM} $(t_0=28d)$ can be used to determine the apparent chloride diffusion coefficient in accordance with Approach B presented in Chapter 2.3.2.2.3 and for durability design. It is not generally necessary to determine values of D_{RCM} at later points in time. However, the development of D_{RCM} in the investigated materials over time was determined for the purposes of this dissertation to enable any specific features of the repair materials to be identified.

With the exception of SPCC 4, the chloride migration coefficients D_{RCM} of the repair material specimens determined at t_0 = 28 d (start of the test) are considerably lower (more favourable) than those of the Portland cement and Portland fly ash cement concretes and are either similar to or lower than those of the blast-furnace cement concretes (see Fig. A.5 and Fig. A.6).

Similar to the development of D_{nss} over time, the parameter D_{RCM} can also be expected to decrease over time as the structure becomes denser owing to post-hydration of the binder. However, it can be seen from the diagrams in Fig. A.5 and Fig. A.6 that this does not apply to all specimens and the decrease is considerably less pronounced than for D_{nss}. While D_{RCM} decreases at approximately the same rate over time as D_{nss} for concrete specimens made with CEM I + FA and at a slightly lower rate for the concrete specimens made with CEM III/B, it remains more or less constant over time for the concrete specimens made with CEM I. The tendency of D_{RCM} to decrease over time can be observed for specimens SPCC 1, SPCC 2, SPCC 3 and PCC I although it is less pronounced than for D_{nss}. The values of D_{RCM} for test specimen SPCC 4 remain more or less constant. For test specimen PCC II, the value of D_{RCM} increases steadily over the first five measurements, at 28 d, 56 d, 90 d, 180 d and 365 d, but decreases at the 550 d and 730 d measurements.

In the literature, D_{RCM} is generally assumed to decrease over time in conventional concretes. In *Lay & Schießl 2006,* the development of D_{RCM} over time was observed for concretes with different types of binder (CEM I, CEM II/A-LL, CEM II-B/T, CEM II/B-S, CEM I + FA, CEM III/A and CEM III/B) over a period of around two years. There was a pronounced decrease in the D_{RCM} over time for concretes containing fly ash, followed by blast-furnace cement concretes. The decrease was considerably lower for concretes made with Portland cement (CEM I) and CEM II/A-LL. The development of D_{RCM} over time was formulated mathematically in *Lay & Schießl 2006* on the basis of the results of the investigations.

Data taken from various publications demonstrates that the behaviour of Portland cement concretes is inconsistent as regards the development of D_{RCM} over time (e.g. *Yu et al. 2013*, *Maage et al. 1996, Tang 1996*). According to these authors, D_{RCM} initially decreases slightly but increases again later on. This effect was observed in Portland cement concretes with high water/cement ratios in particular. In *Yu et al. 2013*, an increase in D_{RCM} after around 180 days of curing (storage in water) was observed for three Portland cement concretes with w/c ratios of 0.40, 0.50 and 0.60. Following more intensive testing, it is suggested in *Yu et al. 2013* that the increase in D_{RCM} may be caused by a transformation from CSH phases with a low density to denser CSH phases as the concrete ages, leading to a shift in the pore size distribution towards the coarser end of the range.

In the search for a possible explanation for the chloride migration coefficients determined in the tests, the structure of the specimens immersed in water was investigated at the ages of 28 d, 365 d, 550 d and 730 d by means of mercury intrusion porosimetry. The median radius of the pore size distribution and the porosity are shown in Table A.5. The results for the CEM I concrete specimens are not unusual in any way. The median radius and porosity are both more or less constant over time. Only a slight reduction in the porosity over time can be seen for CEM I w/b=0.55. The almost constant value of D_{RCM} for the CEM I concretes under investigation can be explained by the fact that hydration of the Portland cement is more or less complete at an early age of the concrete.

The other concretes (CEM I + FA and CEM III/B) did not exhibit any significant change in the median radius over time either. However, their porosity tends to decrease with time.

There was a marked increase in the median radius of repair materials SPCC 1, SPCC 2 and PCC II, while the median radius of SPCC 4 decreased slightly over time. The porosity of SPCC 4 also decreases over time. The results of the investigations into the structure of the materials conducted with mercury intrusion porosimetry do not explain why the chloride migration coefficients of the investigated materials and the conventional concretes develop differently over time. Further investigations are required to find an explanation for this phenomenon.

Table A.5: Derived values from mercury intrusion porosimetry

Material	Median radius [nm]				Porosity [Vol.-%]			
	28 d	365 d	550 d	730 d	28 d	365 d	550 d	730 d
SPCC 1	55	–	149	–	15.4	–	15.2	–
SPCC 2	126	–	173	388	19.5	–	19.0	19.1
SPCC 3	52	–	55	51	15.8	–	15.3	15.4
SPCC 4	117	–	102	88	20.6	–	17.7	18.0
PCC I	50	62	58	62	18.9	18.0	17.6	17.9
PCC II	52	68	66	103	13.5	13.5	12.9	13.2
CEM I w/b=0.45	59	64	59	53	15.2	13.6	14.0	14.6
CEM I w/b=0.50	63	64	59	63	16.0	15.5	13.7	16.0
CEM I w/b=0.55	79	73	75	74	18.9	18.5	18.1	17.5
CEM I + FA w/b=0.45	62	56	61	60	16.2	15.7	14.8	14.5
CEM I + FA w/b=0.50	74	62	46	54	18.6	17.7	17.2	17.2
CEM III/B w/b=0.45	31	34	35	41	14.4	13.1	13.3	13.2
CEM III/B w/b=0.50	32	34	28	33	18.7	15.2	15.0	15.5

The RCM laboratory test method was developed as an alternative to the diffusion test. The RCM test has been shown to be a suitable method of testing and assessing the resistance of concrete to chloride ingress as the testing times are short, it is generally easy to use and reliable and has a sufficient degree of accuracy. A number of publications (*Gehlen 2000, Gehlen & Ludwig 1999, Frederikson et al 1996, Tang et al. 2010*) have pointed out that there is a good correlation between D_{RCM} and D_{nss} for concrete at an early age (between 28 and 90 days). This applies in particular to Portland cement concretes and was confirmed for the Portland cement and Portland fly ash cement concretes investigated in connection with this dissertation. In the case of blast-furnace cement concretes, the values of D_{RCM} at 28 d are lower than the values of D_{nss}. The binder-dependent correlations between D_{RCM} and D_{nss} observed here are in line with the comments on the determination of the chloride diffusion coefficient $D_{app}(t)$ according to Approach B in Chapter 2.3.2.2.3. The much lower values of $D_{RCM}(t_0)$ for blast-furnace cement concretes meant that the difference between the trend line through the $D_{app}(t)$ values obtained for such concretes from structural data and the trend line forced through $D_{RCM}(t_0)$ was greater than for Portland and Portland fly ash cement concretes.

For the repair materials, it can be clearly seen that, with only a few exceptions, the values of D_{RCM} are lower than those of D_{nss}. The differences are particularly pronounced for the SPCC.

The values of D_{RCM} and D_{nss} determined for the investigated repair materials and concretes are compared in Fig. A.7 (on the left and right respectively).

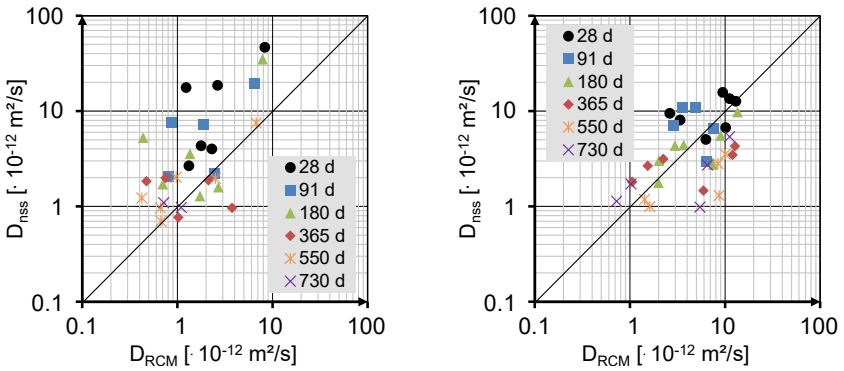

Fig. A.7: Comparison of the derived parameters D_{RCM} and D_{nss} of the investigated repair materials (left) and concretes (right)

The RCM tests on the repair materials were performed with longer test durations (exposure with the catholyte in the measuring cell) than specified in *BAW-Merkblatt 2012* to enable a penetration depth of at least 10 mm to be reached in the specimens. This was because the binder content of PCC and SPCC is considerably higher than that of conventional concretes. According to *NT Build 492:1999*, the test duration must be increased for materials with higher binder contents. In this case, the initial amperage is reduced by a factor equivalent to the ratio of the binder content of conventional concretes (300 – 350 kg/m³) to that of the material and the test duration selected accordingly. In the context of this dissertation, the binder contents of the investigated PCC and SPCC materials were assumed to be twice those of conventional concretes, resulting in a factor of 0.5. The D_{RCM} exhibits a high degree of scatter for penetration depths less than 10 mm (*Tang 1996*).

In addition, the surface zone of 10 mm was disregarded when evaluating the RCM tests, as specified *NT Build 492:1999,* to prevent the test results being affected by the chloride penetration depths in the surface zone as these are frequently greater owing to the porosity of the surface of the test specimens.

A.3.4 Specific electrolyte resistance ρ

The specific electrolyte resistance ρ [Ωm] is determined immediately before starting the RCM test, taking into account the dimensions of the test specimen (factor: cross-sectional

area [m²] / height [m]). It is derived from the electrolyte resistance [Ω] measured by means of the two-electrode method (TEM).

On the whole, the measured specific electrolyte resistances ρ have a tendency to increase over time (see Fig. A.5 and Fig. A.6). However, this tendency and the absolute value of the specific electrolyte resistance ρ differ greatly for the materials under investigation. The specific electrolyte resistance ρ increases very slightly over time for the CEM I concretes and SPCC 4. Compared with the values of ρ for the other materials, the values measured are extremely low. PCC II also has a low specific electrolyte resistance ρ which increases slightly over time. As regard the concretes, the investigated CEM III/B concretes have higher values of ρ than the CEM I +FA concretes. The values of ρ measured for SPCC 1, SPCC 2 and SPCC 3 are in the same range as those of the concretes made with CEM I + FA and CEM III/B.

It can be seen from the results that there is a relatively good correlation between ρ and D_{RCM} as regards both the magnitude and the development over time. The values of D_{RCM} and ρ measured for the investigated repair materials and the concretes are compared separately in Fig. A.8, on the left and right respectively. For both groups of material, the functional correlation between the two parameters can be represented relatively accurately by a power function (R^2 = 0.85 and 0.90). The values of D_{RCM} and ρ measured for the investigated materials are compared in Fig. A.9, left. The accuracy of the functional relationship is lower than when the correlations for the repair materials and the concretes are considered separately (R^2 = 0.80). On the whole, the relationship between D_{RCM} and ρ can be determined with a greater degree of accuracy for the investigated concretes.

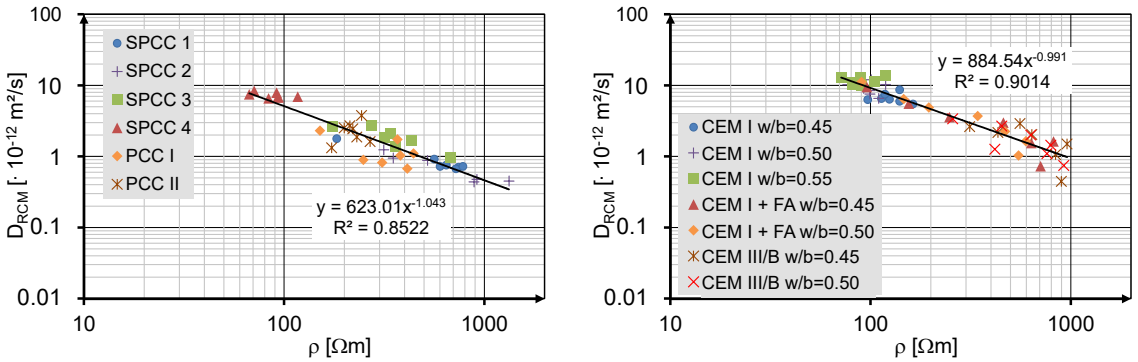

Fig. A.8: Relationship between the measured D_{RCM} und ρ of the investigated repair materials (left) and concretes (right)

Numerous authors have also established a good functional relationship between the electrolyte resistance and the D_{RCM} of concretes (e.g. *Gehlen 2000, Gehlen & Ludwig 1999*, *Bamforth 1997*). The correlation between D_{RCM} and the specific electrolyte resistance measured by Wenner probe, ρ_{WER}, as determined in *Gehlen 2000*, is illustrated

for several concretes in Fig. A.9, right. In *Gehlen 2000*, a proportional correlation was demonstrated between the electrolyte resistance of the concrete measured by the two-electrode method (TEM) and the electrolyte resistance measured using the Wenner probe.

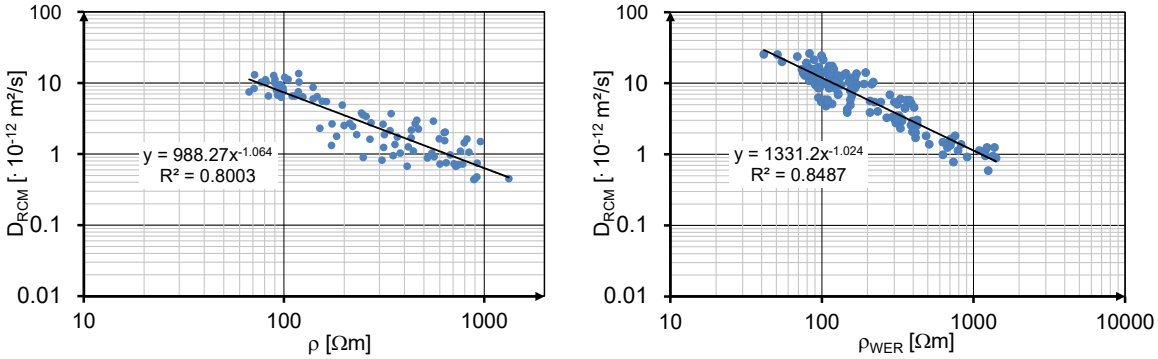

Fig. A.9: Left: relationship between the measured D_{RCM} und ρ of the investigated repair materials and concretes; right: relationship between D_{RCM} und ρ_{WER} of several concretes (from Gehlen 2000)

The specific electrolyte resistance ρ is usually measured by TEM by way of an additional control in the RCM tests as the test is straightforward and requires little time and effort.

A.4 Evaluating the performance of repair materials

The parameters of the investigated materials that are relevant for durability design using the nomograms in Annex D ($D_{nss}(t_0)$, $D_{RCM}(t_0)$, α_{nss}) are shown in Table A.6. The service life was calculated for a randomly selected design case, both with the parameters $D_{nss}(t_0)$ and α_{nss} from the diffusion tests and parameter $D_{RCM}(t_0)$ from the RCM test (Approaches A and B respectively for determining $D_{app}(t)$, see Chapter 2.3.2.2). The binder-dependent value of α_{RCM} from Table 2.5 eingesetzt. Für die Instandsetzungsmaterialien wurde der Altersexponent α_{RCM} = 0,20 gesetzt. Zudem zeigt Table A.6 shows the calculated apparent chloride diffusion coefficient from the diffusion tests after 50 years, $D_{app}(t=50\ a)$.

The service life of the repair materials calculated with the parameters $D_{nss}(t_0)$ and α_{nss} varies widely, ranging from < 10 years to > 100 years. For SPCC 2 and SPCC 3, a maximum value of 0.80 was taken into account for α_{nss} (see Chapter 2.4.4.4). Owing to the great amount of time and effort required to determine α_{nss} by diffusion tests, the durability design of repair materials can be performed with $D_{RCM}(t_0)$ and a conservative value of 0.20 for α_{RCM}. As shown in Table A.6, this option results in a lower service life. An exception is PCC II. In this case, service life design performed with $D_{RCM}(t_0)$ produces better results owing to the very favourable values of $D_{RCM}(t_0)$.and the very unfavourable values of α_{nss}.

As expected, the service life calculated for the investigated concretes also varies to a great extent. Similar to α_{RCM} in Table 2.5, the concretes containing fly ash have, on the whole,

the highest values of α_{nss}, followed by CEM III/B concretes. For these concretes, the values of α_{nss} are higher than their values of α_{RCM}. The CEM I concretes have the most unfavourable values of α_{nss}, in the range of α_{RCM} = 0.30, with the exception of CEM I w/b=0.45 which has a value of α_{nss} = 0.49 and generally has above-average material characteristics. For the majority of concretes, the service life calculated with $D_{RCM}(t_0)$ and α_{RCM} is lower for that calculated with $D_{nss}(t_0)$ and α_{nss}. This is due to the relatively unfavourable values of $D_{RCM}(t_0)$ of the investigated concretes, possibly because the selected constituents (aggregates, grading curve, superplasticizing admixture, etc.) are not as compatible as they might be.

The results of $D_{nss}(t_0)$, $D_{RCM}(t_0)$, $D_{app}(t=50\ a)$ and t_{SL} obtained for the investigated materials are compared in Table A.7. It can be seen that the parameters $D_{nss}(t_0)$ and $D_{RCM}(t_0)$ result in different evaluations of the materials and that, on their own, are insufficient to enable the performance of the materials to be assessed. As expected, the calculated service life t_{SL} and $D_{app}(t=50\ a)$ result in similar evaluations for the materials. The few differences are due to the maximum value of α_{nss} being limited for service life design and for service lives over 50 years.

Table A.6: Determined parameters $D_{nss}(t_0)$, $D_{RCM}(t_0)$, a_{nss} for service life design; calculated $D_{app}(t=50$ years); calculated service life t_{SL} of a structural element under XS2 exposure

Material	$D_{nss}(t_0)$ [$\cdot 10^{-12}$ m²/s]	α_{nss} [1)] [–]	t_{SL} [2)] [year]	$D_{RCM}(t_0)$ [$\cdot 10^{-12}$ m²/s]	t_{SL} [3)] [year]	$D_{app}(t=50$ a) [$\cdot 10^{-12}$ m²/s]
SPCC 1	4.3	0.43	35	1.8	25	0.27
SPCC 2	17.6	0.90	> 100	1.2	40	0.059
SPCC 3	18.6	0.81	> 100	2.6	15	0.096
SPCC 4	46.5	0.53	n. e.	8.3	< 10	1.56
PCC I	4.0	0.52	90	2.3	19	0.13
PCC II	2.7	0.22	17	1.3	36	0.61
CEM I w/b=0.45	5.0	0.49	46	6.3	< 10	0.22
CEM I w/b=0.50	6.7	0.32	< 10	10.2	< 10	1.03
CEM I w/b=0.55	12.6	0.36	< 10	13.0	< 10	1.32
CEM I + FA w/b=0.45	15.7	0.90	> 100	9.5	41	0.063
CEM I + FA w/b=0.50	13.5	0.66	38	11.1	30	0.23
CEM III/B w/b=0.45	9.5	0.67	94	2.6	93	0.15
CEM III/B w/b=0.50	8.0	0.65	> 100	3.4	60	0.099

1) *α_{nss} must be limited to values between 0.20 and 0.80 (see Chapter 2.4.4.4); i.e. for SPCC 2, SPCC 3 and CEM I + FA w/b=0.45 a value $\alpha_{nss} = 0.80$ applies.*

2) *Service life calculated with values determined for parameters $D_{nss}(t_0)$ and α_{nss} using the nomograms in Annex D for the following design situation: XS2, $\beta_0 = 1.5$, $C_{S,\Delta x} = 3.0$ % by mass/b, $c_{min} = 50$mm*

3) *Service life calculated with the values determined for $D_{RCM}(t_0)$ and α_{RCM} according to Table 2.5 using the nomograms in Annex D for the following design situation: XS2, $\beta_0 = 1.5$, $C_{S,\Delta x} = 3.0$ % by mass/b, $c_{min} = 50$mm; the calculations for the repair materials were performed with $\alpha_{RCM} = 0.20$.*

n. e.: cannot be determined as $D(t_0) \leq 20 \cdot 10^{-12}$ m²/s in the nomograms; however, $t_{SL} < 10$ years

Table A.7: Comparative assessment of the investigated materials

	Parameters			
	$D_{nss}(t_0)$	$D_{RCM}(t_0)$	$D_{app}(t=50\ a)$	t_{SL} [1)]
From most unfavourable → to most favourable	PCC II	SPCC 2	SPCC 2	CEM I + FA w/b=0.45
	PCC I	PCC II	CEM I + FA w/b=0.45	SPCC 2
	SPCC 1	SPCC 1	SPCC 3	SPCC 3
	CEM I w/b=0.45	PCC I	CEM III/B w/b=0.50	CEM III/B w/b=0.50
	CEM I w/b=0.50	SPCC 3, CEM III/B w/b=0.45	PCC I	CEM III/B w/b=0.45
	CEM III/B w/b=0.50		CEM III/B w/b=0.45	PCC I
	CEM III/B w/b=0.45	CEM III/B w/b=0.50	CEM I w/b=0.45	CEM I w/b=0.45
	CEM I w/b=0.55	CEM I w/b=0.45	CEM I + FA w/b=0.50	CEM I + FA w/b=0.50
	CEM I + FA w/b=0.50	SPCC 4	SPCC 1	SPCC 1
	CEM I + FA w/b=0.45	CEM I + FA w/b=0.50	PCC II	PCC II
	SPCC 2	CEM I w/b=0.50	CEM I w/b=0.50	CEM I w/b=0.50
	SPCC 3	CEM I + FA w/b=0.50	CEM I w/b=0.55	CEM I w/b=0.55
	SPCC 4	CEM I w/b=0.55	SPCC 4	SPCC 4

[1)] *Service life calculated with the parameters $D_{nss}(t_0)$ and α_{nss} using the nomograms in Annex D for the following design situation: XS2, $\beta_0 = 1.5$, $C_{S,\Delta x} = 3.0$ % by mass/b, $c_{min} = 50$mm*

Finally, it should be noted that the results of the investigations reveal that the behaviour of the repair materials and concretes may differ to some extent. In *Andrade & Whiting 1996,* it is pointed out that the behaviour of polymer-modified cement-bound materials in the RCM test may be inconsistent and may differ from that of concrete. Furthermore, *Hunkeler et al. 2000* drew attention to the particularly large degree of scatter in the results for the chloride content of polymer-modified materials observed in a round-robin test in which the chloride content of concrete was determined chemically. Accordingly, special precautions should be taken when determining the chloride content of such materials. Further research into the possible influence of polymer fibres on the RCM test and the chemical determination of the chloride content is required.

B Annex B: Studies of the chloride transport in repaired concrete members

B.1 Laboratory tests to determine the chloride transport in a two-layer system

To study the chloride transport in two-layer systems, composite specimens comprising a layer of concrete with chloride gradients and a repair layer were prepared, see Fig. B.1. The mechanisms of ingress, "back-diffusion" and redistribution of chloride ions in the new repair layer and concrete layer were studied in long-term diffusion tests (laboratory storage tests) with occasional profile sampling. A summary of the laboratory storage tests, with the specimens and storage conditions, is given in Table B.1. Three types of concrete (CEM I with w/c ratios of 0.55, 0.60 and 0.65) and one type of repair material (PCC I from Annex A) were investigated. The binder and w/c ratios were selected for their high porosity and to obtain a diffusion-open concrete, with the aim of achieving a relatively rapid mobilization of the chloride ions.

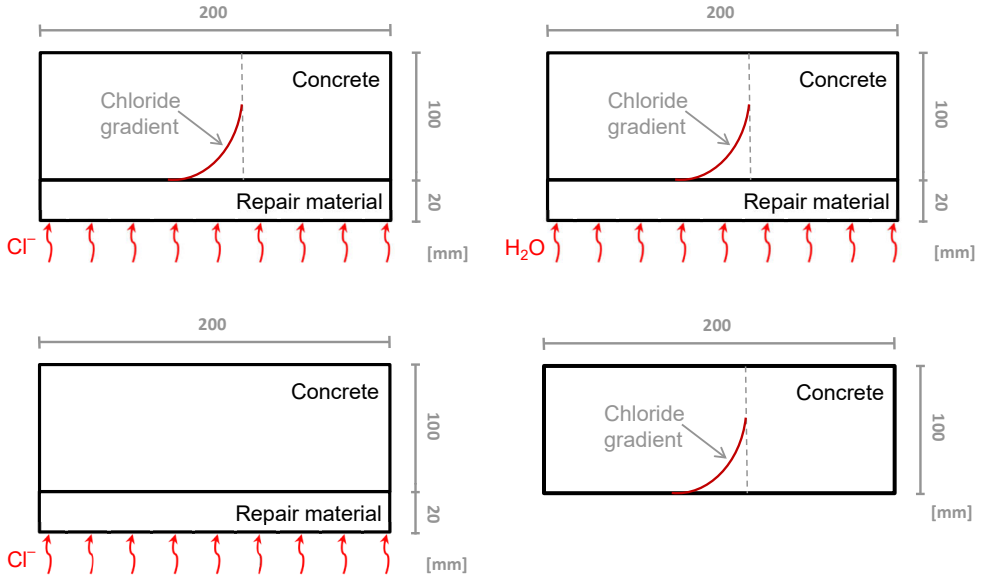

Fig. B.1: Sketch of the specimens used for the laboratory storage tests (width: 200 mm)

Table B.1: Diffusion (storage) tests to investigate the chloride transport in a 2-layer system

Test series	Specimen [1)]	Pretreatment – Prestorage	Mechanism being investigated
1	Composite slabs with residual chlorides	Cl – Cl	D, R, U
2	Composite slabs with residual chlorides	Cl – water	R, U
3	Composite slabs	20 °C / 65 % r.h. – Cl	D
4	Concrete slabs with residual chlorides	Cl – 20 °C / 65 % r.h.	U

D: Diffusion (ingress) of external chlorides into the repair layer and concrete layer
R: "Back diffusion" of residual chlorides into the repair layer
U: Redistribution of residual chlorides in the concrete layer
[1)] two specimens per concrete and test series

The concrete test specimens were first immersed in a 3 % NaCl solution for around 280 days (over 9 months) (unidirectional exposure) after which the resulting chloride gradients were determined. A repair layer (with a thickness of 20 mm) was then applied to the test specimens, Series 1-3. The composite specimens were subsequently stored in the laboratory at 20 °C / 65 % r. h. for 28 days. The change in the chloride gradient was studied during this period, prior to the storage periods shown in Table B.1. In test series no. 1, the composite specimens were stored in a 3 % NaCl solution for the purpose of studying the chloride transport processes in a two-layer system as a whole. In test series no. 2, the composite specimens were stored in water, mainly in order to study the redistribution and back-diffusion in the repair layer. For test series no. 3, the composite specimens with no chlorides in the concrete layer, i.e. which had not previously been exposed, were stored in a 3 % NaCl solution to observe the chloride diffusion in the absence of chloride gradients in the concrete layer. In the last test series, series no. 4, the concrete specimens were sealed with epoxy resin after storage in the chloride solution for 280 days (conditioning) and stored in the laboratory in dry conditions at 20 °C / 65 % r. h. to observe the redistribution of the chlorides in the specimens.

To achieve a better bond between the two layers, the concrete test specimens were sandblasted immediately before the layer of mortar was applied to the surface, the average removal depth being around 1 mm. The concrete specimens were removed from the 3 % NaCl solution around 1.5 days prior to application of the repair mortar and left to dry.

Fig. B.2 and Fig. B.3 show the chloride profiles as average values of the chloride contents determined for two specimens (per concrete and test series) at different times, up to a maximum of two years after storage had started. Test series no. 4 was not taken into account in the tables as the chloride profiles obtained seemed unrealistic and highly implausible, indicating an error in the test procedure for this particular series.

To establish the chloride profiles, slices were sawn from the test specimens at 5 mm intervals and subsequently ground. The overall chloride content of the ground samples was determined by acid digestion and photometric analysis in accordance with DAfStb Heft 401:1989. The chloride contents are given as a percentage by mass of the specimens (% by mass/B), not as a percentage by mass of the cement or binder, as would usually be the case, as the binder content of the repair material (PCC) was not known.

For all three concretes, the chloride profiles of test series 1 and 2 indicate that the residual chlorides are continually extracted from the repair layer. The chloride content at the first measuring level in the repair layer increases almost constantly over time. A pronounced reduction in the chloride content in the concrete closest to the interface can be seen in the first profile (after application of the repair layer and before the beginning of storage). In each of the three concretes, the reduced chloride content is greater than that extracted from the repair layer. This difference can partly be explained by the removal of material from the surface of the concrete during sandblasting prior to application of the repair material. The chloride content in this region increases again slightly during the storage period. A pronounced redistribution of the chlorides in the concrete layer was not noticeable in the period of time under consideration.

It should be noted that the chloride profile prior to application of the repair layer is the mean value of the chloride contents measured for three other specimens. The chloride profile after application of the repair layer and before storage was determined by measuring the chloride content of the two specimens of series no. 1. As the concrete and the specimens are not homogeneous, the chloride profiles shown may differ slightly from the actual values. In this case, the purpose of the chloride profiles is to arrive at a qualitative evaluation of the chloride transport in the repaired structural elements.

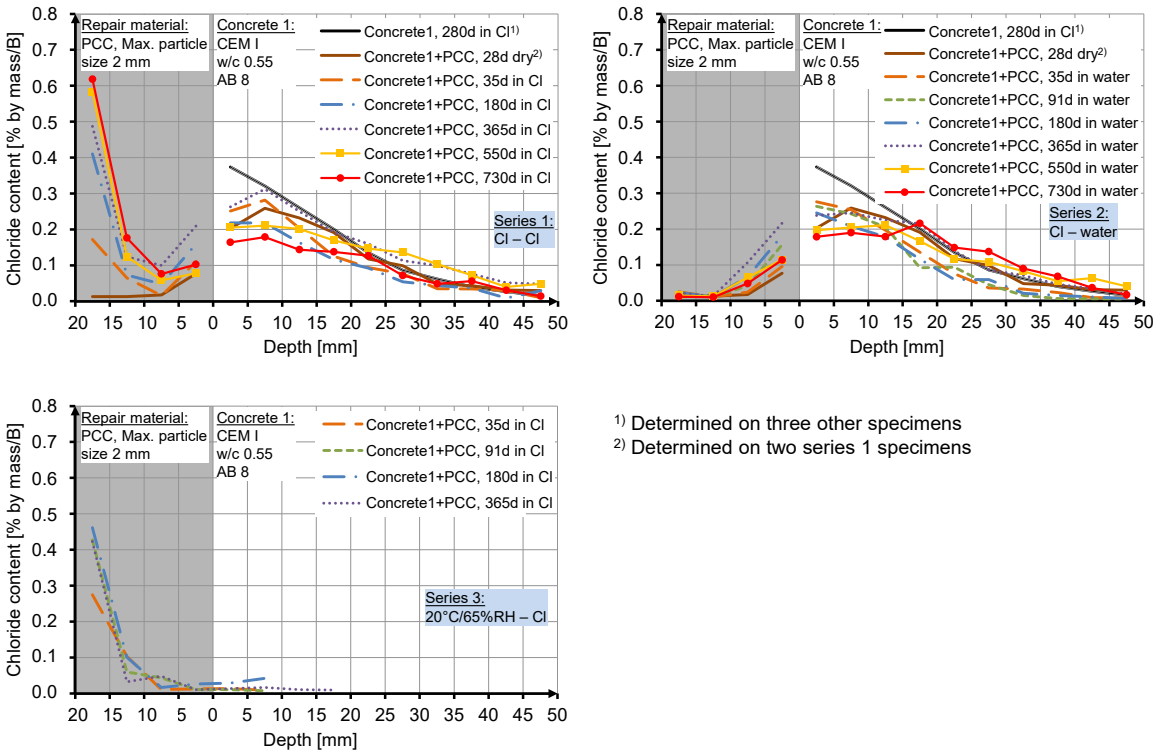

1) Determined on three other specimens
2) Determined on two series 1 specimens

Fig. B.2: Average chloride profile of the specimens made of concrete 1 (w/c = 0.55)

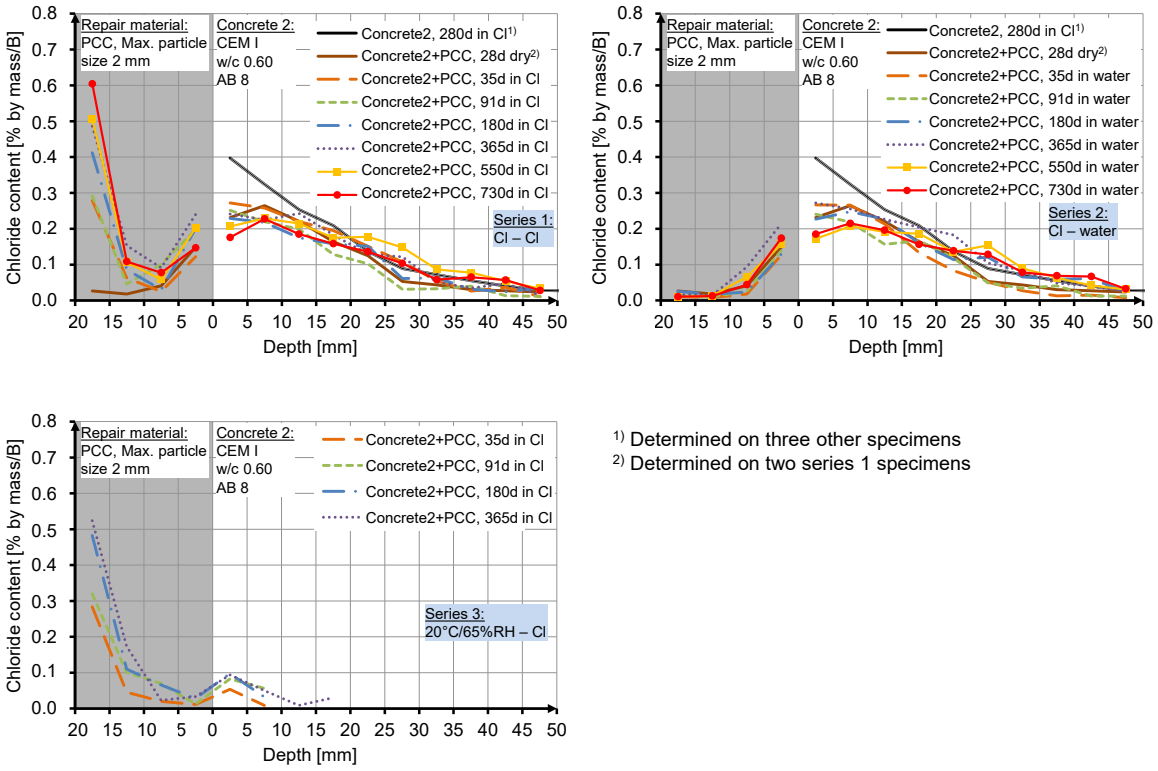

1) Determined on three other specimens
2) Determined on two series 1 specimens

Fig. B.3: Average chloride profiles of the specimens made of concrete 2 (w/c = 0.60)

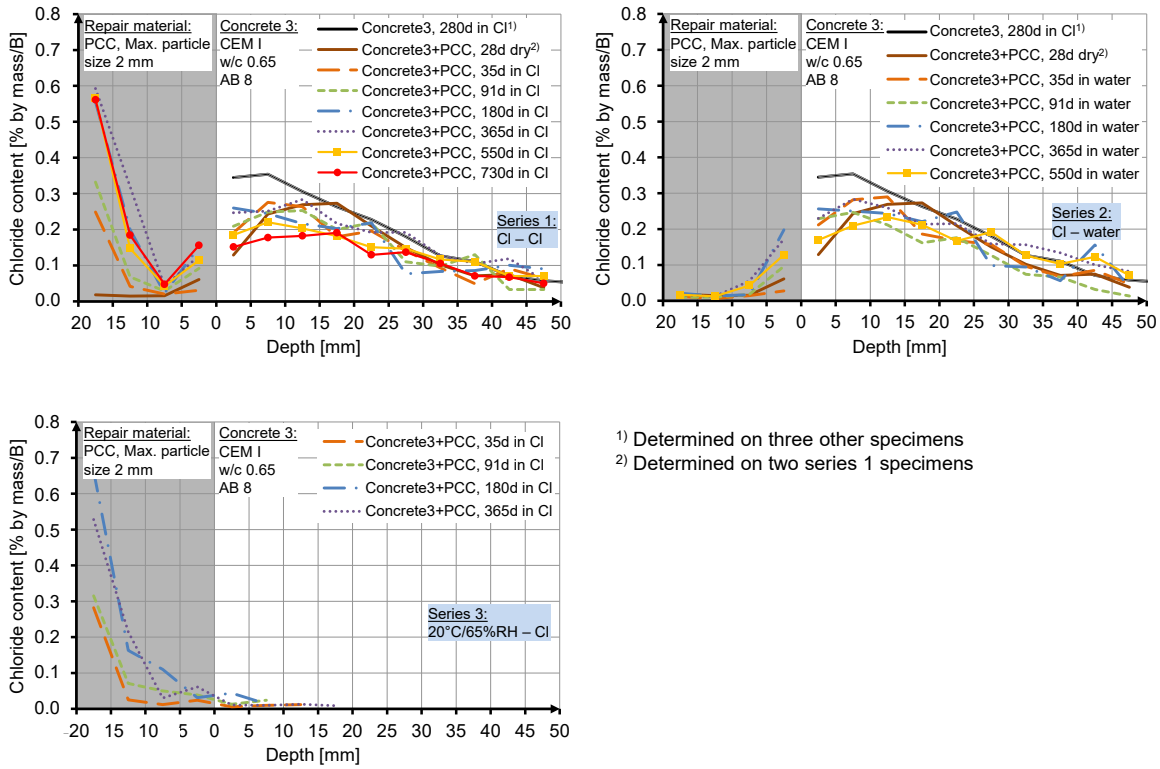

Fig. B.4: Average chloride profile of the specimens made of concrete 3 (w/c = 0.65)

The chloride profiles of test series no. 3 demonstrate, for all of the tested concretes, an almost continuous increase in the chloride content and the depth to which external chlorides penetrate into the repair layer. The chloride front reached the interface with the concrete even though a significant quantity of external chlorides had not yet penetrated into the concrete. The repair material used in this case (PCC) was shown to be very diffusion-tight during the studies of the chloride penetration resistance of repair materials described in Annex A. The values determined for the parameters (chloride migration coefficient $D_{RCM}(t_0)$, non-steady state chloride diffusion coefficient $D_{app}(t_0)$, ageing exponent α_{nss}) are similar to those of a dense CEM III/B concrete. The highest levels of chloride penetration in the concrete layer can be seen in the specimens of concrete no. 2. The chloride contents measured at the first measuring level of the concrete layer (up to a depth of 5 mm) are higher than the values in the adjacent zone of the repair layer. This indicates that the chloride ions accumulate at the interface, possibly due to leakage at this point.

Possible migration of chloride ions into the remaining concrete layer or into the new layer after application of the repair layer was discussed in Chapter 4.2.4.1. Capillary suction, diffusion and “washing-out” may promote the migration of chlorides in both directions. The new mortar layer had a far higher moisture content than the remaining concrete layer. The distinct moisture gradient initially seems to indicate that moisture is being transported from the mortar layer into the concrete layer (capillary suction). This may promote

migration of the chlorides from the surface to zones deep within the specimen. However, the results of the laboratory tests show, as described above, that chlorides are clearly extracted from the repair layer, probably by diffusion. The diffusion-controlled migration of chloride ions into the new layer may be caused by the relatively high moisture content of the concrete specimens prior to application of the repair mortar. The diffusion resistance of the freshly applied repair materials is considerably lower than that of the concrete, resulting in diffusion of the chlorides into the repair layer.

Investigations of repaired reinforced concrete bending beams contaminated with chlorides, described in *Martin 1975,* also indicated that there was considerable migration of the residual chlorides into the repair layer shortly after the layer had been applied. In contrast to the specimens investigated for this dissertation, the test specimens were dry prior to application of the repair material. However, the chloride profiles recorded 2, 3 and 6 years after application of the repair material also indicated that the chlorides present in the concrete of the bending beam had been redistributed.

For practical purposes, it can be safely assumed that the residual chlorides will be extracted by the repair layer, which is generally beneficial for the repair measure. The durability design concept involving the replacement of damaged concrete described in Chapter 4 was based on this assumption.

It is not possible to arrive at any further conclusions or quantitative statements as the results of the diffusion tests exhibited a large degree of scatter in some cases.

B.2 Field testing of the chloride transport in a two-layer system

In 1991, the Federal Waterways Engineering and Research Institute (BAW) and the Institute of Building Materials Research and Chair of Building Materials (ibac) at Aachen University prepared large concrete slabs (2.45 x 1.40 x 0.15 m³ or x 0.17 m³), each covered with a layer of repair material, as part of the research project to investigate the durability of repair materials for underwater applications (*Rössler et al. 2009*). Various repair materials were applied to the concrete slabs. These were exposed at four different locations, including at marine structures on the North Sea and Baltic Sea coasts. The field test site on the Baltic Sea coast is shown in Fig. B.5. The slabs are divided into three exposure zones: an underwater zone (UW; XS2), a splash zone and a zone of fluctuating water levels (SW and WW respectively; XS3). The slabs tested on the North Sea coast are divided into a splash zone and a zone of fluctuating water levels only (SW and WW respectively; XS3).

Fig. B.5: Exposed slabs on the Baltic Sea coast

The studies focused on investigating all of the properties of the eight selected repair systems that are relevant for durability, such as frost resistance, resistance to water penetration, bond strength, and so on. The repair systems used are shown in Table B.2. Repair systems C and D comprised flexible waterproofing slurries applied to the concrete slabs in thin layers. Systems E, F, G and K comprised sprayed concretes with a cement content of around 320 kg/m³ and a maximum particle size of 8 mm. The microsilica-modified sprayed mortar H and the polymer-modified sprayed mortar (SPCC) I each had a maximum particle size of 2 mm. With the exception of sprayed mortar I, the compositions of the supplied mixes for the systems are given in *Rößler et al. 2009*.

Each of the eight repair systems was applied to a CEM III/B concrete with a w/c ratio of 0.47. The concrete layer was 150 mm thick and the mortar or concrete repair systems were each applied to a thickness of around 20 mm. In addition to the slabs with the applied repair systems, two other concrete slabs were prepared, exposed and studied. One of these was made of the same type of concrete (CEM III/B, w/c = 0.47) as used for the base of the composite slabs while the other was made of a CEM I cement with a w/c ratio of 0.47 (concrete B and A, see Table B.2). The concretes each had a cement content of 350 kg/m³.

Table B.2: Concretes and repair materials used for the exposed slabs (from Rößler et al. 2009)

Designations of slab materials	Type of cement [1)] used for the slab base	Repair system
A (concrete)	PZ 45L-NA	–
B (concrete)	HOZ 35L-NW-HS-NA	–
C		Flexible waterproofing slurry
D		Flexible waterproofing slurry
E		Sprayed concrete with PZ 35F
F		Sprayed concrete with HOZ 35L
G		Sprayed concrete with PZ 35F and microbeads
H		Sprayed concrete with PZ 45F-HS and microsilica
I		Polymer-modified sprayed mortar PZ 35F
K		Sprayed concrete with PZ 35F and urea additive

[1)] *Designations for cement types in accordance with DIN 1164-1:1994 – PZ: Portland cement. HOZ: Blast-furnace cement*

The chloride profiles determined after the slabs had been exposed for around 3 and 6 years (see Fig. B.7 to Fig. B.14) and the RCM tests on unexposed reference slabs at an age of around 8.5 years (see Fig. B.6) showed both of the sprayed mortars used, H and I, exhibit a resistance to chloride ingress that makes them suitable for use as repair materials, their behaviour being similar to or in some cases better than that of CEM III/B concrete (*Rößler et al. 2009*). The properties of the sprayed concretes were similar to those of CEM I concrete (*Rößler et al. 2009*). Chloride profiles of the slabs made with the sprayed mortars H and I and of the concrete slabs A and B were established by sounding tests performed in 2012 (after around 21 years of exposure). Cored samples were taken from each of the slabs (A to K) in the summer of 2014, after 23 years of exposure. The slabs were subsequently disposed of.

The chloride profiles after around 3, 6, 21 and 23 years, determined for the drill cores taken from the slabs, are shown in Fig. B.7 to Fig. B.14. The overall chloride contents were determined on ground drill cores by acid digestion and photometric analysis in accordance with *DAfStb Heft 401:1989*. The number of drill cores taken per slab and zone (SW, WW, UW) varied between 1 and 3 per testing time.

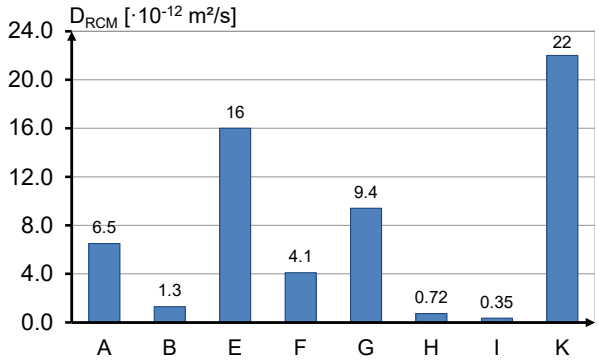

Fig. B.6: Results of the RCM tests on the reference slabs at the age of around 8.5 years (from Rößler et al. 2009)

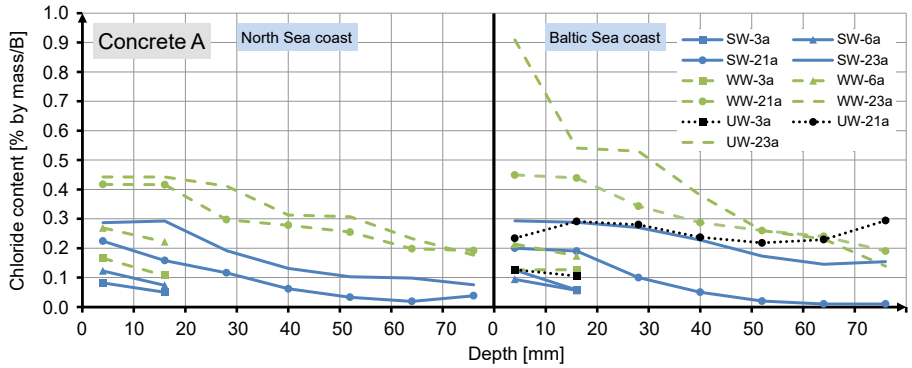

Fig. B.7: Average chloride profiles of the drill cores from the slabs made of concrete A

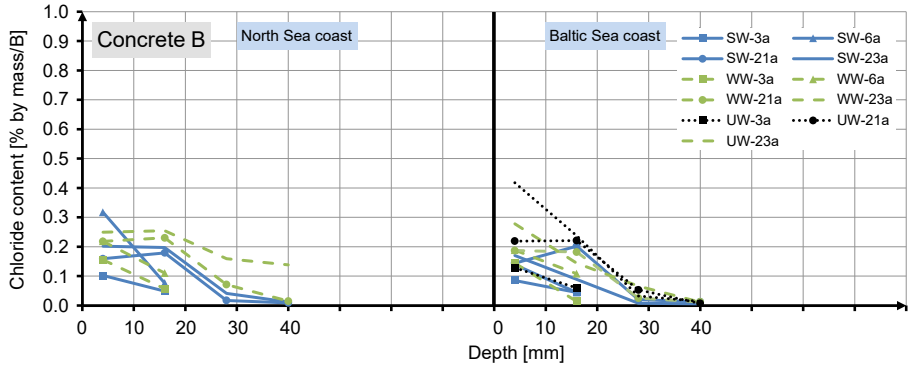

Fig. B.8: Average chloride profiles of the drill cores from the slabs made of concrete B

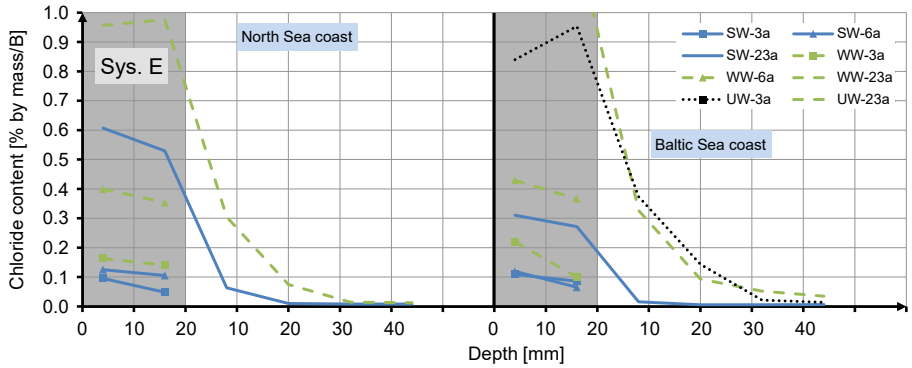

Fig. B.9: Average chloride profiles of the drill cores from the composite slabs made of repair material E

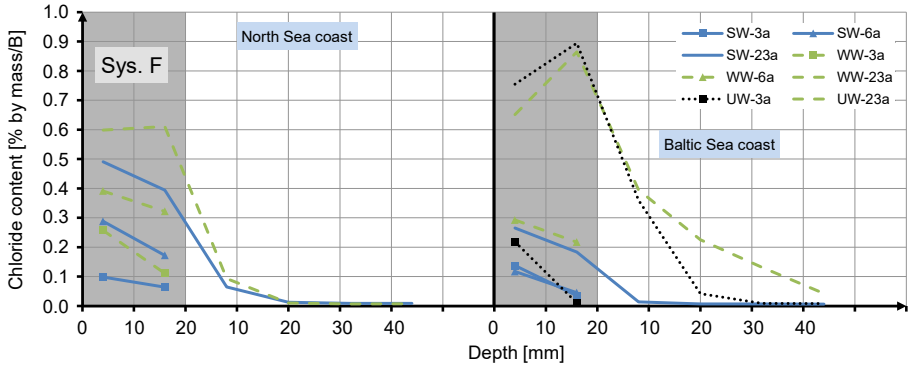

Fig. B.10: Average chloride profiles of the drill cores from the composite slabs made of repair material F

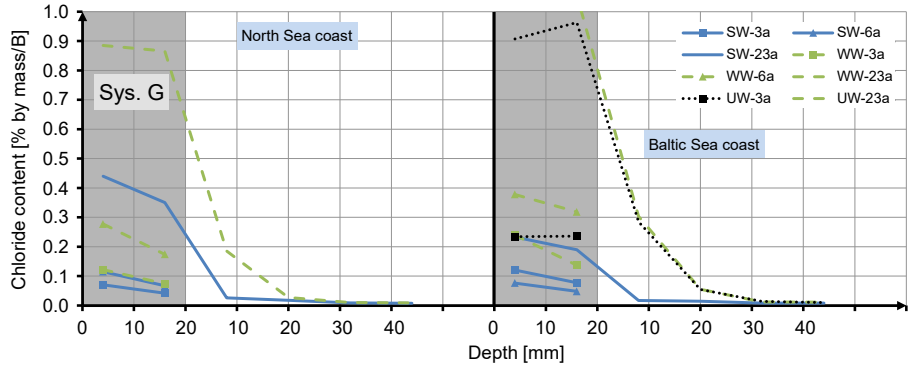

Fig. B.11: Average chloride profiles of the drill cores from the composite slabs made of repair material G

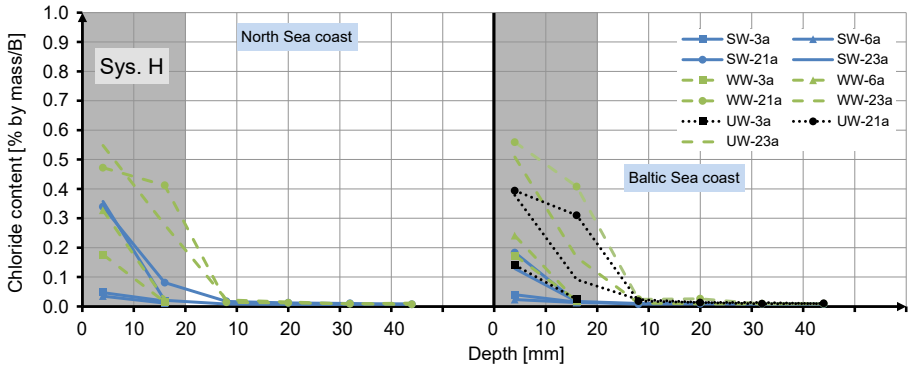

Fig. B.12: Average chloride profiles of the drill cores from the composite slabs made of repair material H

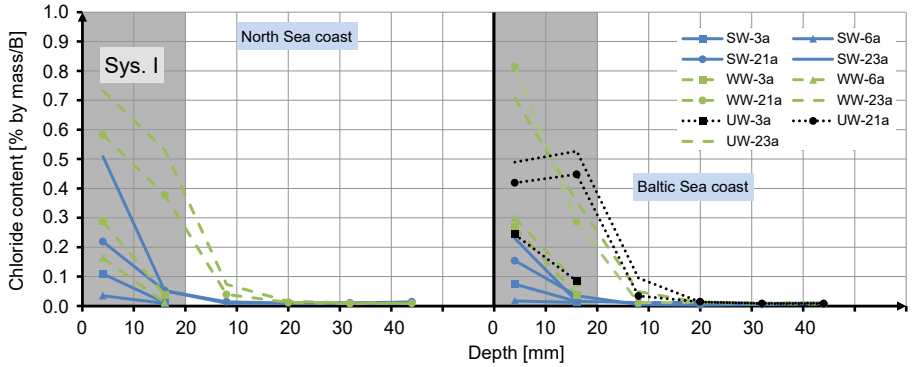

Fig. B.13: Average chloride profiles of the drill cores from the composite slabs made of repair material I

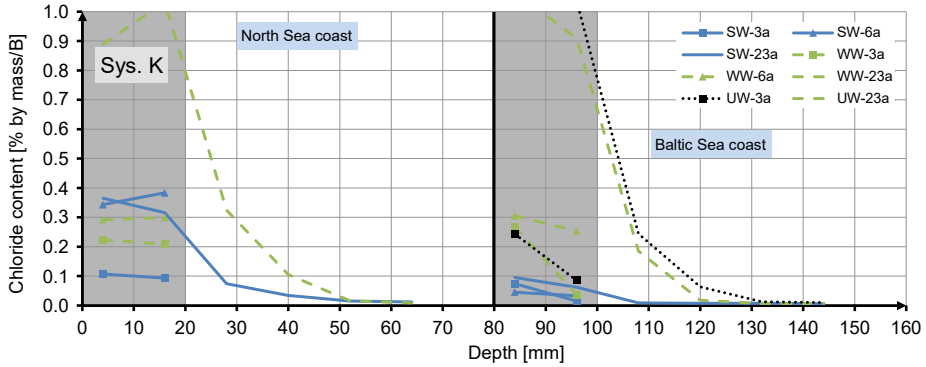

Fig. B.14: Average chloride profiles of the drill cores from the composite slabs made of repair material K

The following can be deduced from the chloride profiles determined for the exposed slabs at various times.

First of all, it should be noted that some of the chloride contents within the defined zones (SW, WW, UW) exhibit a large degree of scatter. The differences were particularly large in the spray water zone, with far lower chloride contents generally being measured in the upper regions of the slabs than in the middle and lower (near WW) regions. This is

demonstrated above all by the results of the investigations after 3 and 6 years of exposure in *Rößler et al. 2009* for which more drill cores were taken than for the later investigations.

The exposure conditions in the zone of fluctuating water levels are far more severe than in the spray water zone (both XS3). The chloride profiles for the underwater zone (XS2) are similar to those for the zone of fluctuating water levels.

It was not possible to identify any systematic influence of the exposure sites (North Sea and Baltic Sea). Although the chloride concentration in North Sea water is twice that of the water in the Baltic Sea, the chloride contents determined on the surface and within the slabs were similar. It was possible to verify the influence of the chloride content of the solution in laboratory tests (see Annex C.2).

With a few exceptions, a steady increase in the chloride content and the penetration depth of the chlorides over time can be seen.

The chloride contents of concrete A were considerably higher than those of concrete B. In the studies after 21 years of exposure, the chloride contents were determined on drill cores taken over the entire thickness of the slabs (A, B, H, I). For concrete A, it could be seen that the chlorides had penetrated the entire depth of the slabs. As expected, this demonstrates that CEM I concretes have a very low resistance to chloride penetration. By contrast, concrete B has a very high resistance to chloride penetration, as is generally the case for blast-furnace cement concretes.

The chloride contents determined for the sprayed concretes were, all in all, higher than those of concrete A. Some of these have chloride contents of around 1 % by mass/B at the first measuring level (up to 8 mm). For WW and UW, the chloride contents in the concrete of the slab bases are similar to those of the slabs made of concrete B. By contrast, the chloride content of the concretes in the base of the slabs ranges from very low to zero in the spray water zone (WS).

The sprayed mortar H has the lowest chloride content of all repair systems, the percentage by mass of concrete being slightly higher than for concrete B. When converting the chloride contents to a percentage by mass of the binder, lower values are obtained for sprayed mortar H as its binder content (approx. 500 kg/m³) is higher than that of concrete B (350 kg/m³). No chlorides at all were measured in the concrete of the slab bases to which sprayed mortar H had been applied.

The chloride contents measured for polymer-modified mortar (SPCC) I are also lower on the whole than for the sprayed concretes. The base concrete has only a low chloride content. These results demonstrate the very high and long-term resistance of SPCC I to chloride penetration.

The chloride transport can generally be seen to stagnate in the outer zone (convection zone) of the concrete slabs while the chloride content of the sprayed mortars greatly decreases with increasing depth. The comparatively dense structure of the sprayed mortars could be the reason why their convection zone is less pronounced, preventing removal of the chloride ions in the outer region (by washing out / back diffusion).

Samples were also taken from slabs C and D with the waterproofing slurries and tested after 3 and 23 years of exposure. No chlorides at all were detected in the concrete of the slab bases after 3 years of exposure while, after 23 years, only very low chloride contents were measured at the first measuring depth in the concrete of the slab bases. Thus the waterproofing slurries can also be seen to have a very high resistance to chloride penetration, similar to the sprayed mortars H and I. The waterproofing slurries significantly delay the penetration of chlorides into the concrete. They maintain a very soft and elastic consistency throughout the entire duration of exposure.

For the tests conducted after the slabs had been exposed for 3, 6 and 21 years, samples were taken from the surfaces facing the wall of the structure to which the slabs had been fixed (i.e. from the back of specimens) and their chloride contents determined. It was possible to identify systematic differences in the chloride penetration behaviour between the front of the slabs (i.e. facing away from the wall of the structure) and the back of the slabs (see *Rahimi et al. 2013*). Higher chloride contents were generally measured at the front of the slabs in the zone of fluctuating water levels. The difference is mainly due to fouling on the back of the slabs which inhibits chloride penetration to some extent. Another possible cause is the lower temperature due to shading of the back of the slabs which could slow down the rate of chloride diffusion. In addition, the differences in the pore structure of both surfaces may also be relevant (front: surface cast against the mould, back: unmoulded surface).

This difference is less pronounced or even reversed in the spray zone. The influences mentioned above could be cancelled out by water rebounding from the wall onto the back of the slabs and the accompanying greater availability of chloride ions, resulting in a slightly higher chloride content at the back of the slabs. As this example demonstrates, the microclimate clearly influences the penetration behaviour of chlorides in structural elements.

A number of drill cores were taken at selected points on the cracked areas of the slabs. The measured chloride profiles indicate a continuous development, with a reduction in the chloride content with increasing depth. Chloride ions were not found to accumulate on the surface of the rebars.

Drill cores were also taken from the region around the rebars. The rebar fragments in the samples do not exhibit any corrosion in spite of the high chloride content at the depth at which the rebars are installed in the concrete. The reinforcement is connected to the holders attaching the slabs to the wall. Thus the slab reinforcement would appear to be protected cathodically and does not corrode even though the passive layer has been destroyed by the high chloride content of the surrounding concrete.

C Annex C: Selected laboratory investigations

C.1 Investigations into the reproducibility of the RCM test and comparison of the methods described in BAW-Merkblatt 2012 and in NT Build 492:1999

The chloride migration coefficients of four materials (of different ages) determined in two different laboratories in accordance with *BAW-Merkblatt 2012* are shown in Fig. C.1, along with the values of D_{RCM} determined as specified in *NT Build 492:1999* (in a laboratory). The test specimens were all prepared and cured in Laboratory 1. The values of D_{RCM} determined in the laboratories as specified in *BAW-Merkblatt 2012* only differ appreciably for PCC 1-180d; very low penetration depths were obtained for this material in Laboratory 2 as a short test duration had been selected. According to *Tang 1996*, a large degree of scatter can be expected for D_{RCM} when the penetration depths are lower than 10 mm.

The values of D_{RCM} determined as specified in *NT Build 492:1999* are all greater than those determined in accordance with *BAW-Merkblatt 2012*, in some cases with significant differences.

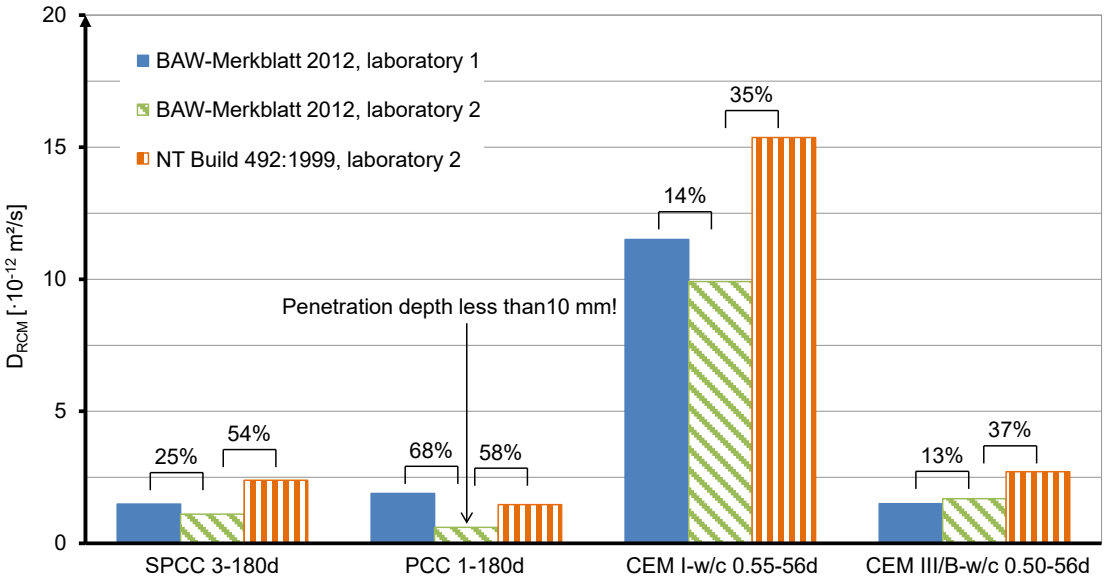

Fig. C.1: Precision of the RCM test and comparison between the values of D_{RCM} determined according to BAW-Merkblatt 2012 and NT Build 492:1999; differences are in relation to the values of laboratory 1 and those according to NT Build 492:1999 respectively

The main differences between the RCM test methods according to *BAW-Merkblatt 2012* and *NT Build 492:1999* are summarized in Table C.1.

Table C.1: Most important differences between the RCM tests according to BAW-Merkblatt 2012 and NT Build 492:1999 (for specimens with a diameter of 100 mm and a thickness of 50 mm)

Operation / component	BAW-Merkblatt 2012	NT Build 492:1999
Preparation of the test	Storage in water	Saturation with $Ca(OH)_2$ at 10-50 mbar
Anolyte	0.2 N KOH	0.3 N NaOH
Catholyte	100g NaCl in 900g water + 0.2 N KOH	100g NaCl in 900g water
Test voltage	U = 30 [V]	$10 \leq U \leq 60$ [V]
Test duration	$4 \leq t \leq 168$ [h]	$6 \leq t \leq 96$ [h]
Indicator solution	Silver nitrate + potassium dichromate or Fluorescein + silver nitrate	Silver nitrate
Measurement of penetration depth	at 9 points	at 7 points (without 2 points at each edge)
Evaluation	A possible loss of voltage due to polarization of the electrodes is not taken into account	A 2 V loss of voltage due to polarization of the electrodes is taken into account

C.2 Investigations into how the chloride content of the test solution affects the chloride penetration behaviour

It can be seen from Fig. C.2 that the surface chloride concentration and chloride penetration depth increase with the chloride content of the test solution. On the whole, the surface chloride concentrations of the Portland cement concrete are higher than those of blast-furnace cement concrete, which is inconsistent with the model according to *Tang 1996* (cf. Chapter 2.4.4.6).

Table C.2: Composition of the test solutions

Constituent	Unit	Test solution		
		North Sea *	Baltic Sea *	0.5 % NaCl
Chloride	mg/l	19900	9000	3035
Sodium		11000	5000	1965
Potassium		400	200	–
Calcium		400	200	–
Magnesium		1300	600	–
Sulfate		2800	1300	–

* *Target composition according to DIN 4030-1:2008*

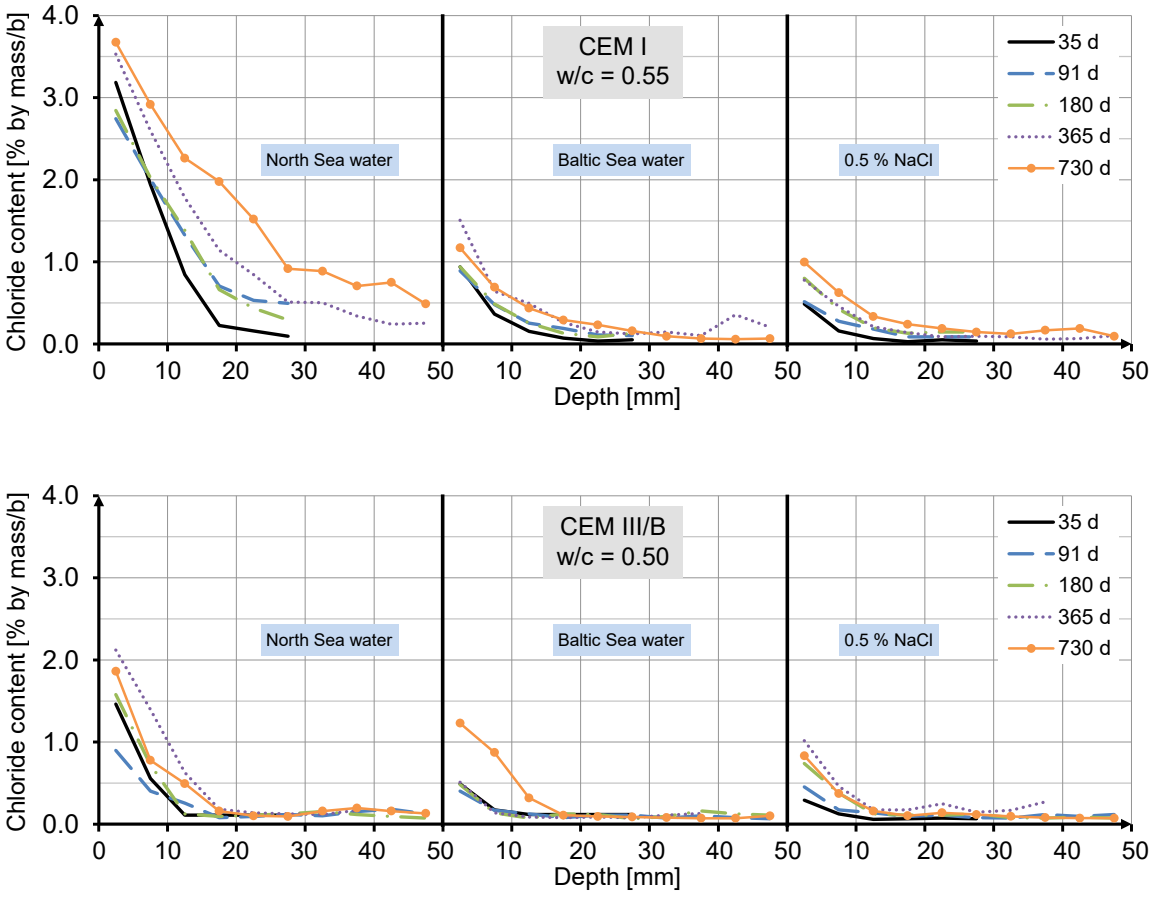

Fig. C.2: Effect of test solution (especially chloride content) on chloride transport in the concrete in diffusion tests. Chloride profiles after approx. 35, 91, 180, 365, 730 and 850 days' storage of the specimens in three different test solutions

C.3 Investigations into how the type of formwork and curing affect the chloride penetration resistance

As already mentioned in Chapter 2.4.4.1, curing and the type of formwork selected significantly affect the development of the properties of the surface zone of the concrete. These parameters, which may affect the chloride penetration resistance of the concrete, are not taken into account in the design model. For design purposes, the 10 mm surface zone (mean value) is disregarded for exposure classes XS3 and XD3 to achieve conservative values. There is very little literature available on systematic studies of the impact of curing and the type of formwork on the chloride penetration resistance of concrete.

The possible influence of the type of formwork (timber beam formwork with film coating, steel plate, timber beam formwork with a permeable formwork liner), secondary curing measures (paraffin-based curing methods, alternative curing methods, applying jute and foil, wetting) and the length of time during which the concrete is in the formwork (1, 3, 7, 14 d) on the chloride migration coefficient was investigated in *Spörel & Müller 2012*. In this case, the RCM tests were performed on more mature concrete (age approx. 6 years), with drill cores being taken from large weathered specimen slabs. In contrast to *BAW-Merkblatt 2012*, the as-cast surface was used as the test surface (instead of the surface 10 mm from the surface that had not been cast against the mould). In this connection, a significant reduction in the chloride migration coefficient was achieved by using permeable formwork liners, partly masking the influence of the type of binder. It was also possible to demonstrate that the duration of curing affects the chloride migration coefficient, even though its impact is considerably weaker. The secondary curing measures did not appear to affect the chloride migration coefficient. *Weizong & Boes 2010* also demonstrated that permeable formwork liners have a very favourable impact on the chloride migration coefficient of concrete.

During the work on this dissertation, it was possible to perform RCM tests on drill cores taken from several of the specimens (age approx. 11 years) prepared and studied in *Spörel & Müller 2012*. Two specimens were taken from each drill core in such a way that both the as-cast surface and concrete from the central region of the slabs (from a depth of around 50 mm) could be used as test surfaces in the RCM test. The values of the chloride migration coefficient D_{RCM} determined in the test and the specific electrolyte resistances ρ determined by the two-electrode method (TEM) are shown in Fig. C.3.

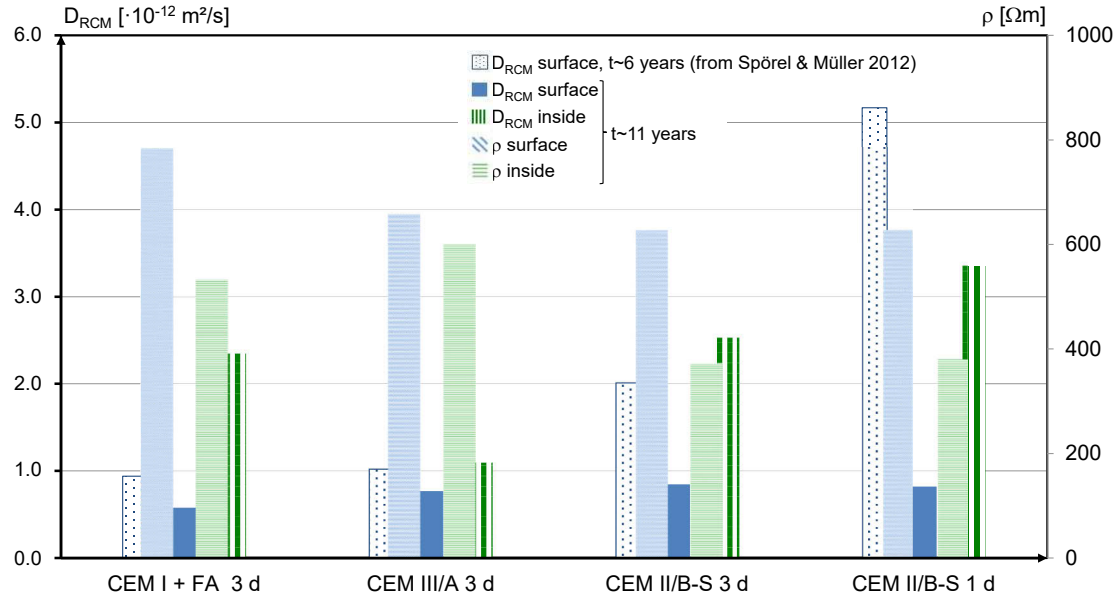

Fig. C.3: Effect of the type of formwork on the chloride migration coefficient and the specific electrolyte resistance of concrete

Fig. C.3 also shows values of D_{RCM} for concrete, measured at an age of around 6 years in *Spörel & Müller 2012* (with the as-cast surface being the test surface), indicating that D_{RCM} is dependent on the type of binder after all. The concretes with CEM I + FA and CEM III/A have almost the same values of D_{RCM}. As expected, D_{RCM} for such concretes is lower than for the concretes with CEM II/B-S, which can be attributed to the fly ash content in CEM I + FA and the higher slag content in CEM III/A.

However, the specimens tested with the as-cast surface at an age of 11 years almost all had the same values of D_{RCM}. The specific electrolyte resistances ρ measured for the specimens were also similar. Only the fly ash concrete had a higher value of ρ and a slightly lower value of D_{RCM} than the other specimens. This is in contrast to the values of D_{RCM} determined for the test surface in the central region of the concretes. The values determined in this case varied, were binder-dependent and were considerably higher than the values of D_{RCM} determined for the as-cast surface. In addition, the measured specific electrolyte resistances correlate well with the values of D_{RCM} and are lower than the values determined for the surface zone of the concretes.

These results demonstrate that the structure of the concrete and thus the resistance to chloride penetration in the surface zone can be optimized by using suitable types of formwork.

When using the RCM and diffusion tests to investigate the possible influence of curing and the type of formwork on the chloride penetration resistance of concrete, the specimens

must be water-saturated before the start of the test. In some investigations, the specimens were tested at an early age after being cured in various ways, in some cases being exposed to outdoor conditions and allowed to lose water (e.g. *Bouwmeester et al. 2010*). The drill cores subjected to the RCM test at an age of around 6 years in *Spörel & Müller 2012* were stored in water for three weeks before testing. This is not sufficient to ensure that the test specimens are fully saturated with water.

D Annex D: Nomograms for the durability design of new structures and for assessing the durability of existing structural elements

The following boundary conditions must be taken into account when using the nomograms, not only when designing new structures but also when determining the remaining service life of existing structures. They also apply when determining how thick the layer of repair material needs to be if the concrete cover is to be completely replaced as part of a repair measure:

- for $D_{RCM}(t_0)$, the largest single value must not exceed 25 % of the mean value;
- for $D_{nss}(t_0)$, the coefficient of determination R^2 must be not less than R^2 95 %;
- for $D_{app}(t_0)$, the coefficient of determination R^2 must be not less than 80 %;
- the allowance for deviation of the concrete cover Δc or layer thickness Δd_E must be between 5 and 15 mm;
- the input values must be based on a mean annual temperature of the structural element of 10° C;
- the input values of the diffusion coefficient must relate to specimens or structural elements with an age of 28 days at the start of the test (t_0 = 28 d);
- the nomograms can be used for concretes with an initial chloride content of not more than 0.1 % by mass/b (Cl 0.10 according to *DIN EN 206:2014*).

The variables $D_{app}(t_0)$ and α_{app} are used when calculating the remaining service life of existing structures. The variable $d_{E,min}$ (=$c_{new,min}$) is the minimum layer thickness for repair measures in which the damaged concrete is completely replaced by a repair material.

Without exception, the input variables must be characteristic values (i.e. mean values). Only c_{min} and $d_{E,min}$ are design values, of the concrete cover and layer thickness respectively.

The action with $C_{S,\Delta x}$ = 1.0 % by mass/b is not generally selected for designs for exposure classes XS2, XS3, XD2 and XD3. The sets of lines with $C_{S,\Delta x}$ = 1.0 % by mass/b have been taken into account in the nomograms to enable the remaining service life of existing structures to be calculated.

An overview of the design nomograms is shown in Table D.1.

Table D.1: Overview of the nomograms for the service life design of new structures and for the durability assessment of existing structures exposed in XS3 / XD3 [1)]

Target reliability index β_0	Target service life $t_{SL\ [years]}$	Fig. No. $D_{RCM}(t_0)$ or $D_{nss}(t_0)$ or $D_{app}(t_0)$ [$\cdot 10^{-12}$ m²/s]		
		0 – 2	2 – 20	0 – 20
1.5	100	D.1	D.2	
	70	D.3	D.4	
	50	D.5	D.6	
	40	D.7	D.8	
	30	D.9	D.10	
	20			D.11
	10			D.12
0.5	100			D.13
	70			D.14
	50			D.15
	40			D.16
	30			D.17
	20			D.18
	10			D.19

[1)] *These nomograms may also be used for exposure classes XS2 / XD2 provided the minimum concrete cover – when used as an **output parameter** - is reduced by 10 mm (convection zone Δx), i.e. c_{min} - 10 mm. However, the minimum concrete cover is increased by 10 mm when used as an **input parameter**, i.e. c_{min} + 10 mm.*

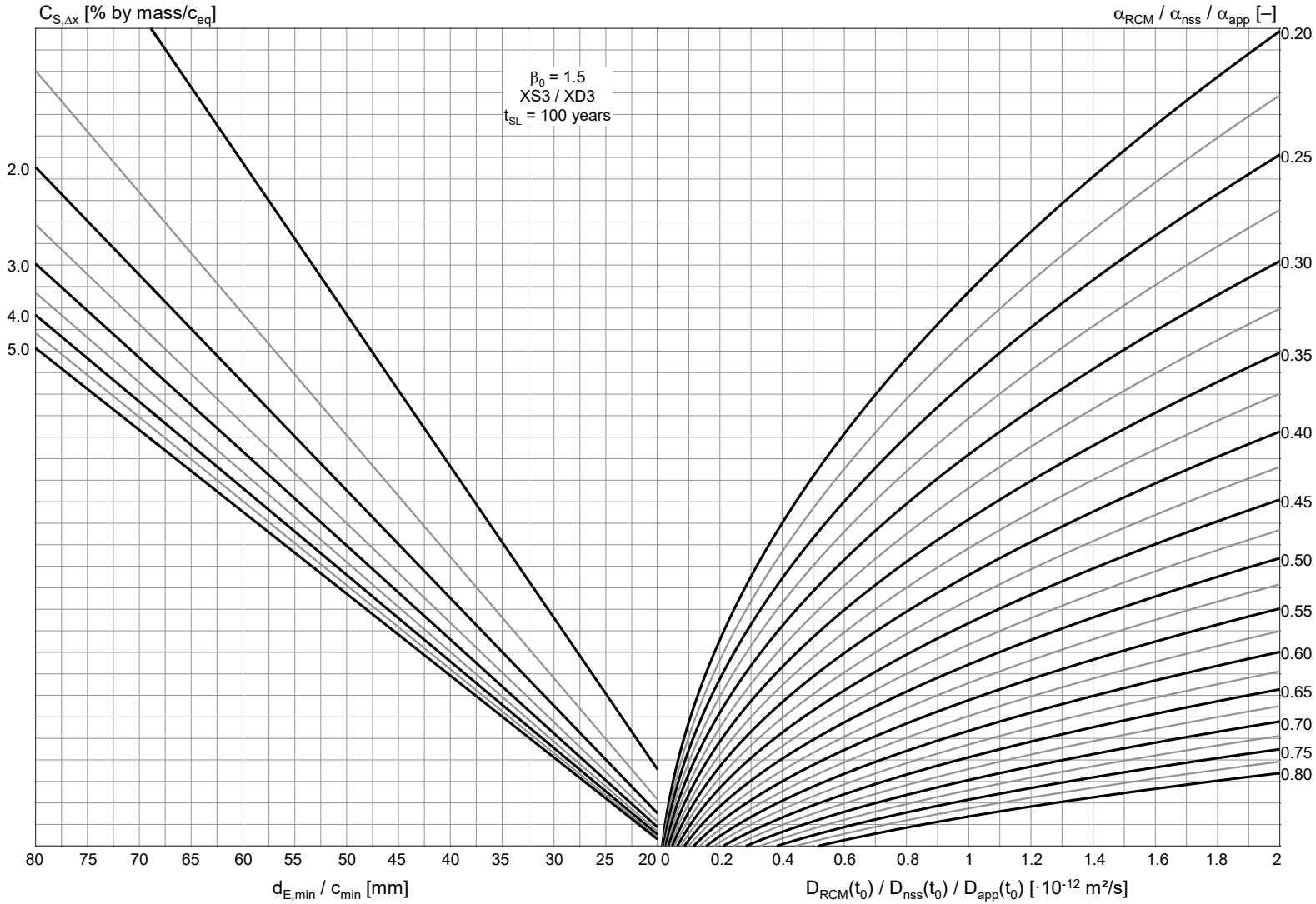

Fig. D.1: Design nomogram for XS3 / XD3, target service life t_{SL}=100 years, target reliability index β_0=1.5, $0 \leq D(t_0) \leq 2$

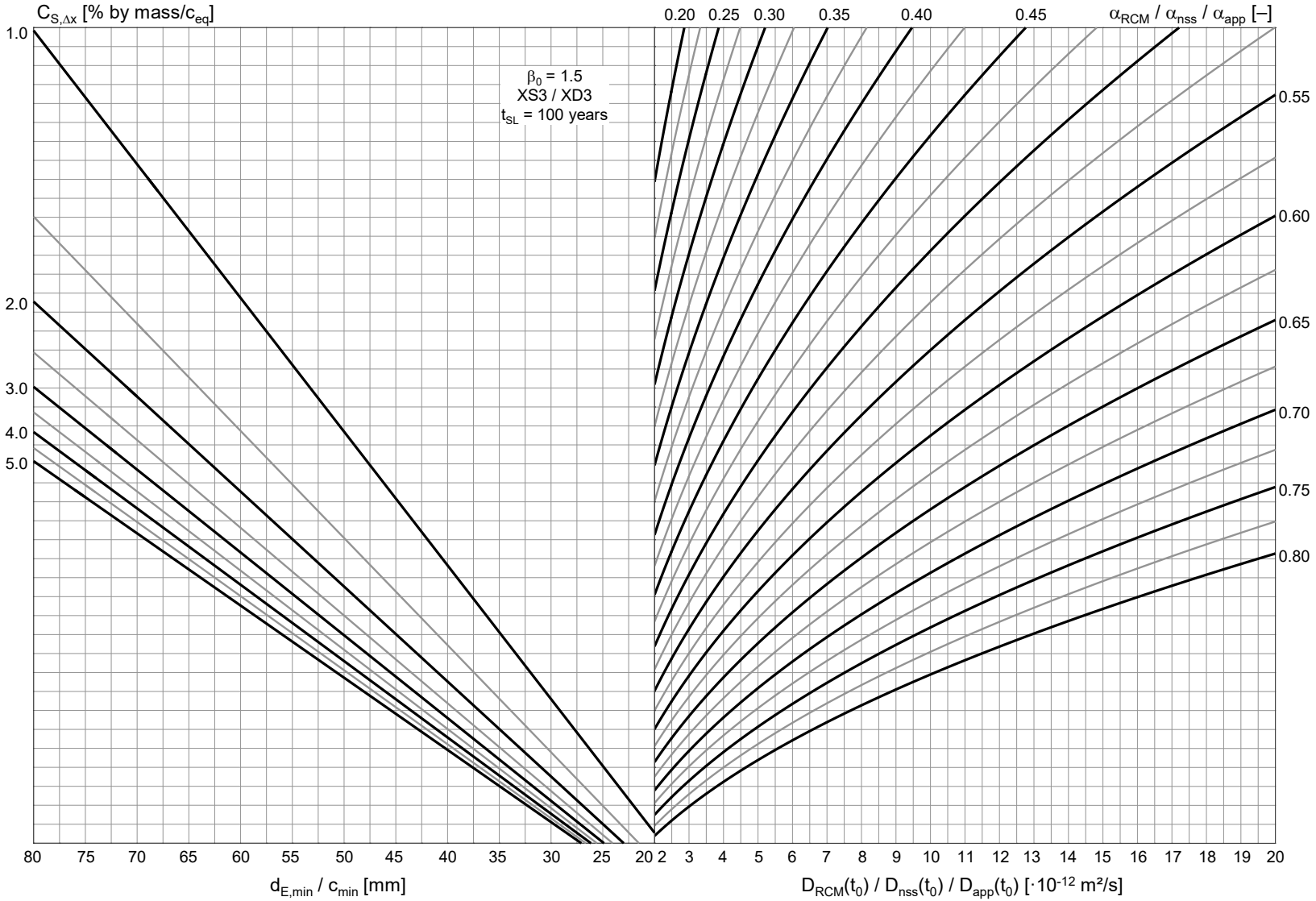

Fig. D.2: Design nomogram for XS3 / XD3, target service life t_{SL}=100 years, target reliability index β_0=1.5, $2 \leq D(t_0) \leq 20$

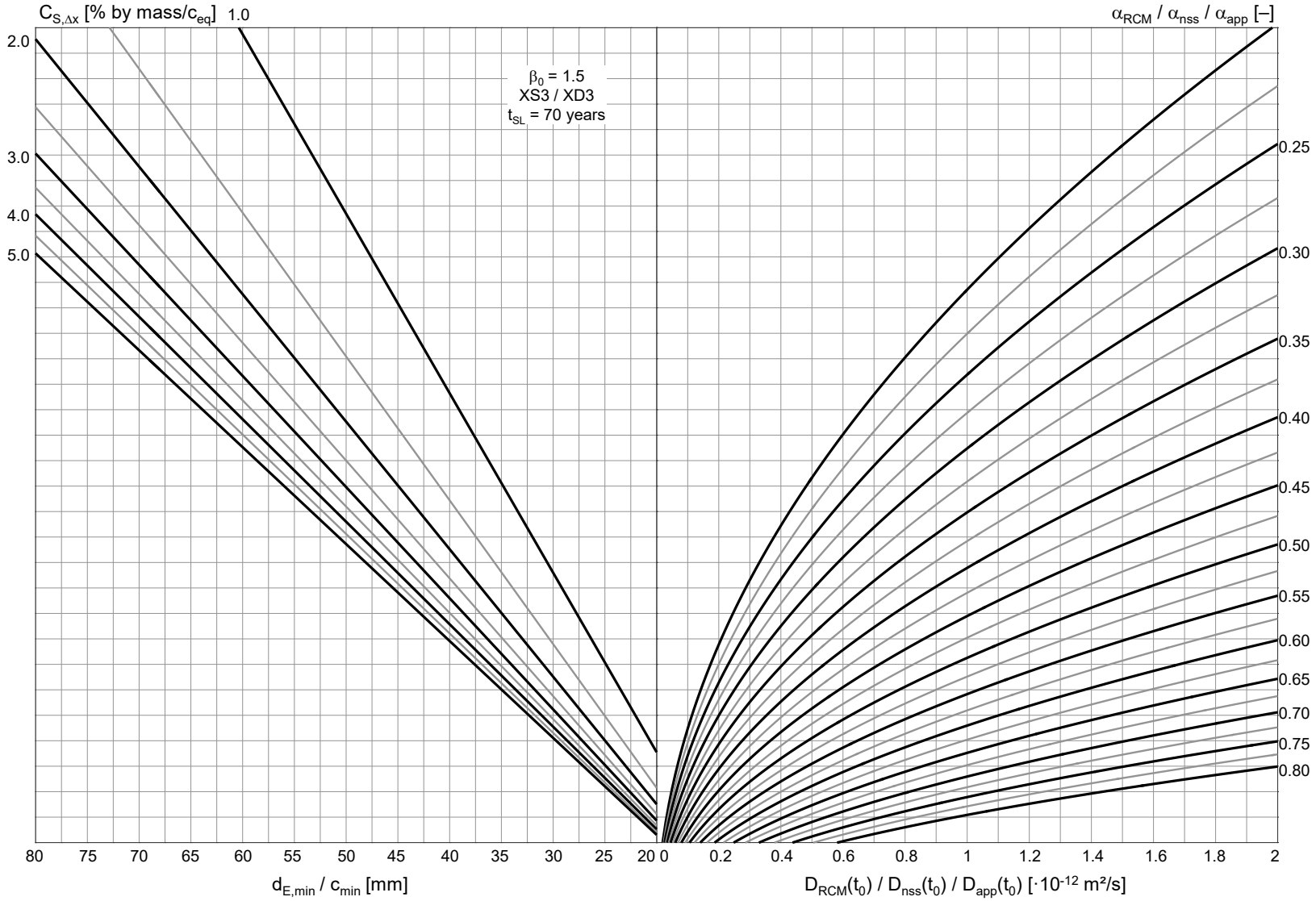

Fig. D.3: Design nomogram for XS3 / XD3, target service life t_{SL}=70 years, target reliability index β_0=1.5, $0 \leq D(t_0) \leq 2$

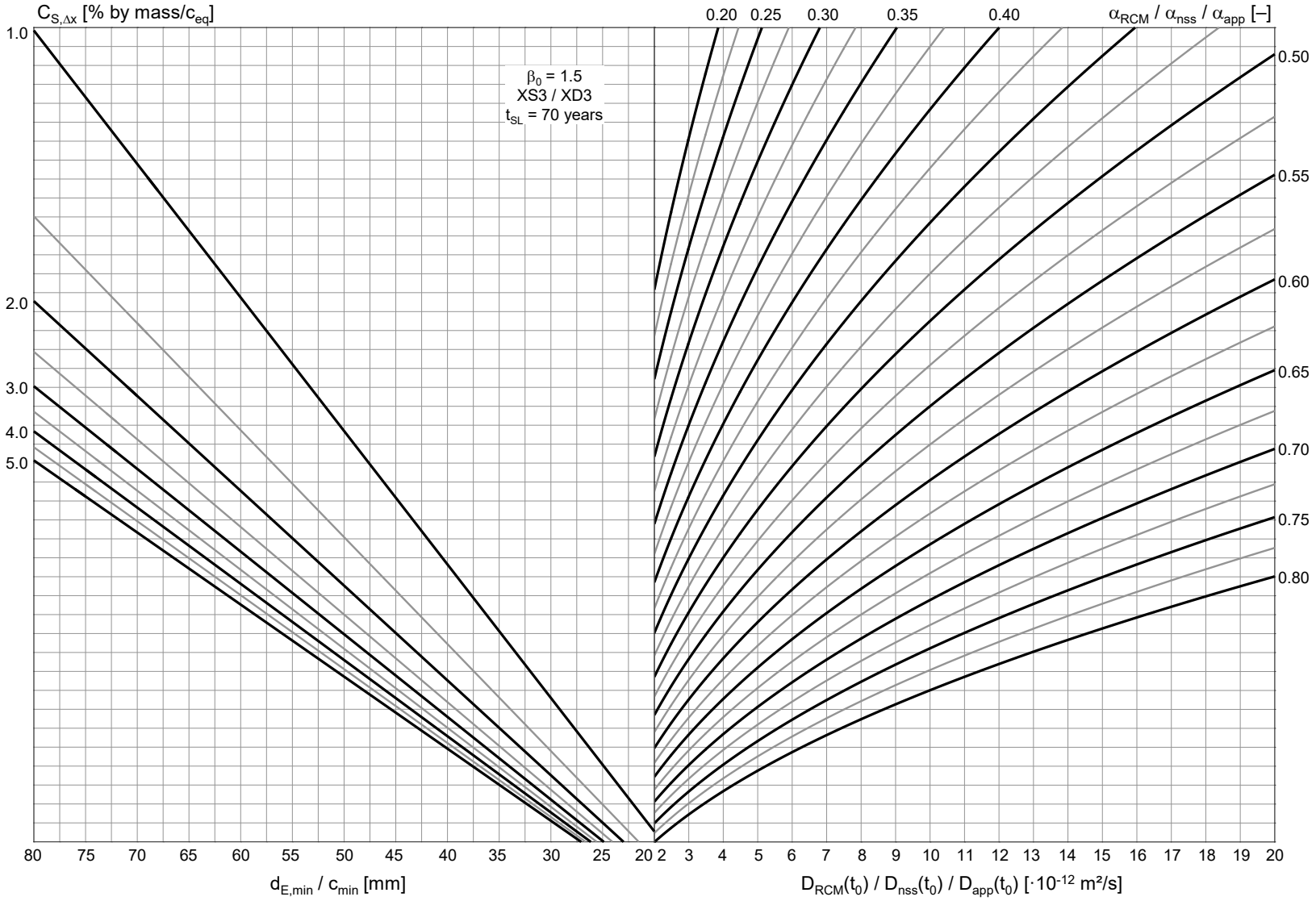

Fig. D.4: Design nomogram for XS3 / XD3, target service life t_{SL}=70 years, target reliability index β_0=1.5, 2 ≤ $D(t_0)$ ≤ 20

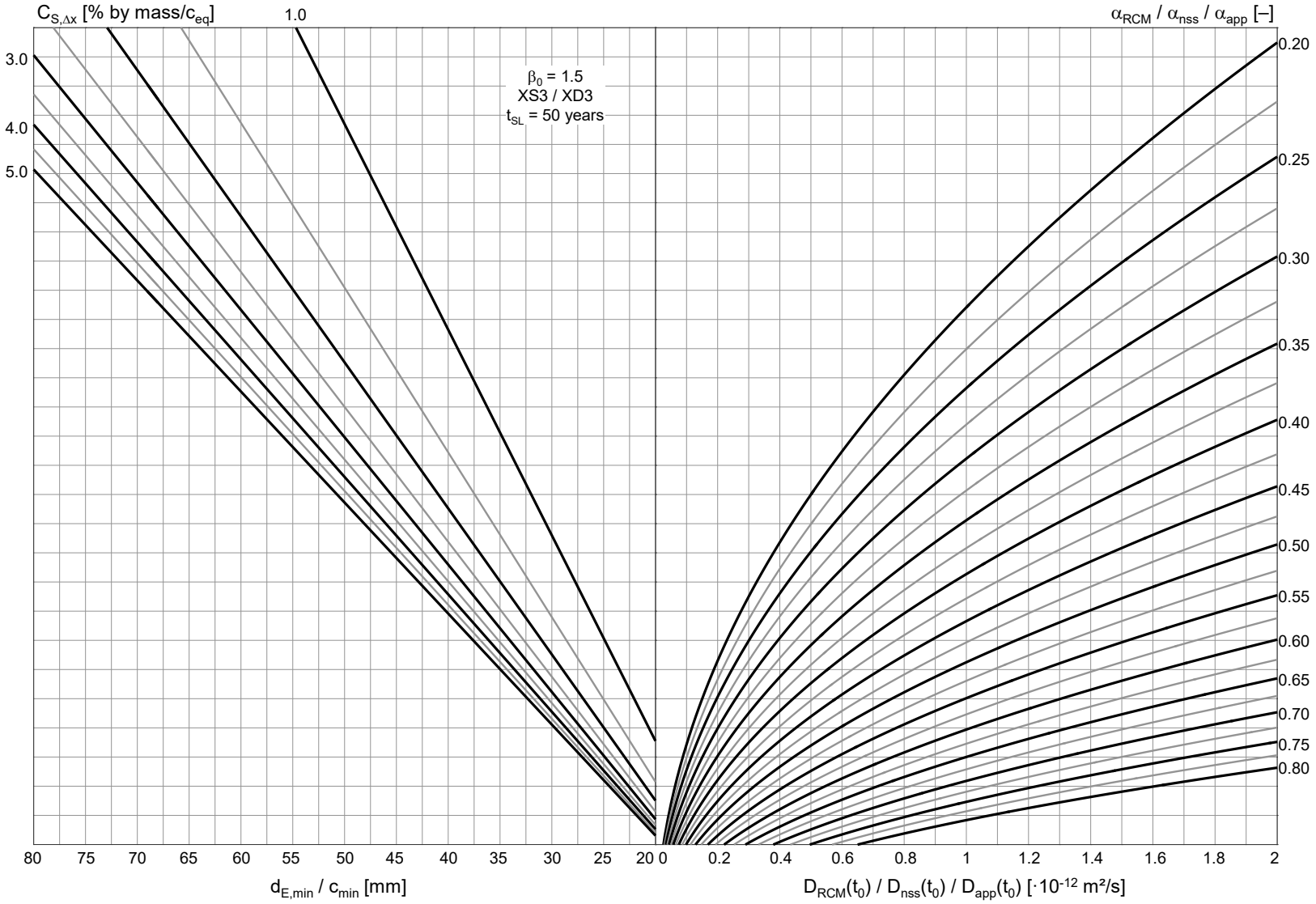

Fig. D.5: Design nomogram for XS3 / XD3, target service life t_{SL}=50 years, target reliability index β_0=1.5, $0 \leq D(t_0) \leq 2$

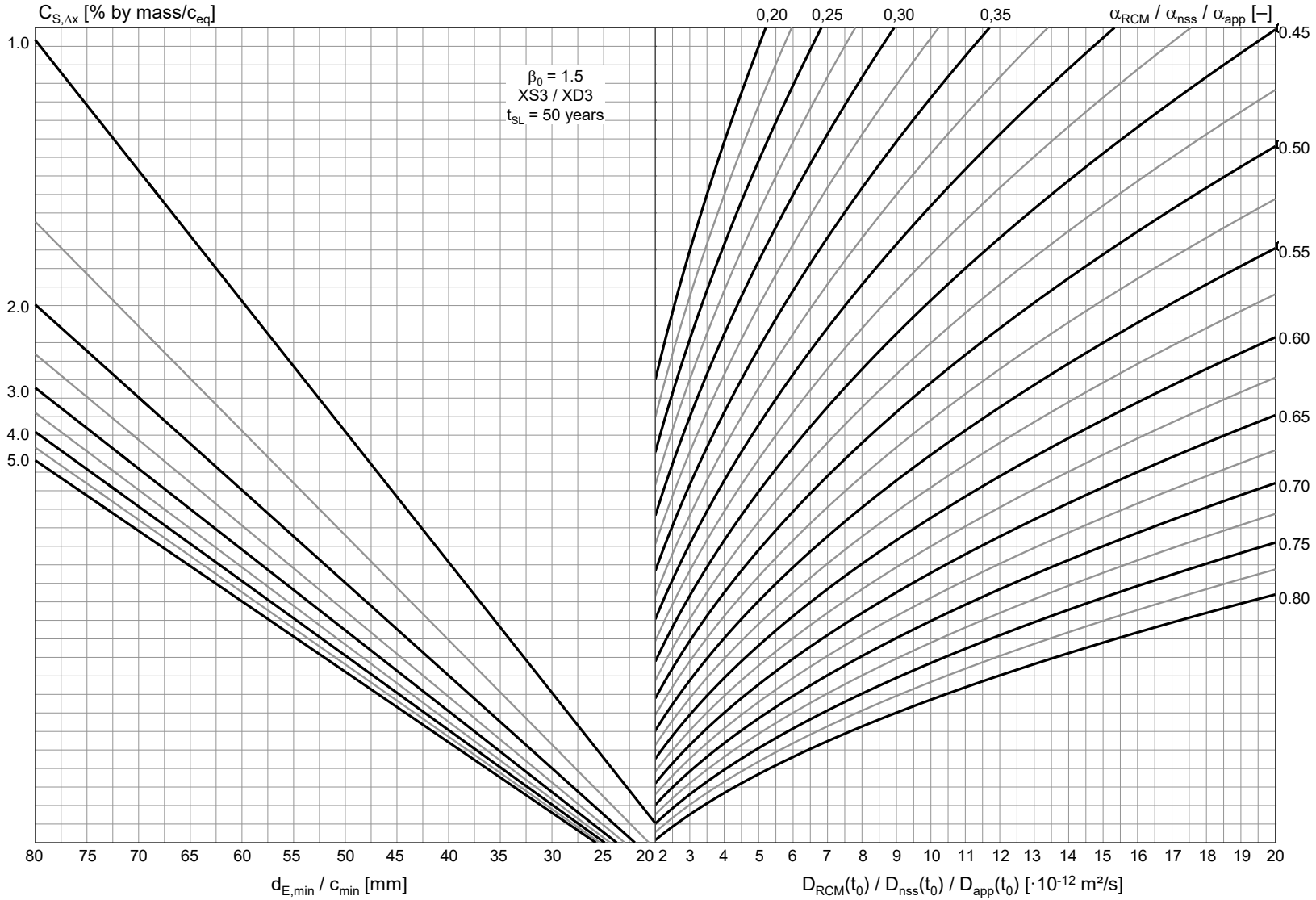

Fig. D.6: Design nomogram for XS3 / XD3, target service life t_{SL}=50 years, target reliability index β_0=1.5, $2 \leq D(t_0) \leq 20$

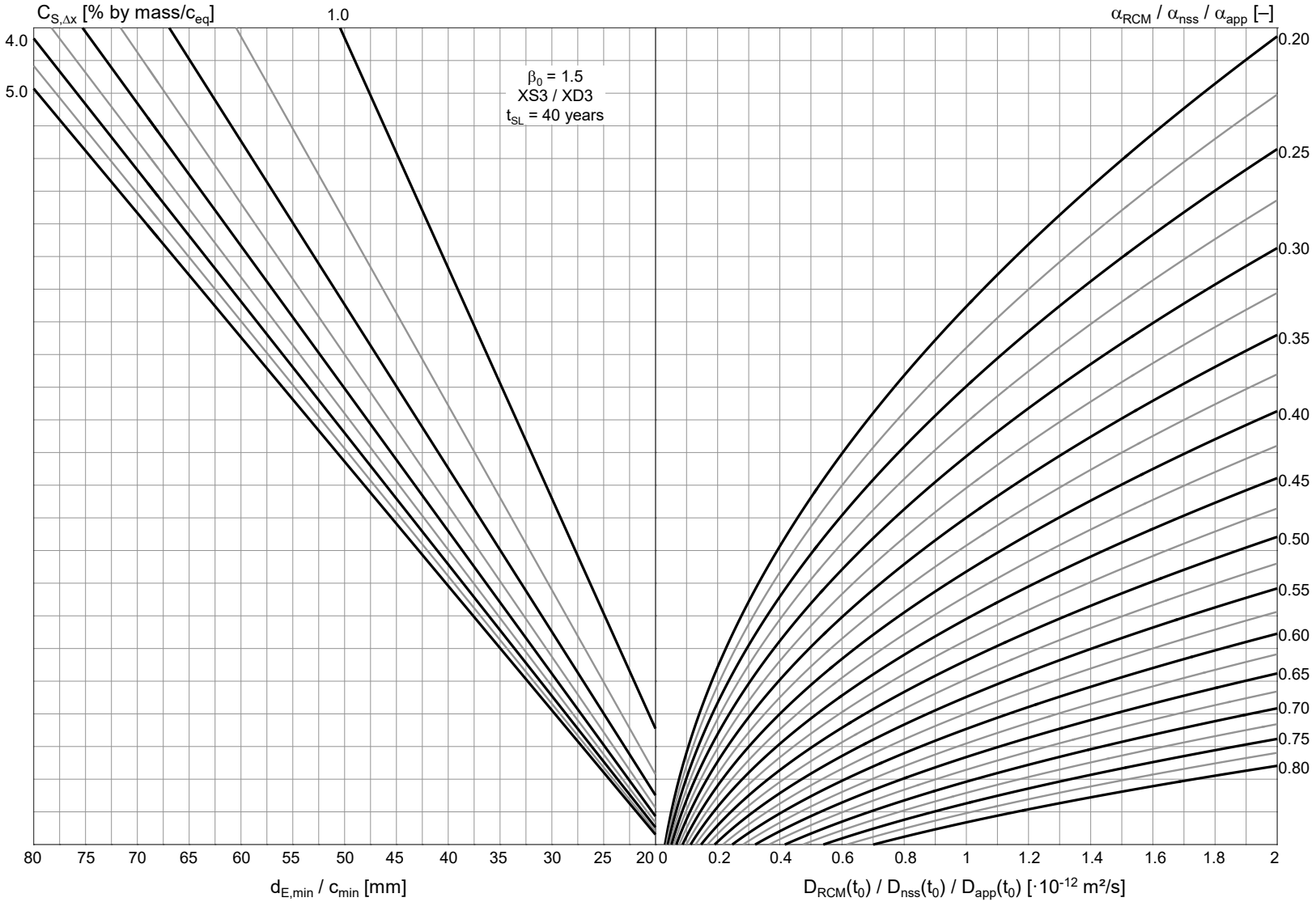

Fig. D.7: Design nomogram for XS3 / XD3, target service life t_{SL}=40 years, target reliability index β_0=1.5, $0 \leq D(t_0) \leq 2$

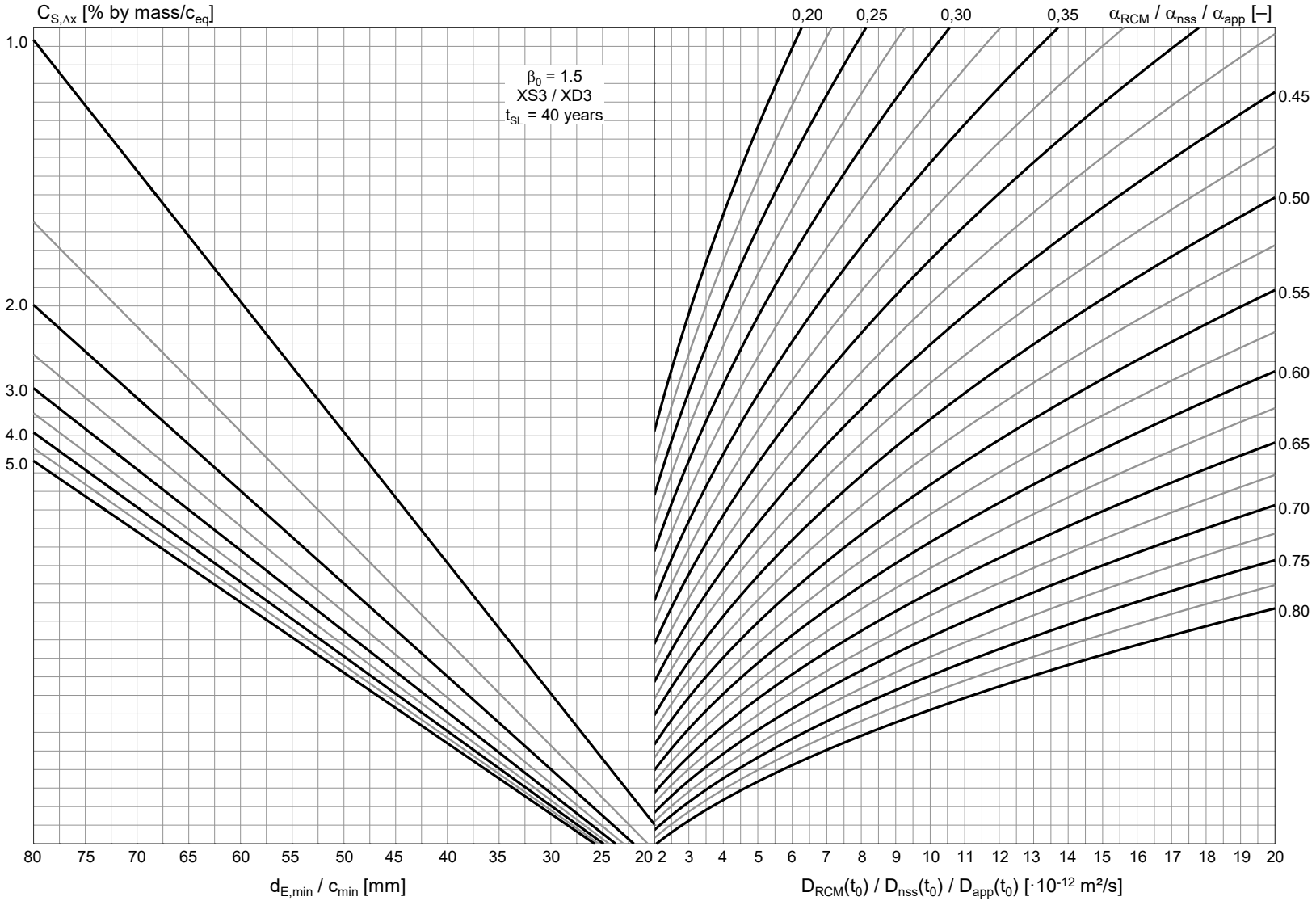

Fig. D.8: Design nomogram for XS3 / XD3, target service life t_{SL}=40 years, target reliability index β_0=1.5, $2 \leq D(t_0) \leq 20$

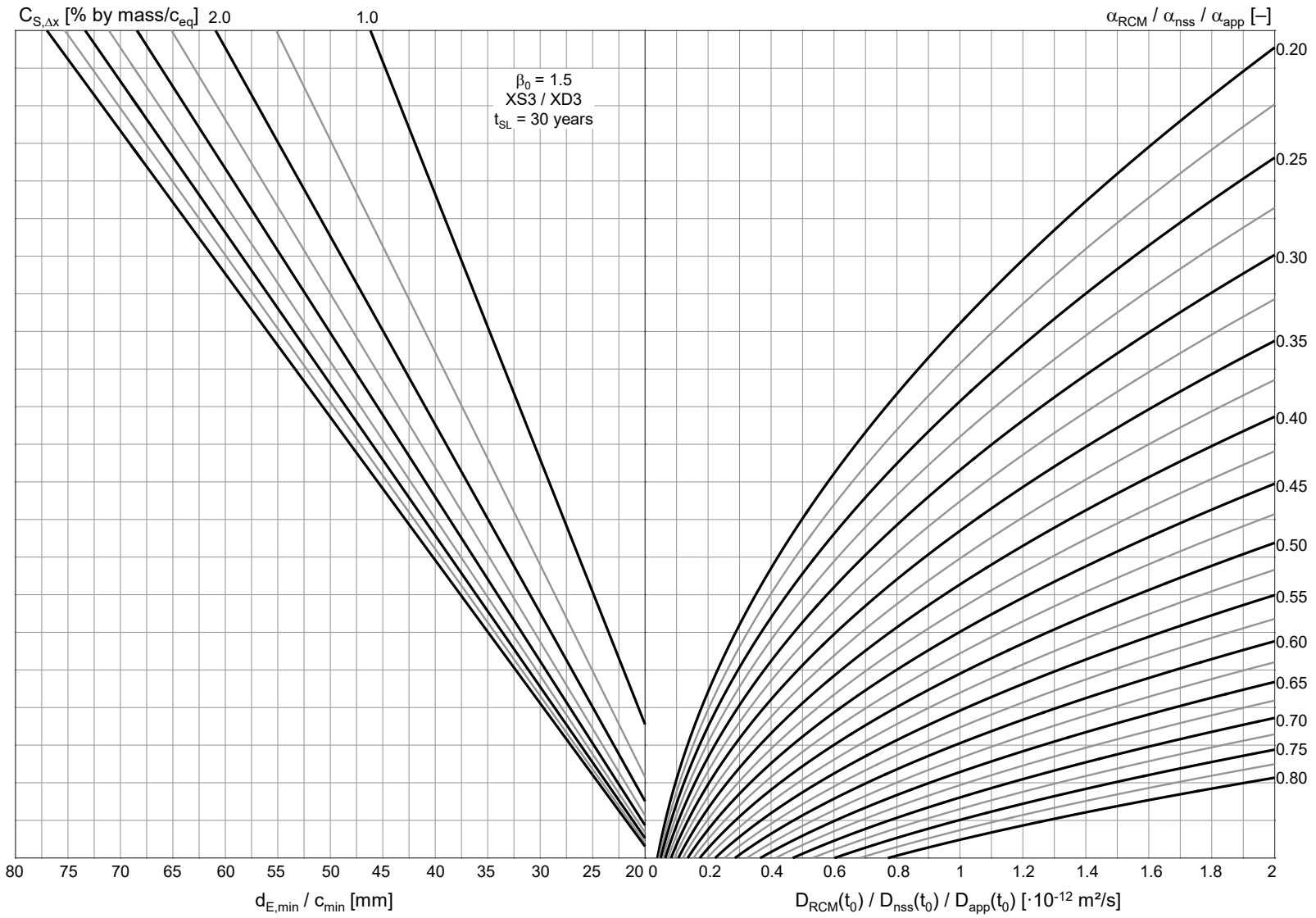

Fig. D.9: Design nomogram for XS3 / XD3, target service life t_{SL}=30 years, target reliability index β_0=1.5, $0 \leq D(t_0) \leq 2$

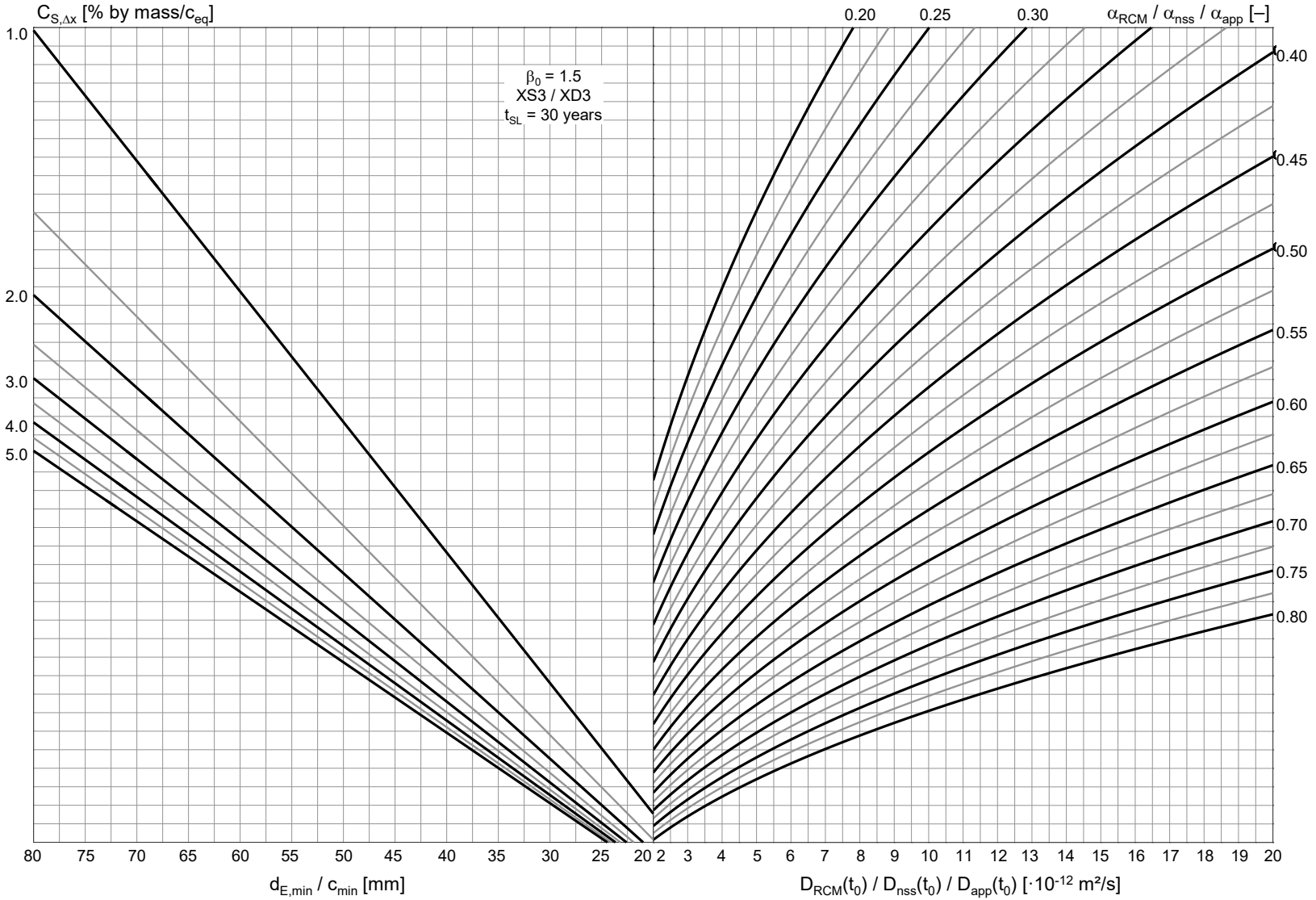

Fig. D.10: Design nomogram for XS3 / XD3, target service life t_{SL}=30 years, target reliability index β_0=1.5, $2 \leq D(t_0) \leq 20$

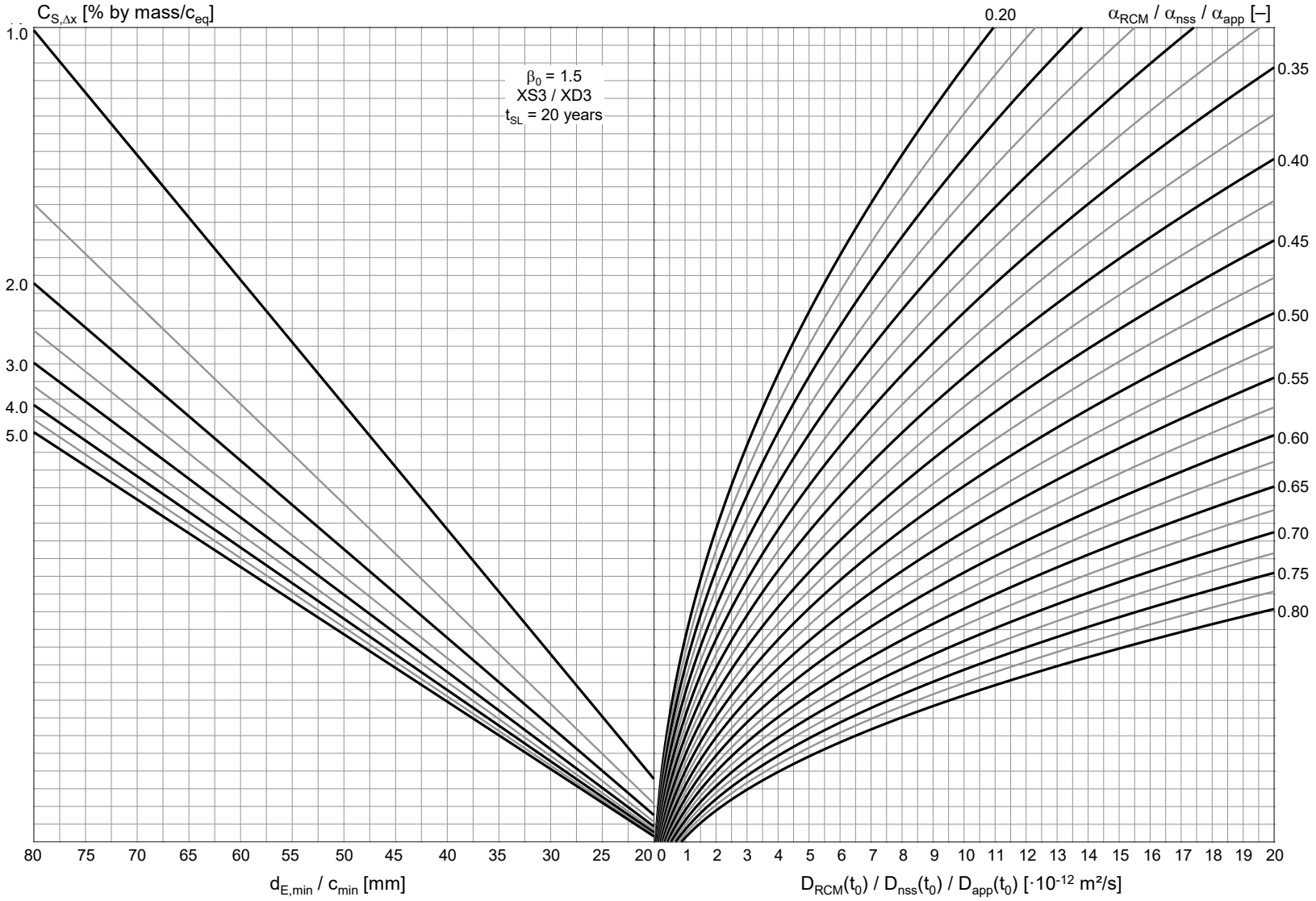

Fig. D.11: Design nomogram for XS3 / XD3, target service life t_{SL}=20 years, target reliability index β_0=1.5, $0 \leq D(t_0) \leq 20$

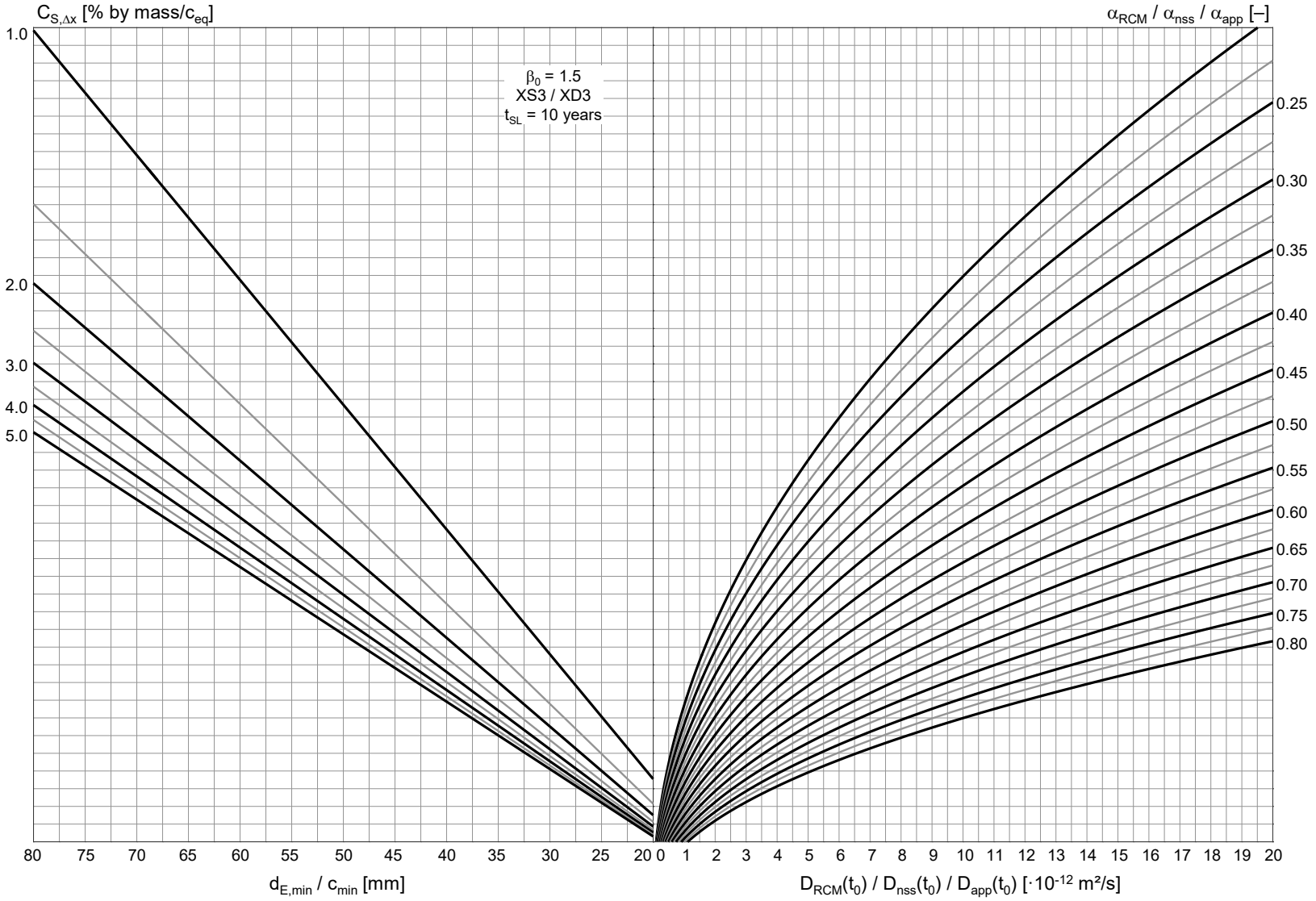

Fig. D.12: Design nomogram for XS3 / XD3, target service life t_{SL}=10 years, target reliability index β_0=1.5, $0 \leq D(t_0) \leq 20$

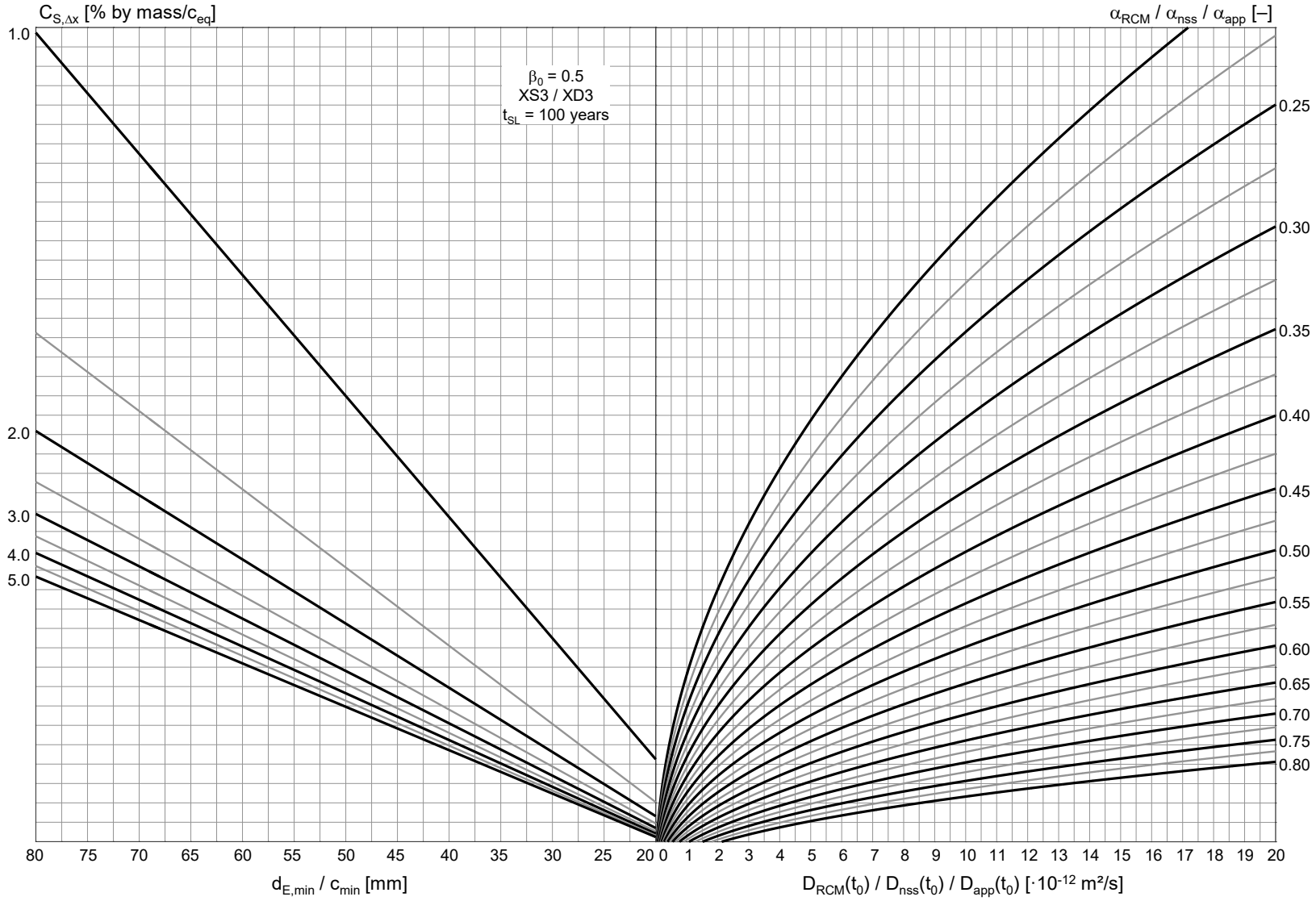

Fig. D.13: Design nomogram for XS3 / XD3, target service life t_{SL}=100 years, target reliability index β_0=0.5, $0 \leq D(t_0) \leq 20$

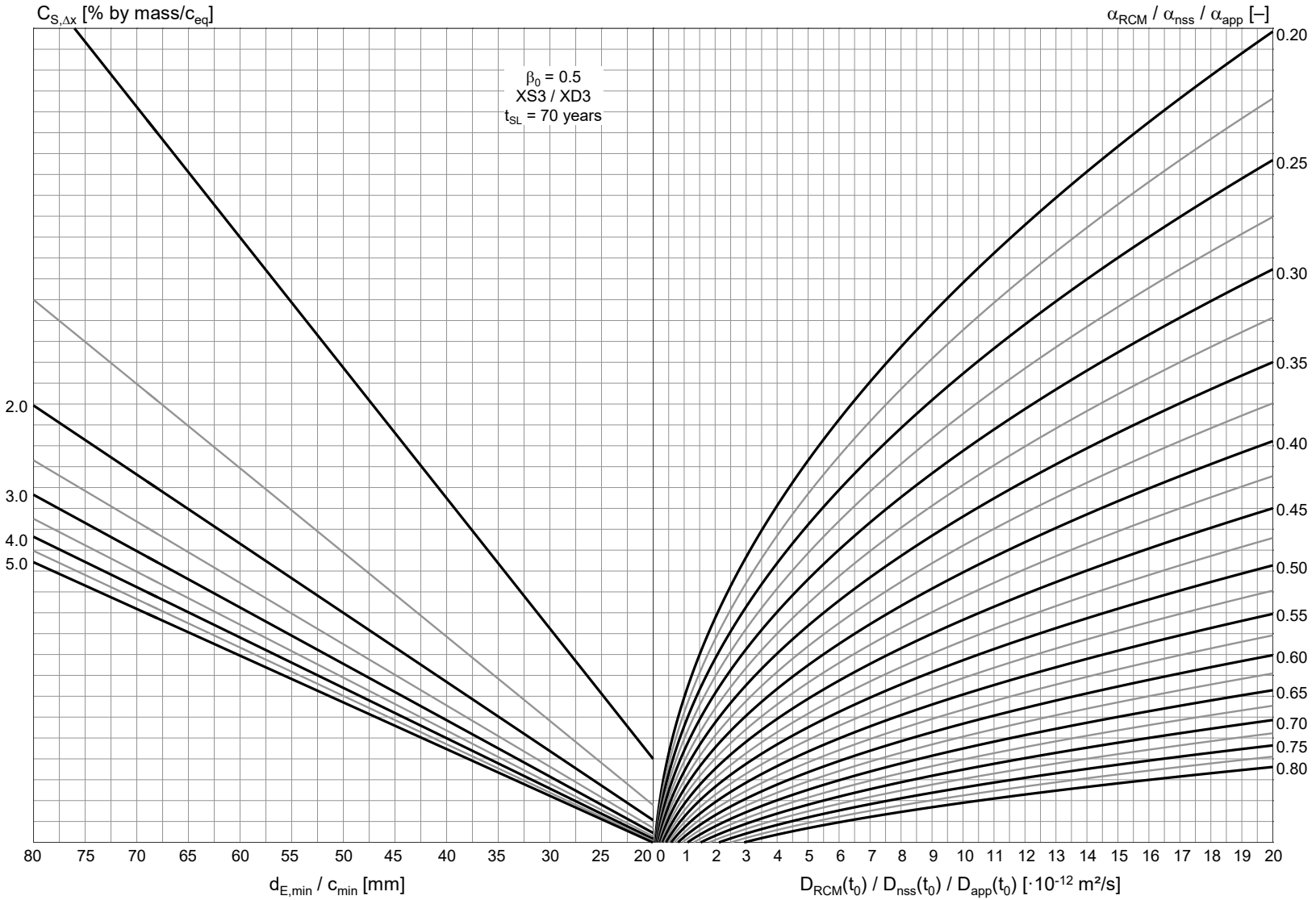

Fig. D.14: Design nomogram for XS3 / XD3, target service life t_{SL}=70 years, target reliability index β_0=0.5, $0 \leq D(t_0) \leq 20$

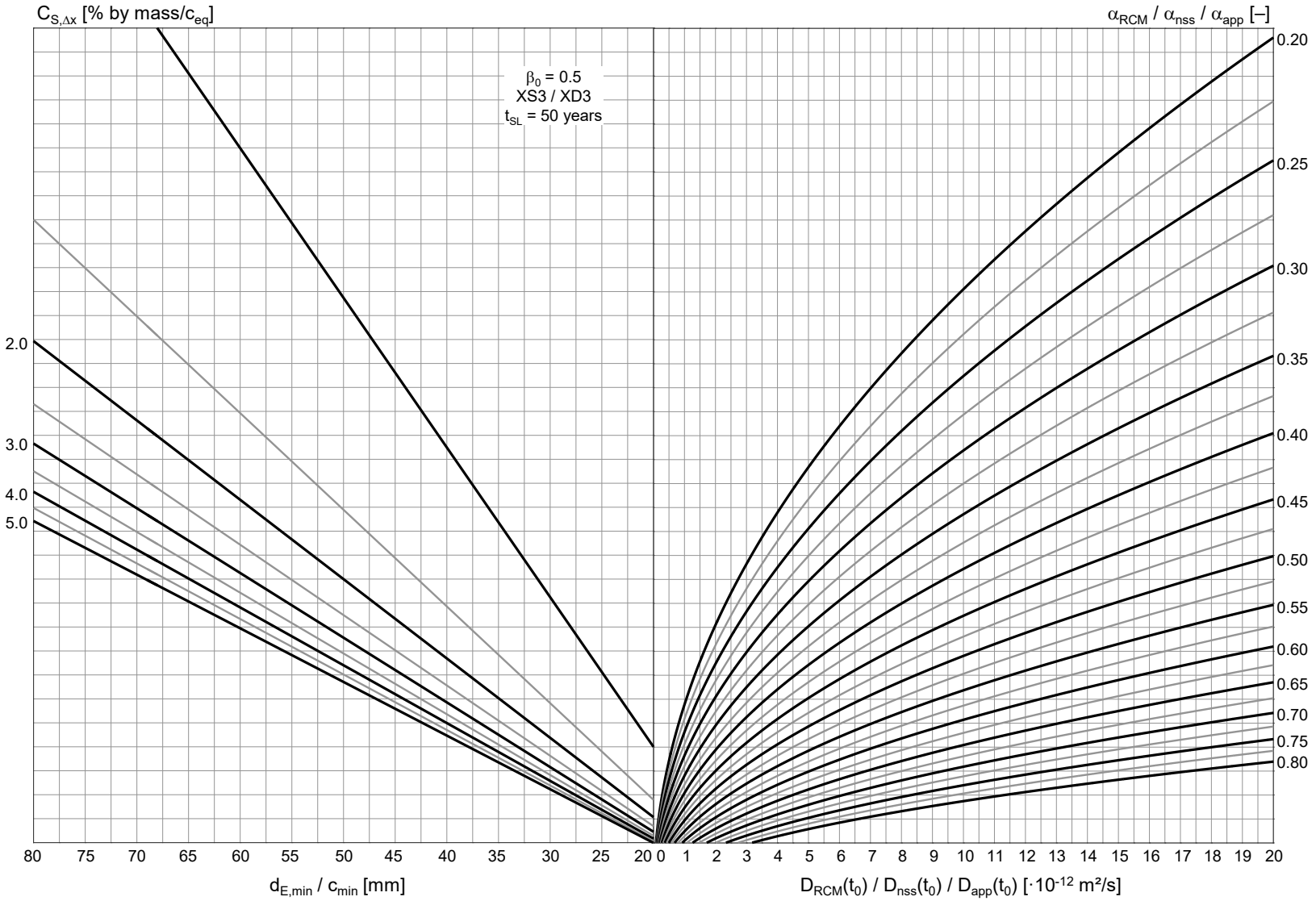

Fig. D.15: Design nomogram for XS3 / XD3, target service life t_{SL}=50 years, target reliability index β_0=0.5, $0 \leq D(t_0) \leq 20$

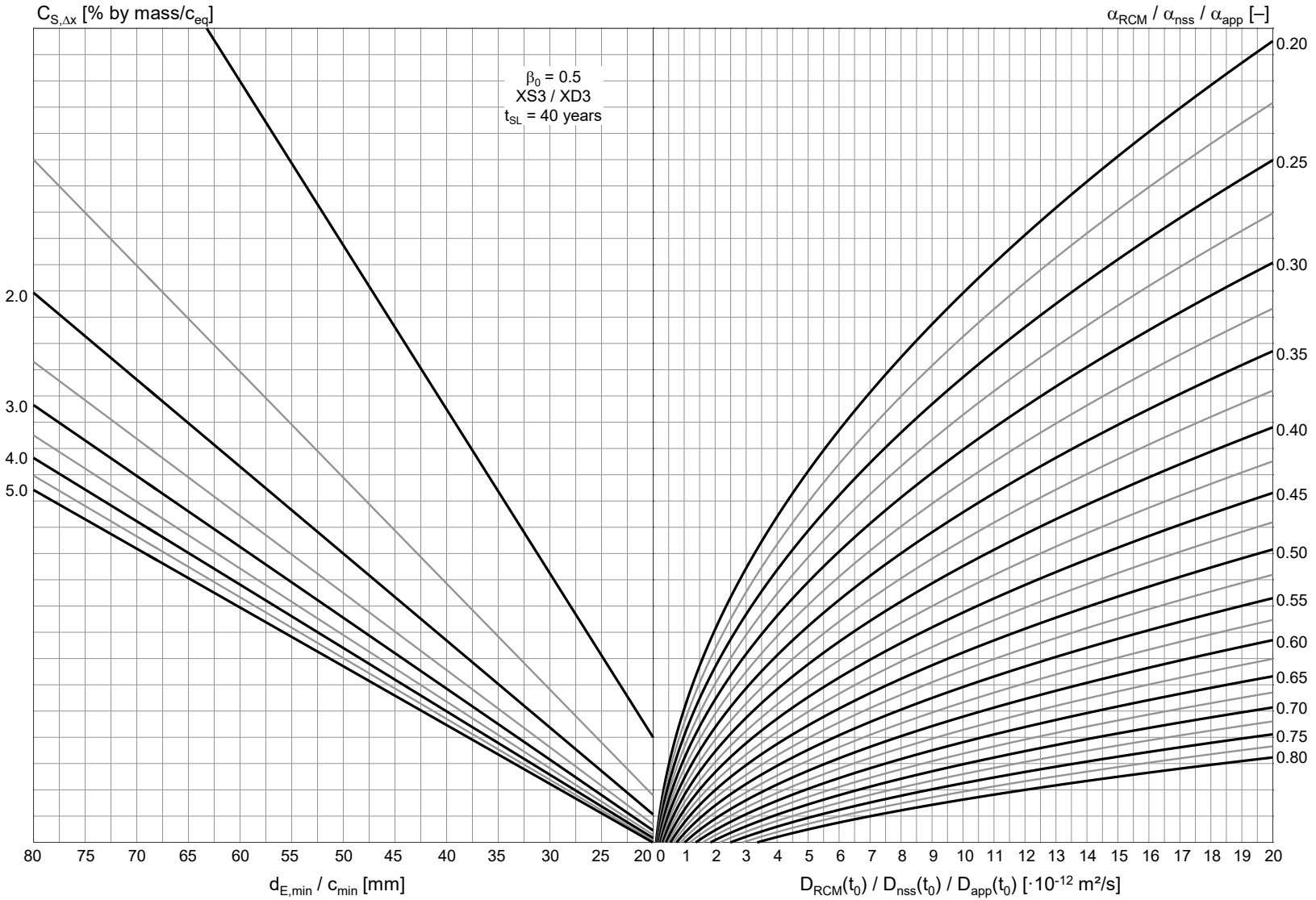

Fig. D.16: Design nomogram for XS3 / XD3, target service life t_{SL}=40 years, target reliability index β_0=0.5, $0 \leq D(t_0) \leq 20$

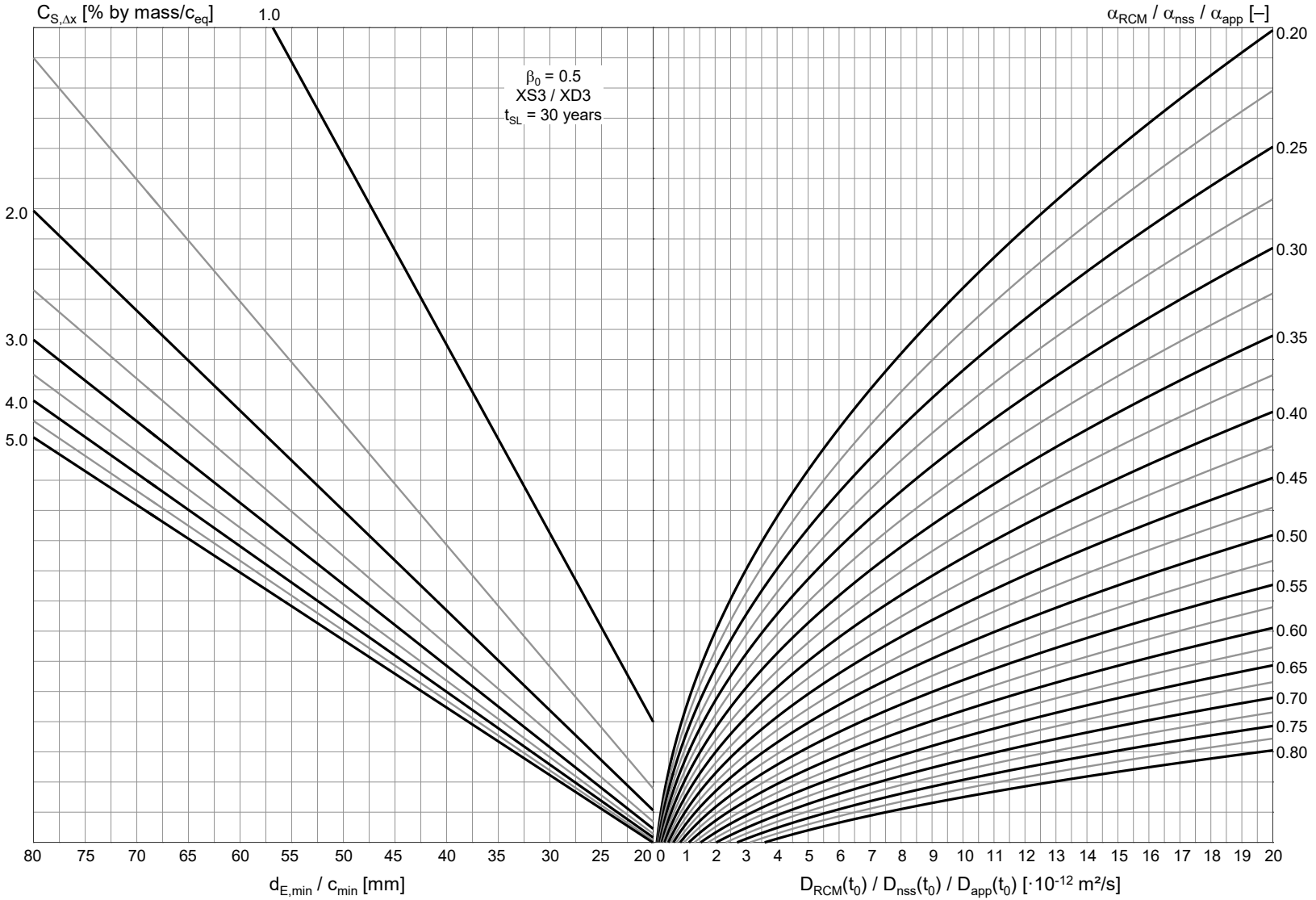

Fig. D.17: Design nomogram for XS3 / XD3, target service life t_{SL}=30 years, target reliability index β_0=0.5, $0 \leq D(t_0) \leq 20$

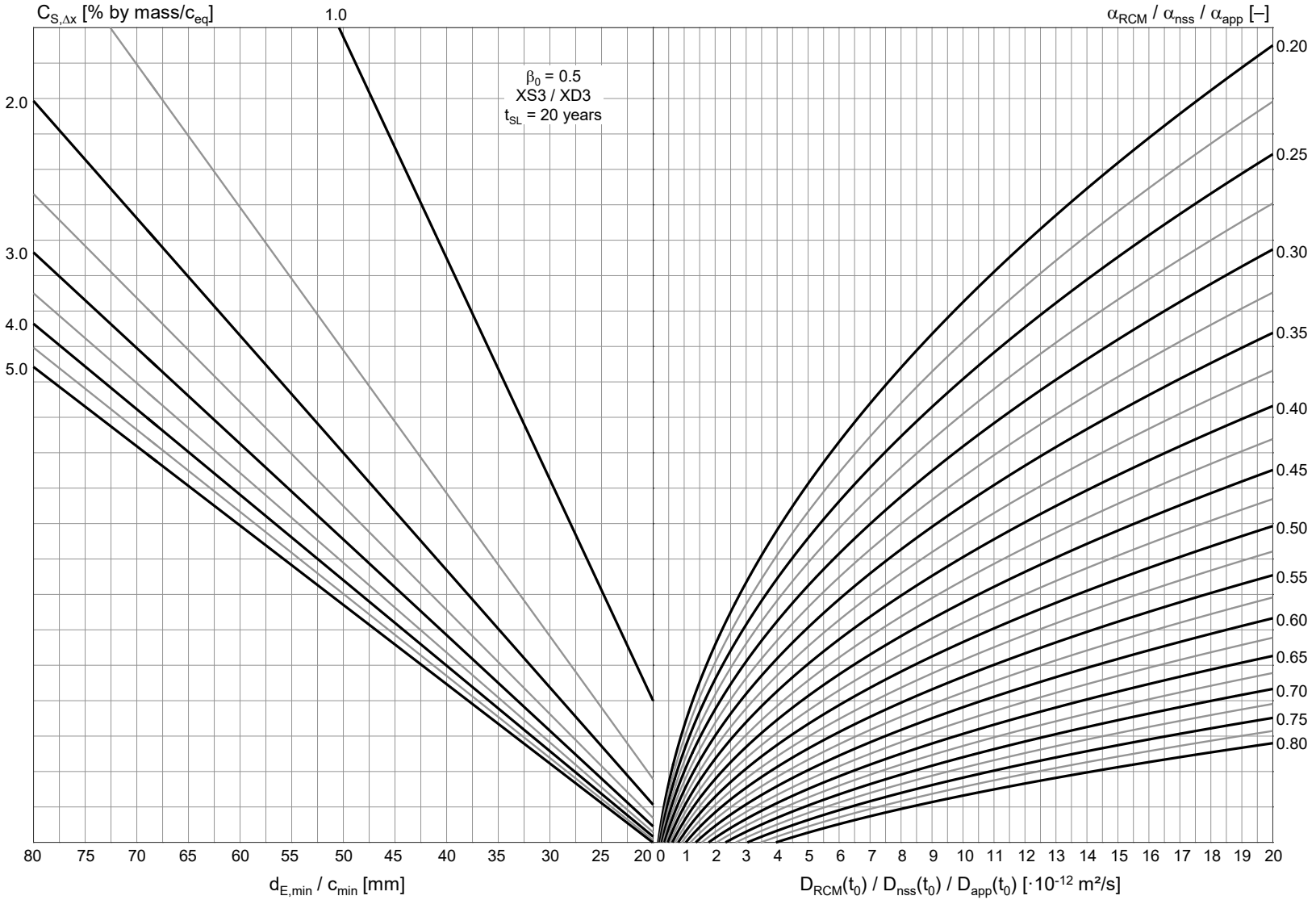

Fig. D.18: Design nomogram for XS3 / XD3, target service life t_{SL}=20 years, target reliability index β_0=0.5, $0 \leq D(t_0) \leq 20$

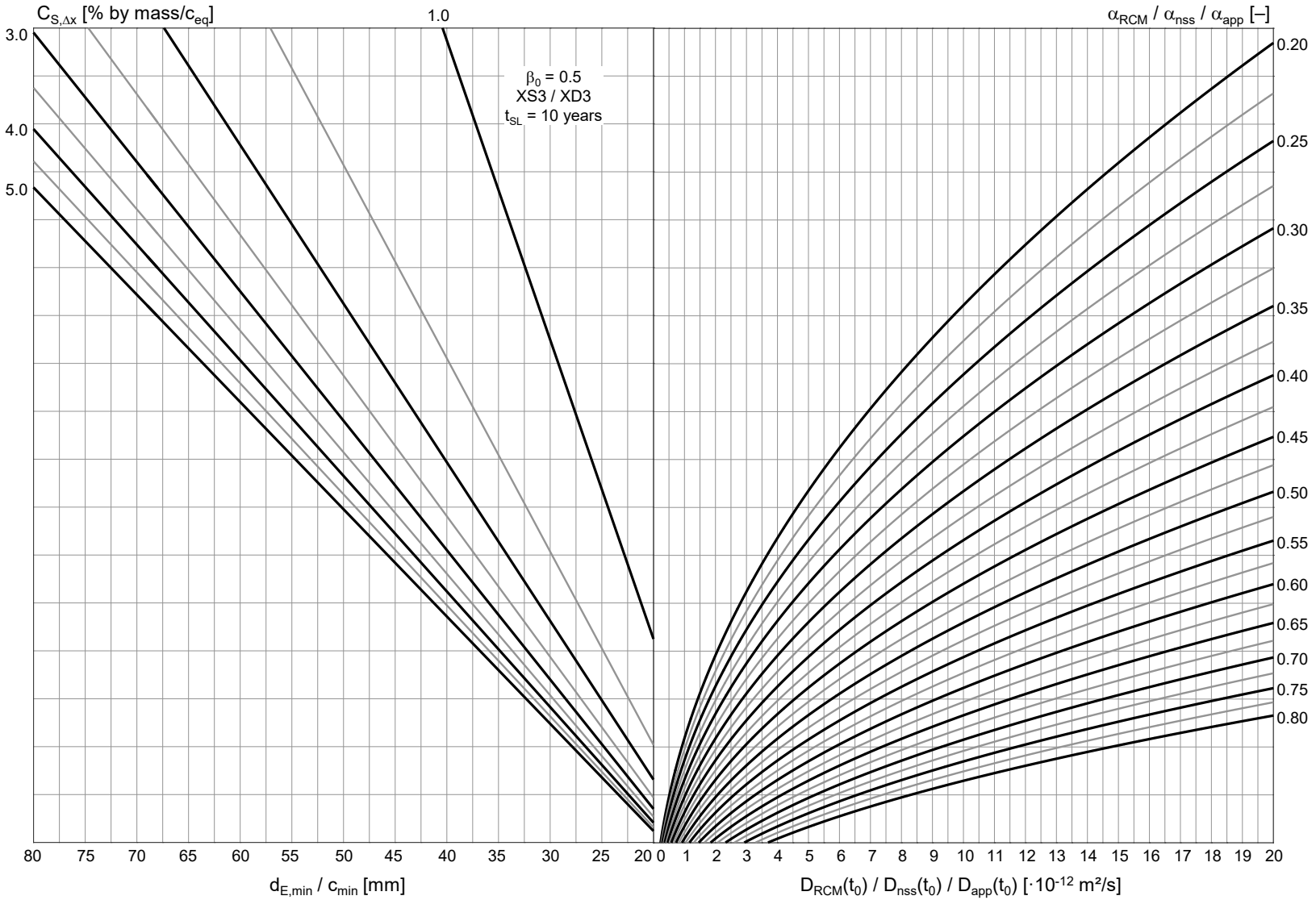

Fig. D.19: Design nomogram for XS3 / XD3, target service life t_{SL}=10 years, target reliability index β_0=0.5, $0 \leq D(t_0) \leq 20$

E Annex E: Nomograms for the durability design of repair measures involving replacement of damaged concrete

The boundary conditions stated in Annex D must be taken into account when using the nomograms.

Durability design is performed with the aid of the nomograms in Annex D for cases in which the damaged concrete cover is completely replaced.

The equations required for application of the design nomograms have been grouped together below:

$$k_{D,d} = 0.04^{\left(\frac{\alpha_{new}}{1.2} - \frac{\alpha_{remain}}{1.1}\right)} \cdot \sqrt{\frac{D_{RCM,new}(t_0) \cdot 1.2}{D_{RCM,remain}(t_0) \cdot 1.1}}$$

$$d_R = \sqrt{k_e \cdot D_{RCM,new}(t_0) \cdot 1.2 \cdot \left(\frac{t_0}{t_{SL}}\right)^{\frac{\alpha_{new}}{1.2}} \cdot t_{SL}}$$

$$d_{E,min} = c_{new,min} = d_c - k_{D.d} \cdot c_{remain,min} + \Delta x$$

$$d_{E,nom} = d_{E,min} + \Delta d_E$$

Δx =10 mm for XS3 and XD3

Δx = 0 mm for XS2 and XD2

5 mm ≤ Δd_E ≤ 15 mm

An overview of the design nomograms is given in Table E.1.

Table E.1: Overview of the nomograms for the service life design of repair measures by means of concrete replacement for exposure classes XS2, XD2, XS3 and XD3

$C_{S,\Delta x}$ [% by mass/b]	C_r [% by mass/b]	Fig. no.	
		β_0 =1.5	β_0 =0.5
2.0	0	E.1	E.17
	0.1	E.2	E.18
	0.2	E.3	E.19
	0.3	E.4	E.20
3.0	0	E.5	E.21
	0.1	E.6	E.22
	0.2	E.7	E.23
	0.3	E.8	E.24
4.0	0	E.9	E.25
	0.1	E.10	E.26
	0.2	E.11	E.27
	0.3	E.12	E.28
5.0	0	E.13	E.29
	0.1	E.14	E.30
	0.2	E.15	E.31
	0.3	E.16	E.32

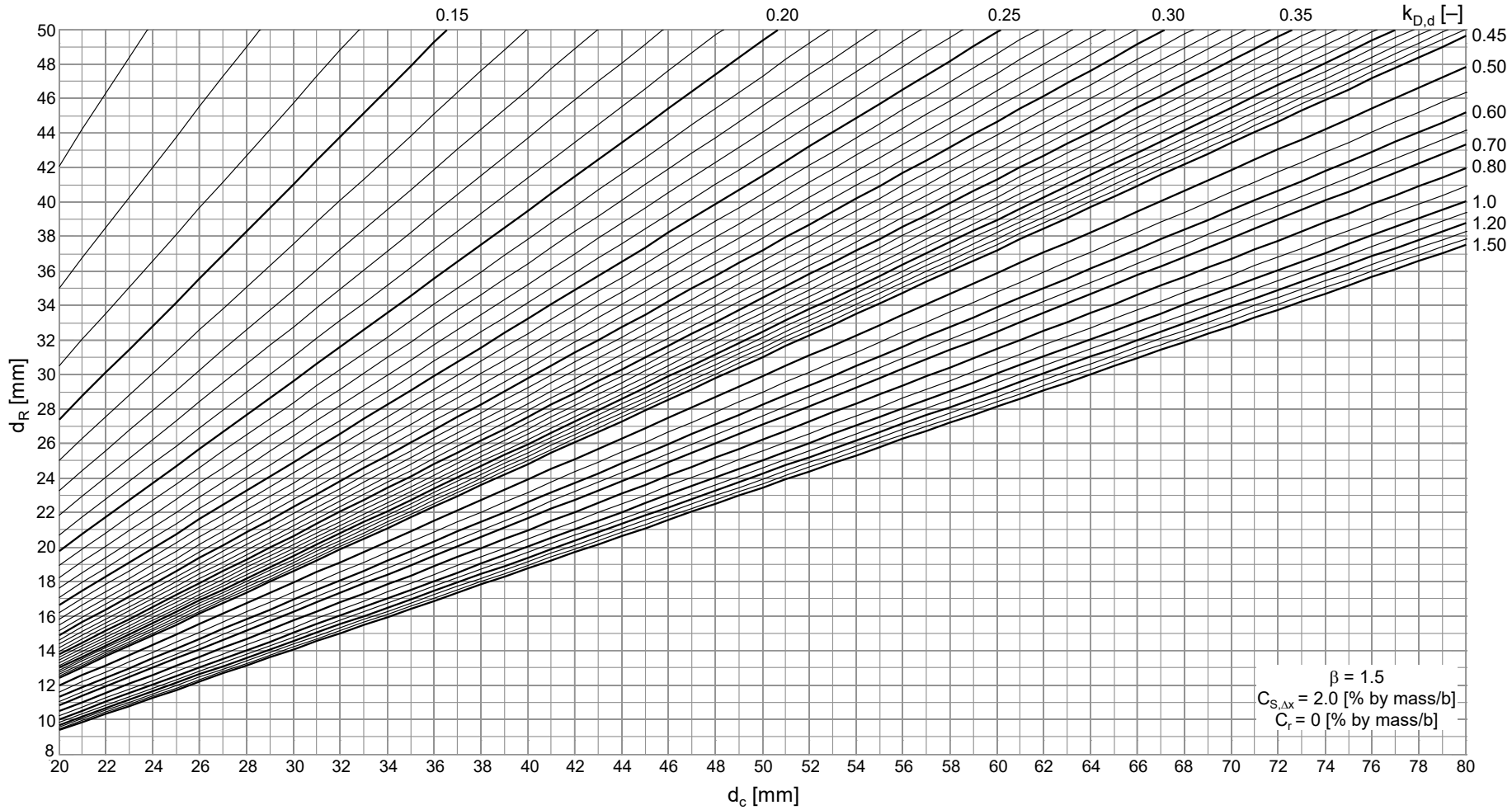

Fig. E.1: Design nomogram for target reliability index β_0=1.5, $C_{S,\Delta x}$=2.0 Wt.-%/b, C_r=0 Wt.-%/b

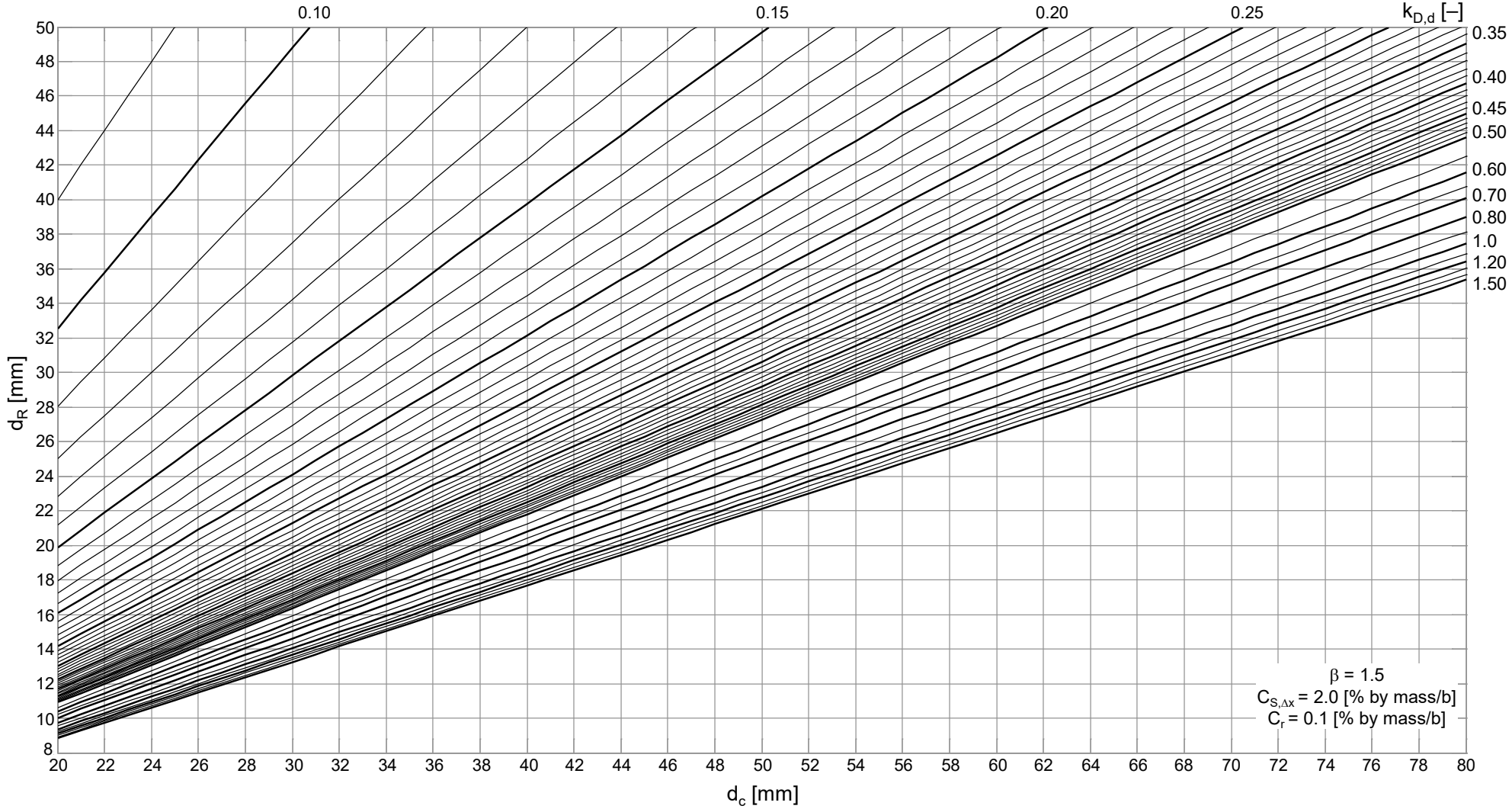

Fig. E.2: Design nomogram for target reliability index β_0=1.5, $C_{S,\Delta x}$=2.0 Wt.-%/b, C_r=0.1 Wt.-%/b

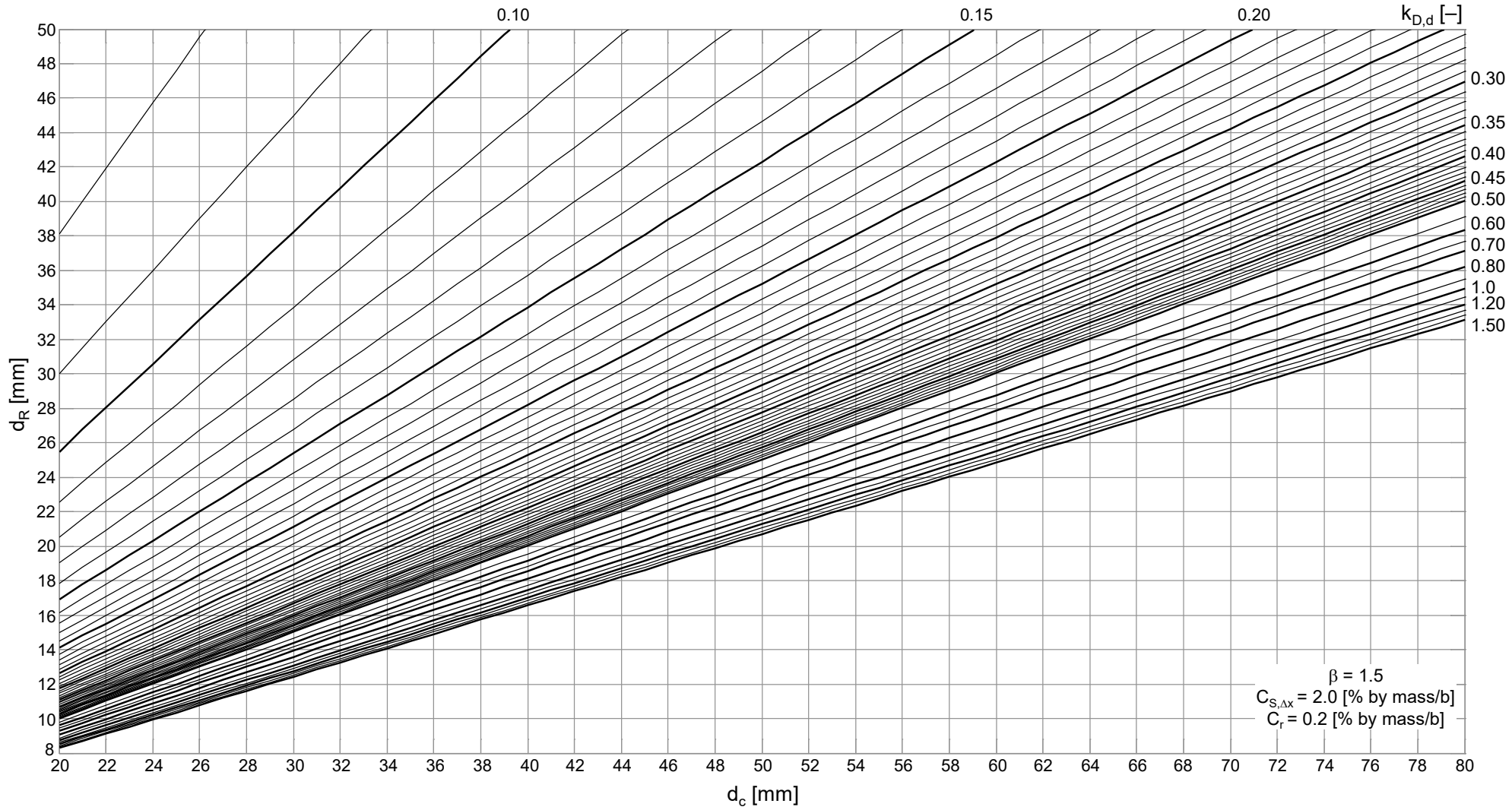

Fig. E.3: Design nomogram for target reliability index β_0=1.5, $C_{S,\Delta x}$=2.0 Wt.-%/b, C_r=0.2 Wt.-%/b

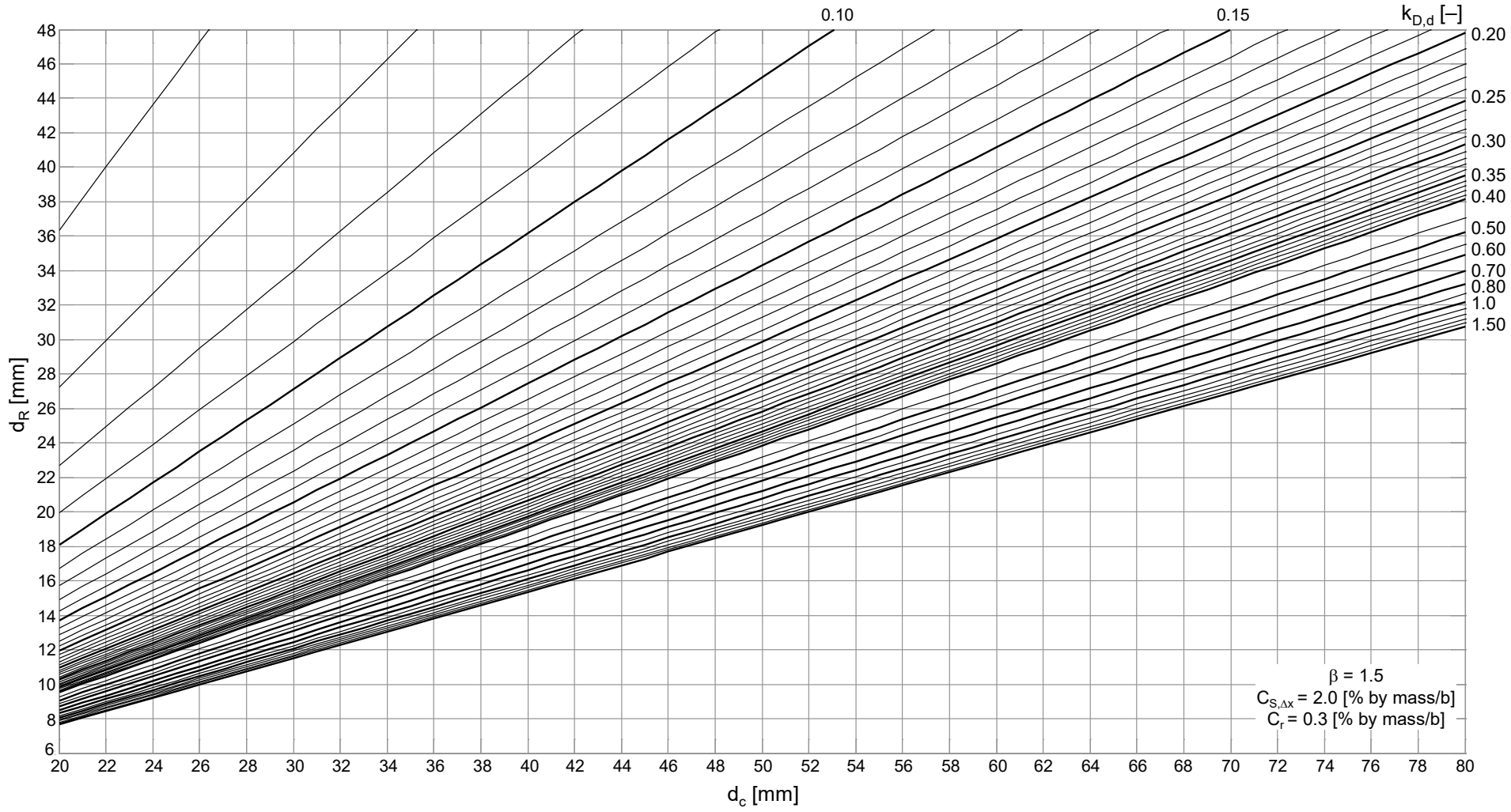

Fig. E.4: Design nomogram for target reliability index β_0=1.5, $C_{S,\Delta x}$=2.0 Wt.-%/b, C_r=0.3 Wt.-%/b

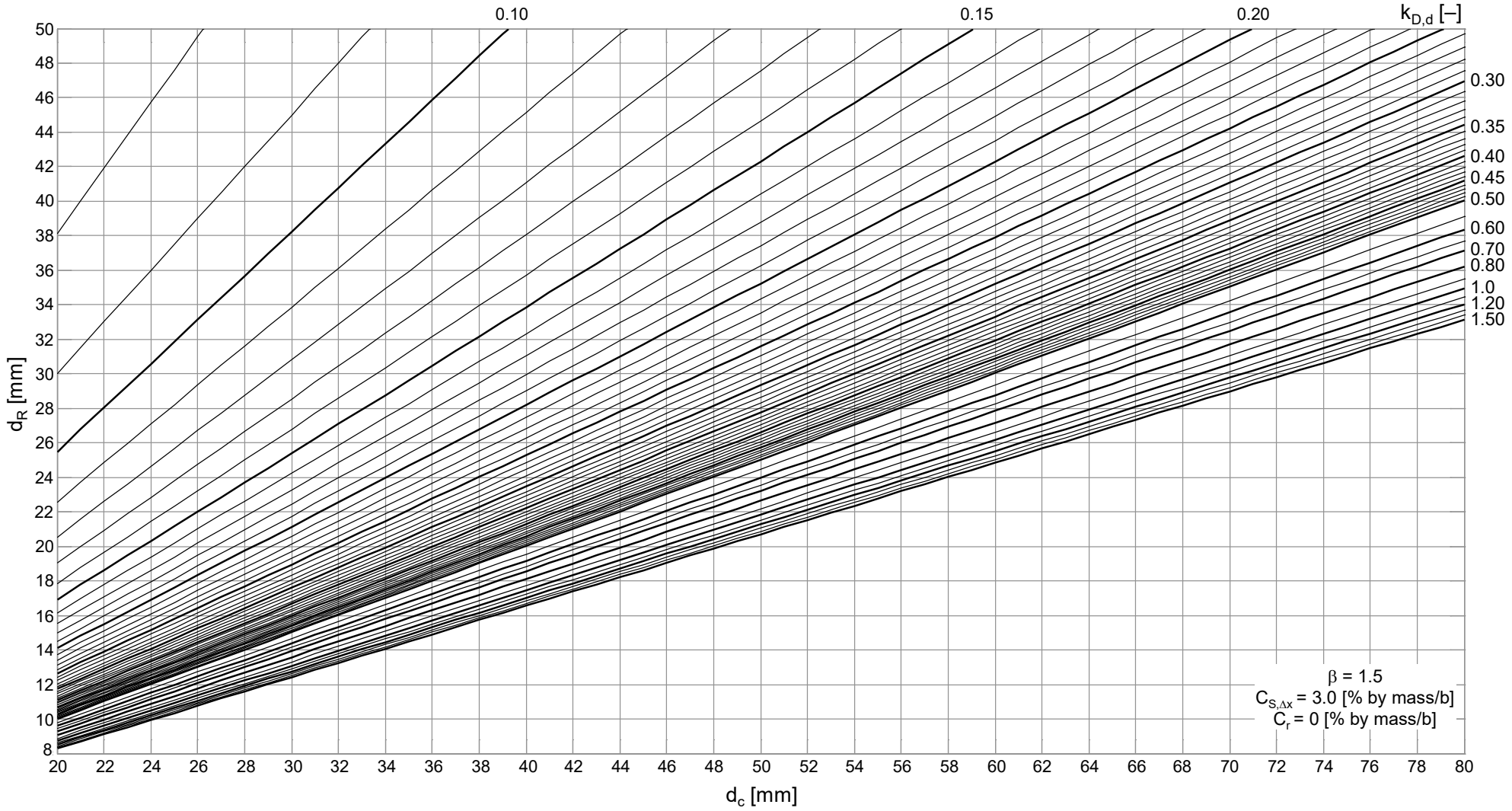

Fig. E.5: Design nomogram for target reliability index β_0=1.5, $C_{S,\Delta x}$=3.0 Wt.-%/b, C_r=0 Wt.-%/b

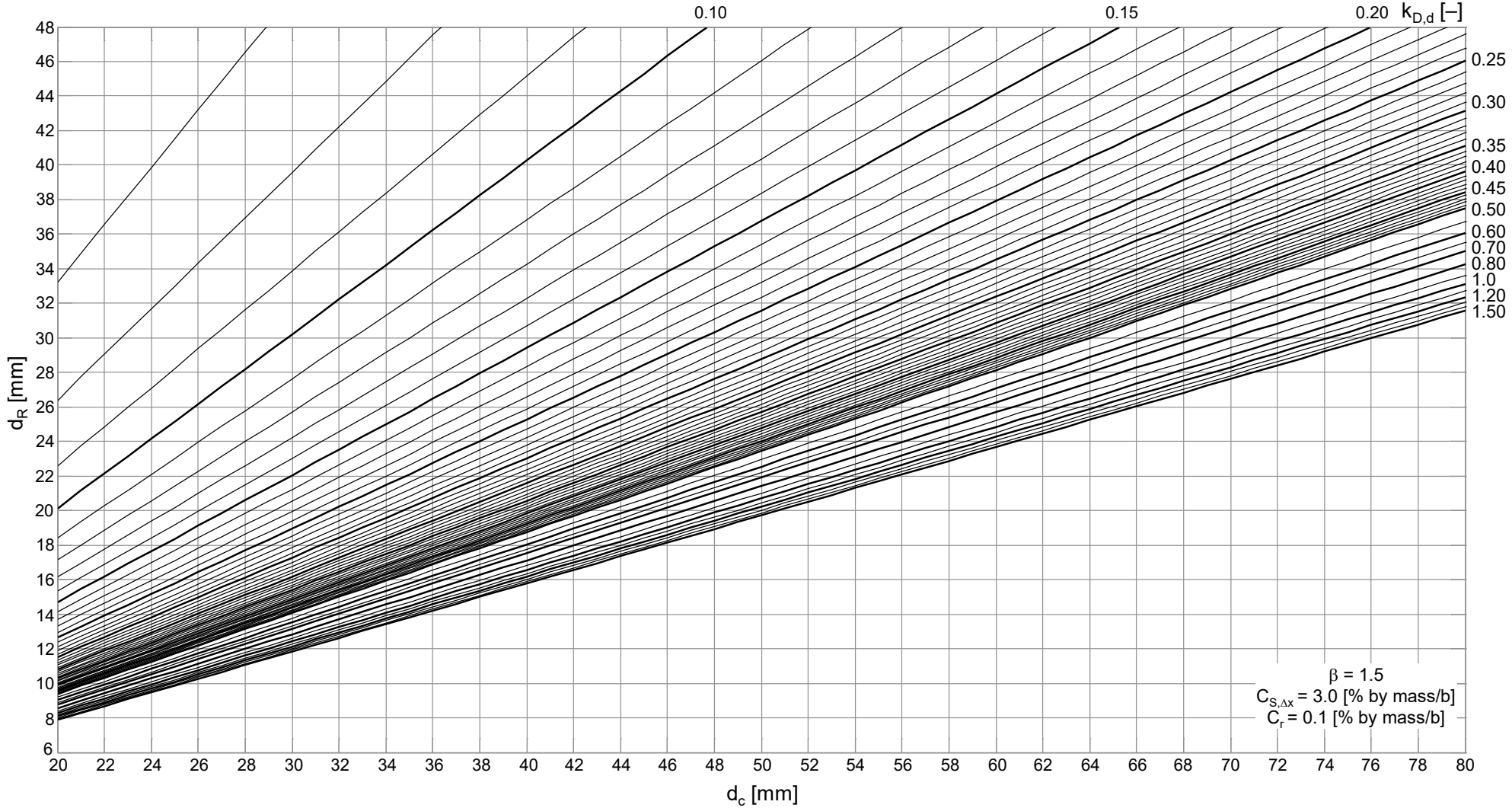

Fig. E.6: Design nomogram for target reliability index β_0=1.5, $C_{S,\Delta x}$=3.0 Wt.-%/b, C_r=0.1 Wt.-%/b

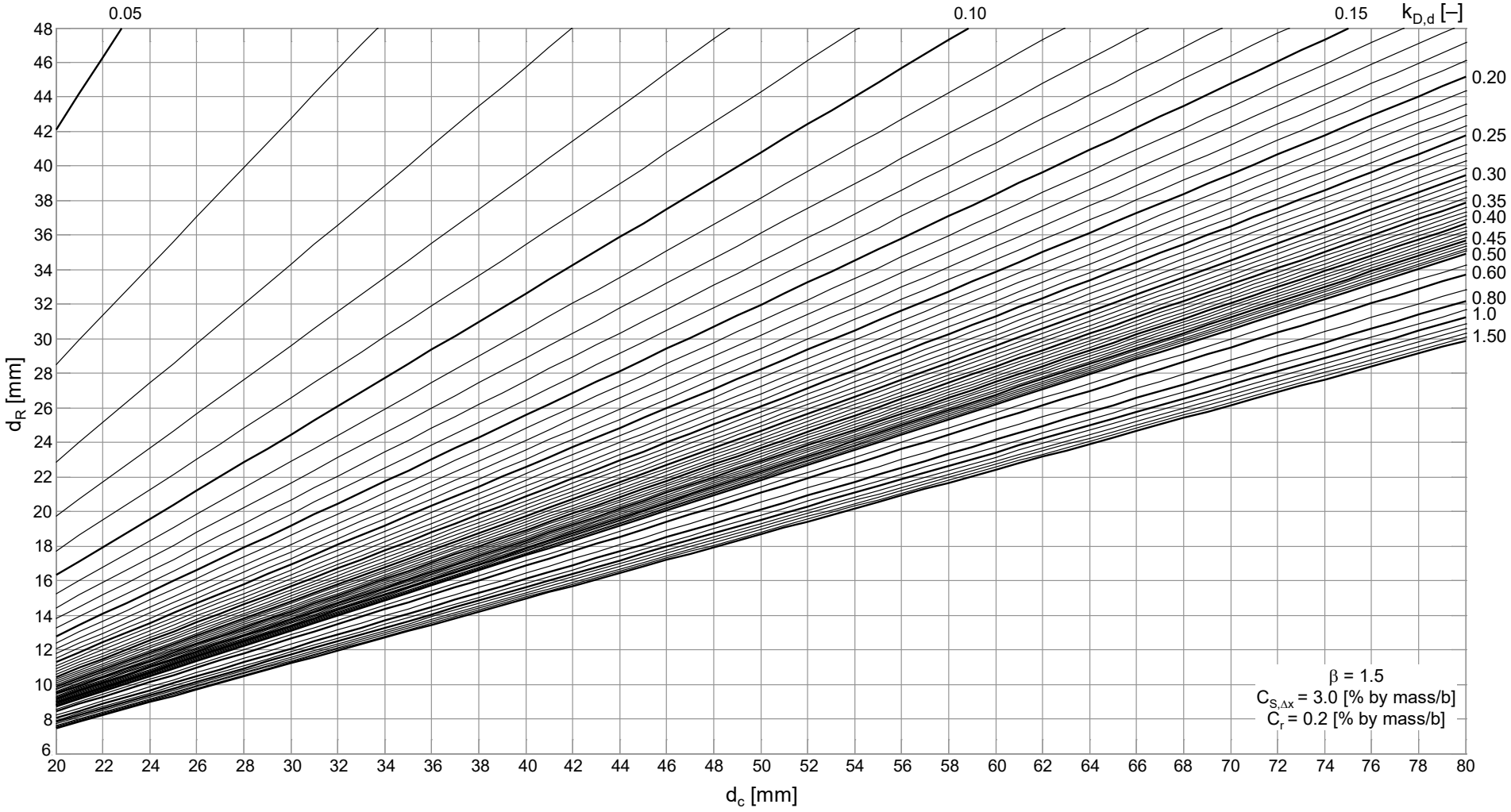

Fig. E.7: Design nomogram for target reliability index β_0=1.5, $C_{S,\Delta x}$=3.0 Wt.-%/b, C_r=0.2 Wt.-%/b

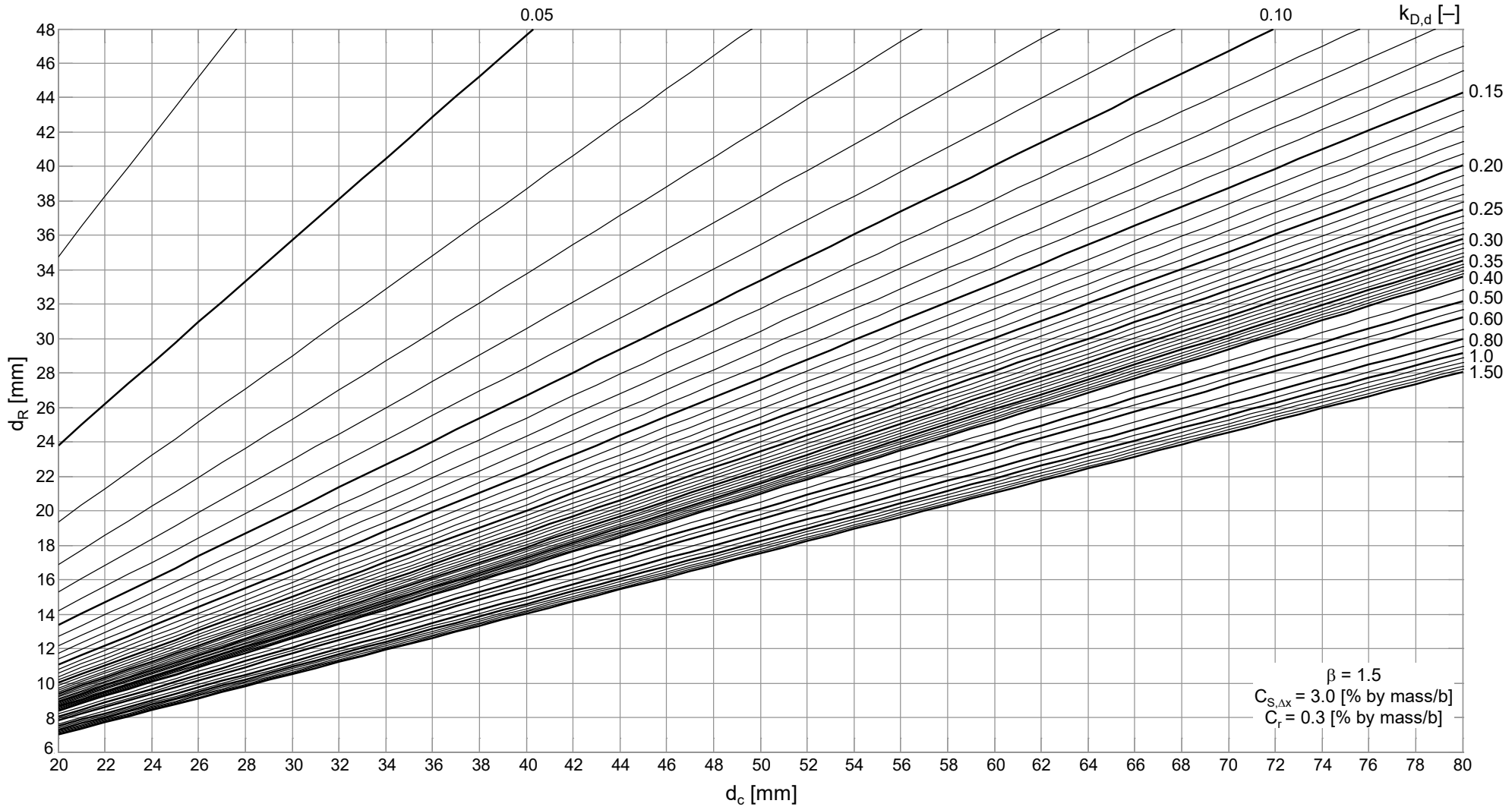

Fig. E.8: Design nomogram for target reliability index β_0=1.5, $C_{S,\Delta x}$=3.0 Wt.-%/b, C_r=0.3 Wt.-%/b

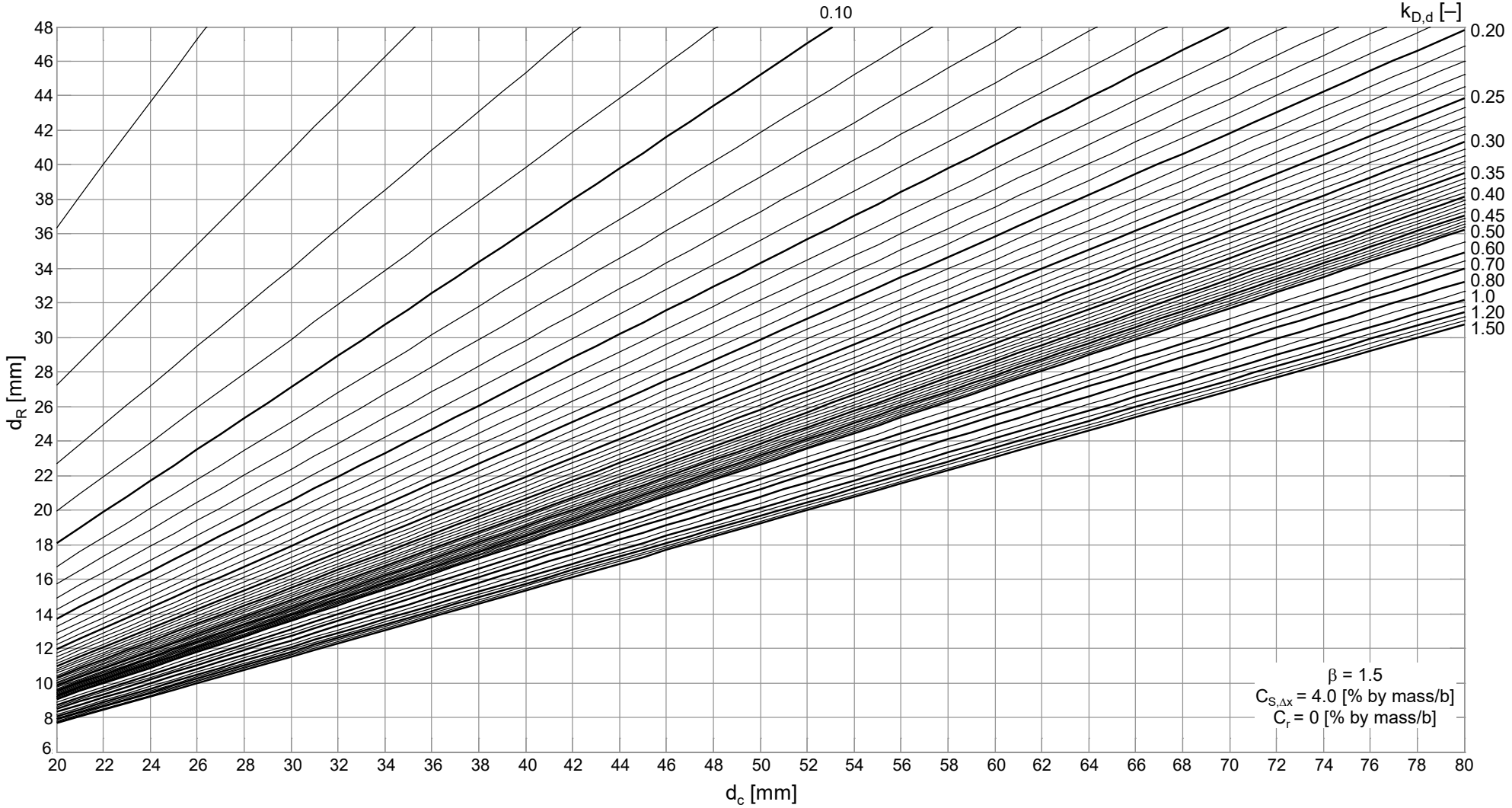

Fig. E.9: Design nomogram for target reliability index β_0=1.5, $C_{S,\Delta x}$=4.0 Wt.-%/b, C_r=0 Wt.-%/b

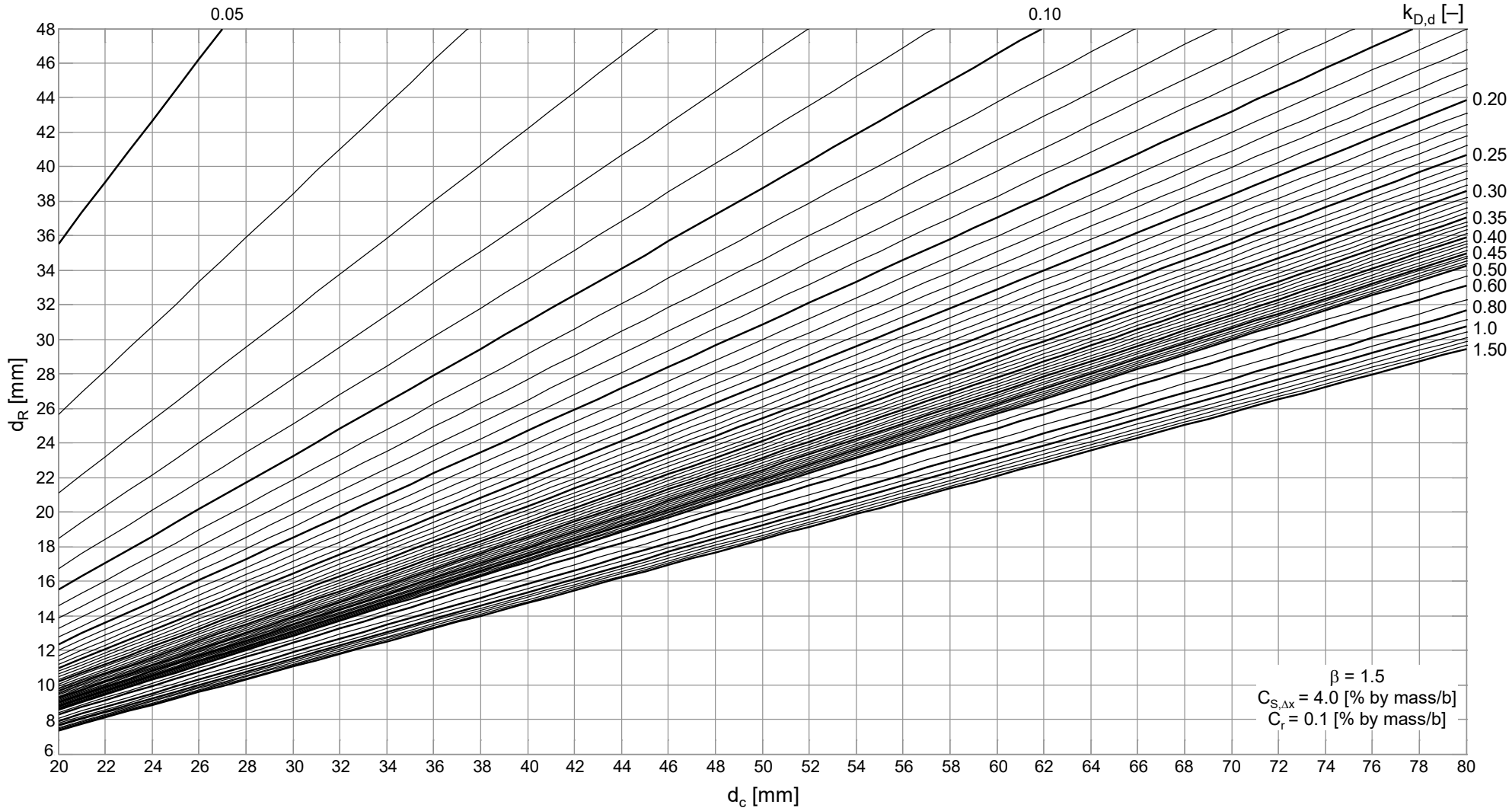

Fig. E.10: Design nomogram for target reliability index β_0=1.5, $C_{S,\Delta x}$=4.0 Wt.-%/b, C_r=0.1 Wt.-%/b

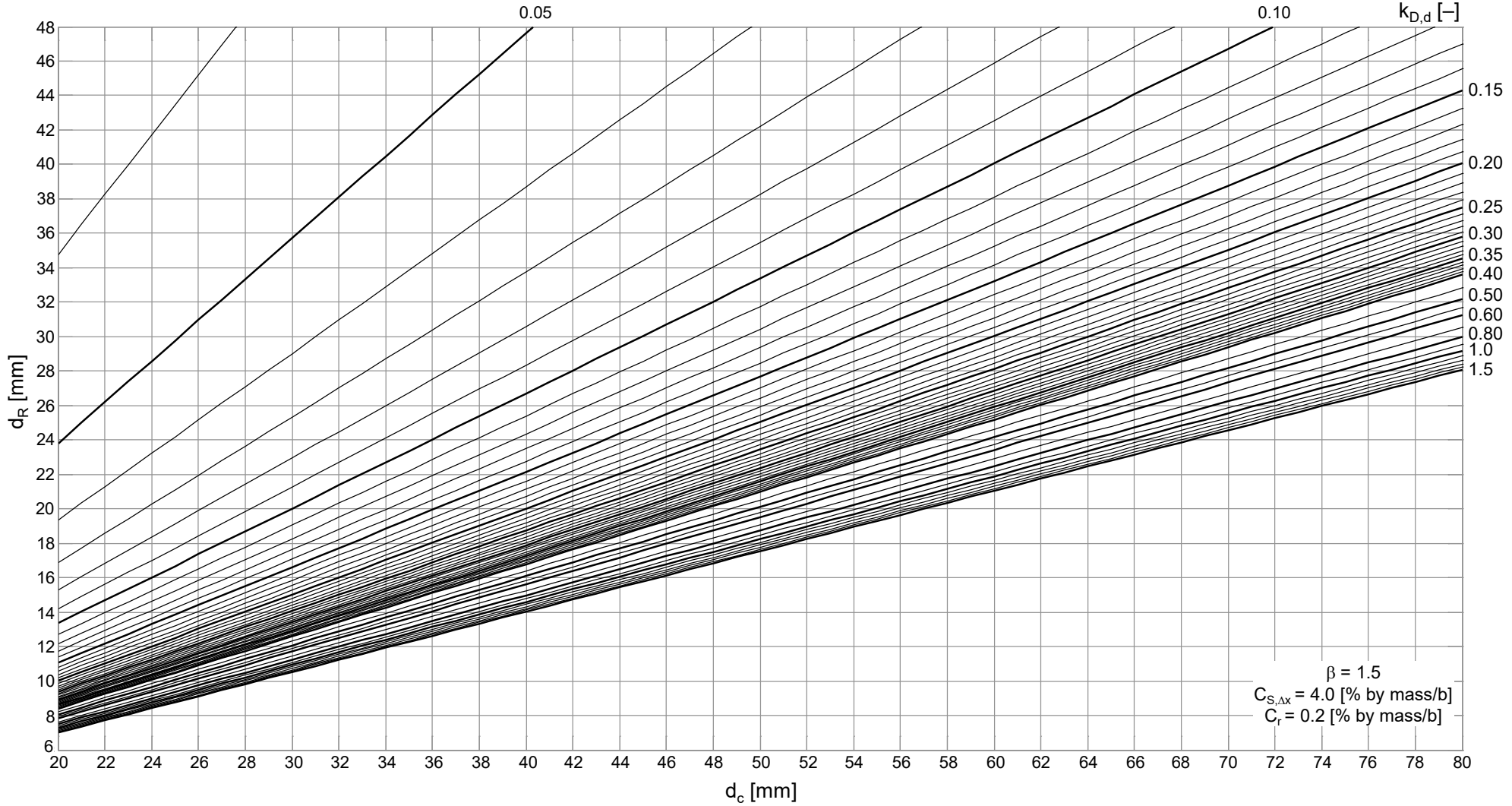

Fig. E.11: Design nomogram for target reliability index β_0=1.5, $C_{S,\Delta x}$=4.0 Wt.-%/b, C_r=0.2 Wt.-%/b

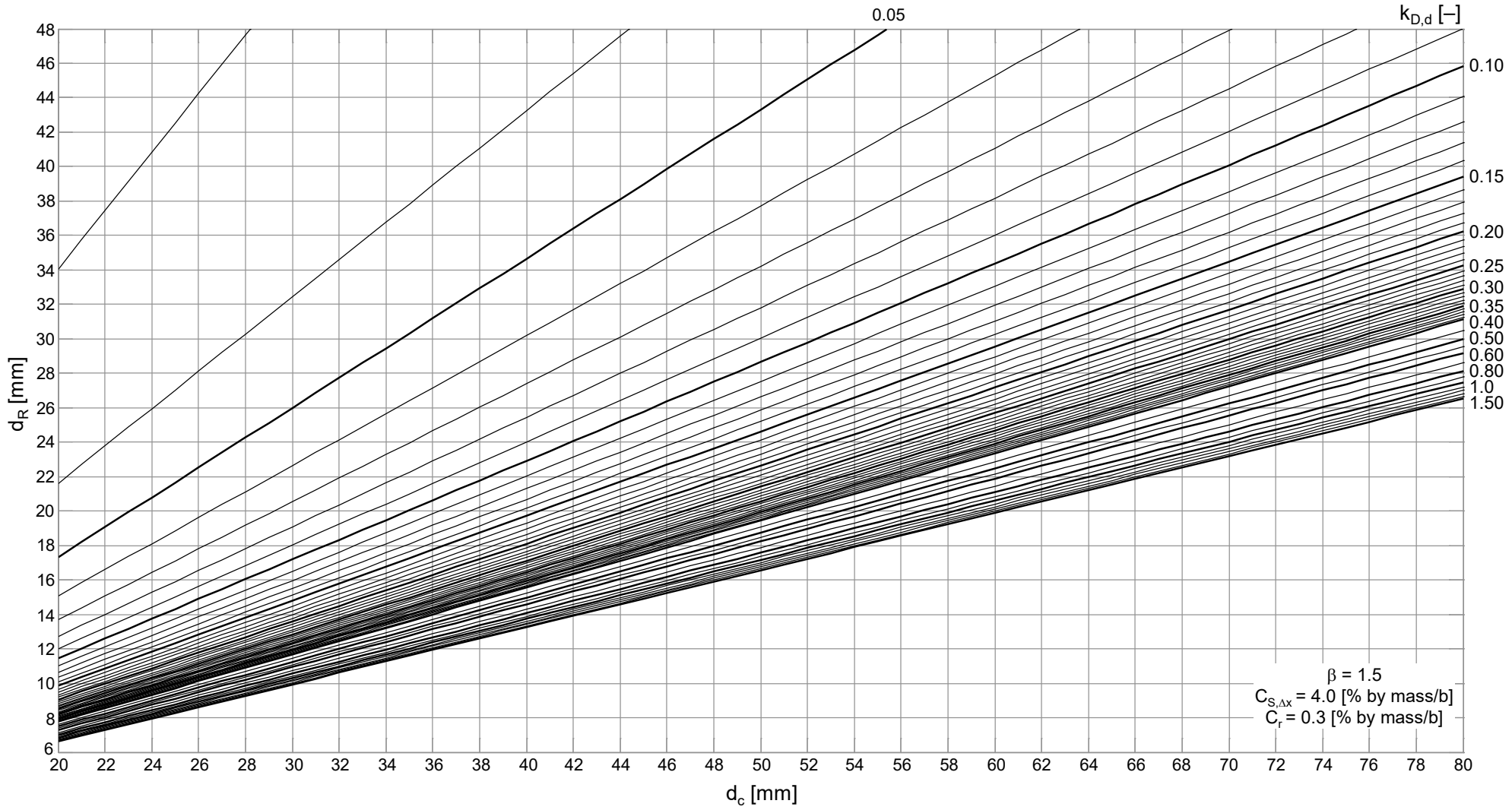

Fig. E.12: Design nomogram for target reliability index β_0=1.5, $C_{S,\Delta x}$=4.0 Wt.-%/b, C_r=0.3 Wt.-%/b

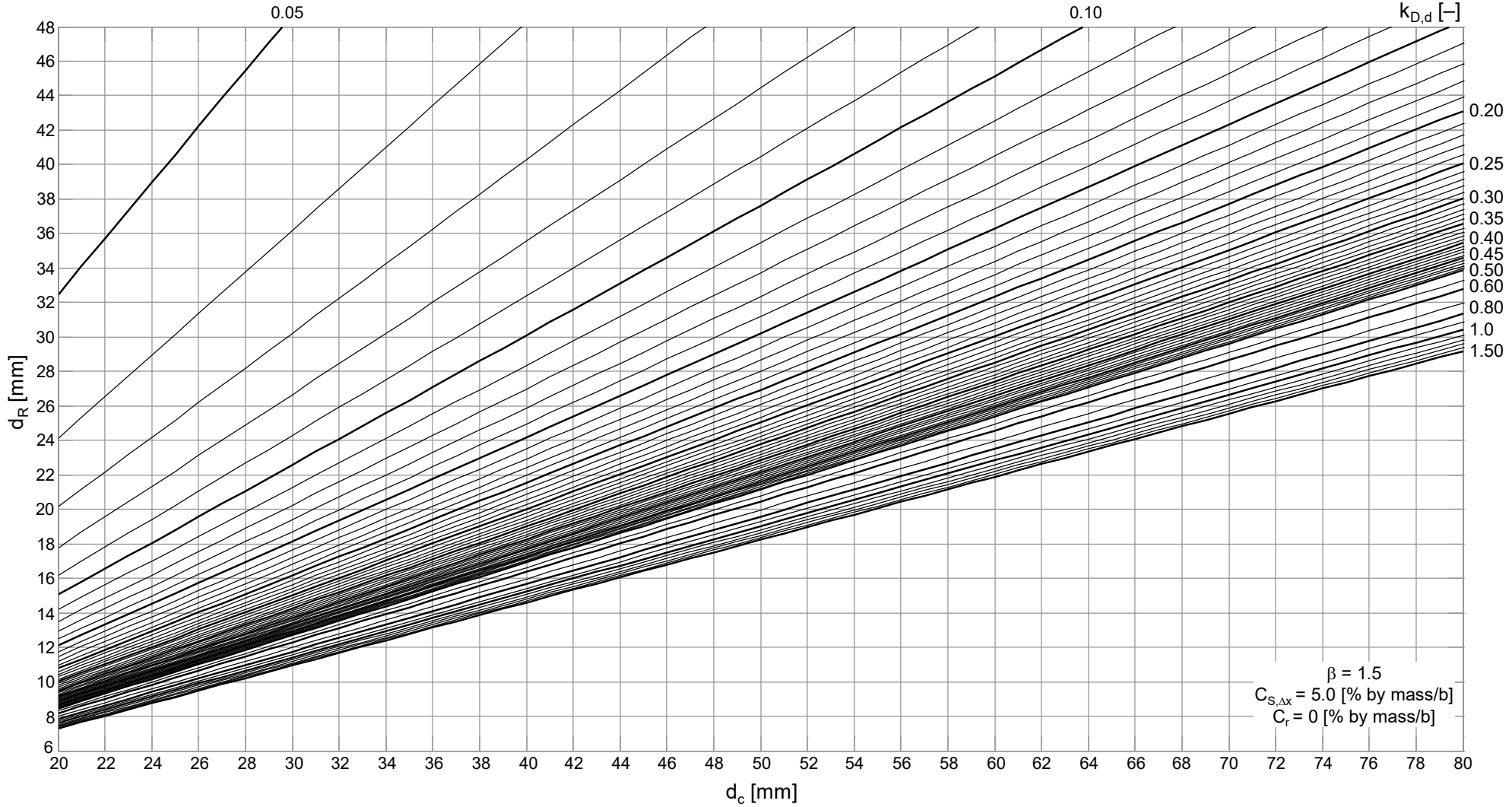

Fig. E.13: Design nomogram for target reliability index β_0=1.5, $C_{S,\Delta x}$=5.0 Wt.-%/b, C_r=0 Wt.-%/b

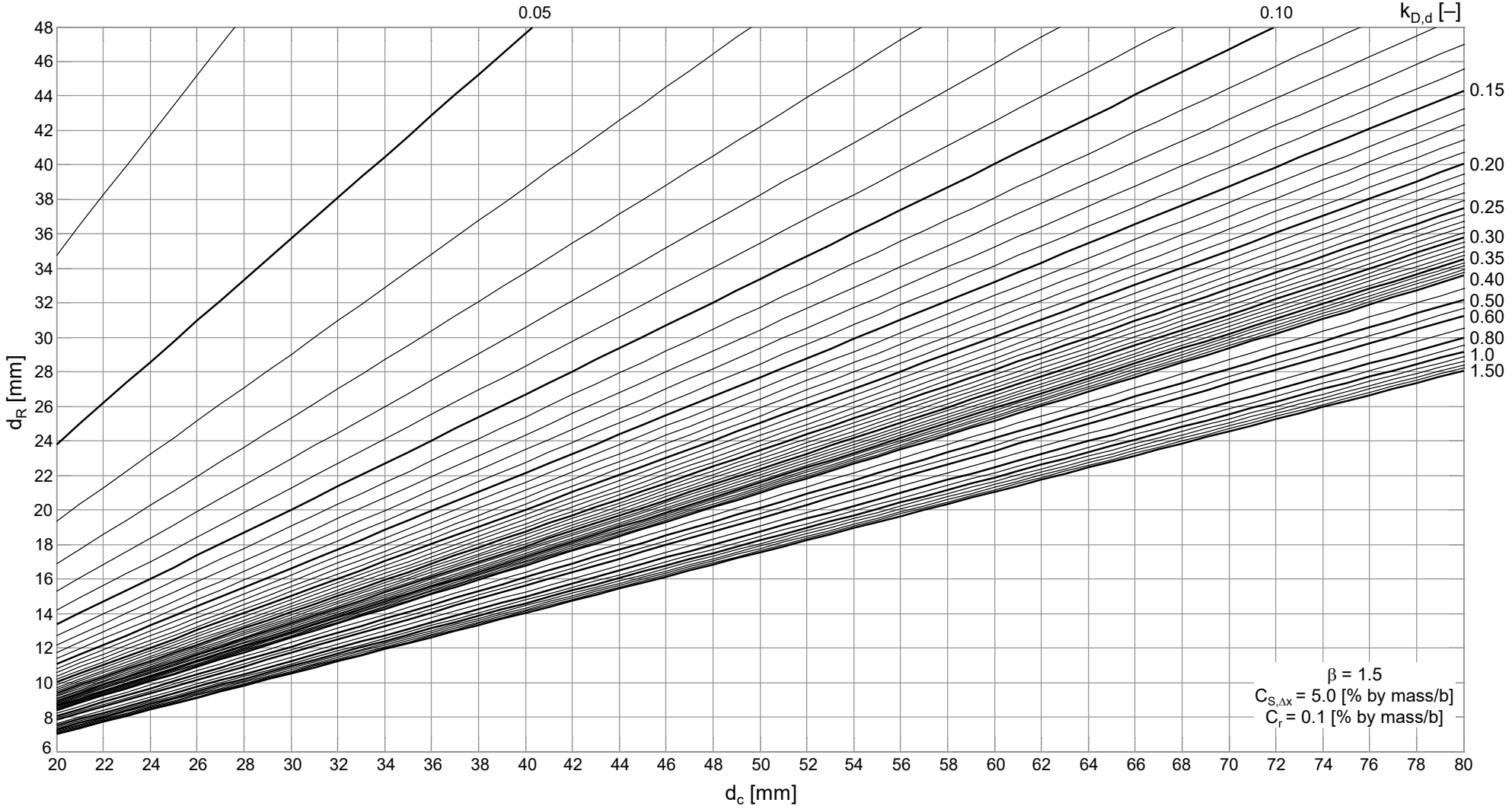

Fig. E.14: Design nomogram for target reliability index β_0=1.5, $C_{S,\Delta x}$=5.0 Wt.-%/b, C_r=0.1 Wt.-%/b

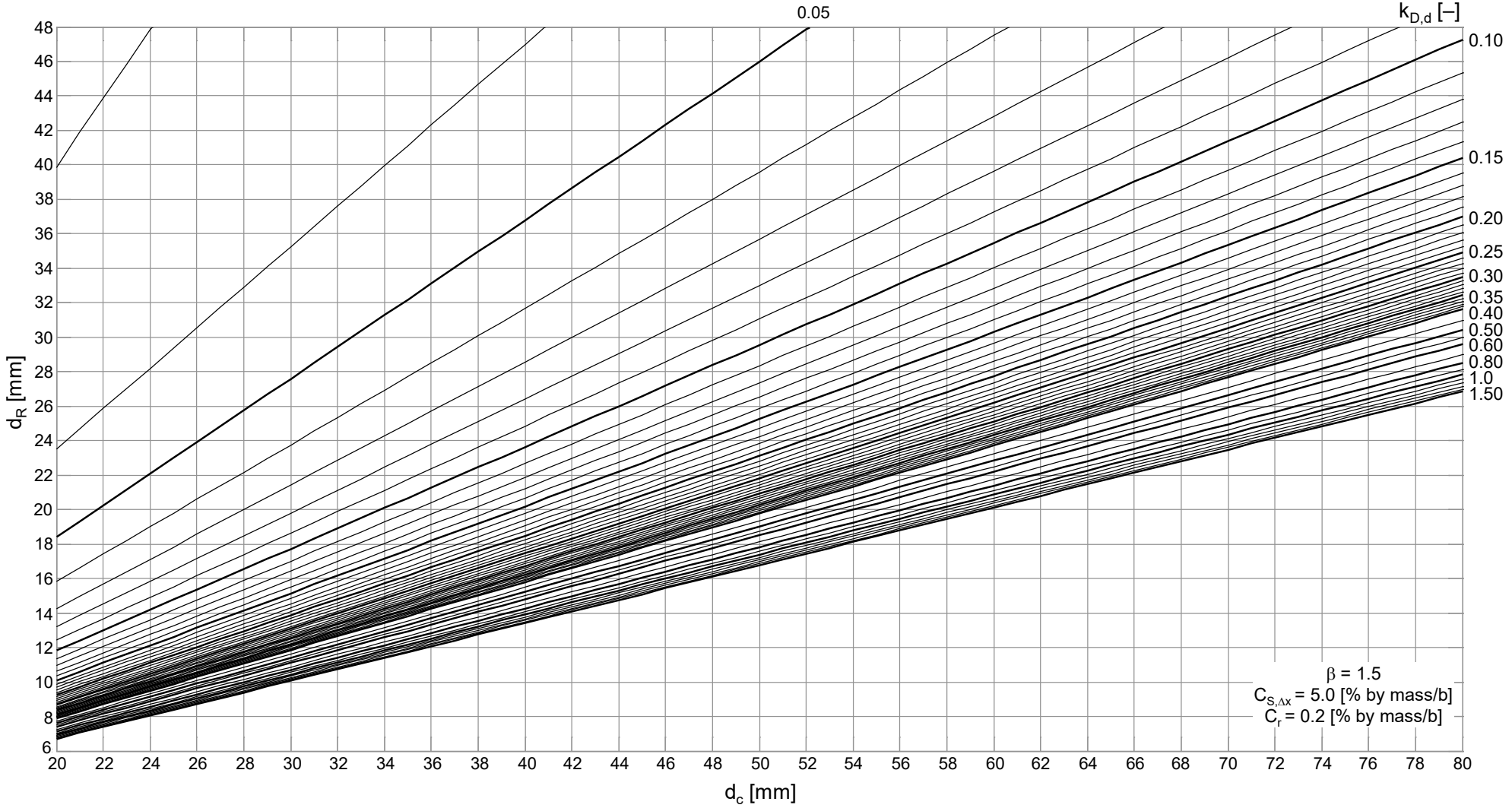

Fig. E.15: Design nomogram for target reliability index β_0=1.5, $C_{S,\Delta x}$=5.0 Wt.-%/b, C_r=0.2 Wt.-%/b

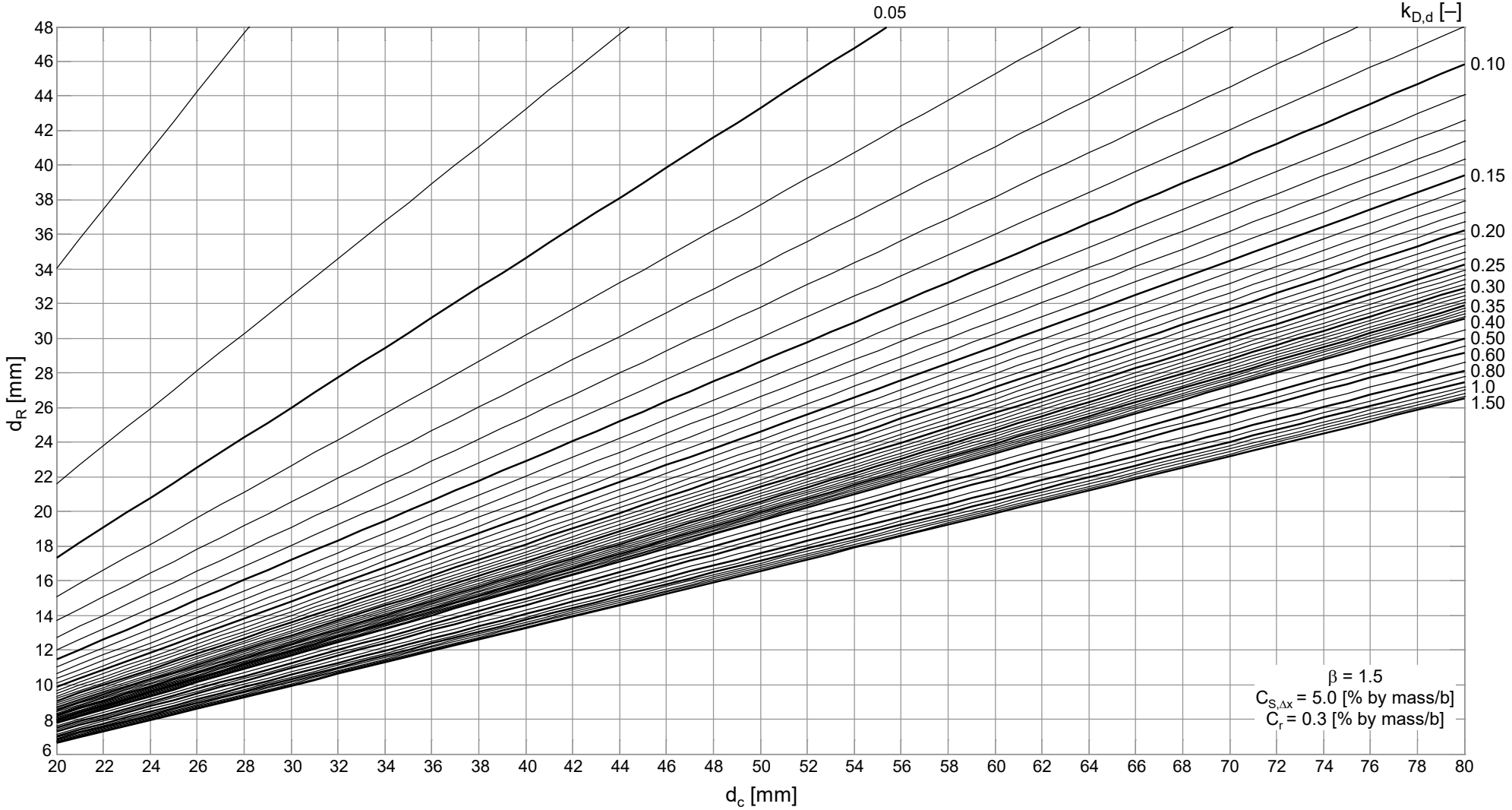

Fig. E.16: Design nomogram for target reliability index β_0=1.5, $C_{S,\Delta x}$=5.0 Wt.-%/b, C_r=0.3 Wt.-%/b

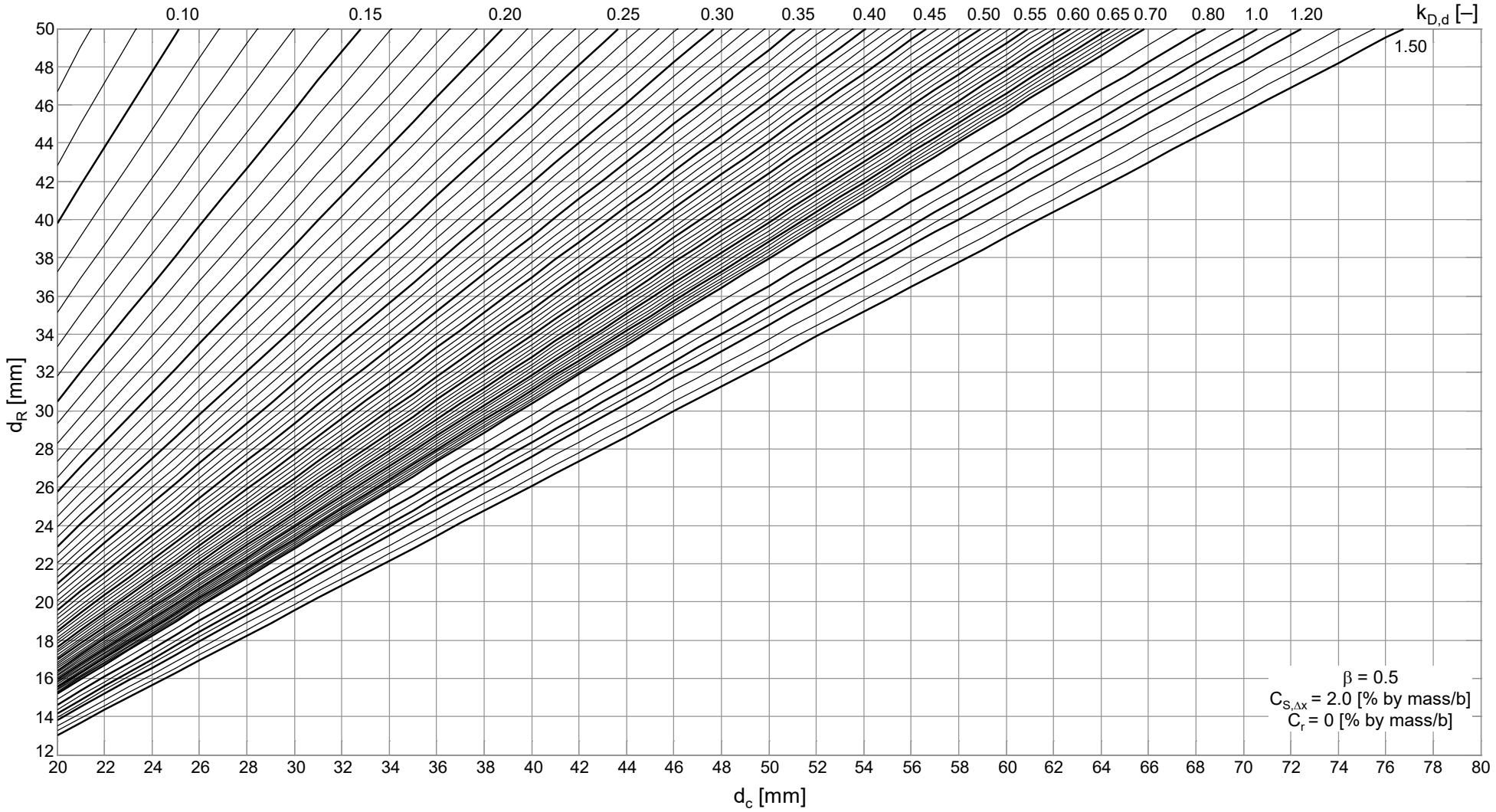

Fig. E.17: Design nomogram for target reliability index β_0=0.5, $C_{S,\Delta x}$=2.0 Wt.-%/b, C_r=0 Wt.-%/b

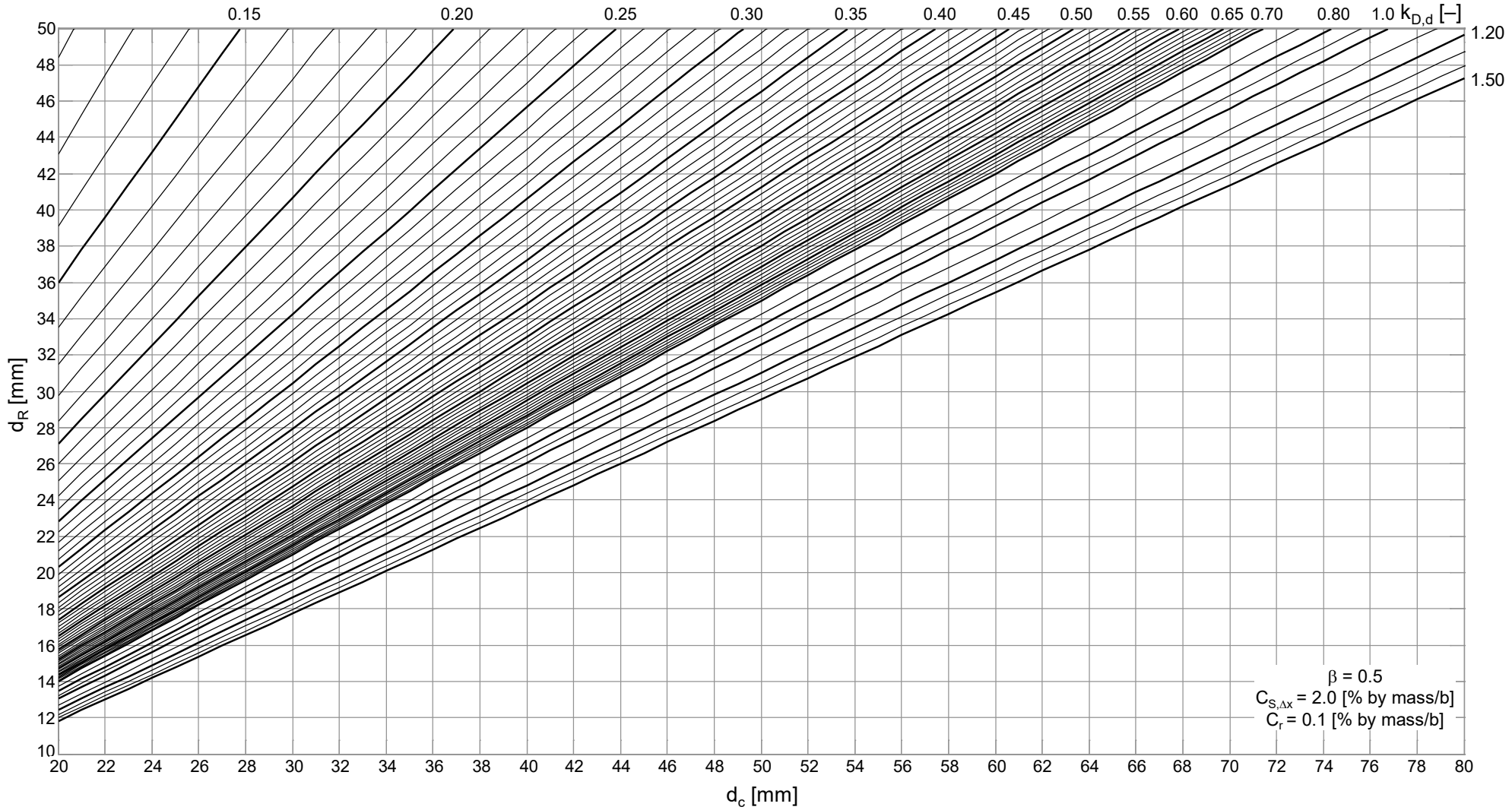

Fig. E.18: Design nomogram for target reliability index β_0=0.5, $C_{S,\Delta x}$=2.0 Wt.-%/b, C_r=0.1 Wt.-%/b

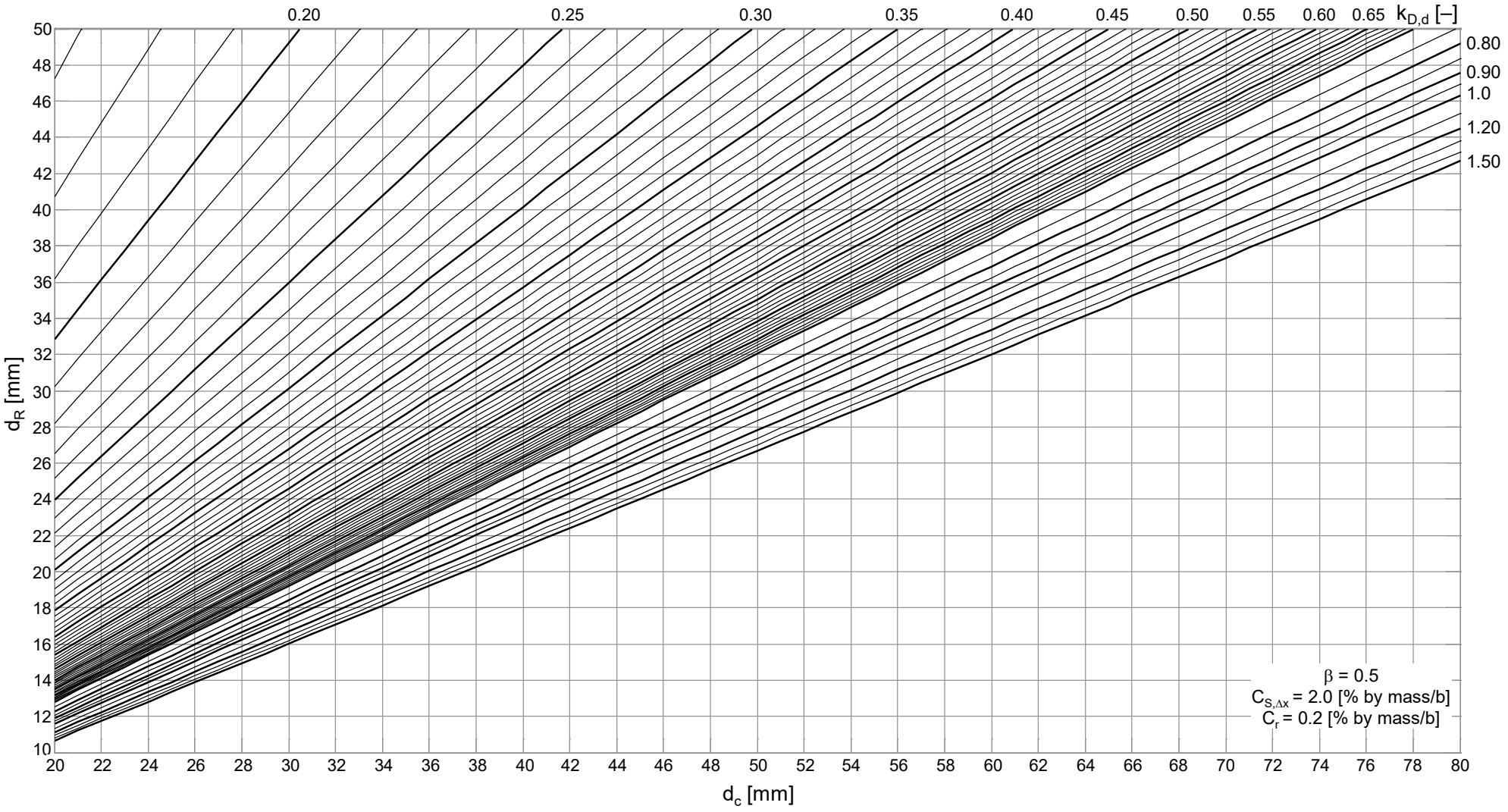

Fig. E.19: Design nomogram for target reliability index β_0=0.5, $C_{S,\Delta x}$=2.0 Wt.-%/b, C_r=0.2 Wt.-%/b

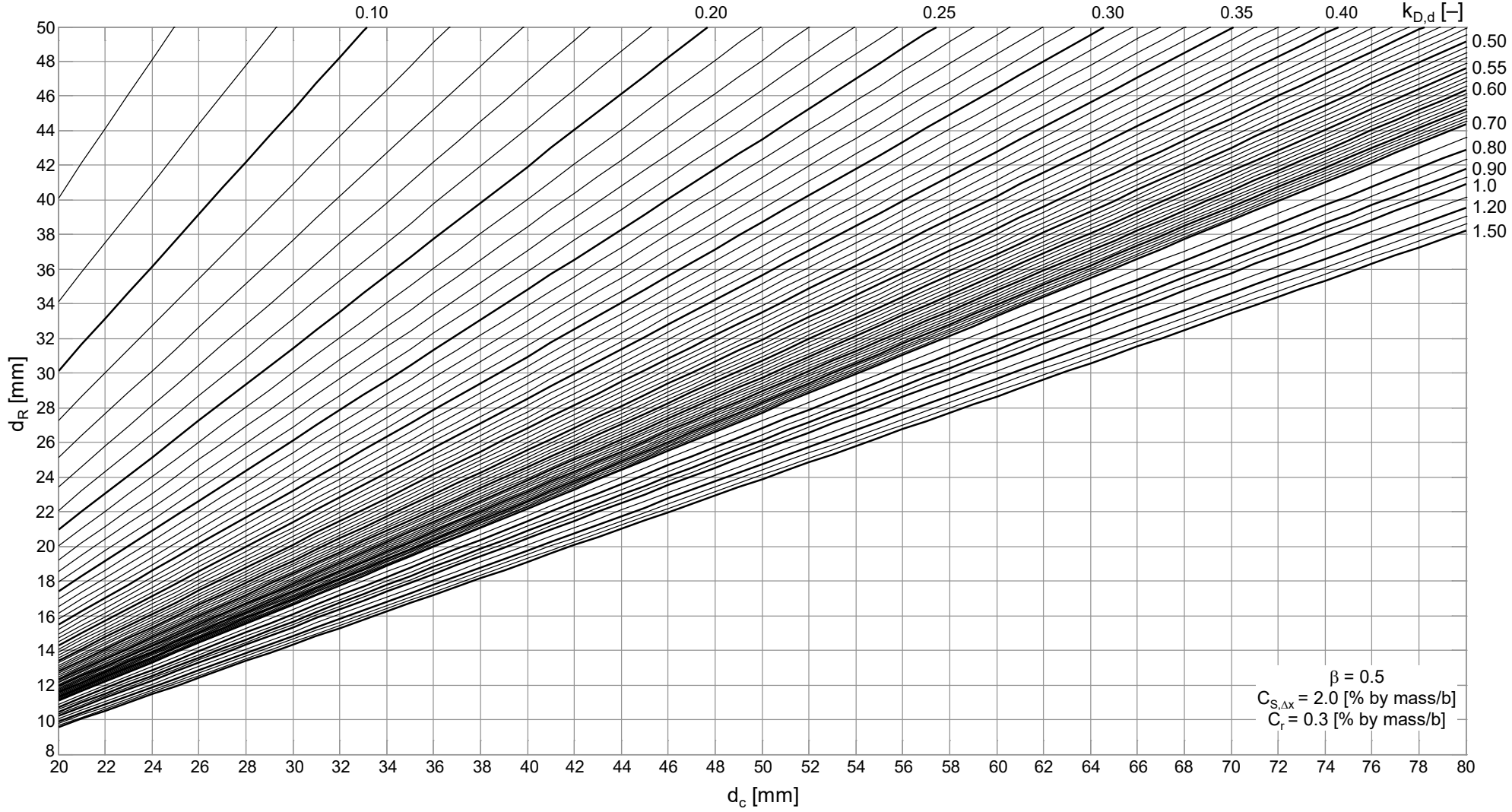

Fig. E.20: Design nomogram for target reliability index β_0=0.5, $C_{S,\Delta x}$=2.0 Wt.-%/b, C_r=0.3 Wt.-%/b

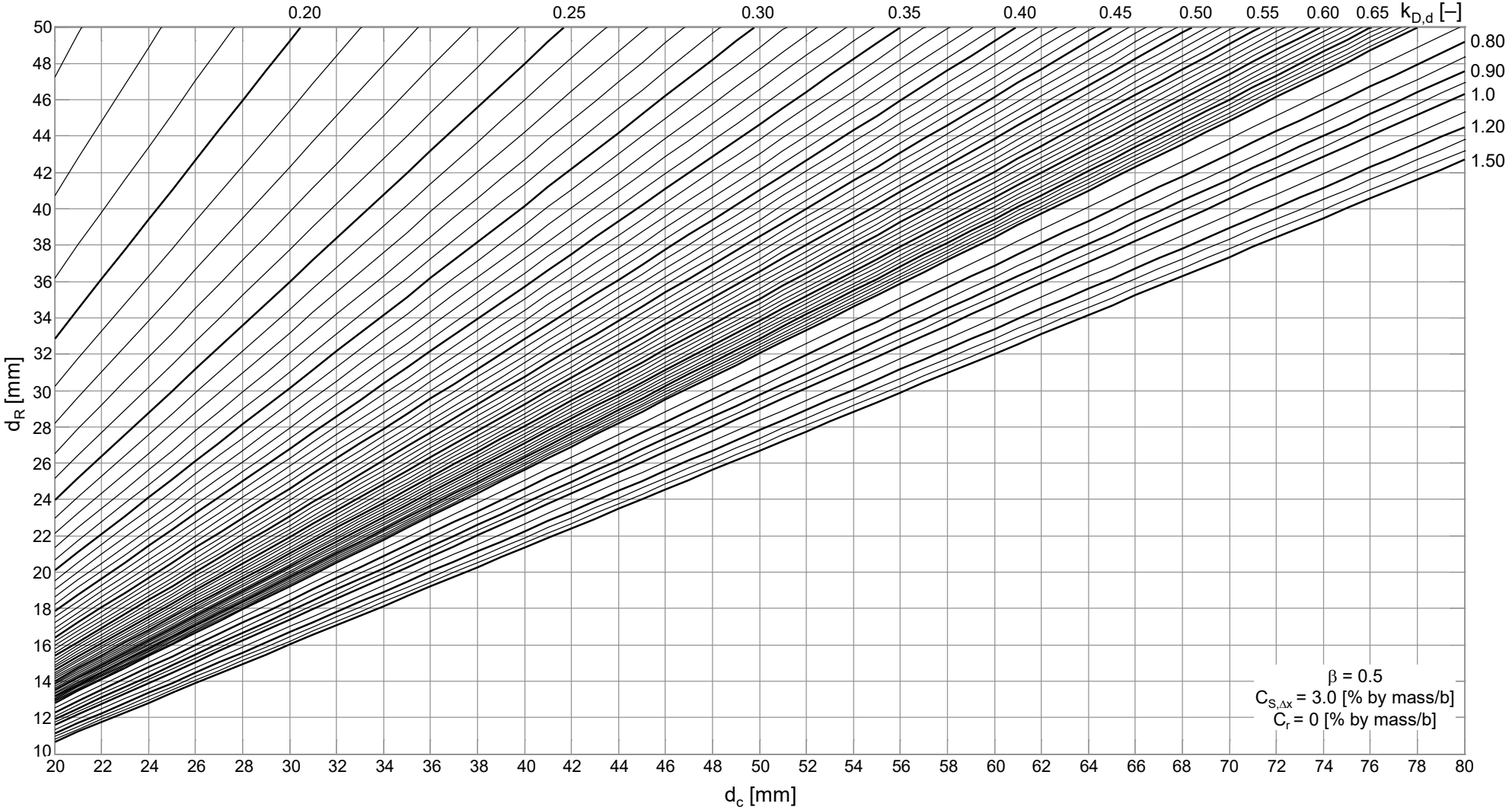

Fig. E.21: Design nomogram for target reliability index β_0=0.5, $C_{S,\Delta x}$=3.0 Wt.-%/b, C_r=0 Wt.-%/b

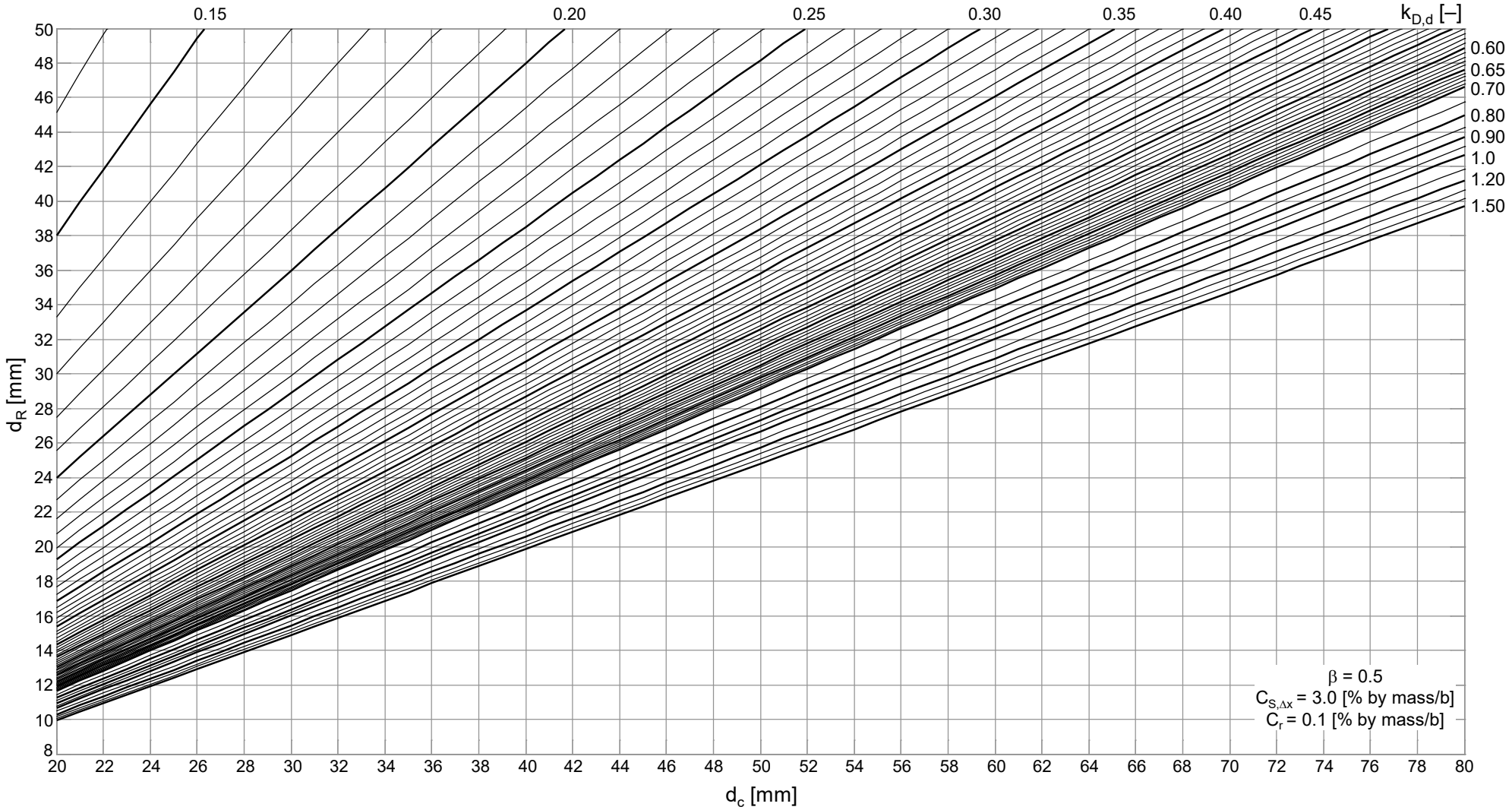

Fig. E.22: Design nomogram for target reliability index β_0=0.5, $C_{S,\Delta x}$=3.0 Wt.-%/b, C_r=0.1 Wt.-%/b

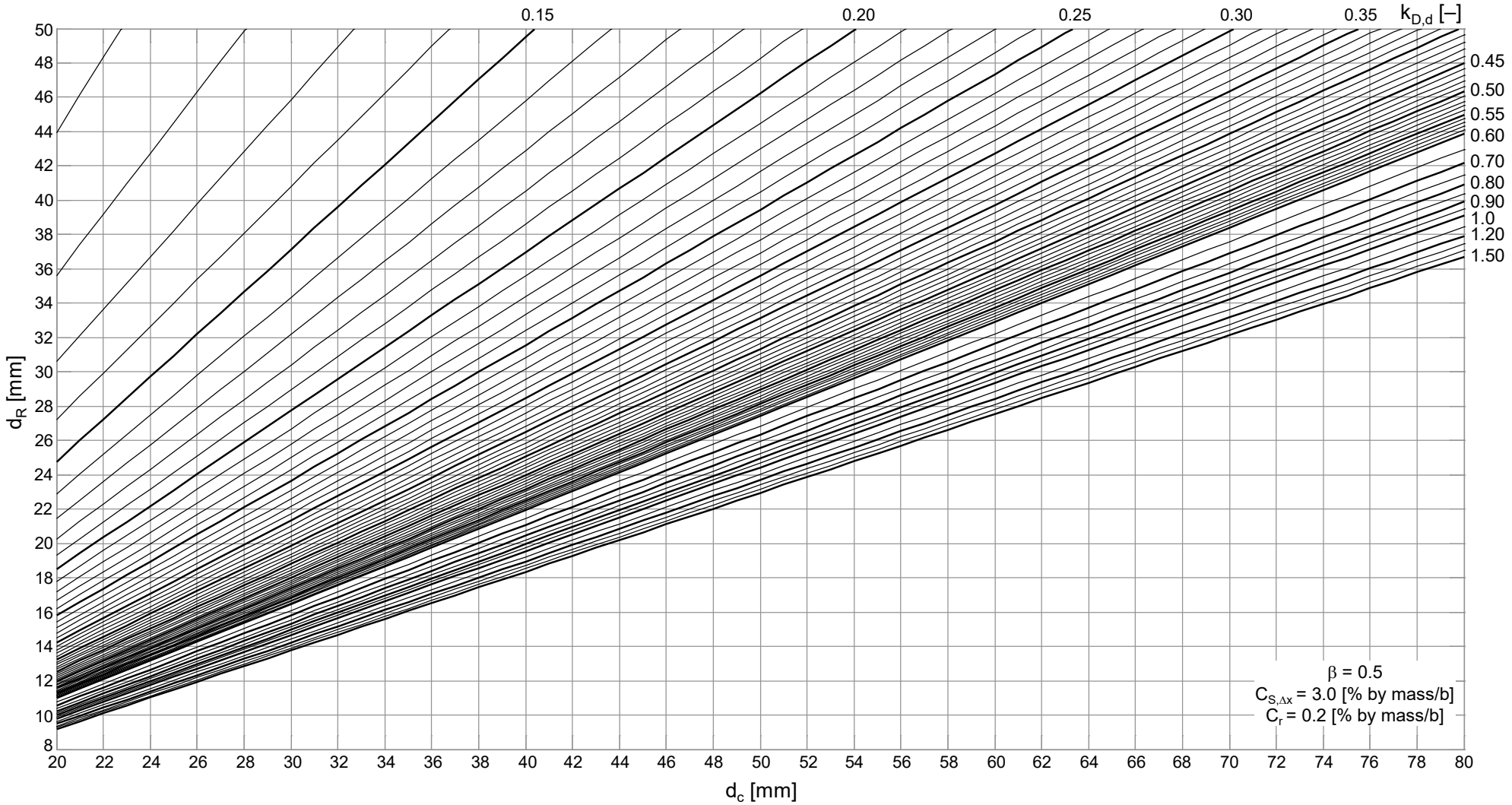

Fig. E.23: Design nomogram for target reliability index β_0=0.5, $C_{S,\Delta x}$=3.0 Wt.-%/b, C_r=0.2 Wt.-%/b

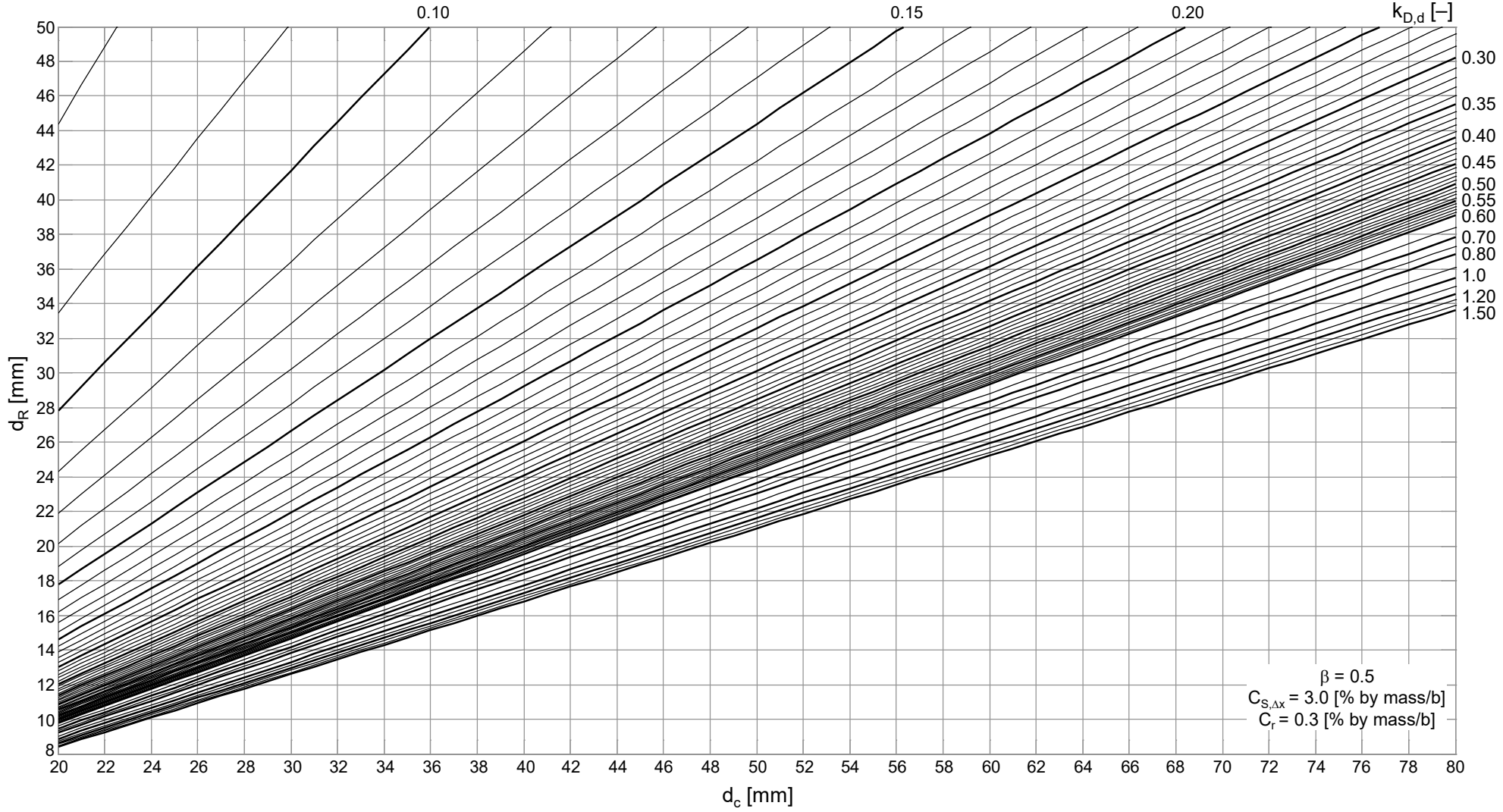

Fig. E.24: Design nomogram for target reliability index β_0=0.5, $C_{S,\Delta x}$=3.0 Wt.-%/b, C_r=0.3 Wt.-%/b

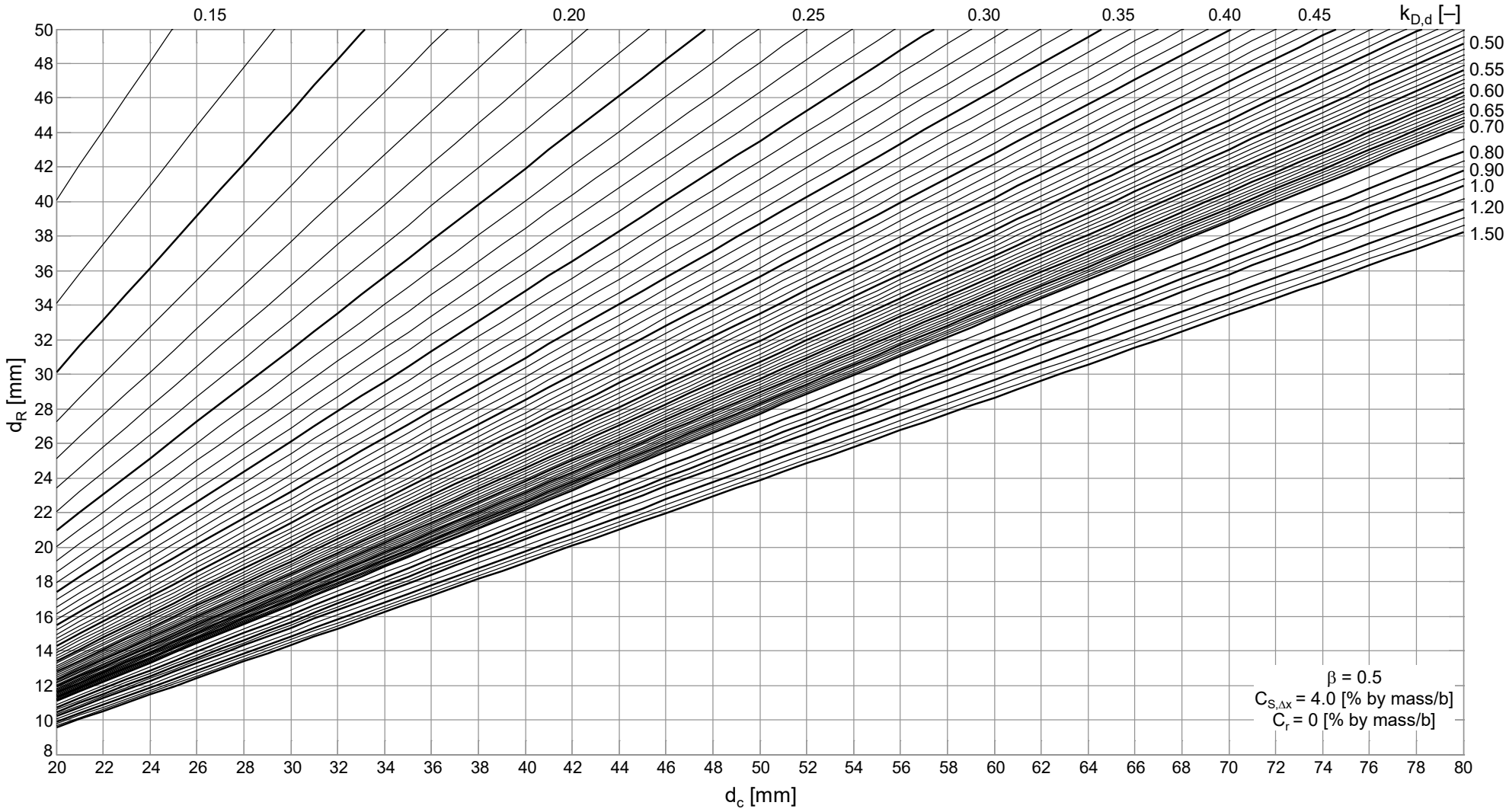

Fig. E.25: Design nomogram for target reliability index β_0=0.5, $C_{S,\Delta x}$=4.0 Wt.-%/b, C_r=0 Wt.-%/b

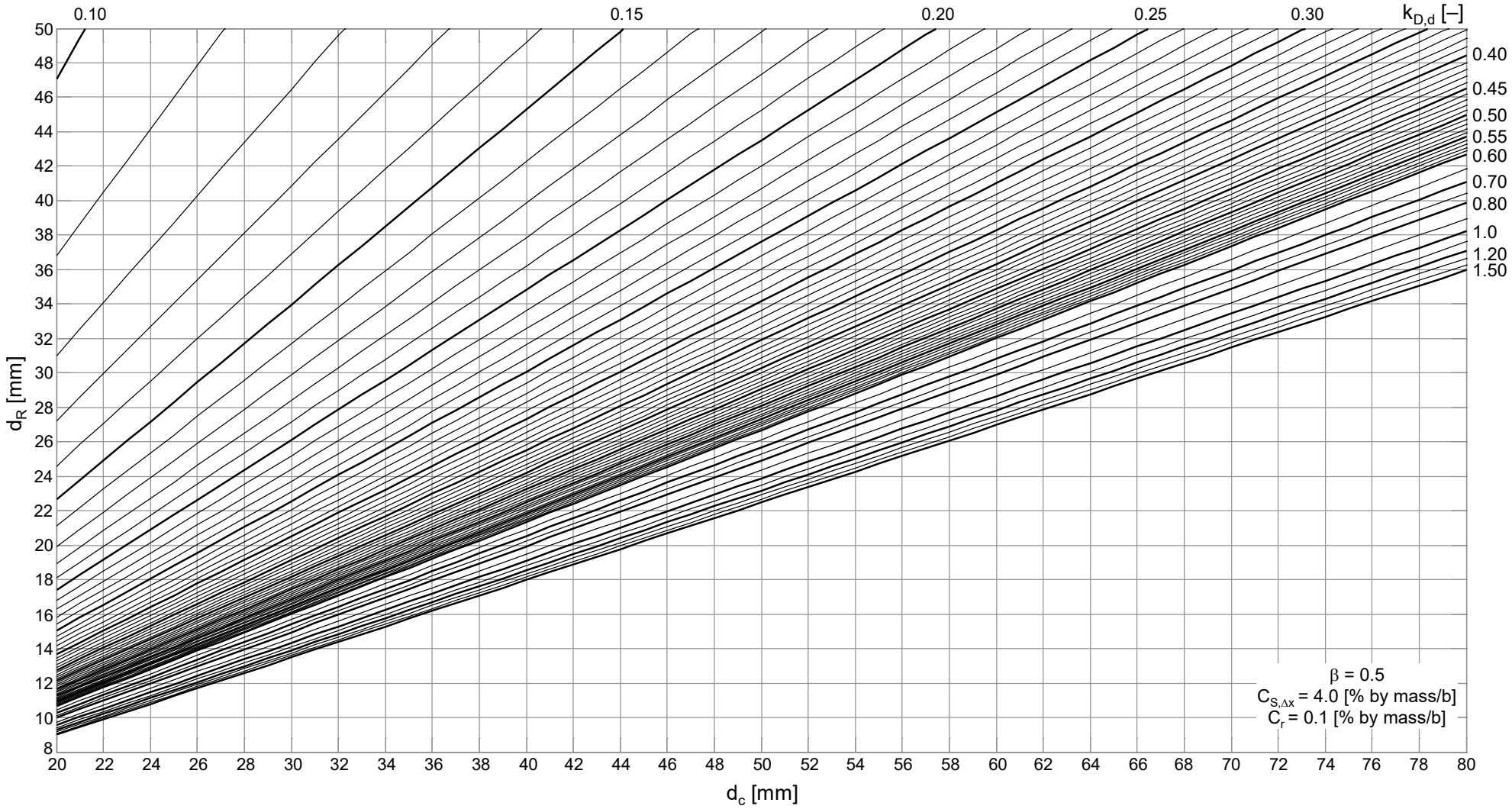

Fig. E.26: Design nomogram for target reliability index β_0=0.5, $C_{S,\Delta x}$=4.0 Wt.-%/b, C_r=0.1 Wt.-%/b b

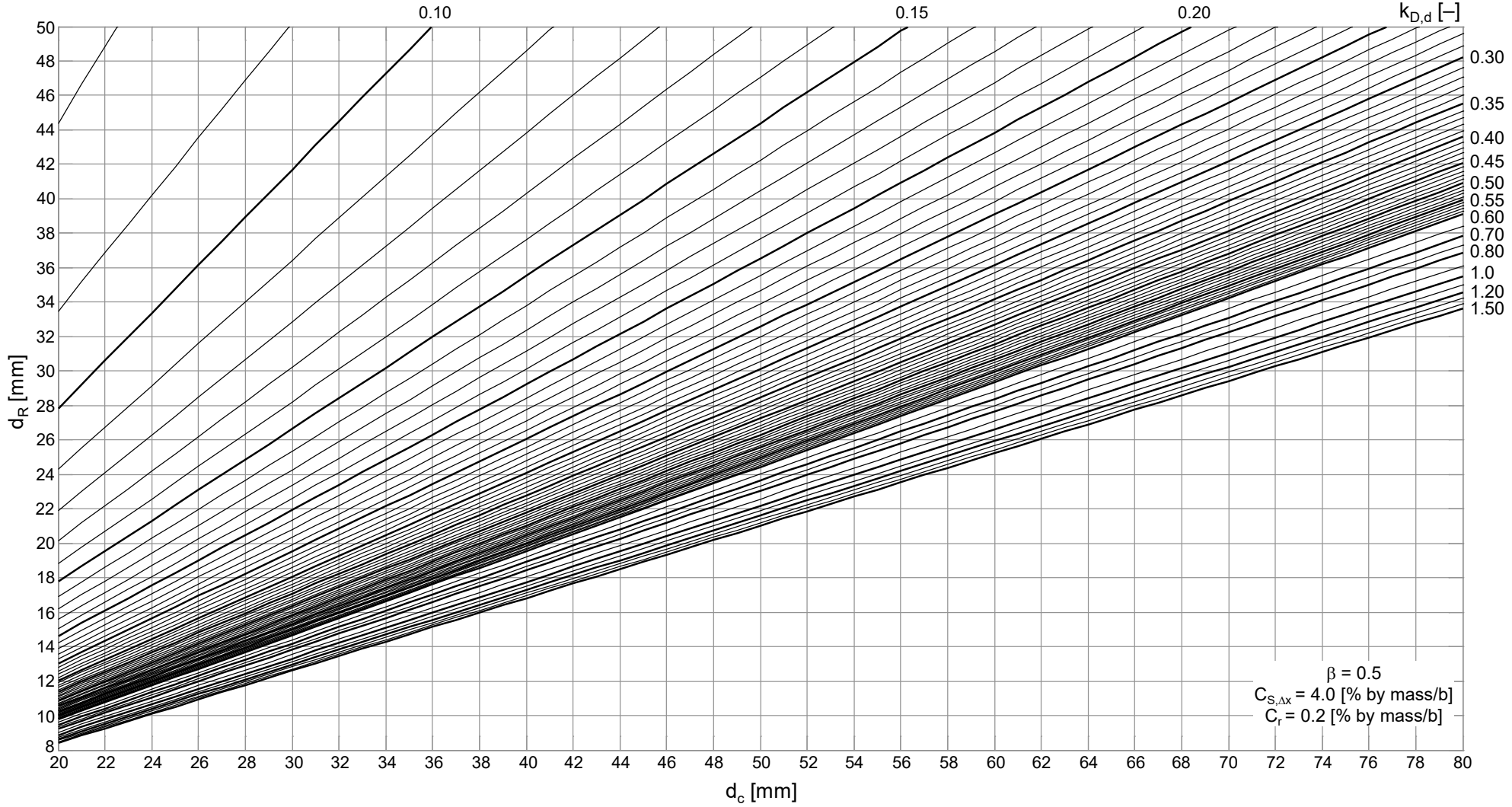

Fig. E.27: Design nomogram for target reliability index β_0=0.5, $C_{S,\Delta x}$=4.0 Wt.-%/b, C_r=0.2 Wt.-%/b

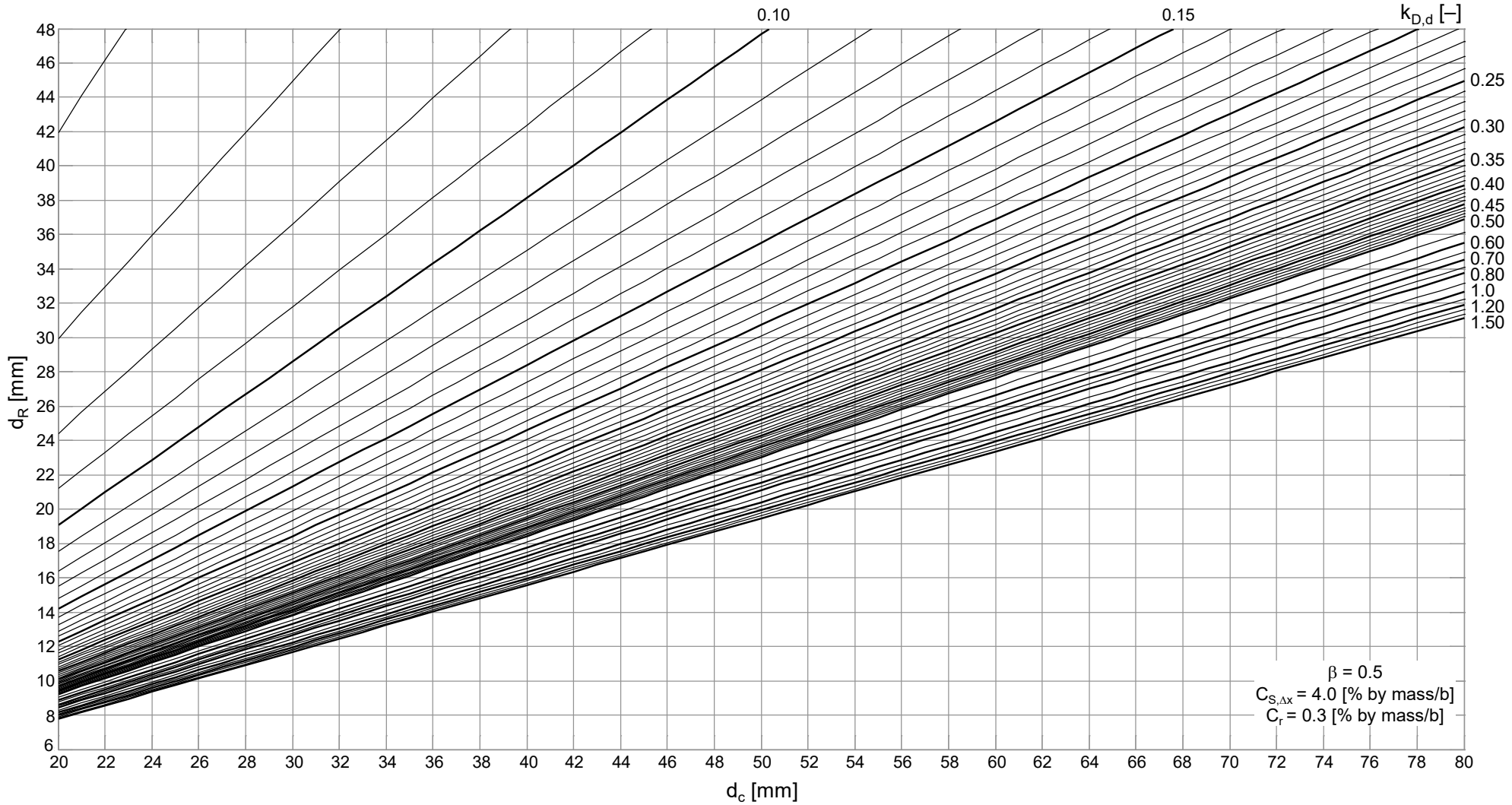

Fig. E.28: Design nomogram for target reliability index β_0=0.5, $C_{S,\Delta x}$=4.0 Wt.-%/b, C_r=0.3 Wt.-%/b

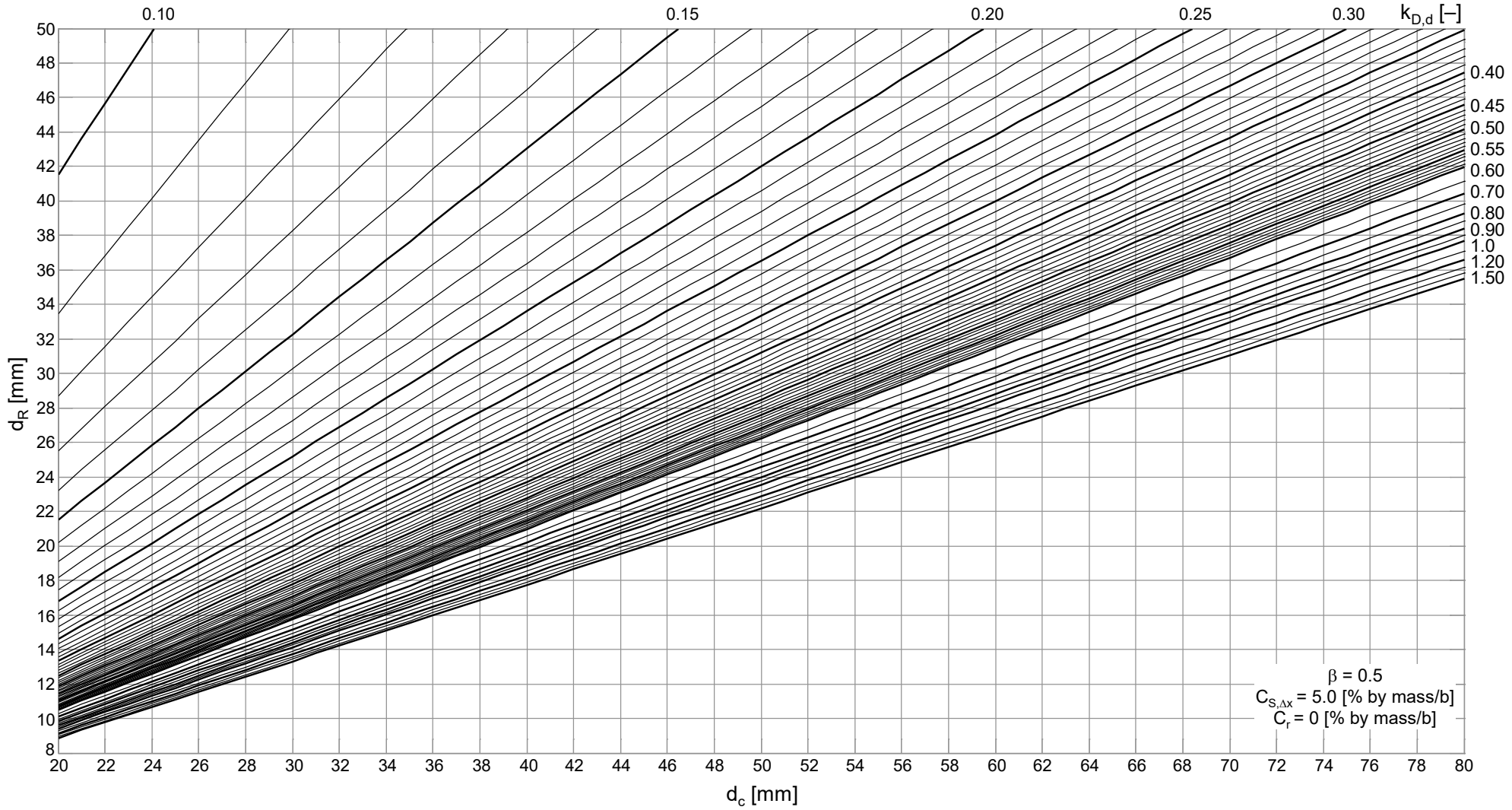

Fig. E.29: Design nomogram for target reliability index β_0=0.5, $C_{S,\Delta x}$=5.0 Wt.-%/b, C_r=0 Wt.-%/b

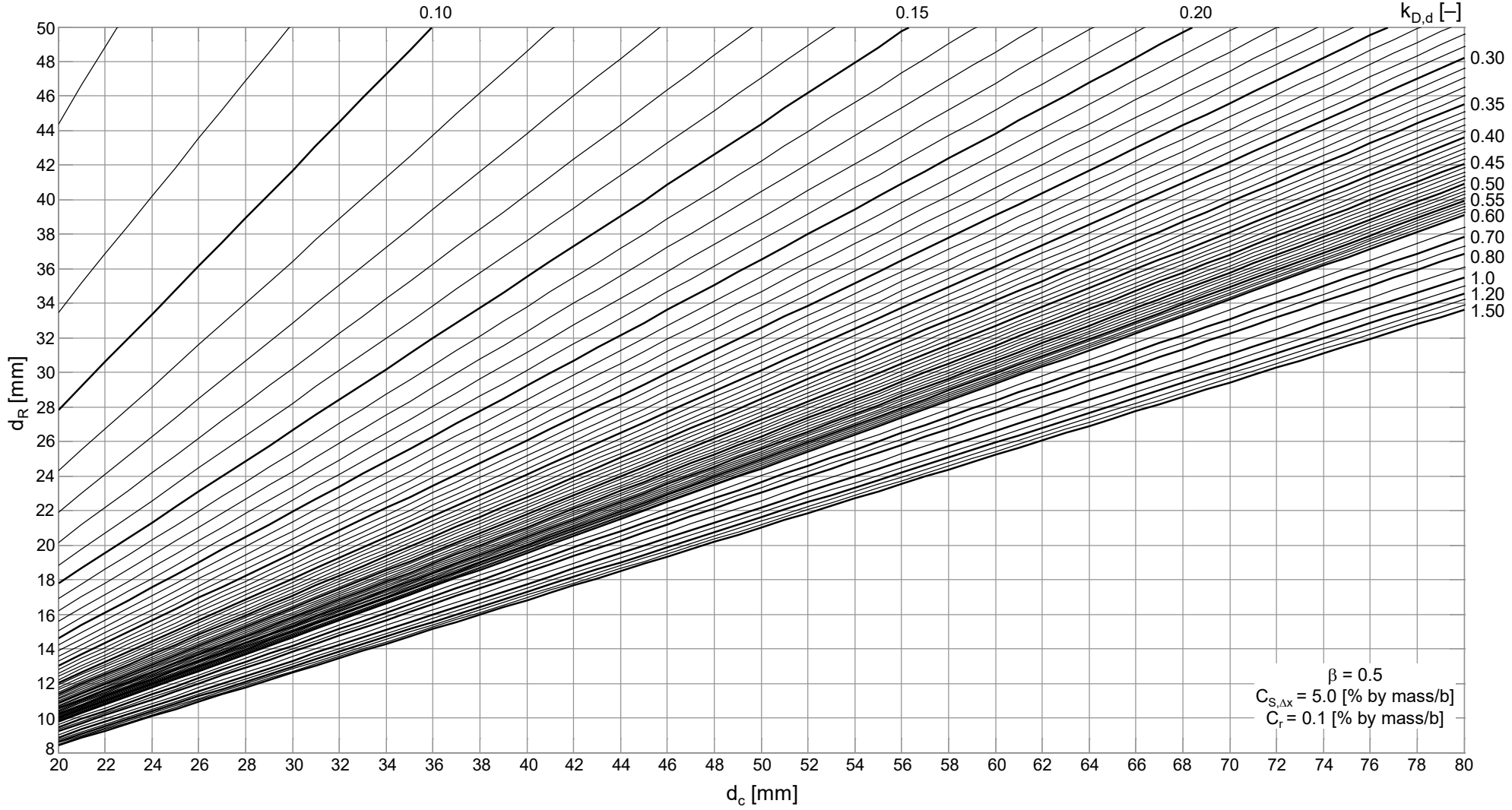

Fig. E.30: Design nomogram for target reliability index β_0=0.5, $C_{S,\Delta x}$=5.0 Wt.-%/b, C_r=0.1 Wt.-%/b

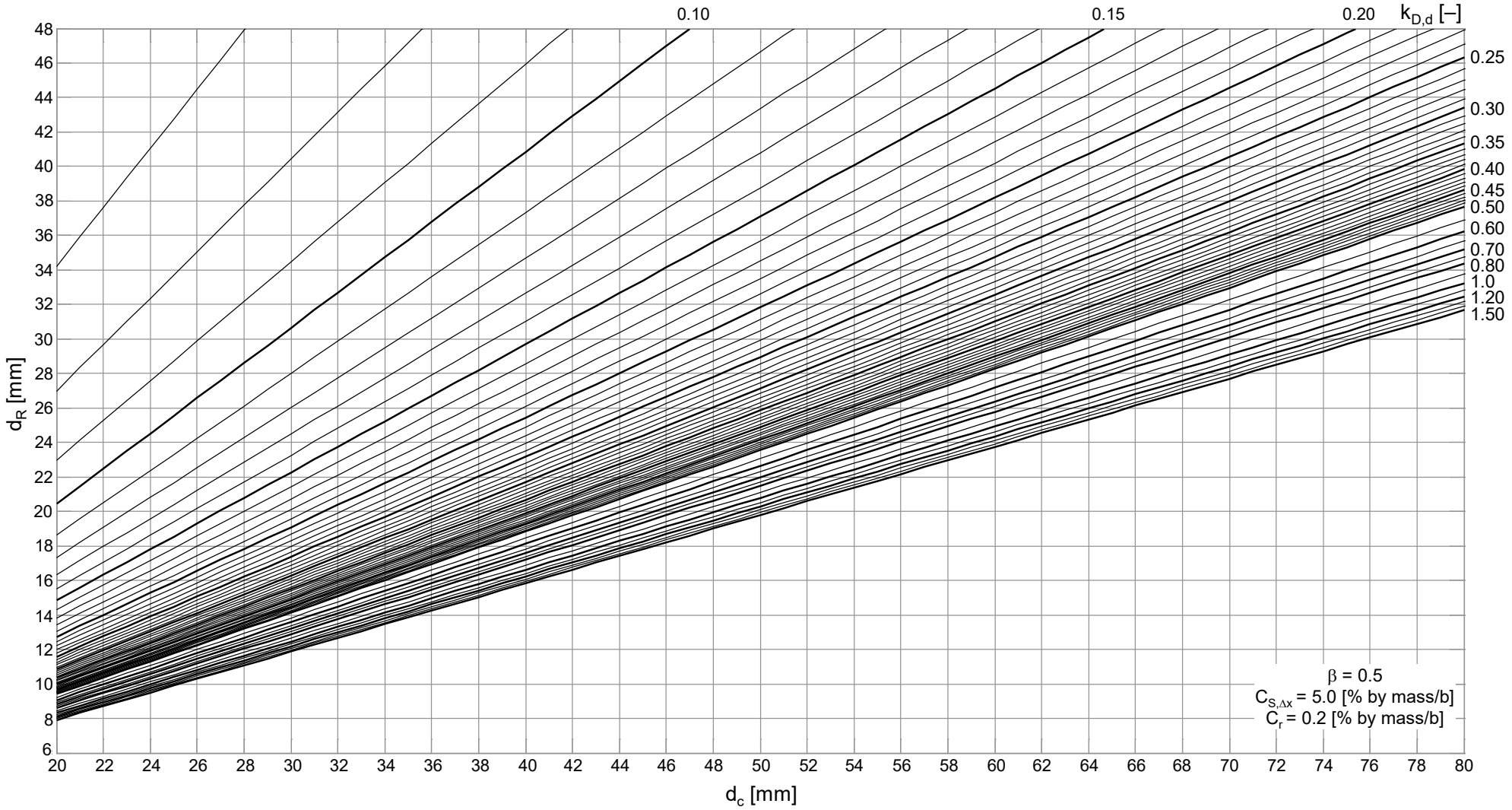

Fig. E.31: Design nomogram for target reliability index β_0=0.5, $C_{S,\Delta x}$=5.0 Wt.-%/b, C_r=0.2 Wt.-%/b

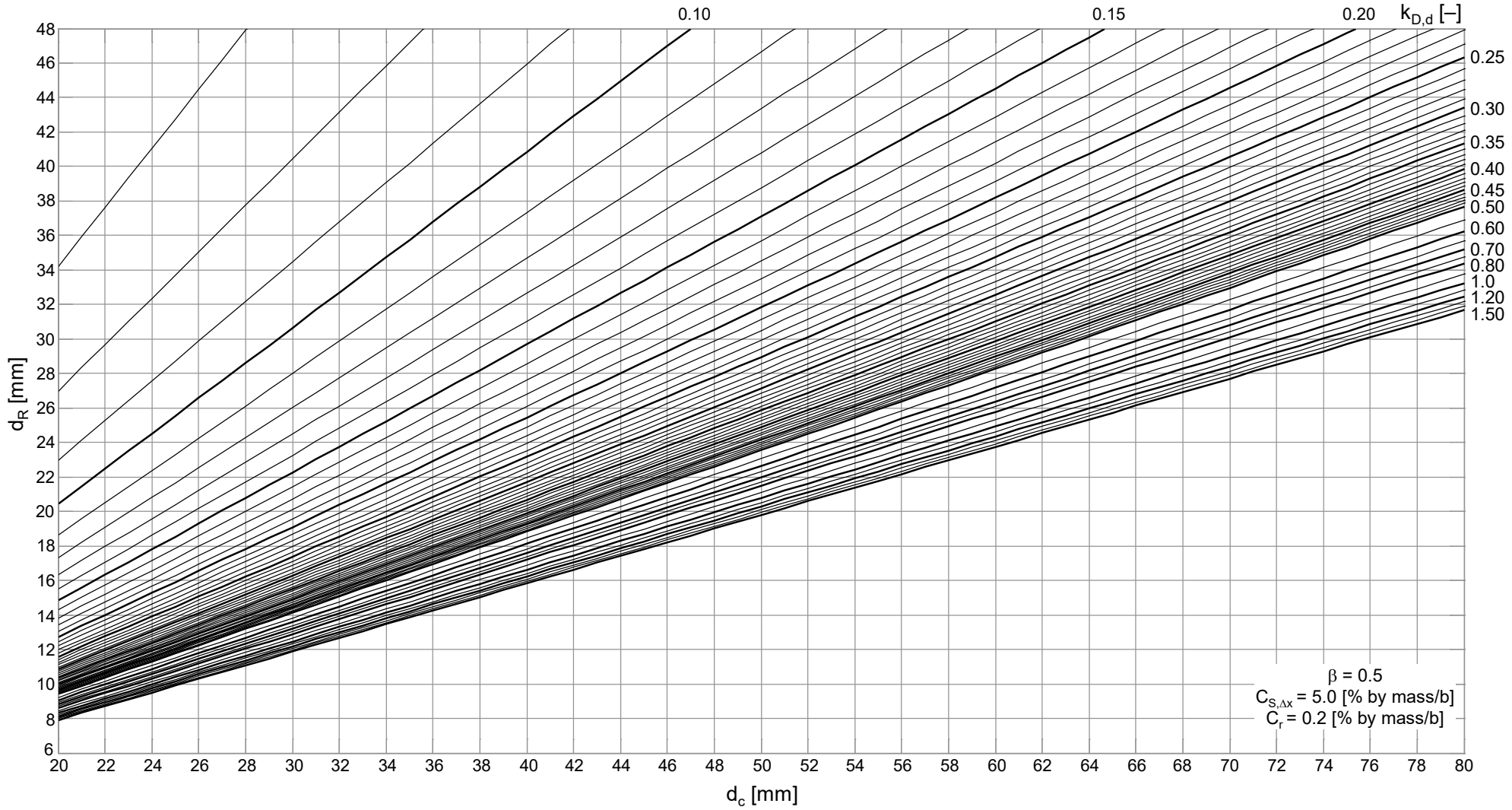

Fig. E.32: Design nomogram for target reliability index β_0=0.5, $C_{S,\Delta x}$=5.0 Wt.-%/b, C_r=0.3 Wt.-%/

Bundesanstalt für Wasserbau
Kussmaulstrasse 17, 76187 Karlsruhe, Germany
www.baw.de

Deutscher Ausschuss für Stahlbeton e. V.
Budapester Strasse 31, 10787 Berlin, Germany
www.dafstb.de